

**Western Australian School of Mines  
Department of Metallurgical and Minerals Engineering**

**A Fundamental Study of Copper and Cyanide Recovery from Gold  
Tailings by Sulfidisation**

**Andrew Murray Simons**

**This thesis is presented for the Degree of  
Doctor of Philosophy  
of  
Curtin University**

**June 2015**

## **STATEMENT OF AUTHENTICITY**

To the best of my knowledge and belief this thesis contains no material previously published by any other person except where due acknowledgment has been made. This thesis contains no material which has been accepted for the award of any other degree or diploma in any university.

A handwritten signature in cursive script that reads "A. Simons".

Andrew Murray Simons

## **ABSTRACT**

Cyanide soluble copper in gold ores causes numerous problems for gold producers. This includes increased costs from high cyanide consumption and a requirement to destroy cyanide in the tailings before discharge into a tailings storage facility. Over recent years a cyanide recycling process known as SART (sulfidisation, acidification, recycle, and thickening) has gained attention as a method to remediate the increased costs and potential environmental impact caused by using cyanidation to process copper bearing gold ores. While sulfidisation processes, such as SART, have been demonstrated within the laboratory to be effective, there are several gold processing operations using sulfidisation which report high sulfide consumption compared to the expected reaction stoichiometry. Further to this problem, there is a lack of fundamental studies of sulfidisation of cyanide solutions resulting in a poor understanding of how various process variables impact the process.

This thesis details work on sulfidisation of copper cyanide solutions to systematically determine the impact of process variables and impurities on the SART process. The work is divided into three distinct areas: modelling of process variables on sulfidisation performance, impact of impurities in sulfidisation, and the impact of residence time on sulfidisation.

Mathematical modelling of sulfidisation of the copper, cyanide, and sulfide system was performed to determine the impact of various factors on sulfidisation. An economic model was then used to determine the overall process optimum and system sensitivity at suboptimal operation. The model showed that to maximise profit during sulfidisation, a sulfide addition of 0.56 moles per mole of copper, a pH of 4, and the lowest possible cyanide to copper ratio should be used. These optimum conditions to maximise profit

remained the same within the range of reagent costs and product values used in the study. The model also showed that it is critical to control sulfide addition at its optimum value, and that the cyanide to copper ratio in the sulfidisation feed should be kept as low as possible, depending on upstream processing constraints.

Impurities in the sulfidisation feed have numerous impacts on sulfidisation performance. It was found that silver and zinc have the largest impact on copper recovery as these two metals consume sulfide preferentially to copper. Gold, iron, nickel, thiosulfate, thiocyanate, and chloride all had no major impact on sulfidisation of copper cyanide solutions. These species did, however, have different minor effects on the process ranging from increases in acid consumption through to shifting the pH range of copper precipitation. It was found that copper can be selectively recovered from other metals, although a small amount of co-precipitation/adsorption occurs. Hence, complete separation of other metals from copper is not possible during sulfidisation.

When sulfidisation is performed on mixed metal cyanide solutions, there are various complex interactions which occur. This includes the potential to precipitate gold at a higher pH than when other metals are not present, likely due to the formation of a silver gold sulfide precipitate. Selective recovery of various metals in sulfidisation is possible, although a small amount of co-precipitation/adsorption will always occur. In any case, selective precipitation would require tight control of sulfide addition and pH.

The most intriguing result from the work is the discovery that long residence times during sulfidisation are the cause of high sulfide consumption experienced in some industrial sulfidisation processes. This is due to

oxidation of the sulfidisation precipitate from a structure similar to  $\text{Cu}_2\text{S}$  towards that of  $\text{CuS}$ . Ultimately, if excess sulfide is not present in solution, copper redissolution occurs reducing the recovery of both copper and cyanide in the process. Industrial surveys of an operational sulfidisation process, along with laboratory scale work using industrial solutions, confirmed the observations from the test work with synthetic copper cyanide solutions. Interestingly, the composition of the industrial solution results in a higher rate of oxidation compared to the synthetic solutions.

## **ACKNOWLEDGEMENTS**

I would firstly like to thank my supervisors Dr Richard Browner from the Western Australian School of Mines (WASM) and Dr Paul Breuer from CSIRO. Both Richard and Paul never ceased to inspire my interest and curiosity in hydrometallurgy and science in general.

I extend many thanks to all of the CSIRO Waterford site staff and fellow PhD students from WASM who have assisted me during my candidature. Of particular mention is Danielle Hewitt whom has assisted me in many aspects of my laboratory work. I'd also like to extend thanks to the Newcrest Telfer metallurgical staff for their assistance in surveying the Telfer SART plant.

I would like to mention the support of my loving parents who have encouraged me over the past four years of my candidature. I am very thankful to have inherited the scientific rational of my father and the creativity of my mother.

Finally, I would like to acknowledge and thank both the CSIRO Minerals Down Under Flagship and the Parker Cooperative Research Centre for Integrated Hydrometallurgy Solutions for their financial support during my candidature.

## CONTENTS

Statement of authenticity .....	i
Abstract .....	ii
Acknowledgements .....	v
Contents .....	vi
Publications .....	xii
List of figures .....	xiv
List of tables .....	xxviii
<b>1 Introduction .....</b>	<b>1</b>
1.1 Importance of gold .....	1
1.2 Processing gold ores .....	3
1.2.1 History of gold processing .....	3
1.2.2 Gold cyanidation .....	4
1.2.3 The impact of copper in gold cyanidation .....	6
1.3 Mitigating the effect of copper in gold processing .....	8
1.3.1 Selective leaching of gold .....	9
1.3.2 Selective leaching of copper .....	9
1.3.3 Cyanide destruction .....	10
1.3.4 Cyanide recycling .....	11
1.3.5 Copper recovery and cyanide recycling by sulfidisation .....	12
1.4 Objectives .....	16
1.5 Thesis structure .....	17
<b>2 Minimising the impact of copper in gold cyanidation .....</b>	<b>19</b>
2.1 Thermodynamic modelling .....	19
2.2 Comparison of technology for separating copper and cyanide .....	19
2.2.1 Direct recycle .....	24
2.2.2 Volatilisation .....	25
2.2.3 Copper cyanide digestion .....	27

2.2.4	Sulfidisation .....	28
2.3	Factors impacting copper-cyanide-sulfide chemistry.....	30
2.3.1	The sulfide system.....	30
2.3.2	Effect of pH .....	32
2.3.3	Effect of sulfide to copper ratio .....	38
2.3.4	Effect of cyanide to copper ratio .....	43
2.3.5	Effect of volatilisation .....	45
2.3.6	Effect of copper concentration.....	46
2.3.7	Effect of residence time .....	47
2.3.8	Effect of temperature .....	48
2.4	Impurities in sulfidisation.....	48
2.4.1	Silver.....	49
2.4.2	Gold .....	52
2.4.3	Iron .....	54
2.4.4	Nickel .....	59
2.4.5	Zinc.....	61
2.4.6	Cyanate .....	65
2.4.7	Thiocyanate .....	65
2.4.8	Thiosulfate.....	66
2.4.9	Chloride .....	66
2.4.10	Carbonate .....	66
2.5	Summary .....	69
<b>3</b>	<b>Methods .....</b>	<b>71</b>
3.1	Reagents and solution preparation.....	71
3.1.1	Distilled and deionised water .....	71
3.1.2	Metal cyanide solutions.....	73
3.1.3	Sulfide solutions .....	73
3.1.4	Diluted sulfuric acid .....	74

3.1.5	Sodium hydroxide solution .....	74
3.2	Reactor design.....	75
3.3	Pre experiment setup .....	77
3.3.1	Reactor configuration .....	77
3.3.2	Acid control and measurement.....	79
3.3.3	Oxidation/reduction potential (ORP) measurement.....	80
3.4	Main experimental procedures .....	80
3.4.1	Staged sulfide addition experiments.....	80
3.4.2	Acid titration experiments .....	81
3.4.3	Residence time experiments .....	82
3.5	Sampling.....	83
3.5.1	Solution sampling .....	83
3.5.2	Solids sampling .....	84
3.6	Analytical techniques .....	84
3.6.1	Atomic absorption spectrometry (AAS) .....	85
3.6.2	Inductively coupled plasma optical emission spectrometry (ICP-OES) .....	85
3.6.3	Potentiometric titration .....	85
3.6.4	High performance liquid chromatography (HPLC) .....	88
3.6.5	Ion selective electrode.....	90
3.6.6	Carbon and sulfur analysis in solids .....	90
3.6.7	X-ray diffraction (XRD) .....	91
3.6.8	Scanning electron microscopy (SEM).....	91
<b>4</b>	<b>Modelling sulfidisation chemistry.....</b>	<b>93</b>
4.1	Introduction .....	93
4.2	Determination of important model factors .....	94
4.2.1	Experimental Methods .....	94
4.2.2	Effect of pH .....	95

4.2.3	Effect of sulfide to copper ratio .....	96
4.2.4	Effect of cyanide to copper ratio .....	98
4.2.5	Effect of initial copper concentration .....	100
4.2.6	Effect of time .....	101
4.2.7	Temperature.....	101
4.3	Response models .....	102
4.3.1	Experimental design .....	102
4.3.2	Experimental Methods .....	105
4.3.3	Copper recovery model.....	106
4.3.4	Cyanide recovery model .....	109
4.3.5	Acid addition model .....	115
4.3.6	Oxidation/reduction potential (ORP) model.....	119
4.4	Economic impacts .....	122
4.4.1	Equations .....	123
4.4.2	System optimum and sensitivity .....	124
4.5	Conclusions .....	133
<b>5</b>	<b>Impact of impurities on sulfidisation.....</b>	<b>136</b>
5.1	Introduction .....	136
5.2	Single impurity experiments .....	137
5.2.1	Experimental methods .....	137
5.2.2	Baseline Experiment .....	138
5.2.3	Silver.....	139
5.2.4	Gold.....	143
5.2.5	Iron (II).....	148
5.2.6	Iron (III).....	152
5.2.7	Nickel .....	156
5.2.8	Zinc.....	159
5.2.9	Thiocyanate .....	163

5.2.10	Thiosulfate.....	165
5.2.11	Chloride .....	167
5.3	Mixed metal experiments.....	169
5.3.1	Experimental methods .....	169
5.3.2	No sulfide addition .....	170
5.3.3	Sulfide to metal molar ratio of 0.2.....	172
5.3.4	Sulfide to metal molar ratio of 0.4.....	175
5.3.5	Sulfide to metal molar ratio of 0.6.....	177
5.3.6	Sulfide to metal molar ratio of 0.8.....	179
5.4	Conclusions .....	181
<b>6</b>	<b>Impact of residence time on sulfidisation .....</b>	<b>185</b>
6.1	Introduction .....	185
6.2	Factorial design screening.....	185
6.2.1	Experimental methods .....	185
6.2.2	Results.....	186
6.3	Large scale residence time tests .....	189
6.3.1	Experimental methods .....	190
6.3.2	Initial precipitate structure .....	190
6.3.3	Effect of sulfide to copper ratio .....	193
6.3.4	Effect of copper concentration.....	201
6.3.5	Effect of oxygen .....	205
6.3.6	Effect of pH .....	217
6.3.7	Effect of cyanide to copper ratio .....	224
6.4	Proposed reactions occurring.....	226
6.5	Industrial implications .....	229
6.6	Conclusions.....	230
<b>7</b>	<b>Industrial implications of residence time on sulfidisation .....</b>	<b>232</b>
7.1	Introduction .....	232

7.2	Newcrest Mining Limited’s Telfer Gold Mine.....	233
7.3	Surveying the Telfer SART plant .....	236
7.3.1	Surveying methods .....	236
7.3.2	Sulfide addition rate .....	239
7.3.3	Nucleation tank experiment .....	240
7.3.4	Surveys.....	242
7.4	Laboratory work using Telfer SART solutions .....	252
7.4.1	Experimental methods .....	252
7.4.2	Analysis of Telfer solutions .....	253
7.4.3	Effect of sulfide dosing.....	254
7.4.4	Effect of oxygen .....	258
7.4.5	Discussion on oxidation in Telfer solutions .....	265
7.4.6	Comparison to synthetic solution experiments .....	266
7.4.7	Effect of impurities.....	269
7.5	Conclusions .....	271
<b>8</b>	<b>Conclusions and recommendations .....</b>	<b>273</b>
8.1	Conclusions .....	273
8.2	Recommendations for future research.....	279
<b>9</b>	<b>References .....</b>	<b>280</b>
<b>10</b>	<b>Appendices.....</b>	<b>290</b>
10.1	Thermodynamic data.....	290
10.2	Calculation of cyanide concentration.....	295
10.3	Coefficients of combined profit equation .....	296

## PUBLICATIONS

Simons, A, and P Breuer. 2011. "The effect of process variables on cyanide and copper recovery using SART" *ALTA 2011 Gold Proceedings, Perth, Australia*: ALTA Metallurgical Services. This paper was also presented.

Dai, X, A Simons, and P Breuer. 2011. "A review of copper cyanide recovery for the cyanidation of copper containing gold ores" *ALTA 2011 Gold Proceedings, Perth*: ALTA.

Re-published as: Dai, X, A Simons, and P Breuer. 2012. "A review of copper cyanide recovery technologies for the cyanidation of copper containing gold ores." *Minerals Engineering* 25 (1): 1-13.

Simons, A, and P Breuer. 2011. "Fundamental investigations of SART for cyanide and copper recovery" *World Gold 2011, Montreal*: Canadian Institute of Mining, Metallurgy, and Petroleum. This paper was also presented.

Re-published as: Simons, A, and P Breuer. 2013. "Fundamental investigations of SART for cyanide and copper recovery." *CIM Journal* 4 (3): 145-152.

Simons, A, and P Breuer. 2013. "The impact of residence time on copper recovery in Telfer Gold Mine's cyanide recycling process" *World Gold 2013, Brisbane*: Australasian Institute of Mining and Metallurgy. This paper was also presented.

Simons, A, P Breuer, and R Browner. 2015. "The impact of metal cyanide species on the recovery of cyanide and copper using SART" *World Gold 2015, Johannesburg*: The Southern African Institute of Mining and Metallurgy.

McGrath, T, A Simons, R Dunne, and W Staunton. 2015. "Cyanide recovery using SART – current status." *World Gold 2015, Johannesburg*: The Southern African Institute of Mining and Metallurgy.

**Planned publications:**

Simons, A, P Breuer, and R Browner. 2015. "The impact of silver, gold, iron, nickel, and zinc during sulfide precipitation of copper from copper cyanide solutions"

Simons, A, P Breuer, and R Browner. 2015. "The impact of residence time on copper and cyanide recovery during SART"

## LIST OF FIGURES

Figure 1.1	Demand for gold in 2011 (World Gold Council 2012a). ....	1
Figure 1.2	Gold price in US dollars per ounce between 1978 and 2012 (World Gold Council 2012c).....	2
Figure 1.3	Generic SART flowsheet.....	15
Figure 2.1	Potential-pH diagram of Cu speciation in the Cu-CN-H <sub>2</sub> O system for a 20 mM Cu solution with a CN:Cu ratio of 4. "a" indicates soluble species. ....	21
Figure 2.2	Potential-pH diagram of Cu speciation in the Cu-CN-H <sub>2</sub> O system for a 20 mM Cu solution with a CN:Cu ratio of 4, where CNO <sup>-</sup> and HCNO <sub>(aq)</sub> are not considered. "a" indicates soluble species.....	21
Figure 2.3	Thermodynamic determination of Cu (I) speciation at different pH values for a 20 mM Cu (I) solution with a CN:Cu ratio of 4 and where redox reactions are not considered. ....	22
Figure 2.4	Potential-pH diagram of S speciation in the S-H <sub>2</sub> O system for a 10 mM S solution. "a" indicates soluble species. ....	31
Figure 2.5	Thermodynamic determination of S speciation at different pH values for a 10 mM S solution where redox reactions are not considered.....	32
Figure 2.6	Potential-pH diagram of Cu speciation in the Cu-CN-S-H <sub>2</sub> O system for a 20 mM Cu solution with a CN:Cu ratio of 4 and a S:Cu ratio of 0.5. "a" indicates soluble species.....	34
Figure 2.7	Potential-pH diagram of Cu speciation in the Cu-CN-S-H <sub>2</sub> O system for a 20 mM Cu solution with a CN:Cu ratio of 4 and a S:Cu ratio of 0.5, where cyanate species are not considered. "a" indicates soluble species. ....	34

Figure 2.8	Potential-pH diagram of Cu speciation in the Cu-CN-S-H <sub>2</sub> O system for a 20 mM Cu solution with a CN:Cu ratio of 4 and a S:Cu ratio of 0.5, where cyanate and sulfur oxide species are not considered. "a" indicates soluble species.....	35
Figure 2.9	Potential-pH diagram of Cu speciation in the Cu-CN-S-H <sub>2</sub> O system for a 20 mM Cu solution with a CN:Cu ratio of 4 and a S:Cu ratio of 0.5, where cyanate, sulfur oxide, and thiocyanate species are not considered. "a" indicates soluble species.....	36
Figure 2.10	Thermodynamic determination of Cu (I) speciation at different pH values for a 20 mM Cu (I) solution with a CN:Cu ratio of 4, a S:Cu ratio of 0.5, and where redox reactions are not considered.....	38
Figure 2.11	Thermodynamic determination of Cu (I) speciation at different S additions for a 20 mM Cu (I) solution with a CN:Cu ratio of 4, a pH of 4, and where redox reactions are not considered. ....	40
Figure 2.12	Thermodynamic determination of Cu (I) speciation at different CN <sup>-</sup> additions for a 20 mM Cu (I) solution with an S:Cu ratio of 0.5, a pH of 4, and where redox reactions are not considered. .	44
Figure 2.13	Thermodynamic determination of Cu (I) speciation at different CN <sup>-</sup> additions for a 20 mM Cu (I) solution with an S:Cu ratio of 0.5, a pH of 6, and where redox reactions are not considered. .	45
Figure 2.14	Thermodynamic determination of a) Ag (I) and b) Cu (I) speciation at different pH for a 20 mM Cu (I) and Ag (I) solution with a CN:metal ratio of 4, a S:Cu ratio of 0.5, and where redox reactions are not considered. ....	51

Figure 2.15	Thermodynamic determination of a) Au (I) and b) Cu (I) speciation at different pH for a 20 mM Cu (I) and Au (I) solution with a CN:metal ratio of 4, a S:Cu ratio of 1.0, and where redox reactions are not considered. ....	53
Figure 2.16	Thermodynamic determination of a) Fe (II) and b) Cu (I) speciation at different pH for a 20 mM Cu (I) and Fe (II) solution with a CN:Cu ratio of 4 plus a CN:Fe ratio of 6, a S:Cu ratio of 0.5, and where redox reactions are not considered. ....	57
Figure 2.17	Thermodynamic determination of a) Fe (III) and b) Cu (I) speciation at different pH for a 20 mM Cu (I) and Fe (III) solution with a CN:Cu ratio of 4 plus a CN:Fe ratio of 6, a S:Cu ratio of 0.5, and where redox reactions are not considered.....	58
Figure 2.18	Thermodynamic determination of a) Ni (II) and b) Cu (I) speciation at different pH for a 20 mM Cu (I) and Ni (II) solution with a CN:metal ratio of 4, a S:Cu ratio of 0.5, and where redox reactions are not considered. ....	60
Figure 2.19	Thermodynamic determination of a) Zn (II) and b) Cu (I) speciation at different pH values for a 20 mM Cu (I) and Zn (II) solution with a CN:metal ratio of 4, a S:Cu ratio of 0.5, and where redox reactions are not considered. ....	63
Figure 2.20	Thermodynamic determination of a) Zn (II) and b) Cu (I) speciation at different pH values for a 20 mM Cu (I) and Zn (II) solution with a CN:metal ratio of 4, a S:Cu ratio of 1.0, and where redox reactions are not considered .....	64
Figure 2.21	Thermodynamic determination of a) CO <sub>3</sub> <sup>2-</sup> and b) Cu (I) speciation at different pH for a 20 mM Cu (I) and CO <sub>3</sub> <sup>2-</sup> solution with a CN:Cu ratio of 4, a S:Cu ratio of 0.5, and where redox reactions are not considered. ....	68

Figure 3.1	Degradation of a sulfide solution over time starting with 406 mM of sulfide. Error bars show standard deviation over 3 samples.....	74
Figure 3.2	Small reactor.....	75
Figure 3.3	Large reactor with funnel in the top section for pouring sodium sulfide solution into the reactor.....	76
Figure 3.4	Small batch reactor mixing test at 0.24 second intervals. ....	77
Figure 3.5	Schematic of reactor configuration for the small batch reactor (not to scale).....	78
Figure 3.6	Staged sulfide addition experiment procedure.....	81
Figure 3.7	Acid titration experiment procedure.....	82
Figure 3.8	Residence time experiment procedure. ....	83
Figure 4.1	Copper recovery at various pH values for a solution initially containing 31.4 mM copper with a CN:Cu ratio of 3 and S:Cu ratio of 0.5. ....	95
Figure 4.2	Copper recovery at various S:Cu ratios for a solution initially containing 29.8 mM copper with a CN:Cu ratio of 3 and pH of 5. Expected recovery is based on Equation 1.3.....	97
Figure 4.3	Copper recovery at various pH values for solutions initially containing 31.4 mM copper with varied CN:Cu ratios and S:Cu ratios of 0.5.....	98
Figure 4.4	Acid addition at various pH values for solutions initially containing 31.4 mM copper with varied CN:Cu ratios and S:Cu ratio of 0.5. ....	99
Figure 4.5	Graphical representation of factor combinations for experiments in the factorial design. ....	103
Figure 4.6	Copper recovery model when pH and S:Cu ratio are varied and CN:Cu ratio is 4.....	107

Figure 4.7	Copper recovery model when pH and CN:Cu ratio are varied and S:Cu ratio is 0.5.....	108
Figure 4.8	Copper recovery model when S:Cu ratio and CN:Cu ratio are varied and pH is 4.75. ....	108
Figure 4.9	Calculated cyanide recovery model when pH and S:Cu ratio are varied and CN:Cu ratio is 4. ....	113
Figure 4.10	Calculated cyanide recovery model when pH and CN:Cu ratio are varied and S:Cu ratio is 0.5. ....	113
Figure 4.11	Calculated cyanide recovery model when S:Cu ratio and CN:Cu ratio are varied and pH is 4.75.....	114
Figure 4.12	Acid addition per copper model when pH and S:Cu ratio are varied and CN:Cu ratio is 4. ....	117
Figure 4.13	Acid addition per copper model when pH and CN:Cu ratio are varied and S:Cu ratio is 0.5.....	117
Figure 4.14	Acid addition per copper model when S:Cu ratio and CN:Cu ratio are varied and pH is 4.75.....	118
Figure 4.15	ORP model when pH and S:Cu ratio are varied and CN:Cu ratio is 4. NB: pH axis has been reversed.....	120
Figure 4.16	ORP model when pH and CN:Cu ratio are varied and S:Cu ratio is 0.5. NB: pH axis has been reversed.....	120
Figure 4.17	ORP model when S:Cu ratio and CN:Cu ratio are varied and pH is 4.75. NB: S:Cu ratio axis has been reversed.....	121
Figure 4.18	Example profit model when pH and S:Cu ratio are varied and CN:Cu ratio = 4. Reagent and product values used are Cu– 6000 US\$/t, NaCN – 1250 US\$/t, Na <sub>2</sub> S – 1000 US\$/t, H <sub>2</sub> SO <sub>4</sub> – 250 US\$/t. Initial Cu concentration used was 1250 mg L <sup>-1</sup> .....	127
Figure 4.19	Example profit model when pH and CN:Cu ratio are varied and S:Cu ratio = 0.56. NB: CN:Cu axis has been reversed.	

	Reagent and product values used are Cu– 6000 US\$/t, NaCN – 1250 US\$/t, Na <sub>2</sub> S – 1000 US\$/t, H <sub>2</sub> SO <sub>4</sub> – 250 US\$/t. Initial Cu concentration used was 1250 mg L <sup>-1</sup> . .....	127
Figure 4.20	Example profit model when S:Cu ratio and CN:Cu ratio are varied and pH = 3. NB: CN:Cu ratio axis has been reversed. Reagent and product values used are Cu– 6000 US\$/t, NaCN – 1250 US\$/t, Na <sub>2</sub> S – 1000 US\$/t, H <sub>2</sub> SO <sub>4</sub> – 250 US\$/t. Initial Cu concentration used was 1250 mg L <sup>-1</sup> . .....	128
Figure 4.21	Profit (% of maximum) for different economic situations when CN:Cu is varied and S:Cu and pH are held constant at 0.56 and 4 respectively.....	130
Figure 4.22	Profit (% of maximum) for different economic situations when S:Cu is varied and CN:Cu and pH are held constant at 4 and 4 respectively.....	131
Figure 4.23	Profit (% of maximum) for different economic situations when pH is varied and CN:Cu and S:Cu are held constant at 4 and 0.56 respectively.....	133
Figure 5.1	a) Metal precipitation, b) sulfide consumption, and c) acid addition when changing the pH from 10 to 3 on a solution containing: 18.0 mM Cu, 8.0 mM Ag, CN:metal ratio of 4, and a S:Cu ratio of 0.5.....	140
Figure 5.2	a) Metal precipitation, b) sulfide consumption, and c) acid addition when changing the pH from 10 to 3 on a solution containing: 16.2 mM Cu, 8.2 mM Ag, CN:metal ratio of 4, and a S:Cu ratio of 1.0.....	142
Figure 5.3	a) Metal precipitation, b) sulfide consumption, and c) acid addition when changing the pH from 10 to 3 on a solution	

	containing: 18.1 mM Cu, 1.7 mM Au, CN:metal ratio of 4, and a S:Cu ratio of 0.5.....	145
Figure 5.4	a) Metal precipitation, b) sulfide consumption, and c) acid addition when changing the pH from 10 to 3 on a solution containing: 17.7 mM Cu, 1.8 mM Au, CN:metal ratio of 4, and a S:Cu ratio of 1.0.....	147
Figure 5.5	a) Metal precipitation, b) sulfide consumption, and c) acid addition when changing the pH from 10 to 3 on a solution containing: 18.3 mM Cu, 9.1 mM Fe(II), CN:metal ratio of 4 for Cu and 6 for Fe, and a S:Cu ratio of 0.5.....	150
Figure 5.6	a) Metal precipitation, b) sulfide consumption, and c) acid addition when changing the pH from 10 to 3 on a solution containing: 15.6 mM Cu, 7.9 mM Fe(II), CN:metal ratio of 4 for Cu and 6 for Fe, and a S:Cu ratio of 1.0.....	151
Figure 5.7	a) Metal precipitation, b) sulfide consumption, and c) acid addition when changing the pH from 10 to 3 on a solution containing: 18.2 mM Cu, 9.2 mM Fe(III), CN:metal ratio of 4 for Cu and 6 for Fe, and a S:Cu ratio of 0.5.....	153
Figure 5.8	a) Metal precipitation, b) sulfide consumption, and c) acid addition when changing the pH from 10 to 3 on a solution containing: 17.1 mM Cu, 10.0 mM Fe, CN:metal ratio of 4 for Cu and 6 for Fe, and a S:Cu ratio of 1.0.....	155
Figure 5.9	a) Metal precipitation, b) sulfide consumption, and c) acid addition when changing the pH from 10 to 3 on a solution containing: 18.1 mM Cu, 8.6 mM Ni, CN:metal ratio of 4, and a S:Cu ratio of 0.5.....	157

Figure 5.10	a) Metal precipitation, b) sulfide consumption, and c) acid addition when changing the pH from 10 to 3 on a solution containing: 16.9 mM Cu, 8.8 mM Ni, CN:metal ratio of 4, and a S:Cu ratio of 1.0.....	158
Figure 5.11	a) Metal precipitation, b) sulfide consumption, and c) acid addition when changing the pH from 10 to 3 on a solution containing: 15.7 mM Cu, 9.4 mM Zn, CN:metal ratio of 4, and a S:Cu ratio of 0.5.....	160
Figure 5.12	a) Metal precipitation, b) sulfide consumption, and c) acid addition when changing the pH from 10 to 3 on a solution containing: 15.7 mM Cu, 9.5 mM Zn, CN:metal ratio of 4, and a S:Cu ratio of 1.0.....	162
Figure 5.13	a) Species precipitation, b) sulfide consumption, and c) acid addition when changing the pH from 10 to 3 on a solution containing: 14.3 mM Cu, 8.1 mM SCN <sup>-</sup> , CN:metal ratio of 4, and a S:Cu ratio of 0.5.....	164
Figure 5.14	a) Species precipitation, b) sulfide consumption, and c) acid addition when changing the pH from 10 to 3 on a solution containing: 14.3 mM Cu, 8.3 mM S <sub>2</sub> O <sub>3</sub> <sup>2-</sup> , CN:metal ratio of 4, and a S:Cu ratio of 0.5.....	166
Figure 5.15	a) Species precipitation, b) sulfide consumption, and c) acid addition when changing the pH from 10 to 3 on a solution containing: 15.3 mM Cu, 2 M Cl <sup>-</sup> , CN:metal ratio of 4, and a S:Cu ratio of 0.5.....	168
Figure 5.16	Metal precipitation when changing the pH from 10 to 2 for a solution containing 12.8 mM Cu, 8.2 mM Fe, 7.1 mM Ni, 8.9 mM Zn, 8.1 mM Ag, 1.8 mM Au, CN:metal ratio of 6 for Fe and 4 for all other metals, and no sulfide addition. ....	171

Figure 5.17	Metal precipitation when changing the pH from 10 to 2 for a solution containing 14.8 mM Cu, 8.0 mM Fe, 6.8 mM Ni, 7.2 mM Zn, 7.5 mM Ag, 1.6 mM Au, CN:metal ratio of 6 for Fe and 4 for all other metals, and an initial S concentration of 6.7 mM. ....	173
Figure 5.18	Metal precipitation when changing the pH from 10 to 2 for a solution containing 14.7 mM Cu, 7.9 mM Fe, 6.7 mM Ni, 7.1 mM Zn, 7.4 mM Ag, 1.6 mM Au, CN:metal ratio of 6 for Fe and 4 for all other metals, and an initial S concentration of 13.3 mM. ...	176
Figure 5.19	Metal precipitation when changing the pH from 10 to 2 for a solution containing 14.5 mM Cu, 10.0 mM Fe, 8.1 mM Ni, 9.9 mM Zn, 8.8 mM Ag, 1.6 mM Au, CN:metal ratio of 6 for Fe and 4 for all other metals, and an initial S concentration of 20 mM. ....	178
Figure 5.20	Metal precipitation when changing the pH from 10 to 2 for a solution containing 14.7 mM Cu, 10.1 mM Fe, 8.2 mM Ni, 10.0 mM Zn, 8.9 mM Ag, 1.6 mM Au, CN:metal ratio of 6 for Fe and 4 for all other metals, and an initial S concentration of 26.7 mM. ....	180
Figure 6.1	a) Species concentration in solution and b) pH over time during sulfidisation for a solution initially containing 62.9 mM copper with a CN:Cu ratio of 4, S:Cu ratio of 0.6, and pH of 5.....	187
Figure 6.2	XRD pattern of a sulfidisation precipitate at time zero from a solution initially containing 15.7 mM Cu, a CN:Cu of 4, a S:Cu of 0.5, and a pH of 4.75. The precipitate was prepared for XRD using powder packing. ....	192
Figure 6.3	SEM image of a sulfidisation precipitate at time zero from a solution initially containing 15.7 mM Cu, a CN:Cu of 4, a S:Cu of 0.5, and a pH of 4.75.....	193

Figure 6.4	a) Species concentration and b) pH over time during sulfidisation for a solution initially containing 13.8 mM copper with a CN:Cu ratio of 4, S:Cu ratio of 1, and pH of 4.65.....	195
Figure 6.5	a) Species concentration and b) pH over time during sulfidisation for a solution initially containing 15.9 mM copper with a CN:Cu ratio of 4, S:Cu ratio of 0.5, and pH of 4.8.....	197
Figure 6.6	a) Species concentration and b) pH over time during sulfidisation for a solution initially containing 14.0 mM copper with a CN:Cu ratio of 4, S:Cu ratio of 0.25, and pH of 4.74.....	199
Figure 6.7	Change in copper concentration over time during sulfidisation for the screening experiment (initial solution containing 62.9 mM copper with a CN:Cu ratio of 4, S:Cu ratio of 0.6, and pH of 5) compared to the large reactor experiments (initial solutions targeting 15.7 mM copper with CN:Cu ratios of 4, initial pH of 4.75, and varied S:Cu ratios). .....	200
Figure 6.8	Change in copper concentration over time during sulfidisation for copper cyanide solutions with CN:Cu ratios of 4, S:Cu ratios of 0.5, target pH of 4.75, and different initial copper concentrations. ....	202
Figure 6.9	Reduction in copper recovery over time during sulfidisation for copper cyanide solutions with initial CN:Cu ratios of 4, S:Cu ratios of 0.5, target pH of 4.75, and with different initial copper concentrations. ....	203
Figure 6.10	Change in thiocyanate concentration over time during sulfidisation for copper cyanide solutions with initial CN:Cu ratios of 4, S:Cu ratios of 0.5, target pH of 4.75, and different initial copper concentrations.....	204

Figure 6.11	Sulfide concentration over time during sulfidisation for solutions initially containing target values of 15.7 mM copper with a CN:Cu ratio of 4, S:Cu ratio of 1.0, pH of 4.75, and different headspace gas. ....	206
Figure 6.12	a) Species concentration and b) pH over time during sulfidisation for a solution initially containing 13.3 mM copper with a CN:Cu ratio of 4, S:Cu ratio of 1, and pH of 4.41, and an oxygenated headspace. ....	208
Figure 6.13	XRD pattern of a sulfidisation precipitate after 4 hours from a solution initially containing 13.3 mM Cu, a CN:Cu of 4, a S:Cu of 1.0, and a pH of 4.41. The precipitate was prepared for XRD using powder packing. ....	210
Figure 6.14	a) Species concentration and b) pH over time during sulfidisation for a solution initially containing 15.8 mM copper with a CN:Cu ratio of 4, S:Cu ratio of 0.5, pH of 4.74, and an oxygenated headspace. ....	212
Figure 6.15	Copper concentration over time during sulfidisation for solutions initially containing target values of 15.7 mM copper with a CN:Cu ratio of 4, S:Cu ratio of 0.5, pH of 4.75, and different headspace gas. ....	214
Figure 6.16	Thiocyanate concentration over time during sulfidisation for solutions initially containing target values of 15.7 mM copper with a CN:Cu ratio of 4, S:Cu ratio of 0.5, pH of 4.75, and different headspace gas. ....	215
Figure 6.17	XRD pattern of a sulfidisation precipitate after 5 hours from a solution initially containing 14.7 mM Cu, a CN:Cu of 4, a S:Cu of 0.5, and a pH of 4.7. The precipitate was prepared for XRD using a zero background plate. ....	216

Figure 6.18	a) Species concentration and b) pH over time during sulfidisation of a solution initially containing 15.1 mM copper with a CN:Cu ratio of 4, S:Cu ratio of 0.5, pH of 2.1, and an oxygenated headspace. ....	218
Figure 6.19	XRD pattern of a sulfidisation precipitate after 4 hours from a solution initially containing 15.1 mM Cu, a CN:Cu of 4, a S:Cu of 0.5, and a pH of 2.1 in an oxygen headspace. The precipitate was prepared for XRD using a zero background plate.....	220
Figure 6.20	XRD pattern of a sulfidisation precipitate from an solution initially containing 15.7 mM Cu, a CN:Cu of 4, a S:Cu of 0.25, and a pH of 2. The precipitate was prepared for XRD using a zero background plate. ....	222
Figure 6.21	Map of sulfide, nitrogen, and copper detected with SEM on a region of precipitate from a solution initially containing 15.7 mM Cu, a CN:Cu of 4, a S:Cu of 0.25, and a pH of 2.....	223
Figure 6.22	Change in copper concentration over time during sulfidisation for solutions initially containing target values of 15.7 mM copper with S:Cu ratios of 0.5, pH of 4.75, and different CN:Cu ratios. ....	224
Figure 6.23	pH over time during sulfidisation for solutions initially containing target values of 15.7 mM copper with S:Cu ratios of 0.5, pH of 4.75, and different CN:Cu ratios. ....	225
Figure 6.24	Change in thiocyanate concentration over time during sulfidisation for solutions initially containing target values of 15.7 mM copper with S:Cu ratios of 0.5, pH of 4.75, and different CN:Cu ratios. ....	226
Figure 7.1	Telfer SART plant flow diagram indicating sample and measurement points.....	234

Figure 7.2	SART feed, sulfide, and acid addition flow rates at the beginning of the nucleation tank experiment.....	241
Figure 7.3	Change in pH over time during the nucleation tank experiment. ....	242
Figure 7.4	Solution pH over time for Telfer SART feed and Telfer sulfide at different S:Cu ratios. ....	255
Figure 7.5	Copper concentration over time for Telfer SART feed and Telfer sulfide at different S:Cu ratios. ....	256
Figure 7.6	Sulfide concentration over time for Telfer SART feed and Telfer sulfide at different S:Cu ratios. ....	257
Figure 7.7	Solution pH over time for Telfer SART feed and Telfer sulfide at an S:Cu ratio of 0.5 and with different headspace gas.....	259
Figure 7.8	Copper concentration in solution over time for Telfer SART feed and sulfide at an S:Cu ratio of 0.5 and with different headspace gas.....	260
Figure 7.9	Solution pH over time for Telfer SART feed and Telfer sulfide at an S:Cu ratio of 1.0, an initial pH of 4.5, and with different headspace gas.....	261
Figure 7.10	Copper concentration in solution over time for Telfer SART feed and Telfer sulfide at an S:Cu ratio of 1.0, an initial pH of 4.5, and with different headspace gas. ....	262
Figure 7.11	Sulfide concentration in solution over time for Telfer SART feed and Telfer sulfide at an S:Cu ratio of 1.0, an initial pH of 4.5, and with different headspace gas. ....	263
Figure 7.12	Sulfide concentration in solution over time for Telfer SART feed and sulfide at an S:Cu ratio of 1.0 with pH controlled at 4.5 and with different headspace gas. ....	264

Figure 7.13	Copper concentration in solution over time for Telfer SART feed and sulfide at an S:Cu ratio of 1.0 with pH controlled at 4.5 and with different headspace gas. ....	264
Figure 7.14	Solution pH over time for various solution mixtures at a S:Cu ratio of 0.5 and initial pH of 4.5. ....	267
Figure 7.15	Change in copper concentration over time for various solution mixtures at a S:Cu ratio of 0.5 and initial pH of 4.5. ....	268
Figure 7.16	Change in copper concentration over time for sulfidisation of a solution initially containing 33.8 mM copper solution with a CN:Cu ratio of 2.3, S:Cu ratio of 0.5, initial pH target of 4.5, and varied amounts of thiosulfate. ....	270
Figure 7.17	Change in copper concentration over time for sulfidisation of a solution initially containing 33.8 mM copper solution with a CN:Cu ratio of 2.3, S:Cu ratio of 0.5, initial pH target of 4.5, and varied amounts of thiocyanate. ....	271

## LIST OF TABLES

Table 1-1	Solubility of various copper minerals in cyanide solutions shown as percentage of mineral dissolved (Sceresini 2005).....	7
Table 1-2	Brief descriptions of various cyanide destruction processes (Environment Australia 2003).....	11
Table 3-1	Details of metal salts used in experiments.....	72
Table 3-2	HPLC elution gradient for sulfide quantification.....	88
Table 3-3	HPLC residence time, wavelength, and standard concentration for sulfide, thiocyanate, thiosulfate, copper, and iron quantification. ....	88
Table 4-1	Acid addition and copper recovery during sulfidisation for solutions (50 mL) containing varied amounts of copper with a CN:Cu ratio of 4, S:Cu ratio of 0.50, and a pH of 4.....	100
Table 4-2	Copper recovery model ANOVA. ....	107
Table 4-3	Cyanide recovery model ANOVA.....	110
Table 4-4	Calculated cyanide recovery model ANOVA.....	112
Table 4-5	Acid addition per amount of copper model ANOVA. ....	116
Table 4-6	ORP model ANOVA.....	119
Table 4-7	Value ranges of reagents and products for the sensitivity analysis of the profit model.....	126
Table 7-1	Survey one solution data for the copper sulfide thickening stage of the Telfer SART plant. The S:Cu ratio during the survey was 0.58 with a residence time of 9.2 hours.....	245
Table 7-2	Survey two solution data for the copper sulfide thickening stage of the Telfer SART plant. The S:Cu ratio during the survey was 0.66 with a residence time of 16.2 hours.....	246

Table 7-3	Survey two solids analysis for the copper sulfide thickening stage of the Telfer SART plant. The S:Cu ratio during the survey was 0.66 with a residence time of 16.2 hours.....	248
Table 7-4	Survey three solution data for the copper sulfide thickening stage of the Telfer SART plant. The S:Cu ratio during the survey was 1.52 with a residence time of 14.3 hours.....	249
Table 7-5	Survey three solids analysis for the copper sulfide thickening stage of the Telfer SART plant. The S:Cu ratio during the survey was 1.52 with a residence time of 14.3 hours.....	250
Table 8-1	S:Cu ratio, CN:Cu ratio, and pH which give the optimum value for various responses during sulfidisation of copper cyanide solutions.....	274
Table 10-1	Source of thermodynamic data.....	290
Table 10-2	Gibbs free energy data used for the Cu-CN-S-H <sub>2</sub> O system. ...	291
Table 10-3	Gibbs free energy data used for Ag species in the Ag-Cu-CN-S-H <sub>2</sub> O system. All data is from reference "a".....	292
Table 10-4	Gibbs free energy data used for Au species in the Au-Cu-CN-S-H <sub>2</sub> O system. All data is from reference "a", except Au <sub>2</sub> S which is from reference "d".....	292
Table 10-5	Gibbs free energy data used for Au-Ag species in the Au-Ag-Cu-CN-S-H <sub>2</sub> O system. All data is from reference "d".....	292
Table 10-6	Gibbs free energy data used for Fe species in the Fe-Cu-CN-S-H <sub>2</sub> O system. All data is from reference "a".....	293
Table 10-7	Gibbs free energy data used for Ni species in the Ni-Cu-CN-S-H <sub>2</sub> O system. All data is from reference "a".....	293
Table 10-8	Gibbs free energy data used for Zn species in the Zn-Cu-CN-S-H <sub>2</sub> O system. All data is from reference "a".....	294
Table 10-9	Explanatory notes for symbols used in MEDUSA.....	295

# 1 INTRODUCTION

## 1.1 Importance of gold

Gold has been a sought after metal by people for thousands of years, with its first use dating back to the Neolithic age in the Middle East (Solis, May, and Hefter 1996; Marsden and House 2006b). With its rarity, beauty, physical properties, and availability in a pure metallic state, gold has been used by many societies around the world for jewellery and as a monetary standard. For this reason, gold is often associated with wealth and prosperity. In modern times gold is also beginning to be used in a growing number of other applications due to its physical properties. These properties include corrosion resistance, ductility, malleability, heat reflectivity, and electrical and thermal conductivity. The demand for gold in 2011 is summarised in Figure 1.1.

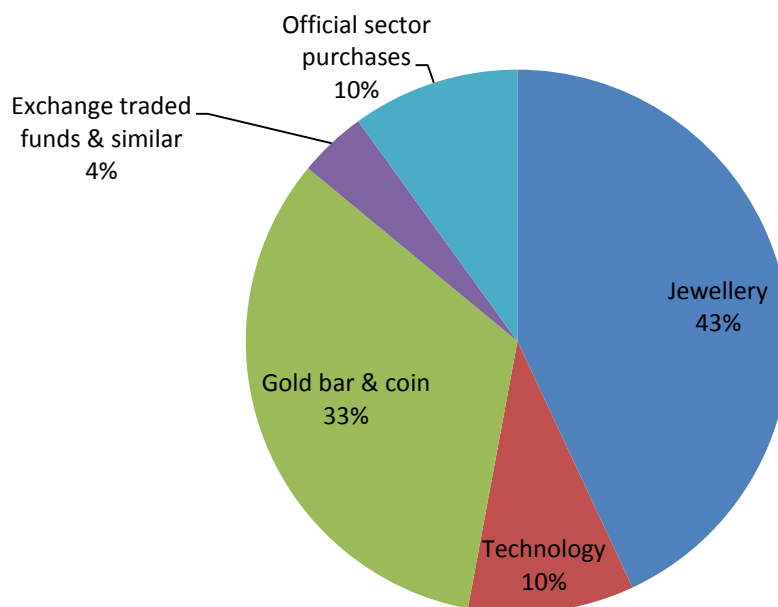
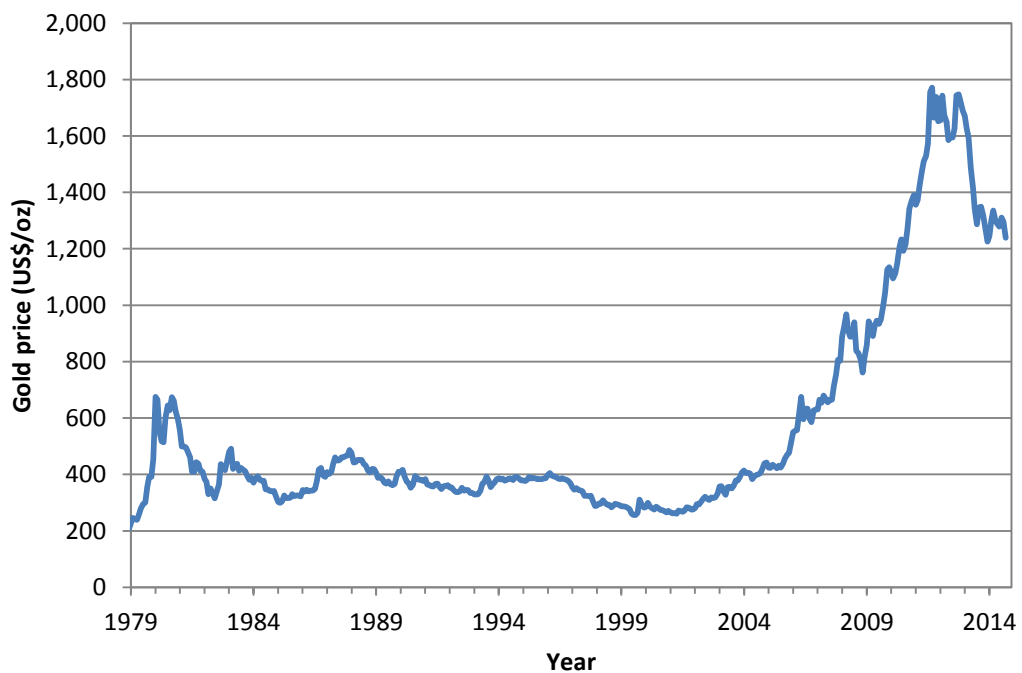


Figure 1.1 Demand for gold in 2011 (World Gold Council 2012a).

Gold is a rare metal with estimates suggesting that only approximately 166000 tonnes of gold have been ever been mined (World Gold Council 2012b). Its rarity has seen gold used as a reliable way to store value especially during times of economic uncertainty. An example of this is the late 2000's financial crisis where people began moving money from other investments to gold causing a surge in gold prices. The price of gold since 1978 is shown in Figure 1.2.



**Figure 1.2 Gold price in US dollars per ounce between 1978 and 2012 (World Gold Council 2012c)**

Australia is one of the largest producers of gold in the world, exporting 13.7 billion Australian dollars of gold in 2010 (Australian Government Bureau of Resources and Energy Economics 2012). This equates to approximately 1% of Australia's Gross Domestic Product (Australian Government Department of Foreign Affairs and Trade 2011). Gold production in Australia is second only to China.

## **1.2 Processing gold ores**

Gold is predominantly found in ores as a native metal or alloyed with silver. Other alloys and chemical compounds can also occur, but these are less common. Gold and gold alloys can occur free of other material, known as alluvial gold, or encapsulated in other minerals, known as reef gold. Gold in reef deposits is usually disseminated, with the minerals encapsulating the gold often being quartz or base metal sulfides including copper sulfides.

### ***1.2.1 History of gold processing***

Early methods of recovering gold were based on exploiting the density of gold, using gravity methods such as panning or sluicing. In these cases, the gold deposits were alluvial allowing easy separation of the gold from the host material.

Around 1400 AD amalgamation became a widespread technique for recovering gold (Marsden and House 2006b). Amalgamation involves contacting liberated gold with mercury to form an amalgam. Gold can then be recovered from the amalgam by distillation. During the 1800's, integrated processing circuits using crushing, gravity recovery, and amalgamation became common. Although amalgamation is a viable way to recover gold, it is a hazardous process due to the health risks of using mercury.

The 1800's also saw the development of chlorination to recover gold. Initially, chlorination was performed by passing chlorine gas over ore and then dissolving the formed gold chloride species in water. Further development of the process then led to the hydrometallurgical leaching of gold with chloride to form soluble  $\text{AuCl}_4^-$ . After chlorination, the solution containing gold chloride is separated from the solid residue. Gold is then

precipitated using a reducing agent such as ferrous sulfide, dihydrogen sulfide, or charcoal. If treating a sulfide ore, roasting was required before chlorination. Roasting had two effects; it converted sulfides to oxides reducing chlorine consumption and it broke down particles exposing more gold. Roasting is still used today as pre-treatment in some cyanidation processes for the same reasons.

Since this first hydrometallurgical process for extracting gold was developed, several other lixiviants have been discovered which will complex with gold. These include bromine/bromide, cyanide, thiosulfate, thiourea, iodine, and ammonia. Of these, only cyanide has seen any large scale commercial success.

### **1.2.2 Gold cyanidation**

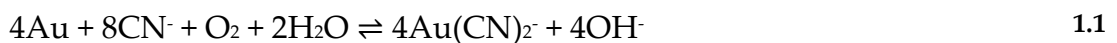
For the past century, gold has been recovered from its ores using cyanidation processes. Of these, cyanidation followed by carbon adsorption has been the dominant technique for gold recovery since the 1980's. The process stages for many gold processing operations are comminution, cyanide leaching, concentration, and recovery.

Comminution refers to crushing and grinding of ore so it is a suitable size for leaching. The main objective is to reduce the ore to particle sizes where gold is either liberated or exposed at the surfaces of the particle. This allows easy interaction between the gold and leaching agent. Usually, a balance is struck between the amount of gold liberated and the cost of crushing and grinding, as finer particle sizes are significantly more costly to produce.

As mentioned previously, roasting can be used to expose gold for leaching fine gold locked in sulfides. Roasting creates fissures in sulfide particles

allowing gold, which may have been locked inside the particle, to be exposed to cyanide. Other technologies such as pressure oxidation and biological oxidation are also used for the same effect. Generally, these methods are used because they are applicable to solid solution gold and they were cheaper than using ultra-fine grinding to expose fine gold.

During leaching the crushed ore is mixed with a dilute cyanide solution. Here, exposed gold and cyanide react to form the aurocyanide complex as per the Elsner equation (Equation 1.1). Leaching usually takes place over 24 or more hours under atmospheric conditions. The pH is maintained above 10 during leaching to maintain cyanide in the ionic form and to prevent loss of cyanide as toxic hydrogen cyanide gas.

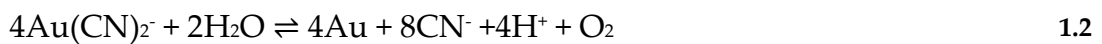


Once the gold has leached, the resulting aurocyanide complex is usually separated from the ore residue using carbon adsorption. This can occur after leaching with a process known as carbon in pulp (CIP), during leaching with a process known as carbon in leach (CIL), or after solid liquid separation in which the leachate is contacted with the carbon in column (CIC) process. While CIP was initially used to recover aurocyanide, CIL has become popular as it minimises gold loss through adsorption of aurocyanide onto certain materials found in the ore including carbonaceous and sulfide minerals (Venter, Chryssoulis, and Mulpeter 2004).

The carbon, which is now loaded with aurocyanide ions, is separated from the slurry by mechanical screening. This is possible as the carbon placed into the slurry is significantly larger than the crushed ore particles in the slurry. Gold is then eluted from the separated carbon using high cyanide

concentrations and temperatures. Once gold has been removed from the carbon, the carbon can be regenerated and reused.

The carbon adsorption and elution process creates a concentrated gold solution where gold can be recovered as metallic gold using electrowinning (Equation 1.2). Usually, this is done on steel wool cathodes where gold is either washed off of the electrodes or the electrodes are dissolved away from the gold using acid. The metallic gold is then smelted and poured into bars where it can be sent for further refining.



### **1.2.3 The impact of copper in gold cyanidation**

Copper is a problem in gold processing for a number of reasons which are all related to the fact that many copper minerals are soluble in cyanide. Copper (I) reacts with cyanide to produce a variety of copper cyanide complex species of the general form  $\text{Cu}(\text{CN})_{x-x+1}$ , where  $x$  is between one and four (Lu, Dreisinger, and Cooper 2002). Copper (II) can oxidise cyanide producing copper (I), which further reacts with cyanide, and cyanogen which in turn breaks down to cyanate. This ultimately results in increased cyanide consumption. The solubility of various copper minerals in cyanide as a percentage of mineral dissolved is shown in Table 1-1.

The copper cyanide species produced from leaching copper are then able to compete with aurocyanide species for adsorption sites on carbon. This results in lower gold recoveries and the appearance of copper in the gold product, in turn lowering the product purity. Copper cyanide, however, does not load onto activated carbon if the ratio of cyanide to copper in the complex remains high (Fleming and Nicol 1984; Dai and Breuer 2009).

**Table 1-1 Solubility of various copper minerals in cyanide solutions shown as percentage of mineral dissolved (Sceresini 2005)**

Mineral	Formula	Source A	Source B	Source C
Azurite	$2\text{Cu}(\text{CO})_3 \cdot \text{Cu}(\text{OH})_2$	94.5%	100%	91.8%
Malachite	$2\text{CuCO}_3(\text{OH})_2$	90.2%	100%	99.7%
Chalcocite	$\text{Cu}_2\text{S}$	90.2%	100%	92.6%
Covellite	$\text{CuS}$	-	-	95.6%
Native copper	$\text{Cu}$	90%	100%	96.6%
Cuprite	$\text{Cu}_2\text{O}$	85.5%	100%	96.6%
Bornite	$\text{FeS} \cdot 2\text{Cu}_2\text{S} \cdot \text{CuS}$	70%	100%	-
Enargite	$\text{Cu}_3\text{AsS}_4$	65.8%	75.1%	-
Tetrahedrite	$(\text{Cu}, \text{Fe}, \text{Ag}, \text{Zn})_{12}\text{Sb}_4\text{S}_{13}$	21.9%	43.7%	-
Chrysocolla	$\text{CuSiO}_3 \cdot n\text{H}_2\text{O}$	11.8%	15.7%	-
Chalcopyrite	$\text{CuFeS}_2$	5.6%	8.2%	-

The practice of keeping cyanide to copper ratios high reduces the impact of copper on the final gold product, but causes other difficulties in processing. Any copper cyanide species that do not adsorb onto activated carbon instead report to the processing plant's tailings (waste) storage facility. Here, copper cyanide species tend to remain stable for long periods of time (Donato et al. 2007). If the copper cyanide comes into contact with wildlife, through ingestion or absorption, it can release cyanide causing death. This is because cyanide binds to the enzymes and proteins which transport oxygen in them.

The stability of copper cyanide can result in wildlife deaths being more likely to occur on tailings storage facilities fed with copper cyanide waste compared to those fed with free cyanide waste (Donato et al. 2007). An example of this issue is the mass bird deaths at Northparkes Gold Mine in

New South Wales during 1995. This incident occurred when copper cyanide levels unexpectedly built up in the tailings storage facility resulting in the deaths of 2700 birds over a four month period (Environment Australia 2003).

The toxicity of cyanide and copper cyanide species, combined with a number of environmental incidents around the world involving cyanide use, has led to many governments enforcing regulations around the use of cyanide (Laitos 2012). Negative public perceptions of using cyanide in mining have also resulted in voluntary regulation of cyanide use through the establishment of “The International Cyanide Management Code for the Manufacture, Transport and Use of Cyanide in the Production of Gold”, commonly referred to as The Cyanide Code (International Cyanide Management Institute 2012a). As of October 2014 there were 41 mining companies, 20 cyanide producers, and 108 cyanide transporters which were signatories to The Cyanide Code (International Cyanide Management Institute 2012b).

The increased cyanide consumption and environmental issues caused by the cyanide processing of gold, without using techniques to mitigate cyanide consumption by copper, can result in the processing of gold copper ores with cyanide being unfeasible.

### **1.3 Mitigating the effect of copper in gold processing**

The processing of ores containing gold and copper varies depending on the levels of copper and gold in the ore. When there is enough copper in the ore, and the mineralogy allows it, then it may be feasible to use flotation to separate the copper from the gold. If the two are not separable, it is also possible to recover the gold as a by-product of copper smelting processes.

When these techniques are used, the environmental issues caused by copper cyanide are no longer present.

It is when copper and gold cannot be separated from each other and copper values do not warrant smelting that cyanidation of the gold copper ore must be performed. The economic and environmental issues caused by cyanide leaching of gold ores containing copper (Section 1.2.3) have the potential to make copper bearing gold ores unfeasible to process. The exhaustion of simple to process gold resources, however, has resulted in the development of numerous technologies for mitigating the adverse effects of copper. These include techniques such as suppressing copper solubility in cyanide, selectively recovering copper from gold, destroying cyanide in the waste, and recycling cyanide from the waste.

### ***1.3.1 Selective leaching of gold***

Selective leaching of gold using the ammonia-cyanide system was one of the first techniques developed to mitigate the impact of copper in gold cyanidation. Muir (2011) provides a review of the process, which has been studied for much of the last century. During ammonia-cyanide leaching, gold is oxidised by a copper ammonia complex species and gold cyanide formed while copper precipitates as  $\text{CuCN}$  or  $\text{Cu(OH)}_2$ . The gold can then be recovered from solution using activated carbon or strong base ion exchange resins. While the process is feasible, it has seen limited commercial success due to the complex chemistry and difficulty controlling the process.

### ***1.3.2 Selective leaching of copper***

The Sceresini process (Sceresini 1992) is another way of selectively separating copper and gold by recovering copper leached by cyanide before gold

recovery. The process relies on maintaining low free cyanide levels in solution, through control of cyanide addition and pH, to generate copper cyanide complexes which have low cyanide to copper molar ratios. These copper cyanide complexes are then removed from solution by carbon absorption. The low free cyanide levels during the copper leaching and absorption stage results in only a small amount of gold being leached from the ore. This in turn allows gold to be leached and recovered in a second cyanidation step.

The copper absorbed on carbon can be recovered by elution with a cold cyanide solution and then recovered from the cyanide using cyanide recycling processes such as acidification and sulfidisation, as discussed later in Section 2.1.

### **1.3.3 Cyanide destruction**

There are many processes available for cyanide destruction, with many reviews in the literature (Fleming 2001; Mudder and Botz 2001; Mudder, Botz, and Smith 2001a, Young 2001). Table 1-2 briefly describes some of the major cyanide destruction processes.

**Table 1-2 Brief descriptions of various cyanide destruction processes (Environment Australia 2003)**

<b>Technology</b>	<b>Description</b>
SO <sub>2</sub> /Air (INCO)	Oxidation with SO <sub>2</sub> /Air and a Cu catalyst
Hydrogen peroxide (Degussa)	Oxidation with H <sub>2</sub> O <sub>2</sub> and a Cu catalyst
Caro's acid	Oxidation with H <sub>2</sub> SO <sub>5</sub>
Alkaline chlorination	Oxidation with Cl <sub>2</sub> or ClO <sup>-</sup> at a pH > 11
Activated carbon	Oxidation with activated C, air, and a Cu catalyst
Biodegradation	Oxidation with bacteria
Wet air oxidation	Oxidation at high temperature and pressure

Due to its simplicity, allowing copper to leach and then destroying the copper cyanide species in the tailings stream is the primary technique used in industry to treat copper cyanide in tailings. Nevertheless, copper cyanide destruction results in not only excess costs due to increased cyanide consumption, but also additional reagent and operating costs to run the destruction process. The outcome is that, while cyanide destruction makes processing copper bearing gold ores environmentally viable, many ores remain economically unviable.

#### **1.3.4 Cyanide recycling**

Cyanide recovery technology offers the same environmental advantages as destruction technology with the additional benefit of recycling cyanide and in turn potentially reducing costs for gold producers. Cyanide recovery technology has been reviewed by several authors (Mudder, Botz, and Smith

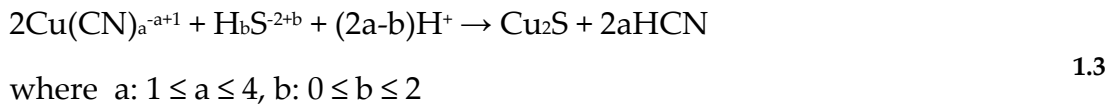
2001a; Mudder and Goldstone 2001; Fleming 2005; Marsden and House 2006c; Dai, Simons, and Breuer 2012) and comprises technology for both extracting and concentrating cyanide from slurries or solutions. These include industrially used processes such as acidification volatilisation and reneutralisation (AVR) (Botz and Mudder 1998; Gönen, Kabasakal, and Özdil 2004; Vapur et al. 2005); technology demonstrated on a pilot scale such as ion exchange and carbon adsorption processes (Fleming and Thorpe 2003; Bachiller et al. 2004; Dai, Breuer, and Jeffrey 2010); and novel processes such as liquid liquid extraction (LLX) (Dreisinger 2000), gas membranes (Han, Shen, and Wickramasinghe 2005; Shen, Han, and Wickramasinghe 2006), and bulk liquid membranes (Aydiner, Kobya, and Demirbas 2005).

The presence of copper cyanides can, however, make many of these cyanide recovery processes inefficient or unusable. This is often due to these processes inability to separate copper and cyanide from each other. Acidification and sulfidisation is one of the few ways to create this separation and provide a copper product as well as cyanide recycle.

### ***1.3.5 Copper recovery and cyanide recycling by sulfidisation***

Sulfidisation for cyanide recovery first makes an appearance in the published literature in two 1960's patents from the American Cyanamid Company (Lower 1965, 1968). The patents detail a process where cyanide is used to leach copper minerals and then the copper cyanide solution is clarified. The copper is recovered from the clarified solution by reducing the pH and adding sulfide. The reaction produces a copper sulfide precipitate releasing cyanide back into solution as aqueous hydrogen cyanide ( $\text{HCN}_{(\text{aq})}$ ). This reaction (Equation 1.3) is the cornerstone of sulfidisation technology for cyanide recovery and is referred to in the rest of this thesis as the primary sulfidisation equation. Equation 1.4 is a simplified version of the same

equation where cyanide to copper molar ratio is 3 and HS<sup>-</sup> is the sulfide source such as when using sodium hydrogen sulfide (NaSH).



In 1986, Metallgesellschaft Natural Resources (MNR) Processing Incorporated patented a process which expanded on the ideas of Lower (1968) and also integrated a silver recovery stage (Potter, Bergmann, and Haidlen 1986). The process became known as the MNR process after the name of the developing company. Like the work of Lower (1968), the MNR process was never commercially adopted.

In the 1990's, a paper was published by MacPhail, Fleming, and Sarbutt (1998) detailing a process called SART. The name SART stands for sulfidisation, acidification, recycle, and thickening which describes the major steps involved in the process. SART has since become the most common technique for separation of copper and cyanide from each other on an industrial scale.

For most SART installations, a clarified tailings stream containing copper cyanide is mixed in a pipe with a sulfide source, sulfuric acid, and seed recycled from within the process. In most cases sodium sulfide (Na<sub>2</sub>S) or sodium hydrogen sulfide (NaSH) are used as the sulfide source, although the use of biologically produced dihydrogen sulfide gas (H<sub>2</sub>S) has been proposed (Adams, Lawrence, and Bratty 2008; Marchant 2008).

Once the clarified copper cyanide solution is mixed with sulfide and acid, the primary sulfidisation reaction (Equation 1.3) occurs rapidly. The resultant slurry is then fed to a nucleation tank to allow precipitate size growth. After nucleation, the slurry is thickened and filtered to separate the chalcocite (Cu<sub>2</sub>S) from the aqueous hydrogen cyanide solution. Thickening is one major area where the SART process differs from the MNR process. As there is no thickening stage in the MNR process, the process requires filtration of slurries with very low percent solids (0.5 %). Thickening to 10 to 15 % solids in SART results in a significant decrease in slurry volume and, hence, a reduction in the filter equipment size requirement (MacPhail, Fleming, and Sarbutt 1998). The SART process also uses some of the thickened slurry as seed during precipitation, promoting crystal growth.

The aqueous hydrogen cyanide solution produced is then re-neutralised, often with lime, converting aqueous hydrogen cyanide back to cyanide (Equation 1.5). Generally, this whole system is covered and kept under a slight negative pressure to prevent the release of hydrogen cyanide gas. A generic SART flowsheet is shown in Figure 1.3.



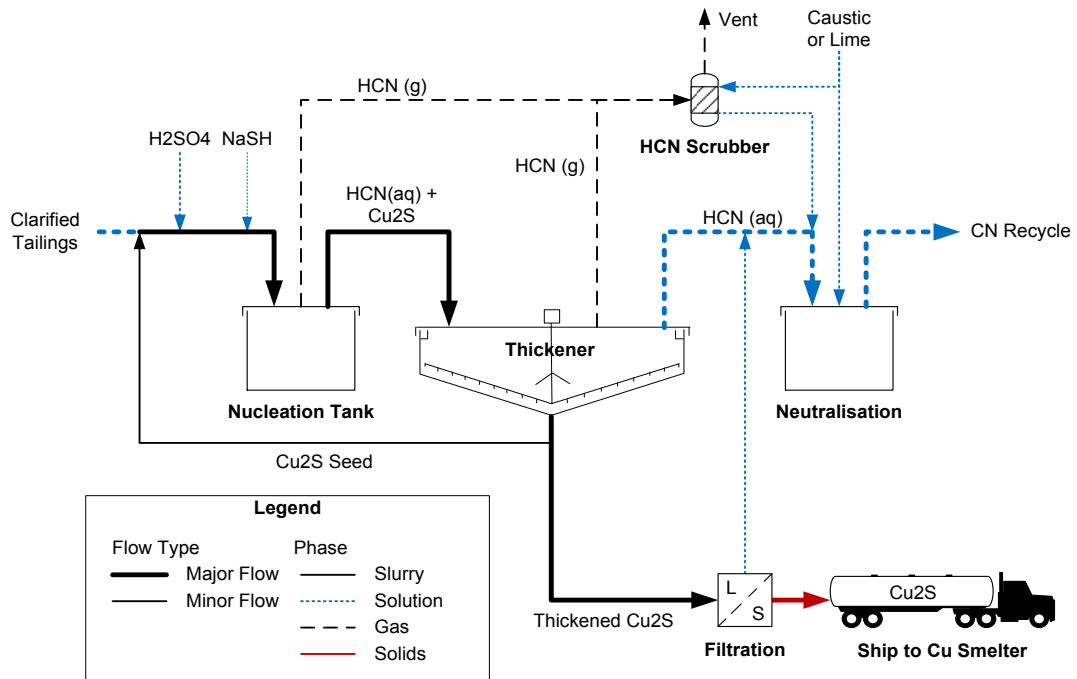


Figure 1.3 Generic SART flowsheet

The results of most bench scale (e.g. MacPhail, Fleming, and Sarbutt 1998; Barter et al. 2001; Dreisinger et al. 2008; Ford, Fleming, and Henderson 2008) and pilot plant (e.g. MacPhail, Fleming, and Sarbutt 1998; Botz and Acar 2007) studies of the SART process have shown that the technique can separate and recover more than 90% of copper and cyanide. This does not include cyanide that is oxidised or has reacted with a strongly complexing metal such as iron. In every case, a ratio of around 0.5 to 0.6 stoichiometric sulfide to copper addition yielded a precipitate which analysed as being close to chalcocite ( $\text{Cu}_2\text{S}$ ) (Lower 1965, 1968; Potter, Bergmann, and Haidlen 1986; Fleming and Trang 1998; MacPhail, Fleming, and Sarbutt 1998; Dreisinger et al. 2008). Operational data from Newmont Mining Corporation's Yanacocha Gold Mill in Peru shows, however, that SART will mainly produce other products such as covellite ( $\text{CuS}$ ) and digenite ( $\text{Cu}_{1.8}\text{S}$ ) (Guzman et al. 2010). Sulfide additions can also be much larger than expected (Equation 1.3) and difficult to control (Botz and Acar 2007; Guzman

et al. 2010). Similar problems have been experienced at Newcrest Mining Limited's Telfer Gold Mine (Turton-White, personal communication, 2010). Such issues have not been reported in any bench or pilot studies of the process.

Apart from copper, SART may also be useful in the separation of other metals which are complexed with cyanide. There is an understanding that silver and zinc precipitate at a higher pH than copper and that this could allow for a selective precipitation process to be established (Potter, Bergmann, and Haidlen 1986; Dymov, Ferron, and Fleming 1997; Milosavljevic, Solujic, and Kravetz 2004). Nevertheless, separation efficiency and required pH ranges are not well defined.

Sulfidisation has the ability to create a recyclable cyanide solution, reducing costs and producing a saleable copper product. This combination allows the sulfidisation processes, such as SART, to unlock the value from copper gold ores that were previously uneconomic to be processed with cyanidation. In addition, it has considerable environmental advantages. Nonetheless, there are problems with this process surrounding high sulfide consumption and low precipitate grade. Also, the response of other species in solution during sulfidisation is largely unexplored. This thesis will therefore focus on developing a fundamental understanding of sulfidisation for cyanide and copper recovery.

#### **1.4 Objectives**

The unexpected problems encountered when using sulfidisation processes such as SART on an industrial scale highlight a requirement for better fundamental understanding of sulfidisation chemistry. An improved fundamental understanding of the process could then lead to reduced

reagent consumptions, higher precipitate grades, and selective metal recovery during sulfidisation. Hence, the overall objective of this research is to develop a better fundamental understanding of the chemistry which occurs in the sulfidisation process. This understanding could then be used to improve sulfidisation and make the process more efficient. The specific objectives of the research are:

- 1) To create a model of sulfidisation that shows the optimum operational values for the process;
- 2) To gain an understanding of how other species in the tailings respond to and affect sulfidisation including other metals and anionic species formed during gold leaching;
- 3) To deduce selective precipitation scenarios between different metals found in gold tailings; and
- 4) To determine the cause of high sulfide consumption and low precipitate grades seen in the SART process and verify this cause at an industrial scale.

## **1.5 Thesis structure**

This thesis is divided into the following chapters:

Chapter 2 discusses the state of the art in sulfidisation for cyanide and copper recovery from gold tailings.

Chapter 3 shows the experimental methods and analytical techniques used during this study.

Chapter 4 details the building of a fundamental model of sulfidisation and

- shows the process optima through economic sensitivity analysis.
- Chapter 5 shows how various impurities impact sulfidisation and their ability to be selectively recovered.
- Chapter 6 explores the impact of residence time on sulfidisation at the laboratory scale and shows how this could be the cause of high sulfide consumption experienced at industrial sulfidisation processes.
- Chapter 7 shows the result of industrial scale studies which verify that long residence time is the cause of performance issues in sulfidisation at the industrial scale.
- Chapter 8 provides conclusions and recommendations for further research.

## **2 MINIMISING THE IMPACT OF COPPER IN GOLD CYANIDATION**

### **2.1 Thermodynamic modelling**

Thermodynamic modelling is used during this chapter to help verify and understand concepts presented in the literature. Diagrams were generated using the thermodynamic packages HSC Chemistry 7 (Roine et al. 2012) and MEDUSA (Puigdomenech 2010). HSC Chemistry 7 was used for the generation of potential-pH diagrams with MEDUSA being used for the generation of simple speciation diagrams that do not consider redox reactions. The algorithms behind the operation of the two programs can be found in their respective software documentation.

As the thermodynamic database in HSC Chemistry 7 was found to be more comprehensive than the MEDUSA database, it was selected as the main database for the modelling. Gibbs free energy data for some species were adjusted in the database based on a literature search of metal cyanide and metal sulfide species. The Gibbs free energy data and sources used for the data are shown in the Appendices (Section 10.1).

### **2.2 Comparison of technology for separating copper and cyanide**

While there are many proposed techniques to recycle cyanide on an industrial scale, there are only limited methods to separate cyanide and copper from each other. All processes proposed to date for this purpose (detailed in this section) are based on the concept that cyanide has a reduced affinity to form complex species with copper under acidic conditions. This is due to the protonation of cyanide at low pH to form hydrogen cyanide via Equation 2.1. The protonation of cyanide as the pH is decreased reduces the cyanide ion concentration in solution. Hence, the cyanide in copper cyanide complexes is released via the reverse of Equation 2.2, 2.3, 2.4, and 2.5.



A potential-pH diagram of the copper cyanide water system, with a copper concentration of 20 mM and a cyanide to copper molar ratio (CN:Cu ratio) of 4, is shown in Figure 2.1. Due to the ability for cyanide to oxidise to cyanate, there are no regions where copper cyanide species are predominant within the region where H<sub>2</sub>O is stable, except for a small region of CuCN predominance at low pH and potential. Nevertheless, oxidation of cyanide to cyanate is not expected in most cyanide recycling processes, because reaction kinetics are slow without the presence of strong oxidants or a catalyst, as is required in cyanide destruction processes (Section 1.3.3). Due to this, Figure 2.1 does not give an accurate representation of the copper cyanide system as usually observed in cyanide recovery processes. Hence, a metastable potential-pH diagram of the same system was generated (Figure 2.2), where cyanate and hydrogen cyanate are not considered. Here the effect of pH on the formation of copper cyanide species is apparent. A more detailed thermodynamic study of the copper cyanide system is shown in Lu, Dreisinger, and Cooper (2002).

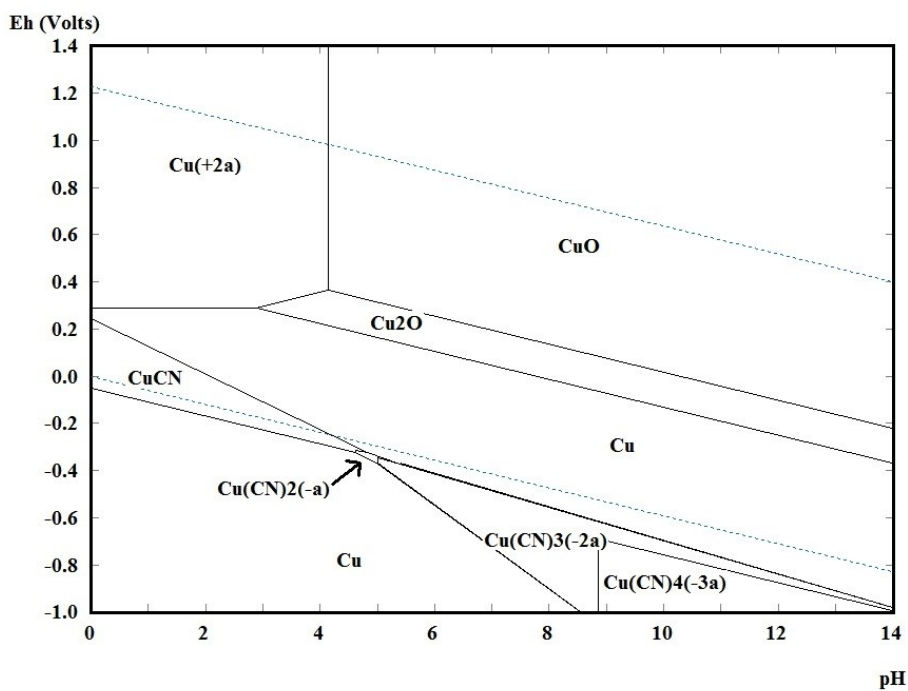


Figure 2.1 Potential-pH diagram of Cu speciation in the Cu-CN-H<sub>2</sub>O system for a 20 mM Cu solution with a CN:Cu ratio of 4. "a" indicates soluble species.

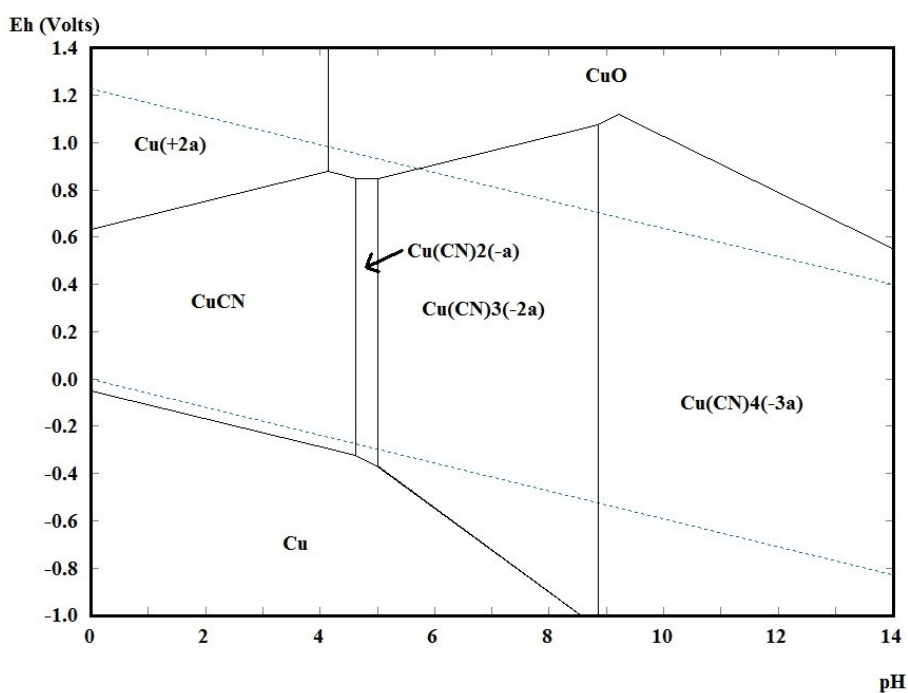
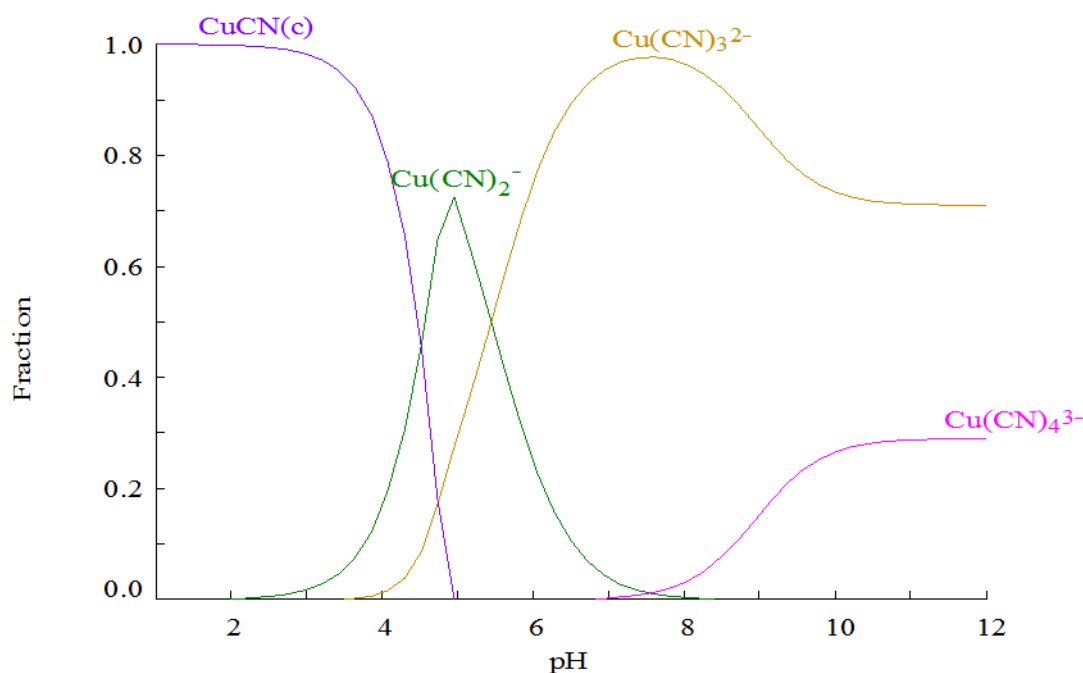


Figure 2.2 Potential-pH diagram of Cu speciation in the Cu-CN-H<sub>2</sub>O system for a 20 mM Cu solution with a CN:Cu ratio of 4, where CNO<sup>-</sup> and HCNO<sub>(aq)</sub> are not considered. "a" indicates soluble species.

It is apparent from Figure 2.2 that a sufficiently low pH ultimately results in the formation of a copper cyanide precipitate ( $\text{CuCN}$ ) by combination of Equation 2.1 and the reverse of Equation 2.3. Thus, in this situation some cyanide remains bound with the precipitated copper.

While the potential-pH diagram shows the region where a copper cyanide precipitate is the predominant species, the diagram does not clearly indicate how much cyanide is liberated from copper at a given pH. Figure 2.3 shows a simple speciation diagram for copper in a 20 mM copper solution with a cyanide to copper molar ratio (CN:Cu ratio) of 4. As there is no oxidation of cyanide, all cyanide not attached to copper is liberated as cyanide ions or aqueous hydrogen cyanide. Figure 2.3 shows that the optimum pH for formation of copper cyanide is below 4 in the system shown.



**Figure 2.3 Thermodynamic determination of Cu (I) speciation at different pH values for a 20 mM Cu (I) solution with a CN:Cu ratio of 4 and where redox reactions are not considered.**

Other precipitates can also form during acidification depending on the solution composition including, but not limited to, copper thiocyanate (CuSCN) and copper iron cyanide double salts ( $\text{Cu}_{(y+6)^x}[\text{Fe}^y(\text{CN})_6]_x$  where  $x: x = 1, 2$   $y: y = 2, 3$ ). The reactions for the formation of these species are discussed in more detail in Section 2.4. The formation of copper thiocyanate and copper iron cyanide double salts is often preferable in cyanide recovery processes based on acidification only. This is due to the cyanide in iron cyanide species ( $\text{Fe}(\text{CN})_6^{3-}$  and  $\text{Fe}(\text{CN})_6^{4-}$ ) and thiocyanate ( $\text{SCN}^-$ ) being strongly bonded and therefore considered unrecoverable. Hence, no loss in recoverable cyanide occurs from the formation of copper iron cyanide salts and copper thiocyanate in the precipitate. For a process using acidification only, the formation of a copper cyanide precipitate is unavoidable, as it is unlikely that there is enough iron and thiocyanate in solution to prevent its formation.

Due to their fundamental requirement for acidification, a potential problem with all technologies for separating copper and cyanide is a build-up of gypsum in the process. This is caused by the use of sulfuric acid in solutions with large amounts of calcium. Additional gypsum precipitation can also occur after neutralisation if lime is used (Riveros, Molnar, and Basa 1996; Barter et al. 2001). If a solution which has undergone acidification and neutralisation is required to be used in the processing plant, scale formation in the plant can be limited through the use of a gypsum thickener. Prevention of scale is also possible through the use of other acids but these are often more expensive and can cause additional problems such as corrosion.

### **2.2.1 Direct recycle**

Weak acid dissociable (WAD) cyanide comprises the cyanide ion, aqueous hydrogen cyanide, and complexed cyanide that will be released in an acid of pH 4 to 4.5. One of the simplest techniques to recover cyanide from WAD cyanide species is to clarify the tailings solution, acidify it, separate out any precipitates, reneutralise the solution, and finally recycle the cyanide rich solution. Alonso-González, Nava-Alonso, and Uribe-Salas (2009) showed that, for a group of solutions with copper concentrations ranging from 264 to 730 mg L<sup>-1</sup> and cyanide concentrations ranging from 375 to 2700 mg L<sup>-1</sup>, greater than 90% of copper is recovered at a pH of 2.5. Cyanide recovery was greater than 80% for three of the solutions with one solution only reporting a recovery of 66%. The authors do not discuss why this occurred, but is likely related to a low initial cyanide to copper molar ratio of the solution resulting in a comparatively large loss of cyanide due to the formation of a copper cyanide (CuCN) precipitate.

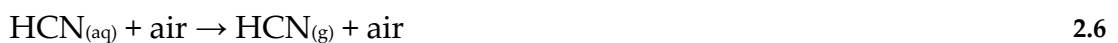
A study by Riveros, Molnar, and Basa (1996) reported that sedimentation problems occurred with the precipitates produced by an acidification and direct recycle process. Flocculation was found to increase the settling rate but did not help to compact the solids once settled. The work ultimately recommended that filtration would be the preferred method of solids separation from the acidified solution. This may be hazardous due to the requirements to filter large volumes of solutions containing aqueous hydrogen cyanide.

Once separated, the hydrogen cyanide rich solution is neutralised and sent back to leaching. The drawback of doing this is that the cyanide is not concentrated. This results in a positive water balance in operations where the tailings are washed using counter current decantation (CCD) to obtain the

clarified liquor for acidification. Ultimately, an amount of cyanide rich solution would need to exit the circuit and go to tailings. This would not be an issue in a heap leach operation where clarification may not be required or if the excess water from a milling operation was able to be used in a heap leach. Alternatively, concentration after solid liquid separation could be performed using volatilisation (Section 2.2.2), liquid-liquid extraction (Dreisinger 2000), or membrane technology (Aydiner, Kobya, and Demirbas 2005; Han, Shen, and Wickramasinghe 2005; Shen, Han, and Wickramasinghe 2006). Volatilisation during precipitation is also possible as discussed below.

### **2.2.2 Volatilisation**

Volatilisation processes take advantage of the volatility of hydrogen cyanide (HCN). They work by bubbling air through acidified cyanide solution to remove hydrogen cyanide gas via Equation 2.6. The hydrogen cyanide gas is then adsorbed into an alkaline solution, usually lime (Equation 2.7). Hence, cyanide is both separated from the solution and concentrated, potentially up to the solubility limit of the cyanide salt formed.



The reactions leading to the formation of hydrogen cyanide are rapid, with volatilisation being the rate limiting step in the process (Fleming and Trang 1998; MacPhail, Fleming, and Sarbutt 1998). Increasing the rate of hydrogen cyanide volatilisation is a high energy process due to the large volumes of air required (Riveros, Molnar, and McNamara 1993; Riveros, Molnar, and Basa

1996). This problem is further exacerbated when low residual cyanide concentrations ( $<1 \text{ mg L}^{-1}$ ) are required.

To help overcome the slow kinetics of volatilisation and reduce energy consumption, packed towers can be used to break up and reduce the size of air bubbles passing through the solution during volatilisation. The reduction of air bubble size, in turn, increases the surface area for diffusion of hydrogen cyanide from the liquid to gas phase. The Cyanide Recovery Process (CRP) and the Cyanisorb process are both based on this concept.

In addition to better reactor design, process variables have been shown to have varying effects on the volatilisation of HCN. Several authors (Vapur et al. 2005; Alonso-González, Nava-Alonso, and Uribe-Salas 2009) have shown that the volatilisation time required can be reduced by using increased air flow rates. It has also been reported that lowering pH can reduce volatilisation time of hydrogen cyanide generated from free and WAD cyanide species (Gönen, Kabasakal, and Özdil 2004). The same work showed a 40 % increase in cyanide recovery when the temperature is raised from 15 °C to 25 °C. Vapur et al. (2005) reported, however, only a 3 to 4 % increase in cyanide recovery when temperature is changed from 10 °C to 30 °C. These two studies differed mainly in the use of a packed column by Vapur et al. (2005) which facilitates air bubble size reduction in the same way a packed tower does on an industrial scale. The difference in results when temperature is varied shows that the interaction of variables during volatilisation is complex.

Volatilisation processes can be used for the treatment of solutions or slurries. The processing of slurries is more difficult with volatilisation from a pulp requiring a significantly longer residence time to remove the hydrogen

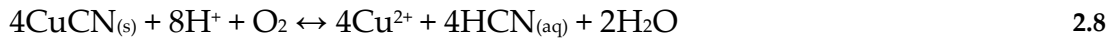
cyanide compared to from a solution. Fleming and Trang (1998) found that the cyanide recovered in 120 minutes from the volatilisation stage reduced from 96.5 % for a solution to 54 % for a pulp. Vapur et al. (2005) achieved 97.3 % recovery of cyanide from a pulp in 90 minutes using a packed column, again highlighting the importance of the gas/slurry or gas/solution contact. A limitation reported in all studies with slurries is increased acid consumption due to acid consuming constituents in the solids.

If copper cyanide species are present during volatilisation, copper will precipitate as copper cyanide. When processing a solution, the copper cyanide generated can be recovered using thickening or filtration after volatilisation of cyanide. When processing a slurry, however, the precipitated copper cyanide is not separable from the rest of the slurry creating an environmental risk when the slurry is sent to tailings storage. Ultimately, while volatilisation is a useful process for generating concentrated cyanide solutions, the presence of copper may limit the use of volatilisation processes to solutions only.

### **2.2.3 Copper cyanide digestion**

Copper and cyanide in copper cyanide precipitates generated during acidification processes can be separated from each other using digestion techniques. Sceresini and Richardson (1991) propose a digestion method as part of the Sceresini Process. The technique releases hydrogen cyanide and oxidises copper to give copper (II) ions according to Equation 2.8. The copper cyanide precipitate is filtered and thoroughly washed to achieve a very low chloride level prior to the digestion with sulphuric acid and oxygen at about 75 °C for approximately eight hours. The produced copper sulfate solution can be used for direct sale or for producing copper cathode via

electrowinning. The hydrogen cyanide gas liberated during digestion is scrubbed by lime and recycled.



This technique has been used at Mt Gibson for treating copper cyanide precipitates generated from the Sceresini process. Sceresini (2005), however, stated that while the process is effective, a sulfidisation technique was more effective for maximising cyanide recovery (Section 2.2.4). In addition, the digestion process mentioned does not detail how copper thiocyanate and copper iron cyanide double salts react during digestion, as these species are not present in the Sceresini process precipitate.

CANMET proposed thermal decomposition under reducing conditions to release cyanide species from copper iron cyanide double salts (Riveros, Molnar, and McNamara 1993). Specific details of the process, however, are not mentioned and the limitation of the technique to copper iron cyanide double salts is likely to make this process not applicable for most gold processing operations.

#### **2.2.4 Sulfidisation**

The basis of sulfide precipitation for cyanide recovery is that, at low pH and in the presence of sulfide, copper precipitates as a copper sulfide releasing cyanide into solution as aqueous hydrogen cyanide (Equation 1.3). It is generally reported in the literature (e.g. Lower 1968; Potter, Bergmann, and Haidlen 1986; MacPhail, Fleming, and Sarbutt 1998) that the precipitation of copper and release of cyanide is rapid and goes to near completion with stoichiometric sulfide addition at a pH of approximately five or less. This gives sulfidisation processes several advantages over acidification only

processes such as increased cyanide recovery and a precipitate which is less difficult to filter (Fleming 2005). Further, MacPhail, Fleming, and Sarbutt (1998) show that acid consumption can be less in sulfidisation compared to volatilisation if sulfide is added as a protonated species (NaHS). Acid consumption would be further reduced if dihydrogen sulfide gas was used (Adams, Lawrence, and Bratty 2008). The addition of dihydrogen sulfide gas, however, may add additional complexities to the process, which is discussed further in (Section 2.3.5). It should be noted here that while sulfide can be added in many ways, the low pH used in sulfidisation will result in the majority of sulfide being present as aqueous dihydrogen sulfide (H<sub>2</sub>S) (Section 2.3.1).

A major disadvantage of sulfidisation technology is that the cyanide is not concentrated. This creates the same positive water balance issue as processes using precipitation followed by direct recycle (Section 2.1.1). In addition, as cyanide is not separated from other aqueous species after SART is performed, thiocyanate and iron cyanides can build up in the circuit (Fleming and Trang 1998; MacPhail, Fleming, and Sarbutt 1998). Bleeding an amount of excess solution to a heap leach or using concentration techniques such as volatilisation, LLX, or membrane technology could potentially solve the water balance issue. Such techniques have been proposed for some SART plants including in the original designs for Newcrest Mining Limited's Telfer Gold Mine (Goulsbra et al. 2003) and tested in piloting work for Newmont's Yanacocha Project (Botz and Acar 2007). It also forms a part of a proposed cyanide recycling process called tailings washing and pond stripping (WPS) (Adams and Lloyd 2008).

As sulfidisation is the focus of this research, an in depth review of the literature surrounding sulfidisation processes for cyanide and copper recovery is presented for the remainder of the chapter.

### **2.3 Factors impacting copper-cyanide-sulfide chemistry**

Although sulfidisation processes are used industrially, little information is available in the literature around the optimum conditions to operate such processes. Generally, pH (Section 2.3.2) and sulfide to copper ratio (Section 2.3.3) have been the focus in sulfidisation experiments and piloting. This is presumably because these process variables are adjustable in a sulfidisation process like SART, whereas other process variables like copper and cyanide concentration are dictated by conditions during gold leaching.

Nevertheless the impact of other variables, such as copper and cyanide concentration, may be important when considering the economic viability of cyanide recycling using sulfidisation. Important factors affecting sulfidisation are reviewed in this section. Thermodynamic modelling (Section 2.1) has also been used where possible to aid in assessing the impact of these factors.

#### **2.3.1 The sulfide system**

Before considering the copper-cyanide-sulfide system it is important to show the speciation of sulfide species without copper and cyanide present. A potential-pH diagram of the sulfide system where the concentration of sulfide is 10 mM is shown in Figure 2.4. It is apparent from Figure 2.4 that the oxidation of sulfide causes sulfate and hydrogen sulfate to be the most predominant species at most pH values and potentials.

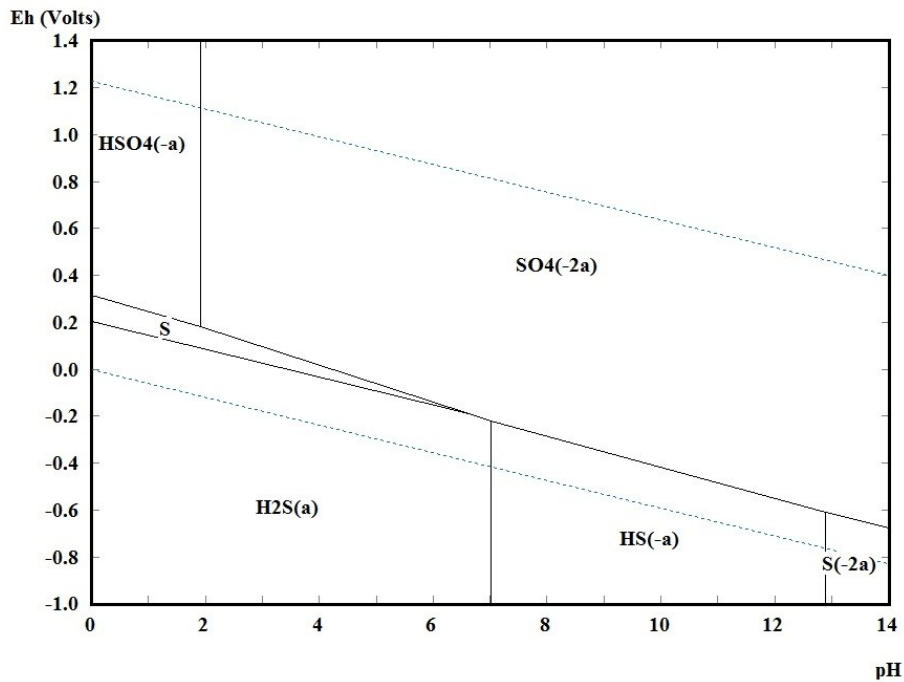


Figure 2.4 Potential-pH diagram of S speciation in the S-H<sub>2</sub>O system for a 10 mM S solution. "a" indicates soluble species.

While the formation of sulfate species is the ultimate oxidation state of the sulfide system, the rate at which sulfide oxidises to sulfate is slow without the presence of a catalyst (Paul 1984). For that reason the analysis of a simple sulfide system that does not consider oxidation is useful for this study. Figure 2.5 shows a simple speciation diagram of the sulfide system where sulfide concentration is 10 mM. From Figure 2.5 it is clear that sulfide forms either dihydrogen sulfide, hydrogen sulfide, or sulfide depending on pH.

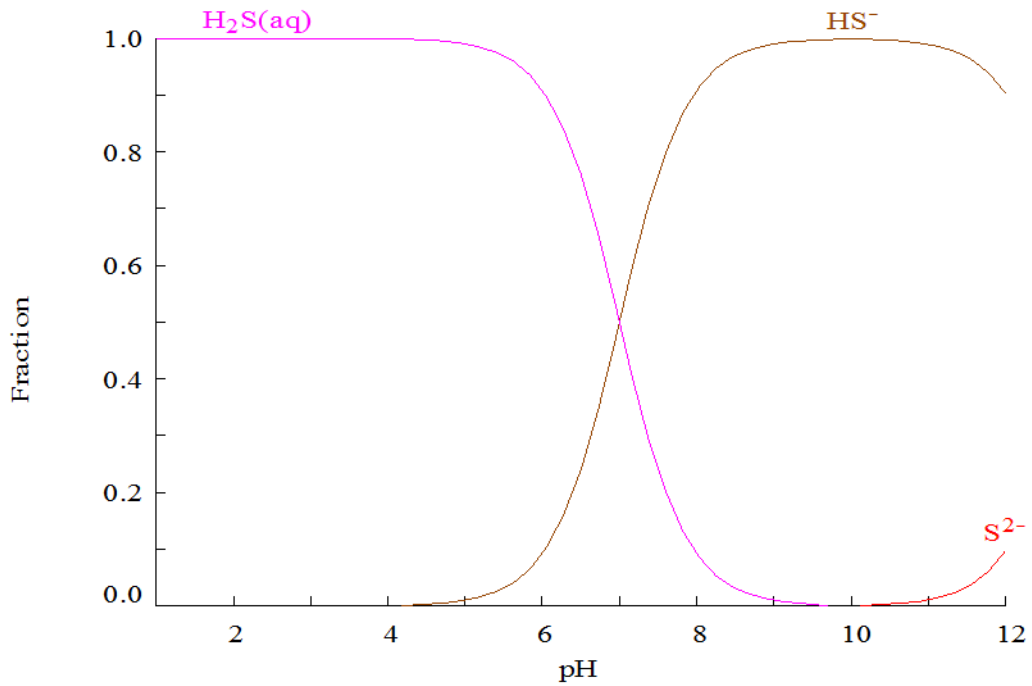


Figure 2.5 Thermodynamic determination of S speciation at different pH values for a 10 mM S solution where redox reactions are not considered.

### 2.3.2 Effect of pH

Little to no recovery of cyanide and copper occurs at high pH values when sulfide is added to copper cyanide solutions. The initial patents (Lower 1965, 1968) describing sulfidisation state that a pH of less than 5 is sufficient for high recoveries of copper and cyanide. The MNR process later suggested lower pH values of around 1.5 are required (Potter, Bergmann, and Haidlen 1986). Initial work on the SART process was done at the slightly higher pH value of 3 (MacPhail, Fleming, and Sarbutt 1998). None of the early work on the topic states the reasoning for the selection of the various pH values used.

More recent work on sulfidisation has seen pH values between the range of 4 and 5 being recommended for the SART process on an industrial scale (Barter et al. 2001; Botz and Acar 2007; Dreisinger et al. 2008; Ford, Fleming, and Henderson 2008; Guzman et al. 2010). The recent trend of selecting pH

between 4 and 5 is due to reduced acid and base consumption compared to lower pH values, while still achieving high cyanide and copper recoveries (Barter et al. 2001; Botz and Acar 2007).

Figure 2.6 shows a potential-pH diagram of the copper cyanide sulfide water system with a copper concentration of 20 mM, a cyanide to copper molar ratio (CN:Cu ratio) of 4, and a sulfide to copper molar ratio (S:Cu ratio) of 0.5. In the pH range where sulfidisation is commonly operated (4 to 5), Figure 2.6 shows that a variety of species can form depending on the potential of the system. As seen with Figure 2.1, this diagram does not show any stable copper cyanide species within the stability region for water because it considers the oxidation of cyanide to cyanate. As oxidation of cyanide is unlikely to occur during sulfidisation (Section 2.2), a metastable potential-pH diagram was generated where cyanide oxidation is not considered (Figure 2.7).

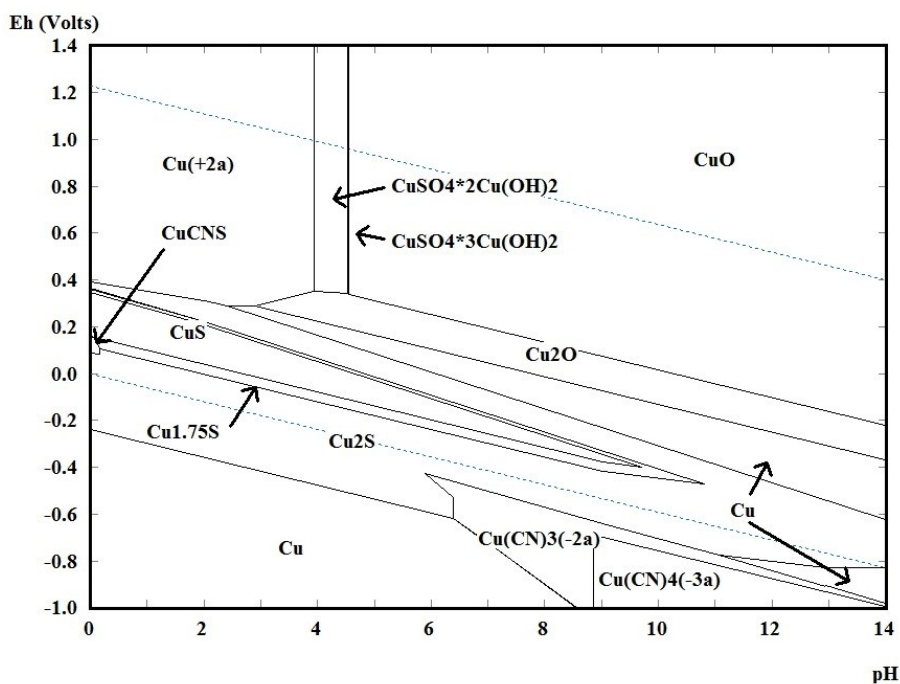


Figure 2.6 Potential-pH diagram of Cu speciation in the Cu-CN-S-H<sub>2</sub>O system for a 20 mM Cu solution with a CN:Cu ratio of 4 and a S:Cu ratio of 0.5. "a" indicates soluble species.

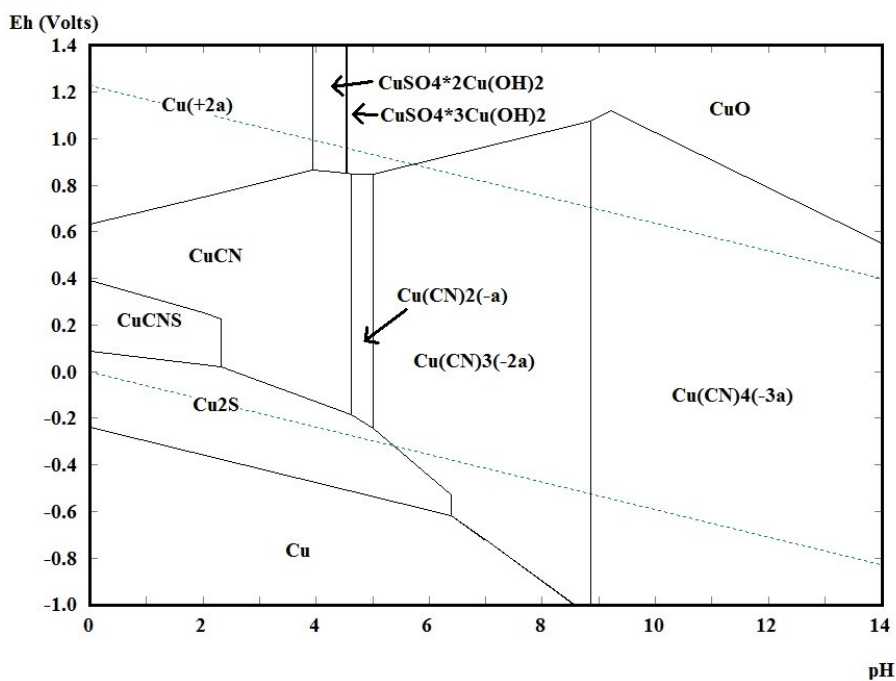


Figure 2.7 Potential-pH diagram of Cu speciation in the Cu-CN-S-H<sub>2</sub>O system for a 20 mM Cu solution with a CN:Cu ratio of 4 and a S:Cu ratio of 0.5, where cyanate species are not considered. "a" indicates soluble species.

Figure 2.7 predicts that in the pH range where sulfidisation processed are operated (4 to 5), the most predominant species at most potentials is CuCN. The formation of CuCN over the expected species of Cu<sub>2</sub>S (Equation 1.3) is due to the oxidation of sulfide species to sulfate in the thermodynamic model. Nevertheless, based on observations from the literature (Lower 1965, 1968; Potter, Bergmann, and Haidlen 1986; Fleming and Trang 1998; MacPhail, Fleming, and Sarbutt 1998; Dreisinger et al. 2008), oxidation of sulfide species to sulfate is not expected to occur to any appreciable extent during sulfidisation. This is due to the rapid kinetics of metal sulfide precipitation compared to sulfide oxidation. Hence, a second metastable potential-pH diagram of the system from Figure 2.6 was generated, where neither cyanide oxidation to cyanate nor sulfide oxidation to sulfur oxide species is considered (Figure 2.8).

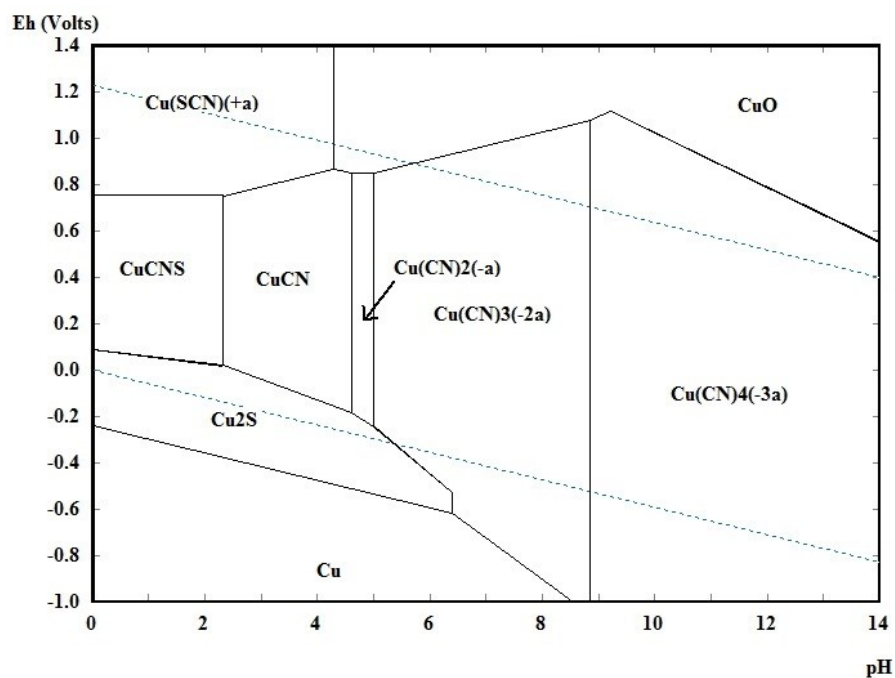


Figure 2.8 Potential-pH diagram of Cu speciation in the Cu-CN-S-H<sub>2</sub>O system for a 20 mM Cu solution with a CN:Cu ratio of 4 and a S:Cu ratio of 0.5, where cyanate and sulfur oxide species are not considered. "a" indicates soluble species.

As with Figure 2.7, Figure 2.8 predicts that CuCN is the most predominant species in the pH region where sulfidisation processes are operated. In this case it is due to sulfide oxidation to thiocyanate in the thermodynamic model. As with other sulfide oxidation reactions, sulfide oxidation to thiocyanate is expected to be slow (Breuer, Jeffrey, and Hewitt 2008; Hewitt et al. 2009) with only small amounts of thiocyanate observed during sulfidisation (MacPhail, Fleming, and Sarbutt 1998). For this reason, a third metastable potential-pH diagram of the system in Figure 2.6 was generated, where no cyanide or sulfide oxidation reactions are considered (Figure 2.9).

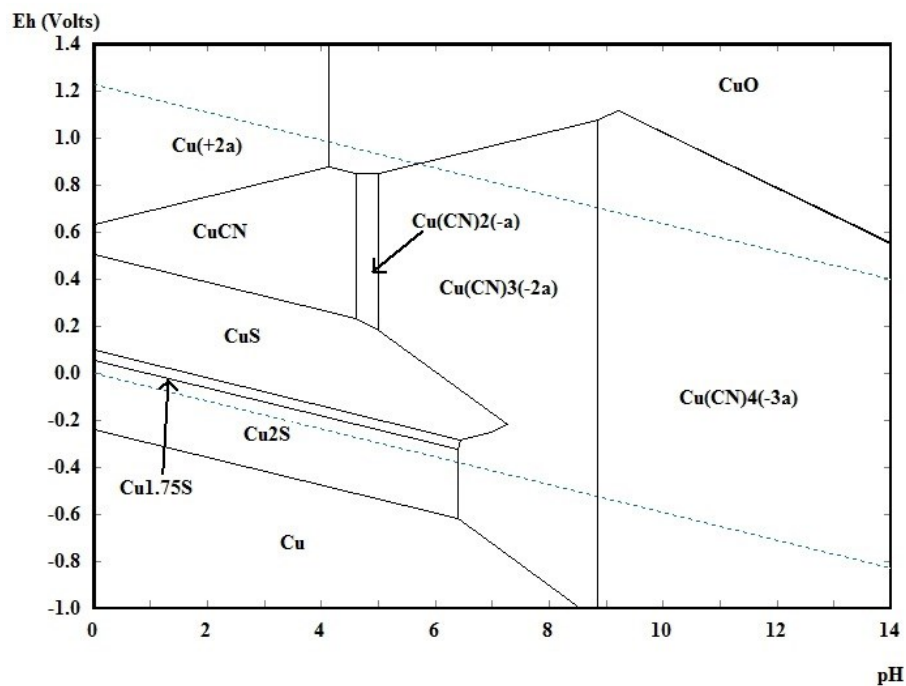
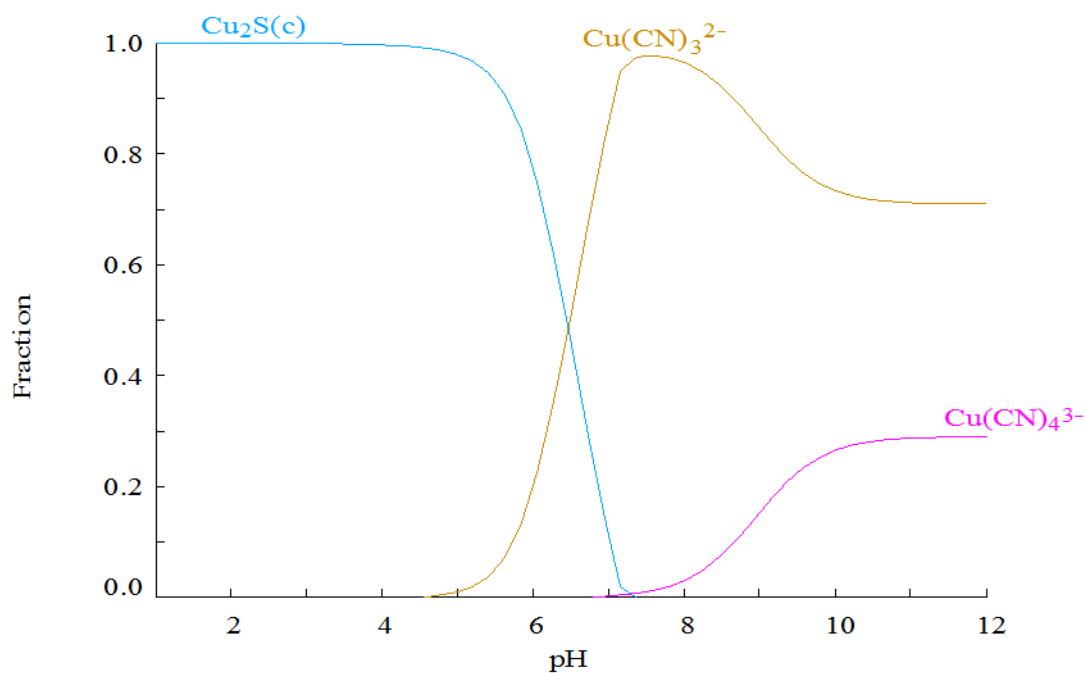


Figure 2.9 Potential-pH diagram of Cu speciation in the Cu-CN-S-H<sub>2</sub>O system for a 20 mM Cu solution with a CN:Cu ratio of 4 and a S:Cu ratio of 0.5, where cyanate, sulfur oxide, and thiocyanate species are not considered. "a" indicates soluble species

Figure 2.9 shows that in the optimal pH range for sulfidisation reported in the literature, the predicted predominant precipitates are Cu<sub>2</sub>S, Cu<sub>1.75</sub>S, CuS, and CuCN depending on potential. With the exception of work by Guzman et al. (2010), which is discussed in more detail in Section 2.3.3, all available

research on sulfidisation of copper cyanide solutions show  $\text{Cu}_2\text{S}$  to be the precipitate produced in the process as per Equation 1.3. While it could be possible that all of the studies performed on sulfidisation in the literature were done at potentials where  $\text{Cu}_2\text{S}$  is predominant, it is far more likely the  $\text{Cu}_2\text{S}$  forms at all potentials initially and that other species predicted in Figure 2.9 are caused by slower redox reactions not observed in the short time periods that sulfidisation experiments in the literature are conducted for.

Since redox reactions were causing the potential-pH diagrams to predict the formation of species that are not observed during sulfidisation work in the literature, a simple speciation diagram of the same system shown in Figure 2.6 was generated (Figure 2.10) where redox reactions are not considered. Generation of a simple speciation diagram is also useful for evaluation of the amount of copper and cyanide recovered at a specific pH. Figure 2.10 shows that at a pH of 5, copper conversion from aqueous copper cyanide to a copper sulfide precipitate is high (97%). This increases to 99% conversion at pH 4. Hence, the thermodynamic model shown in Figure 2.10 agrees with the consensus in the recent literature, that there is an optimum pH range between 4 and 5 to generate  $\text{Cu}_2\text{S}$ .



**Figure 2.10 Thermodynamic determination of Cu (I) speciation at different pH values for a 20 mM Cu (I) solution with a CN:Cu ratio of 4, a S:Cu ratio of 0.5, and where redox reactions are not considered.**

Potential-pH diagrams have not been generated in subsequent sections of this review as the kinetics of metal sulfide precipitation reactions are fast compared to the redox reactions that are predicted in potential-pH models. Hence, simple speciation diagrams that do not consider redox reactions should be adequate for prediction of species generated in sulfidisation processes, as the objective of such processes are to precipitate and recover the metal in as short a time as possible. The rapid precipitation of metal sulfides is also likely to be the reason why potential is not a commonly considered factor in metal sulfide precipitation studies (see Lewis 2010).

### **2.3.3 Effect of sulfide to copper ratio**

The sulfide dosing requirements during sulfidisation are dictated by reaction stoichiometry of the primary sulfidisation equation (Equation 1.3). Reaction

stoichiometry shows a S:Cu ratio of 0.5 is required to precipitate all of the copper and release cyanide. Recommendations for sulfide dosing in the literature agree with this, with dosing of slightly above stoichiometry often used (S:Cu ratio of 0.5 to 0.6) (Dreisinger et al. 2008).

The two early sulfidisation patents from the 1960s (Lower 1965, 1968) are an exception to the recommended S:Cu ratio of 0.5 to 0.6. Instead, these patents suggest adding less sulfide when iron or thiocyanate are present as these two species can also separate recoverable cyanide from copper. It is likely that this has not been suggested for more recent sulfidisation processes due to the difficulty in measurement and control of a sulfidisation plant using this kind of sulfide dosing strategy. Further to this, if sulfide is under dosed and other impurities are not present, then cyanide recoveries will be reduced. There is also potential to precipitate copper cyanide which could be detrimental in marketing the copper sulfide precipitate (MacPhail, Fleming, and Sarbutt 1998).

As adding sulfide at stoichiometry or slightly above is sufficient to achieve high cyanide and copper recoveries, there is no need to add sulfide in large excess as it would be a waste of reagent. Further, sulfide and cyanide can react to form thiocyanate (Equation 2.9). While this reaction occurs slowly, it can be catalysed by other species in solution and some mineral surfaces (Breuer, Jeffrey, and Hewitt 2008; Hewitt et al. 2009). The result is that, even if thiocyanate were not generated during sulfidisation, it would likely be generated if sulfide is present in the cyanide return when the solution was recycled to leaching. Excess sulfide may also result in the generation of dihydrogen sulfide gas (Barter et al. 2001; Botz and Acar 2007).



2.9

A thermodynamic analysis of a 20 mM Cu solution with a CN:Cu ratio of 4 and at a pH of 4 (Figure 2.11) shows that, once a stoichiometric amount of sulfide is added to solution (10 mM), all copper is precipitated as  $\text{Cu}_2\text{S}$ .

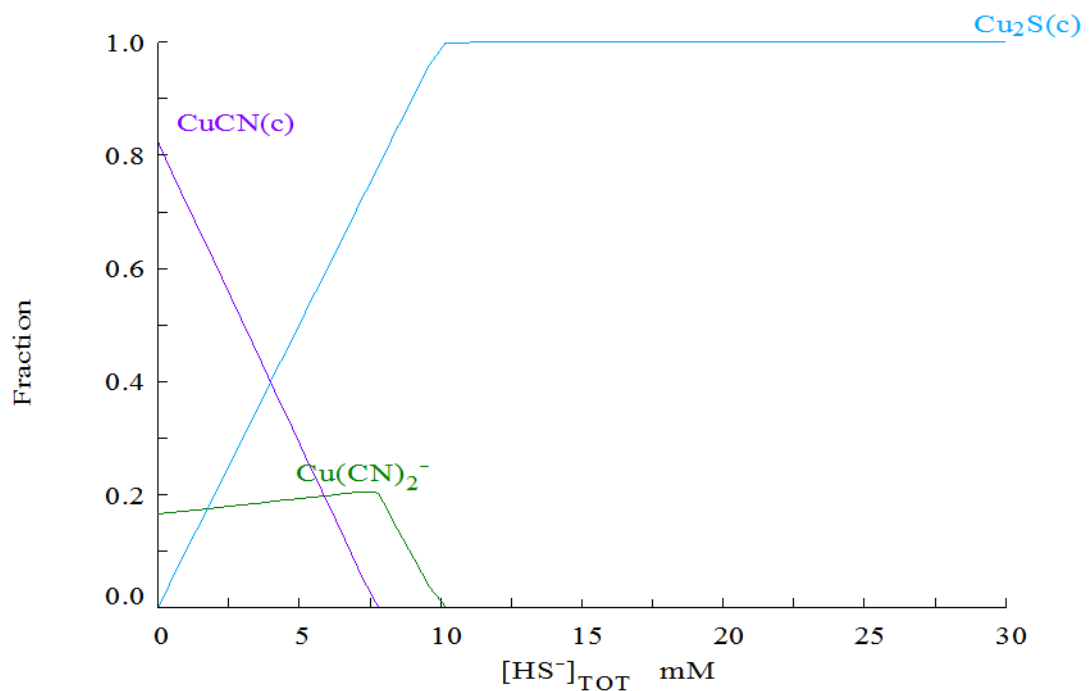


**Figure 2.11 Thermodynamic determination of Cu (I) speciation at different S additions for a 20 mM Cu (I) solution with a CN:Cu ratio of 4, a pH of 4, and where redox reactions are not considered.**

While a S:Cu ratio of 0.5 or slightly above appears acceptable to achieve high recoveries during sulfidisation, there is some research that suggest higher S:Cu ratios are required (Botz and Acar 2007; Guzman et al. 2010). Some pilot tests for Newmont Mining Corporation's Yanacocha Project show that a S:Cu ratio of approximately 1.7 is required based on the amount of copper in the ore (Botz and Acar 2007). This is based on adding sulfide to the system until a slight excess of sulfide is detected in the solution. The solution used did not contain significant amounts of impurities that would be expected to be

consuming sulfide. A second paper (Guzman et al. 2010) using operational data from the Yanacocha plant showed the issue was also present on an industrial scale with sulfide to total metal (copper and silver) ratios near one being required for high copper recoveries. As the ratio accounted for the formation of silver sulfide ( $\text{Ag}_2\text{S}$ ), the high value cannot be attributed to the presence of silver (Section 2.4.1) in the SART feed.

Interestingly, Guzman et al. (2010) also showed that the mineralogical makeup of the copper sulfide precipitate was not chalcocite ( $\text{Cu}_2\text{S}$ ) as expected from Equation 1.3. Instead the composition of the precipitate was predominantly covellite ( $\text{CuS}$ ), with smaller amounts of digenite ( $\text{Cu}_{1.8}\text{S}$ ) and copper thiocyanate ( $\text{CuSCN}$ ) also occurring. Analysis of the precipitates from the Yanacocha pilot work shows that 61.5% of the precipitate is copper, with a small amount of silver (0.33%) and gold ( $< 0.01\%$ ) and the remaining 38.1% presumably being sulfur (Botz and Acar 2007). Based on this outcome, Botz and Acar (2007) suggest the precipitate is 76.9%  $\text{Cu}_2\text{S}$  and 0.38%  $\text{Ag}_2\text{S}$  with the remaining unknown. When considered in conjunction with the plant data from Guzman et al. (2010), however, it is also possible that the unaccounted mass is due to formation of precipitates with higher S:Cu ratio (i.e.  $\text{CuS}$ ).

Newcrest Mining Limited's Telfer Gold Mine has had similar problems to that seen at Yanacocha, with S:Cu ratios of near one required to get high copper and cyanide recoveries (Turton-White, personal communication, 2010). The Newcrest SART feed is not known to contain large amounts of any other sulfide consuming metals and hence the high S:Cu ratio cannot be attributed to impurities in the solution. An internal report from Telfer also shows the copper concentration in the precipitate is low, at only around 50 wt% copper. This may also be related to the precipitate mineralogy being

similar to covellite instead of chalcocite as seen at Yanacocha. Nonetheless, this cannot be confirmed without mineralogical analysis.

The reason for covellite formation as observed at Yanacocha is not discussed in the literature. Based on the potential pH diagrams from Section 2.3.2, it is possible that oxidation of the precipitate may be the cause of covellite formation (Figure 2.9). While the potential formation of covellite is not discussed by Guzman et al. (2010), the authors do postulate that copper thiocyanate seen in the precipitate is caused by the excess sulfide addition. Much of the literature reports increases in thiocyanate in solution during SART although the amount varies between publications. Small increases of around 5 ppm were seen in bench scale work (Dreisinger et al. 2008) while larger increases of around 60 ppm were seen in pilot scale work (MacPhail, Fleming, and Sarbutt 1998; Botz and Acar 2007).

MacPhail, Fleming, and Sarbutt (1998) attribute thiocyanate generation during pilot plant work to reagent addition order suggesting that, by adding sulfide before acid, there is time for the sulfide and free cyanide to react and form thiocyanate. MacPhail, Fleming, and Sarbutt (1998) then suggest that, by acidifying the solution first, the problem could be resolved as all the cyanide would be in its protonated form (HCN). The authors, however, did not test this concept.

The difference in thiocyanate generation is not speculated on by any authors with the only notable difference between the works being that the tests with high thiocyanate generation were pilot scale while the tests with low thiocyanate generation were laboratory scale. Generally, the laboratory scale experiments were performed on leach solutions and therefore the difference

in thiocyanate generation cannot be attributed to laboratory experiments using synthetic solutions.

#### **2.3.4 Effect of cyanide to copper ratio**

The effect of cyanide to copper molar ratio on sulfidisation is not detailed in the literature. This is presumably because the feed solution composition is a result of gold leaching conditions and hence not a variable that is changed for the purpose of sulfidisation. CN:Cu ratio may, however, have an effect on sulfidisation which in turn may require a more holistic approach to running both a gold leaching and cyanide recovery process.

From the primary sulfidisation equation (Equation 1.3), it is apparent that higher CN:Cu ratios will impact on the amount of acid and base required by sulfidisation processes. Nonetheless, the sulfide dose should be unaffected. Thermodynamic analysis of a 20 mM copper solution with a S:Cu ratio of 0.5 and at a pH of 4 (Figure 2.12) shows that variation of the amount of cyanide in solution from a CN:Cu ratio of 1 to 6 has no effect on the formation of the copper sulfide product. Hence, at this pH cyanide and copper recovery is high no matter the amount of cyanide present. Thermodynamic analysis of the same solution at a pH of 6 (Figure 2.13), however, shows that CN:Cu ratio can have an impact on copper recovery at this pH.

The results of the thermodynamic analysis at pH 4 (Figure 2.12) and 6 (Figure 2.13) show that there is an interaction between pH and CN:Cu ratio. The result of this interaction is that the selection of the appropriate pH for sulfidisation may be influenced by the CN:Cu ratio in the sulfidisation feed.

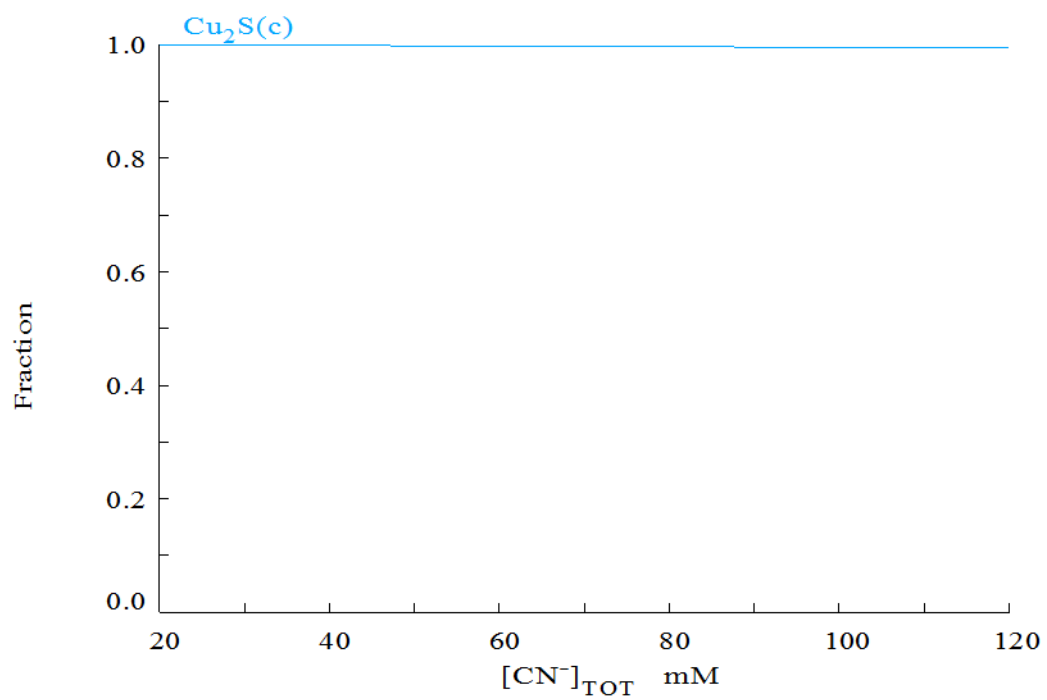


**Figure 2.12 Thermodynamic determination of Cu (I) speciation at different  $\text{CN}^-$  additions for a 20 mM Cu (I) solution with an S:Cu ratio of 0.5, a pH of 4, and where redox reactions are not considered.**

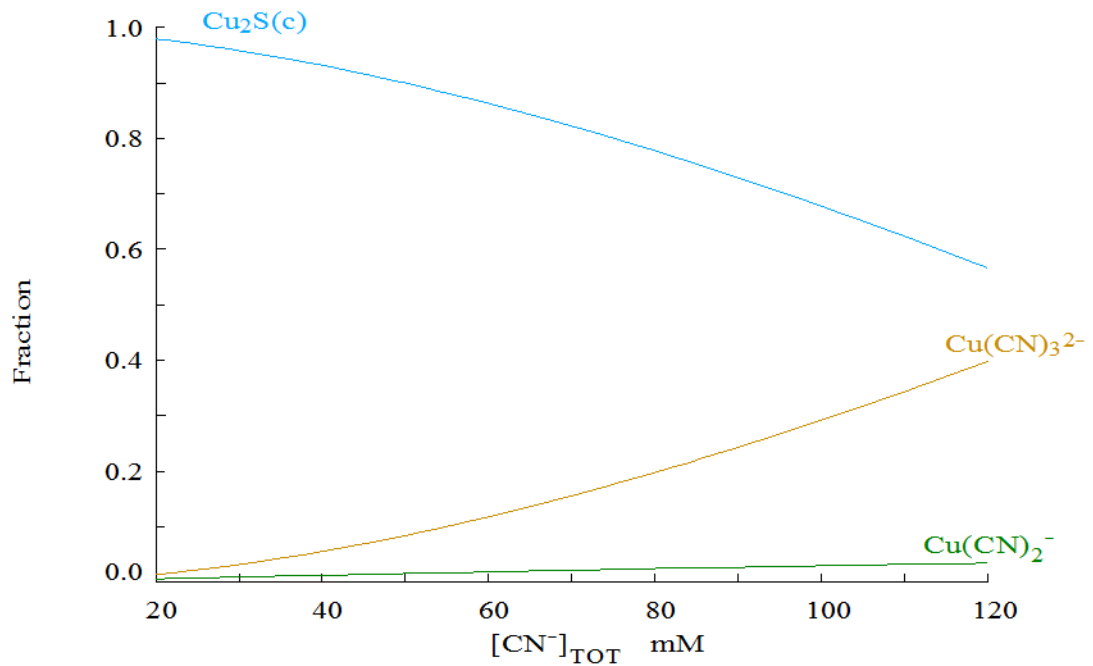


Figure 2.13 Thermodynamic determination of Cu (I) speciation at different CN<sup>-</sup> additions for a 20 mM Cu (I) solution with an S:Cu ratio of 0.5, a pH of 6, and where redox reactions are not considered.

### 2.3.5 Effect of volatilisation

To recovery copper during sulfidisation, the process can only be used on solutions and not slurries. This often results in a requirement for washing of the tailings slurry before sulfidisation such as at Newcrest Mining Limited's Telfer SART plant (Goulsbra et al. 2003). The use of tailings washing, such as counter current decantation (CCD), can in turn cause a positive water balance for a processing operation.

To overcome the problem of a positive water balance, volatilisation during SART has been proposed (Fleming and Trang 1998). Fleming and Trang (1998) show that, by performing volatilisation at the same time as sulfidisation, some sulfide is volatilised. This is due to sulfide being present as aqueous dihydrogen sulfide (H<sub>2</sub>S) at the pH where sulfidisation is

performed (< 5). The result of volatilisation was a reduction in the amount of sulfur available for precipitation leading to an increase of cyanide and iron in the precipitate. The authors reported an increase from <0.15% and <0.7% to 4% and 4.8% for cyanide and iron respectively. Due to this issue, the authors propose that volatilisation could be performed on the recycle stream after sulfidisation. This idea was also proposed in the initial designs for Newcrest Mining Limited's Telfer Operation (Goulsbra et al. 2003).

Another potential source of hydrogen cyanide and dihydrogen sulfide volatilisation during sulfidisation is caused by the use of closed reactors which are under a vacuum and connected to a scrubbing system. This is done to prevent the release of toxic hydrogen cyanide and dihydrogen sulfide gas to the atmosphere. As the scrubber system draws air in, it creates airflow over the solution surfaces during sulfidisation. Estay et al. (2012) developed a mathematical model showing that the loss of hydrogen cyanide from the reactor is small due to small amounts of mass transfer from the liquid phase. Loss of sulfide gas during sulfidisation is considered in some work (Barter et al. 2001; Botz and Acar 2007), but has not been formally researched in the available literature.

### **2.3.6 Effect of copper concentration**

There were no studies found that identified copper concentration as having any effect on the efficiency of cyanide and copper recovery. Logically, based on the primary sulfidisation equation (Equation 1.3), acid, base, and sulfide consumption would vary with the amount of copper present. Copper concentration may also have an effect on the physical properties of the precipitate generated. This would depend largely on the precipitate crystallisation mechanisms (Demopoulos 2009).

The crystallisation mechanism during sulfidisation from a cyanide solution to produce chalcocite ( $\text{Cu}_2\text{S}$ ) has not been researched in the available literature. Crystallisation of covellite ( $\text{CuS}$ ) from copper (II) sulfate solutions, however, has been extensively researched with a comprehensive review by Lewis (2010). The crystallisation mechanism of covellite in the copper (II) sulfate system is one of primary nucleation followed by aggregation and attrition of the fine precipitates formed (Lewis and van Hille 2006). Aggregation is known to increase with more particles in solution (Demopoulos 2009). Therefore, larger copper concentrations in the copper (II) sulfate system cause larger covellite precipitates.

As precipitation of copper sulfide from sulfate or cyanide solutions are similar, increased copper concentration is likely to result in larger chalcocite precipitates being formed in sulfidisation from cyanide solutions. This may explain why settling rates during thickening are improved during SART when some of the thickener underflow is recycled (MacPhail, Fleming, and Sarbutt 1998), as the amount of copper in the system is increased.

### **2.3.7 Effect of residence time**

The effect of residence time on sulfidisation has not been extensively covered in the literature due to the rapid kinetics of the primary sulfidisation reaction (Equation 1.3). Work that has been done on residence time in pilot SART plants suggests that it has little to no effect on copper or cyanide recovery (MacPhail, Fleming, and Sarbutt 1998; Barter et al. 2001). Nonetheless, the residence times used in these pilot trials were comparatively short compared to what may be experience on an industrial scale. As the pH-potential models generated in Section 2.3.2 predict that the precipitate generated in sulfidisation can be oxidised to release copper into solution, long residence times may negatively impact the process.

### **2.3.8 Effect of temperature**

Temperature is expected to influence all the rates and equilibrium involved in sulfidisation processes. Ford, Fleming, and Henderson (2008), however, show that identical solutions at 4 °C and 20 °C had little to no difference in cyanide recovery, copper recovery, or reagent consumptions. The lack of impact of temperature is likely due to the rapid kinetics of the primary sulfidisation reaction (Equation 1.3).

Temperature will affect the volatility of hydrogen cyanide gas (Estay et al. 2012). While this is not critical, as hydrogen cyanide gas can be captured during scrubbing, there is also potential for dihydrogen sulfide gas to be volatilised. Estay et al. (2012) did not cover the impact of temperature on the volatility of dihydrogen sulfide gas during sulfidisation and it is not mentioned elsewhere in the literature surveyed.

## **2.4 Impurities in sulfidisation**

Other species in gold cyanidation tailings may have several impacts on sulfidisation processes such as consumption of sulfide and acid, decrease in precipitate grade, and precipitation of cyanide species. The impact of various species found in gold cyanidation tailings are reviewed in this section. For ease of reference, such species will be referred to as impurities in the rest of this thesis.

The impurities reviewed were based on common impurities seen in cyanidation leach tails. These were silver, gold, iron, nickel, zinc, cyanate, thiocyanate, and thiosulfate. Chloride was also studied as sulfidisation could potentially be used after a resin recovery process for copper cyanide (Dai,

Breuer, and Jeffrey 2010), which would result in the treatment of high chloride solutions.

As with the previous sections, thermodynamic modelling was used to assist in understanding observations in the literature and to help make predictions on how different impurities will affect the process. Thermodynamic modelling was performed using the software MEDUSA, as described in Section 2.1, to generate simple speciation diagrams that do not consider redox reactions. For every cationic impurity, two thermodynamic models were made. Both models used 20 mM of copper and 20 mM of impurity with CN:metal molar ratios of 4. One model for each impurity was set with a S:Cu ratio of 0.5 to evaluate how the impurity impacted an ideal sulfidisation process. The second model for each impurity was set with a S:Cu ratio of 1.0 to evaluate if the impurity reacts differently when excess sulfide is present in solution. Simple speciation diagrams have been used for the impurity studies due to the fast kinetics of metal sulfide precipitation making them sufficient for analysis of sulfidisation processes (Section 2.3.2).

#### **2.4.1 Silver**

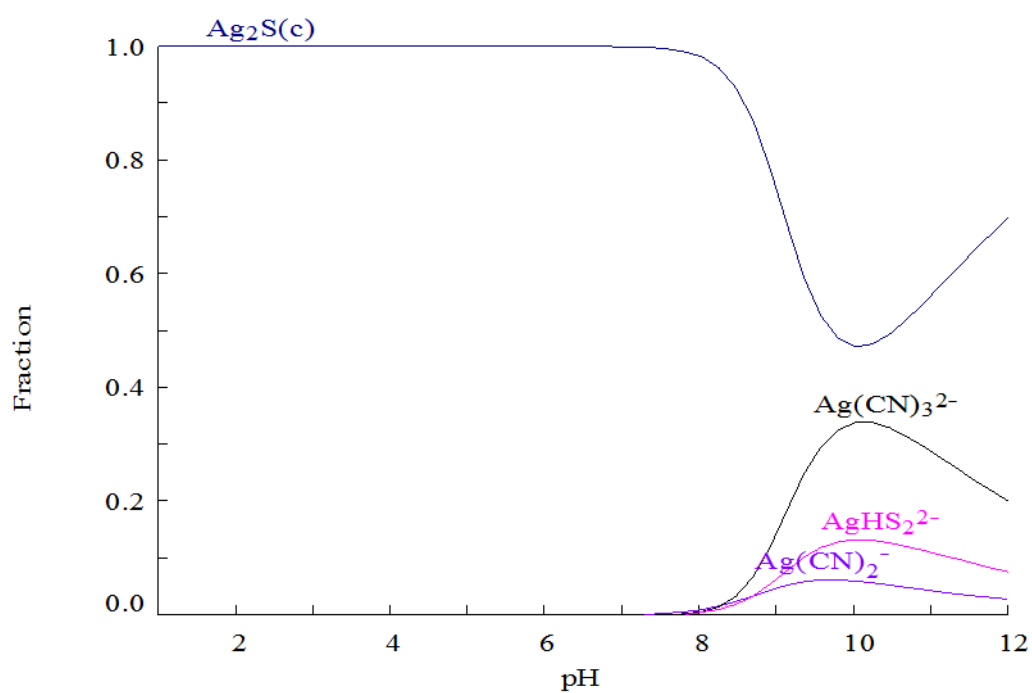
It is well understood that silver cyanide species will react with sulfide to form a silver sulfide precipitate as shown in Equation 2.10. This was first discussed in the MNR patent where a silver recovery stage is suggested before copper recovery (Potter, Bergmann, and Haidlen 1986) and is also mentioned in many other sulfidisation papers (Milosavljevic, Solujic, and Kravetz 2004; Dreisinger et al. 2008; Guzman et al. 2010).



Unlike copper, silver can be recovered at the same pH that is used during leaching of gold with cyanide. This results in the ability to selectively recover silver from copper with high separation efficiency. Milosavljevic, Solujic, and Kravetz (2004) report 99% silver recovery with only 7% recovery of copper. The authors, however, do not report the conditions which yield this selectivity. Newmont Mining Corporation's Yanacocha Project recovers silver in the copper precipitate and receives credits for its presence (Guzman et al. 2010). Recoveries at Yanacocha are usually high (>75%).

Thermodynamic analysis of a 20 mM copper and silver solution with a CN:metal molar ratio of 4 and an S:Cu ratio of 0.5 (Figure 2.14) shows that silver precipitates as silver sulfide preferentially to copper over the pH range 1 to 9. Thermodynamic analysis of the same system at a S:Cu ratio of 1.0 (not shown) gives a similar result. These results agree with observations in the literature.

a)



b)

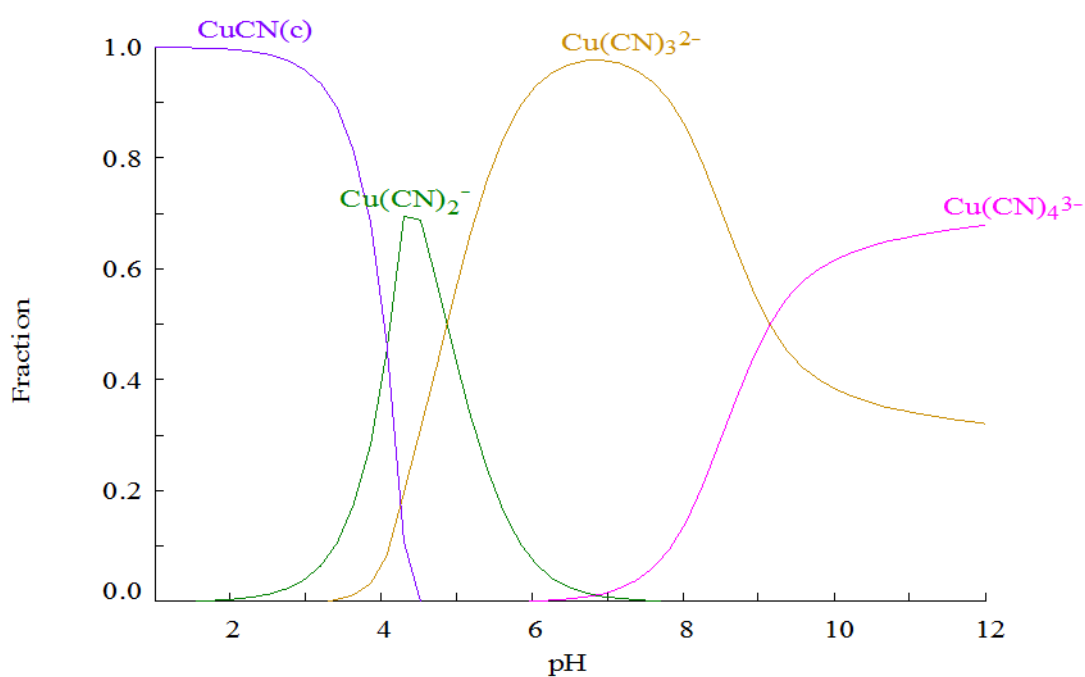


Figure 2.14 Thermodynamic determination of a) Ag (I) and b) Cu (I) speciation at different pH for a 20 mM Cu (I) and Ag (I) solution with a CN:metal ratio of 4, a S:Cu ratio of 0.5, and where redox reactions are not considered.

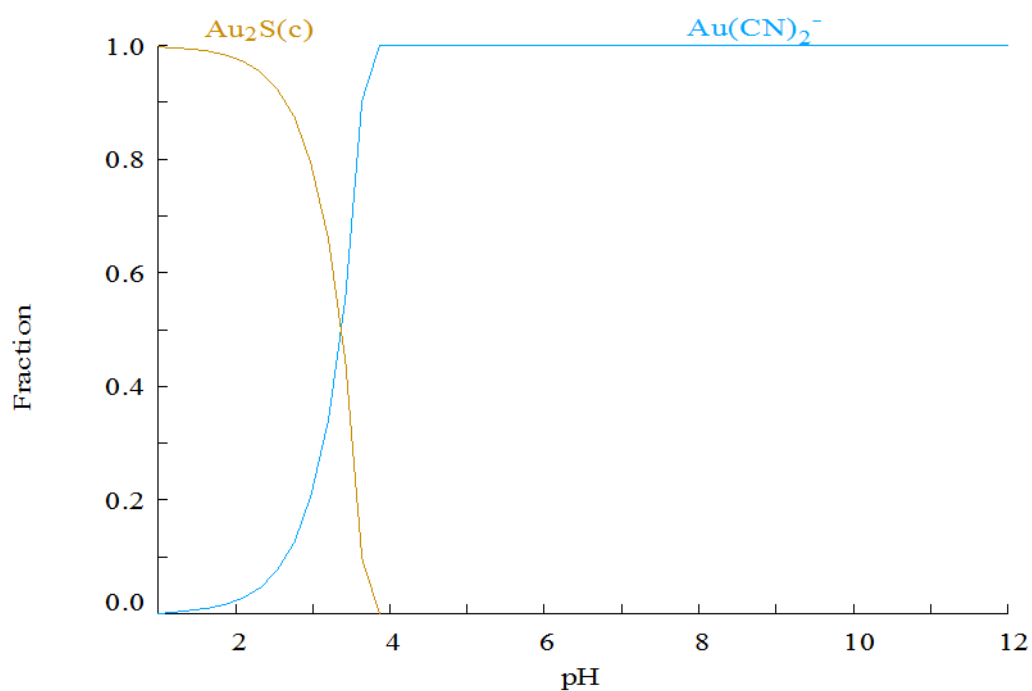
### **2.4.2 Gold**

The recovery of gold during sulfidisation appears possible, although the recoveries reported vary between studies. Dreisinger et al. (2008) reported recovering around 20% to 30% of gold in a leach solution when the leach solution was treated using SART before gold recovery by carbon adsorption. Work by Littlejohn, Kratochvil, and Hall (2013), however, shows that only a small amount (<1.5%) of gold is precipitated during sulfidisation of a gold leach solution before carbon adsorption. Guzman et al. (2010) shows gold recovery during sulfidisation is dependent on pH and sulfide dosing. Nonetheless, this does not explain the differences in results from Dreisinger et al. (2008) and Littlejohn, Kratochvil, and Hall (2013), as both authors use a pH greater than 4 while the work of Guzman et al. (2010) shows little gold recovery above pH 4.

Thermodynamic analysis of a 20 mM copper and gold (I) solution with a CN:metal molar ratio of 4 and an S:Cu ratio of 0.5 showed no precipitation of gold for the pH range modelled (not shown). Thermodynamic modelling of the same solution when S:Cu is 1.0 (Figure 2.15) shows that gold precipitation as gold sulfide can occur below pH 4. The thermodynamic model suggests that copper sulfide formation is preferential to gold sulfide.

The result of the modelling is partly consistent with the research of Guzman et al. (2010), who showed that at pH 4 there is no gold recovered, with recovery increasing to 20% by pH 2. The exact solution composition is not given for the experiment which may explain the inconsistency in gold recovery compared to the thermodynamic model data.

a)



b)

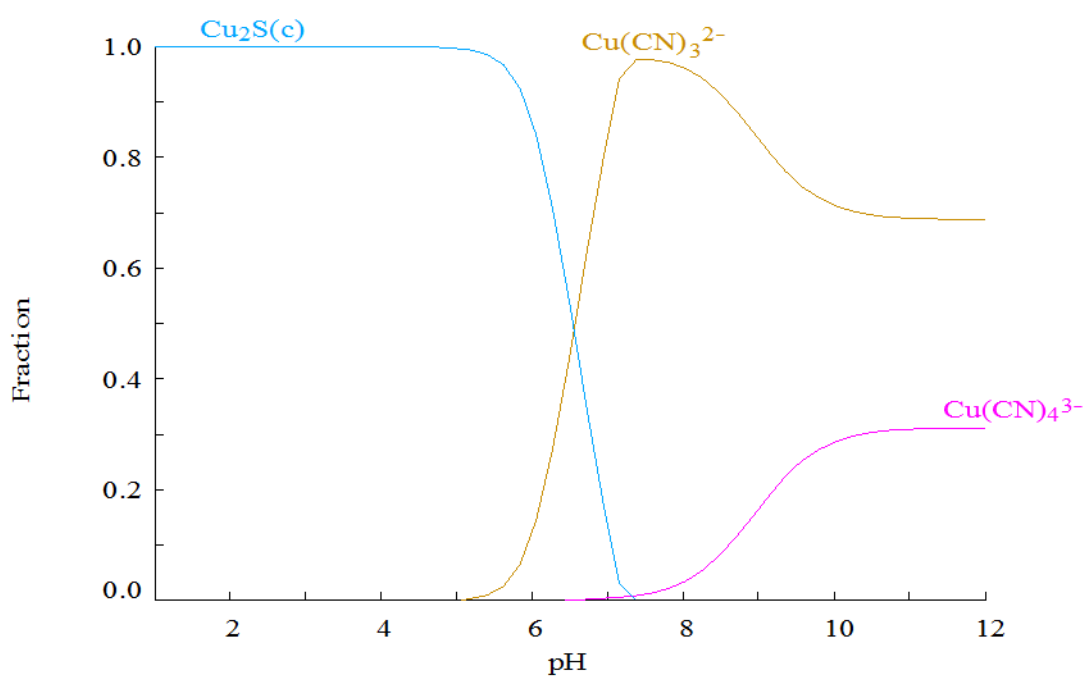


Figure 2.15 Thermodynamic determination of a) Au (I) and b) Cu (I) speciation at different pH for a 20 mM Cu (I) and Au (I) solution with a CN:metal ratio of 4, a S:Cu ratio of 1.0, and where redox reactions are not considered.

As mentioned earlier, the 20% to 30% gold recovery from Dreisinger et al. (2008) was seen at pH values between 4 and 5. These gold recoveries are higher than expected for the pH range tested considering the thermodynamic model data and results of Guzman et al. (2010) and Littlejohn, Kratochvil, and Hall (2013). The solutions used by Dreisinger et al. (2008) did, however, contain silver which can result in the formation of gold silver sulfide precipitates (Osadchii and Rappo 2004). The formation of gold silver sulfide may explain the unusually high recovery of gold observed by Dreisinger et al. (2008).

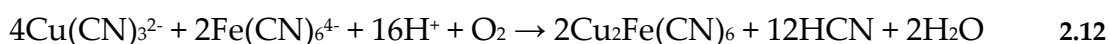
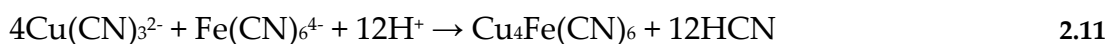
Gold precipitated during sulfidisation may be beneficial as it can result in credits given on its presence when marketing the sulfidisation precipitate to smelters. It should, however, be noted that this would only be the case where the gold recovered was taken from a tailing solution treated with sulfidisation. If sulfidisation was used on a solution before gold recovery with carbon adsorption (Kratochvil, Chan, and Hall 2013) then gold recovery during sulfidisation may be undesirable.

### **2.4.3 Iron**

In cyanide solutions, iron can form  $\text{Fe}(\text{CN})_6^{4-}$  and  $\text{Fe}(\text{CN})_6^{3-}$  for iron (II) and iron (III) respectively. The iron cyanide species formed are highly stable and hence cyanide in the form of iron cyanide can be considered unrecoverable. This strong bond between iron and cyanide results in iron not reacting with sulfide during sulfidisation processes (Fleming and Trang 1998).

Although iron is not known to react with sulfide during sulfidisation, it is able to react with copper to form copper iron cyanide precipitates. Copper and iron (II) cyanide form copper iron cyanide precipitates at low pH ( $\text{pH} < 4$ ) as per Equations 2.11, and 2.12. The formation of  $\text{Cu}_2\text{Fe}(\text{CN})_6$  is caused by

the oxidation of copper when oxygen is available such as in processes like acidification, volatilisation, and reneutralisation (AVR) (Fleming and Trang 1998). Additional oxidation of  $\text{Cu}_2\text{Fe}(\text{CN})_6$  results in the conversion of iron (II) to iron (III) and potential formation of  $\text{Cu}_3[\text{Fe}(\text{CN})_6]_2$  (Moritz 1954).



Copper (I) can also react with iron (III) cyanide to form  $\text{Cu}_3\text{Fe}(\text{CN})_6$  (Adams and Kyle 2000). The formation of the copper iron (III) cyanide precipitates ( $\text{Cu}_3\text{Fe}(\text{CN})_6$  and  $\text{Cu}_3[\text{Fe}(\text{CN})_6]_2$ ) from copper cyanide solutions, however, has not been studied in the available literature.

While copper iron cyanide precipitates can form during sulfidisation, the formation of copper sulfide is indicated to occur preferentially (Fleming and Trang 1998). Hence, copper iron cyanide precipitates may only occur during sulfidisation if sulfide dosing is less than what is required to react with all the copper. As discussed in Section 2.3.3, this chemistry was exploited in the patents by Lower (1968) who suggested that copper should be allowed to precipitate with iron cyanide and then only enough sulfide added to precipitate the remaining copper in solution.

Dreisinger et al. (2008) showed a recovery of iron between 20% and 99% during sulfidisation with sulfide addition slightly above stoichiometry (Equation 1.3). Two different solutions were used during the study: one a gold leach solution before gold recovery, and the other a gold leach solution after gold recovery by carbon adsorption. The amount of iron in solution was small ( $<10 \text{ mg L}^{-1}$ ) and recovery above 90% only occurred in solutions which

had not undergone carbon recovery of gold. The authors do not attempt to explain the variation in iron recovery.

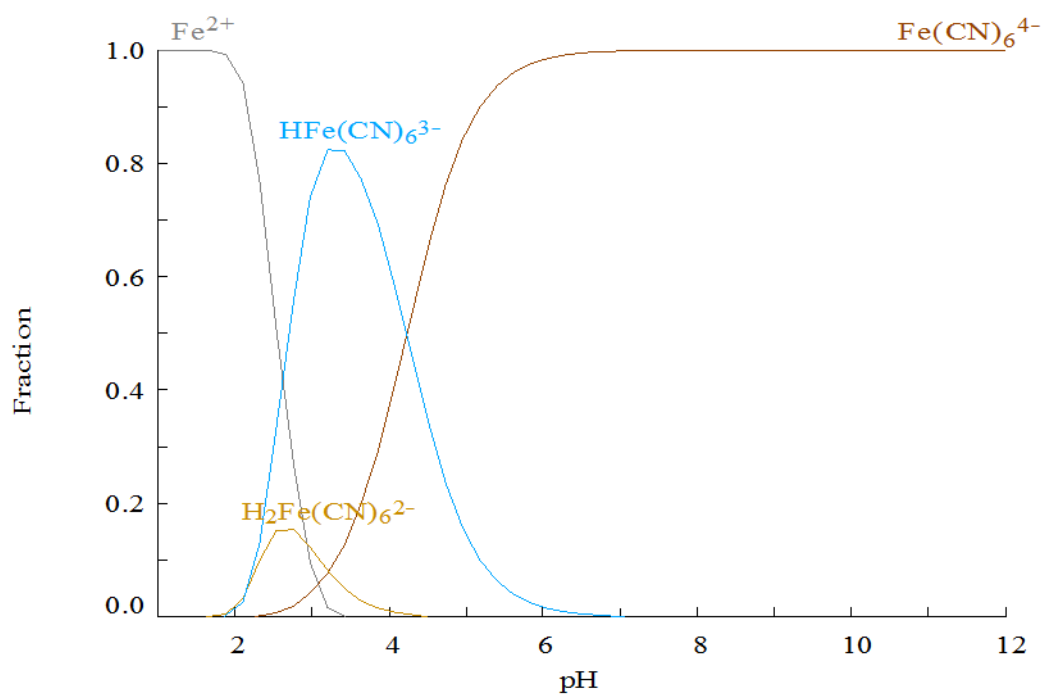
Thermodynamic analysis of a 20 mM copper and iron (II) solution with a CN:Cu ratio of 4, plus a CN:Fe molar ratio of 6, and an S:Cu ratio of 0.5 (Figure 2.16) shows that iron (II) is not expected to interfere with copper recovery. It also shows that iron (II) does not release cyanide attached to it until very low pH values are reached (pH < 3). The same is true when the S:Cu ratio is 1.0 (not shown). These results agree with the literature.

Figure 2.17 shows the thermodynamic analysis of the same system as Figure 2.16 except using iron (III) instead of iron (II). At low pH, the iron (III) model shows release of cyanide from iron due to the formation of a copper iron sulfide precipitate and iron (III) ions. It should be noted here that no thermodynamic data could be found for copper (I) iron (III) cyanide precipitates and hence they are not included in the model. The iron (III) system with a S:Cu ratio of 1.0 (not shown) gave a similar result.

Iron can also react with zinc to produce zinc iron cyanide precipitates according to Equation 2.13. As copper recovery is usually the focus of sulfidisation from cyanide solutions, the interaction of zinc or other metals with iron has not been reported in this context in the literature surveyed.



a)



b)

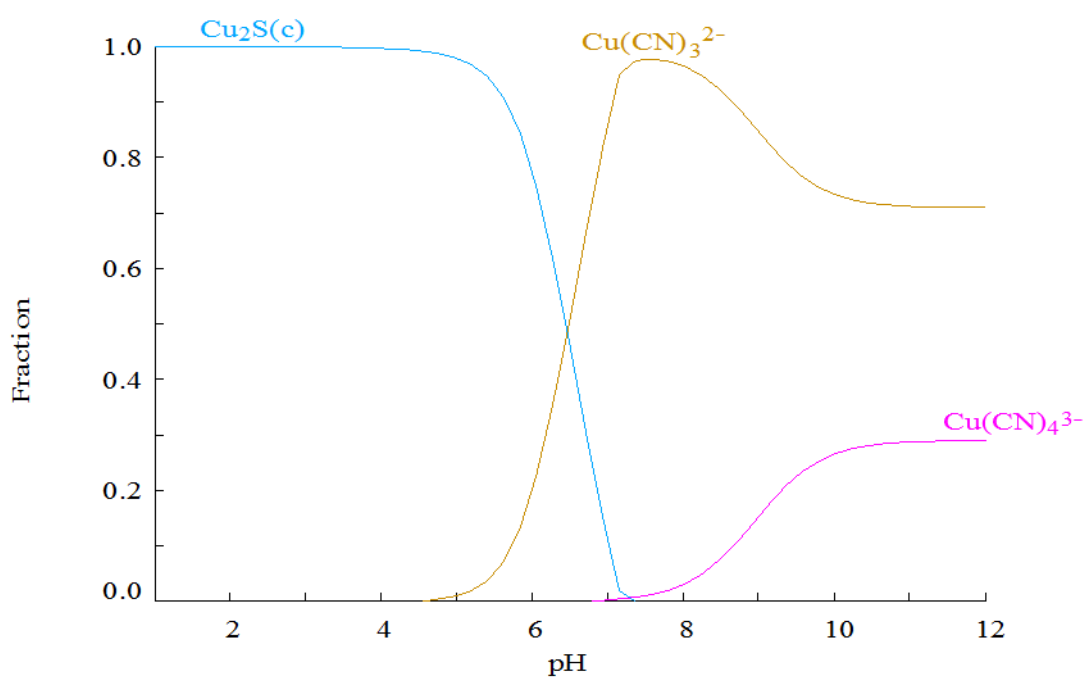


Figure 2.16 Thermodynamic determination of a) Fe (II) and b) Cu (I) speciation at different pH for a 20 mM Cu (I) and Fe (II) solution with a CN:Cu ratio of 4 plus a CN:Fe ratio of 6, a S:Cu ratio of 0.5, and where redox reactions are not considered.

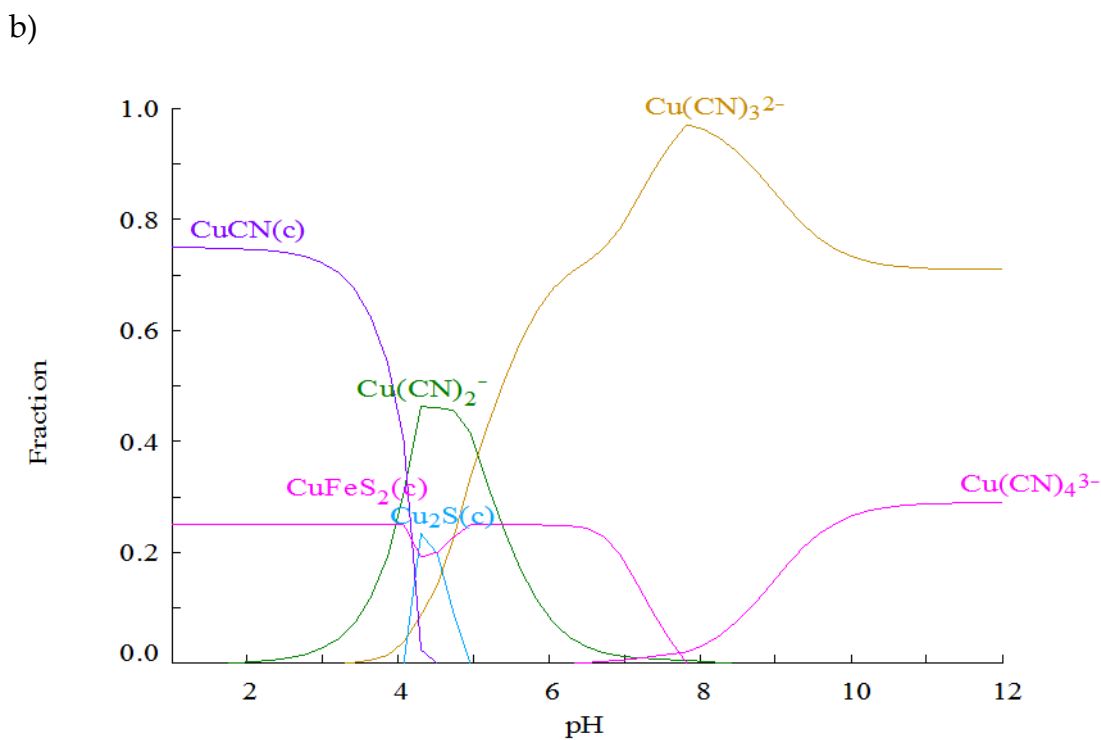
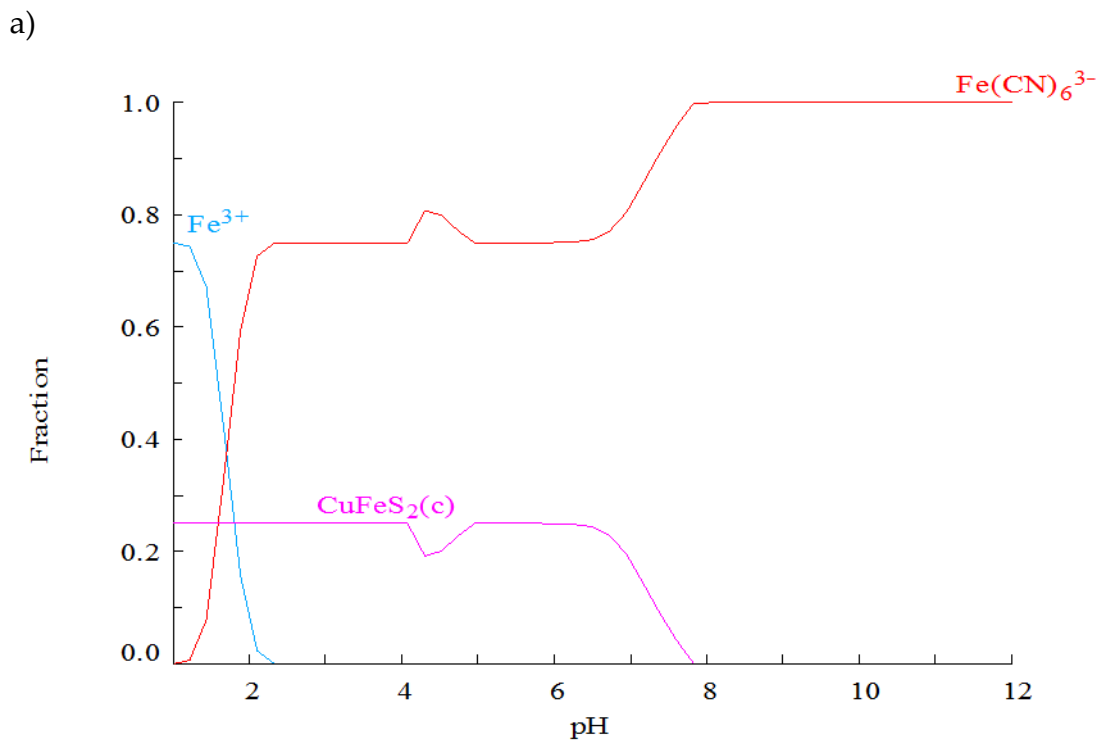
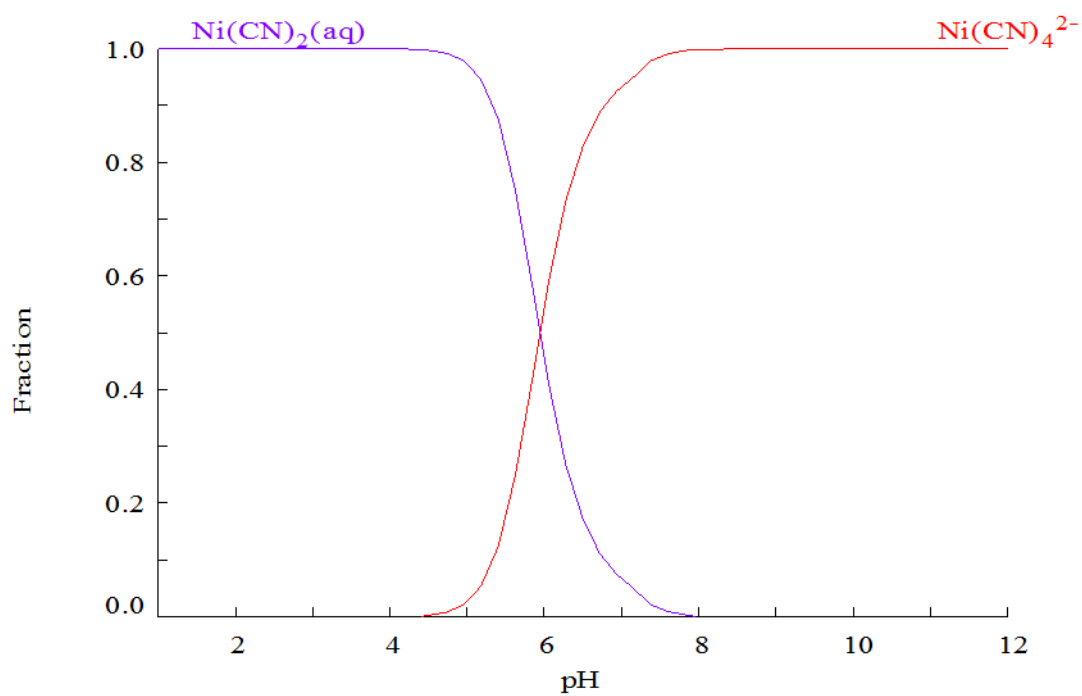


Figure 2.17 Thermodynamic determination of a) Fe (III) and b) Cu (I) speciation at different pH for a 20 mM Cu (I) and Fe (III) solution with a CN:Cu ratio of 4 plus a CN:Fe ratio of 6, a S:Cu ratio of 0.5, and where redox reactions are not considered.

#### **2.4.4 Nickel**

The impact of nickel in sulfidisation processes is not covered in any of the available literature. Thermodynamic analysis of a 20 mM copper and nickel solution with a CN:metal molar ratio of 4 and an S:Cu ratio of 0.5 (Figure 2.18) shows that nickel does not form a sulfide or precipitate over the entire pH range. There is also no precipitate in the same system when the S:Cu ratio is 1.0 (not shown). Nickel is known to form sulfide precipitates at neutral pH values when cyanide is not present (Lewis 2010). The stability of nickel cyanide, however, appears to prevent this.

a)



b)

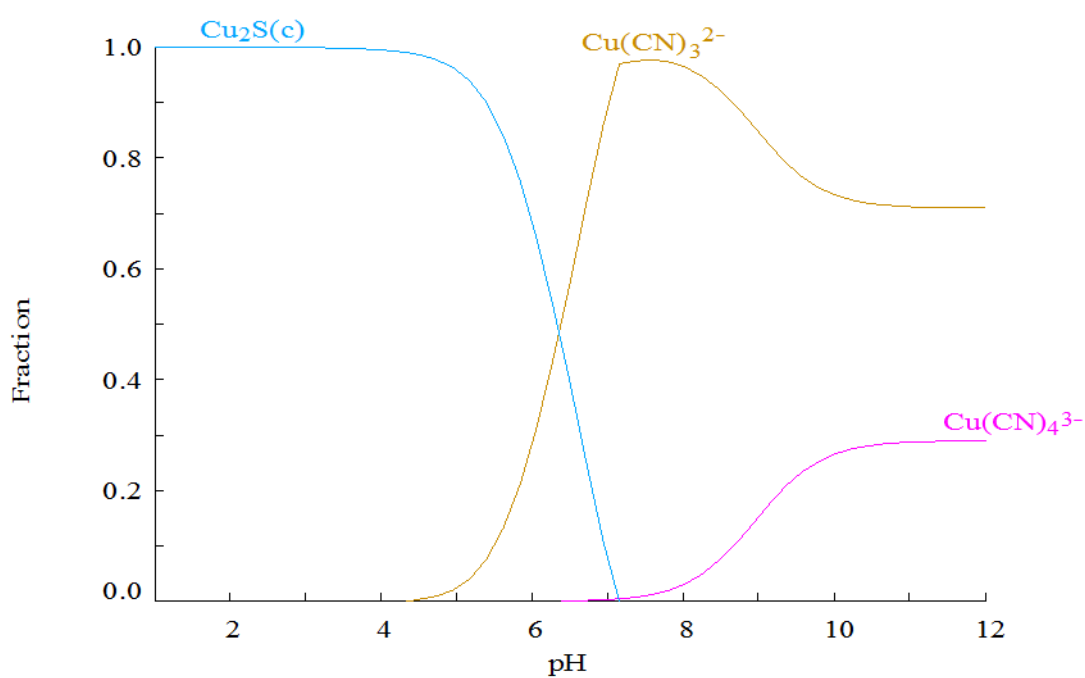


Figure 2.18 Thermodynamic determination of a) Ni (II) and b) Cu (I) speciation at different pH for a 20 mM Cu (I) and Ni (II) solution with a CN:metal ratio of 4, a S:Cu ratio of 0.5, and where redox reactions are not considered.

### 2.4.5 Zinc

Zinc reacts with hydrogen sulfide ions to form zinc sulfide as shown in Equation 2.14. Due to this, a sulfidisation process for zinc recovery from the Merrill-Crowe process was developed by Dymov, Ferron, and Fleming (1997). The process was capable of precipitating 64% of zinc from solution when stoichiometric sulfide was added to solution and pH was not adjusted from that experienced after zinc cementation. The advantage of not adjusting pH is that the precipitated zinc sulfide would not need to be separated from the recovered cyanide before it is recycled to gold leaching.



The recovery of zinc in sulfidisation processes, where pH is adjusted, can result in high zinc recoveries as well as the ability to selectively recover zinc and copper as separate precipitates (Milosavljevic, Solujic, and Kravetz 2004; Littlejohn, Kratochvil, and Hall 2013). Littlejohn, Kratochvil, and Hall (2013) show that, when enough sulfide is present to react with both zinc and copper (Equation 2.14 and Equation 1.3 respectively), zinc can be precipitated as zinc sulfide at pH 7 (90%) with minimal copper precipitation (5%). The pH was then reduced to pH 4.5 to give a zinc recovery of 100% and copper recovery of 91%. Milosavljevic, Solujic, and Kravetz (2004) also demonstrated this selective precipitation with the use of organo-sulfur reagents. Nevertheless, the specific conditions used to achieve the selective separation of these metals are not mentioned.

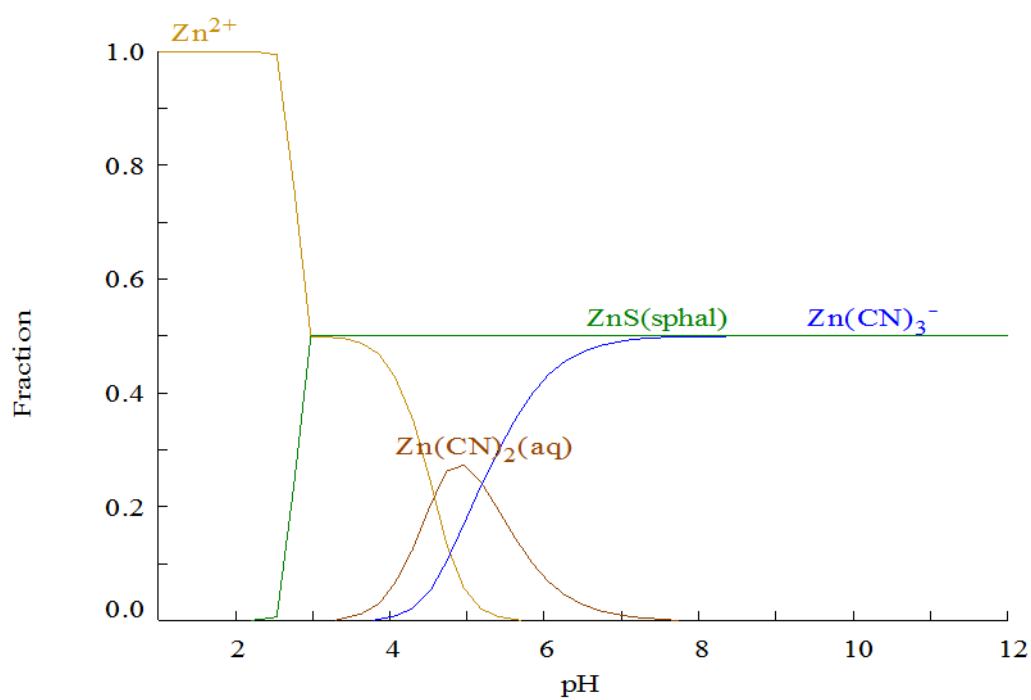
Thermodynamic analysis of a 20 mM copper and zinc solution with a CN:metal molar ratio of 4 and a S:Cu ratio of 0.5 (Figure 2.19) shows that zinc precipitates as zinc sulfide. Due to the sulfide dosing being stoichiometric with respect to copper (Equation 1.3), zinc precipitation is incomplete

because zinc sulfide (ZnS) requires twice as much sulfide per metal as copper sulfide (Cu<sub>2</sub>S). The model suggests that zinc precipitation will consume all of the sulfide and precipitate preferentially to copper above a pH of 2.5. Interestingly, at low pH (<2.5), zinc redissolves from the sulfide precipitate. This results in high copper recovery due to the release of sulfide from zinc. Also notable is that, in the pH region where zinc precipitation does occur, the precipitation is incomplete due to zinc requiring one sulfide molecule per zinc atom (Equation 2.14).

Thermodynamic analysis of a 20 mM copper and zinc solution with a CN:metal molar ratio of 4 and a S:Cu ratio of 1.0 (Figure 2.20) gave a similar result to Figure 2.19. The two notable differences being the complete precipitation of zinc as sulfide at high pH, due to excess sulfide, and increased zinc sulfide stability at low pH.

The thermodynamic model is in disagreement with the results of Dymov, Ferron, and Fleming (1997) as it suggests that zinc will react with all available sulfide at high pH. Dymov, Ferron, and Fleming (1997), however, only reported a zinc recovery of 64% when stoichiometric sulfide was added in accordance with Equation 2.14. The difference is potentially caused by slow kinetics of zinc sulfide precipitation.

a)



b)

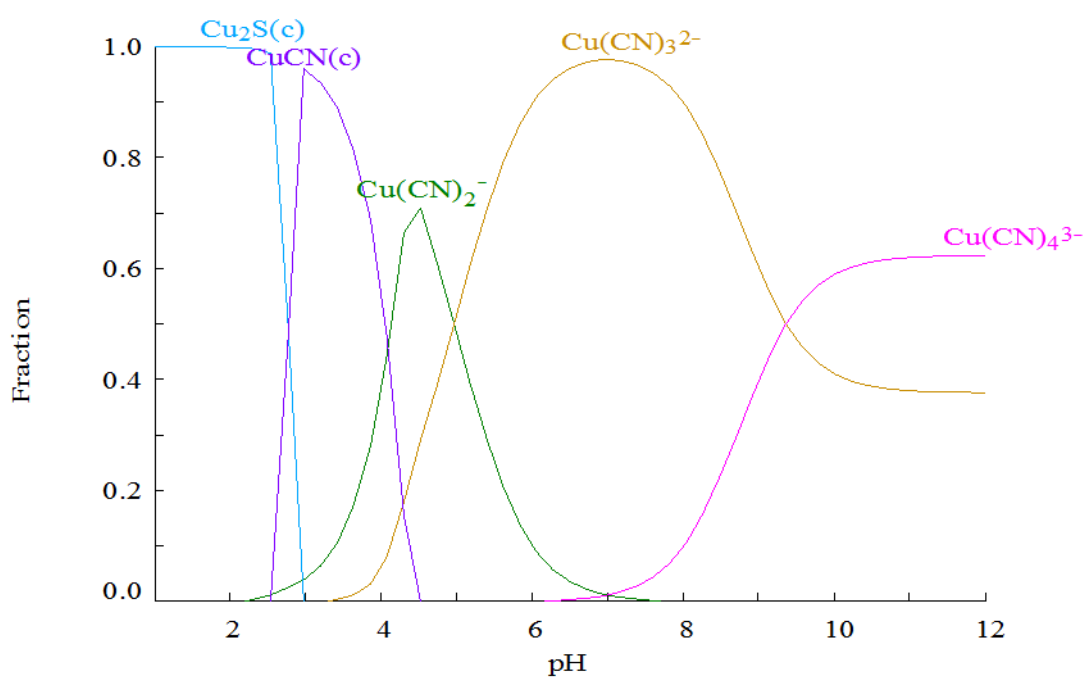
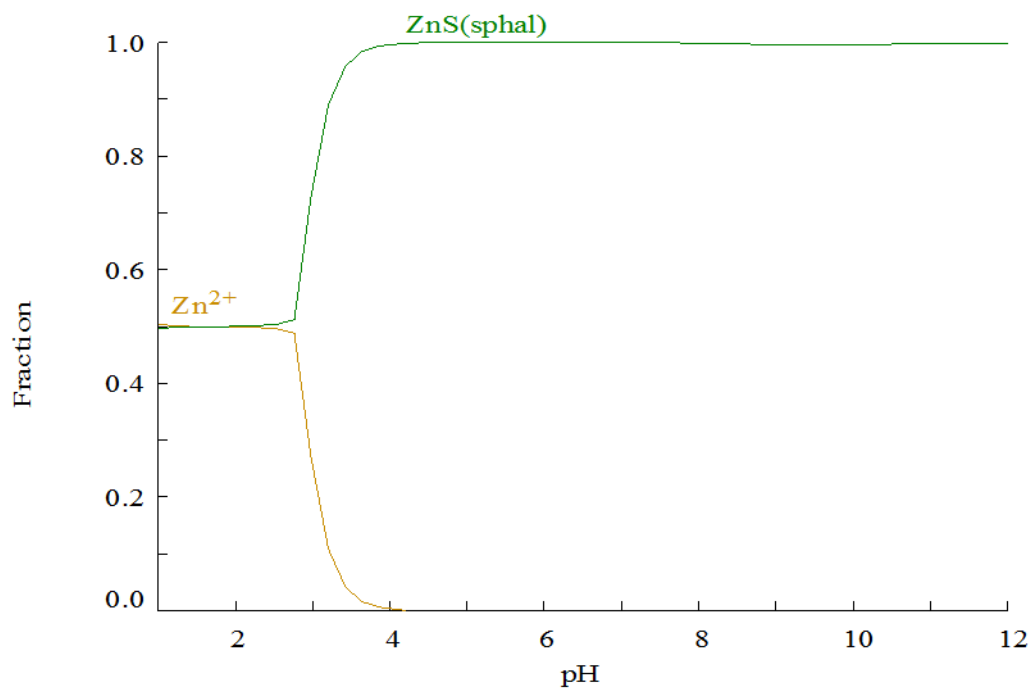


Figure 2.19 Thermodynamic determination of a) Zn (II) and b) Cu (I) speciation at different pH values for a 20 mM Cu (I) and Zn (II) solution with a CN:metal ratio of 4, a S:Cu ratio of 0.5, and where redox reactions are not considered.

a)



b)

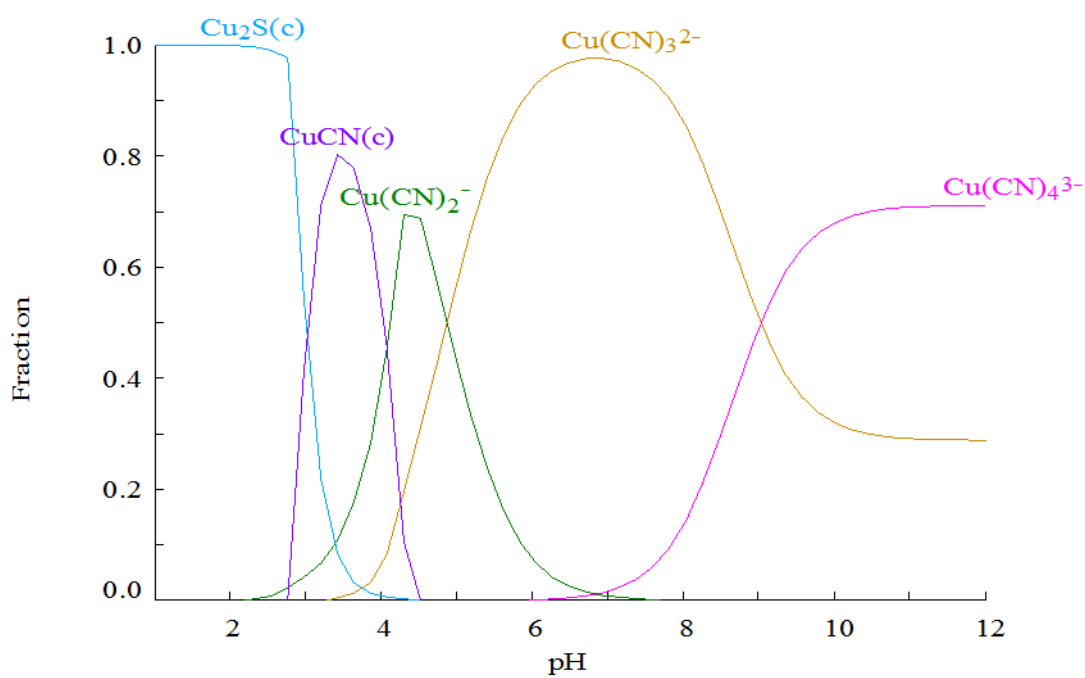


Figure 2.20 Thermodynamic determination of a) Zn (II) and b) Cu (I) speciation at different pH values for a 20 mM Cu (I) and Zn (II) solution with a CN:metal ratio of 4, a S:Cu ratio of 1.0, and where redox reactions are not considered

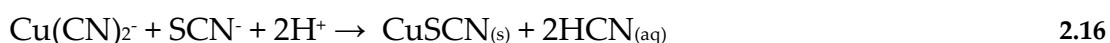
### **2.4.6 Cyanate**

Under acidic conditions, cyanate is hydrolysed to form bicarbonate and ammonium according to Equation 2.15 (Lorösch 2001). Due to this, cyanate is usually not seen in the cyanide recycle stream from sulfidisation processes (MacPhail, Fleming, and Sarbutt 1998). While this results in cyanate having little impact on sulfidisation, MacPhail, Fleming, and Sarbutt (1998) note that the hydrolysis of cyanate may slightly increase acid consumption for the process.



### **2.4.7 Thiocyanate**

Thiocyanate can react with copper cyanide species to form copper thiocyanate as shown for  $\text{Cu}(\text{CN})_2^-$  in Equation 2.16. The primary sulfidisation reaction (Equation 1.3) occurs preferentially to this reaction and hence thiocyanate has no impact on sulfidisation provided that sufficient sulfide is present in solution. As with iron cyanide, the reaction to produce a copper thiocyanate precipitate was utilised in the patent by Lower (1968) to minimise sulfide consumption during sulfidisation. Fleming (2005) also suggests the use of this technique as a way to prevent the build-up of thiocyanate in the recirculating solution from leaching to cyanide recovery and back to leaching.



Formation of copper thiocyanate occurs at a low pH (<3), with the reaction taking up to 30 minutes at a pH of 2 (Fleming and Trang 1998). The same authors reported that the reaction occurs faster at lower pH.

#### **2.4.8 Thiosulfate**

The impact of thiosulfate during sulfidisation is not reported in any of the available literature. Thiosulfate may, however, be present in reasonable quantities in the leach tails from cyanidation of sulfide ores (Breuer, Jeffrey, and Hewitt 2008; Hewitt et al. 2009). As noted in Section 2.3.3, thiosulfate may also be generated in small quantities during sulfidisation.

#### **2.4.9 Chloride**

Chloride is not expected to be a major species in gold cyanidation tailings, but is included in this review due to the potential for sulfidisation to be used after ion exchange resin recovery of copper cyanide. There are numerous proposals for using ion exchange to recover copper cyanide from gold cyanidation tailings as a way to concentrate copper cyanide before the two species are separated from each other (Fleming and Thorpe 2003; Bachiller et al. 2004; Dai, Breuer, and Jeffrey 2010).

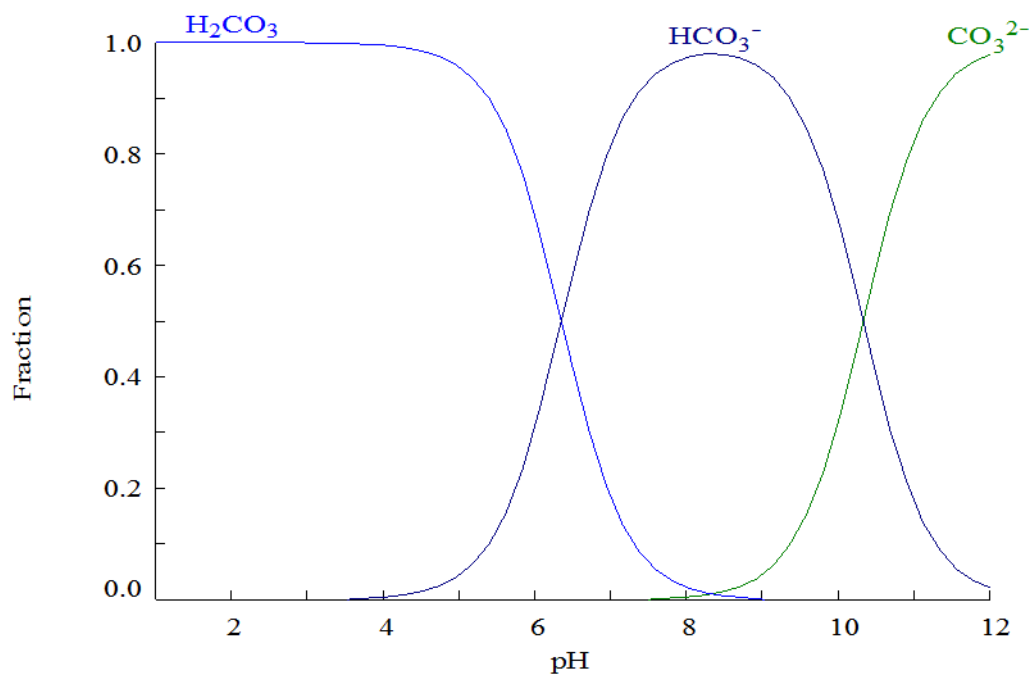
The use of ion exchange would result in a copper cyanide solution with a high chloride concentration. There was no work found in the available literature detailing what effect high chloride would have on sulfidisation from a cyanide solution.

#### **2.4.10 Carbonate**

The impact of carbonate on sulfidisation has not been reported in the available literature. This is presumably because it is not expected to interfere with the primary sulfidisation reaction (Equation 1.3). Thermodynamic analysis of a 20 mM copper and carbonate solution with a CN:Cu molar ratio of 4 and an S:Cu ratio of 0.5 (Figure 2.21) shows that carbonate species do not interfere with copper sulfide precipitation. Figure 2.21a does show, however,

that the presence of carbonate will increase acid consumption during the process, because it is converted to hydrogen carbonate as pH is reduced.

a)



b)

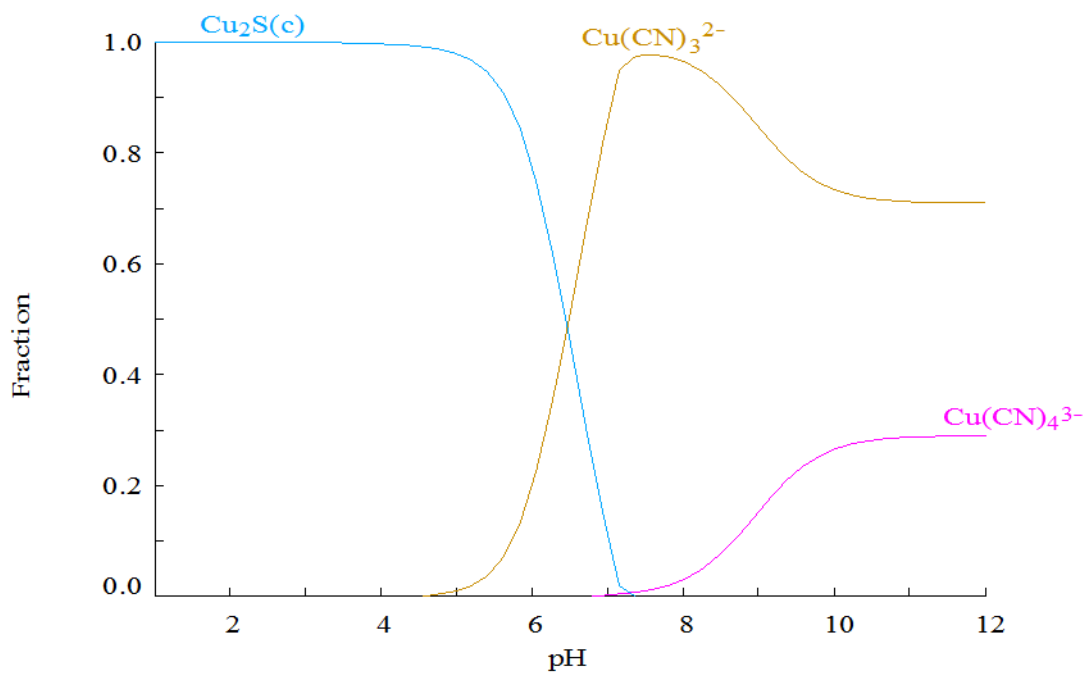


Figure 2.21 Thermodynamic determination of a)  $\text{CO}_3^{2-}$  and b) Cu (I) speciation at different pH for a 20 mM Cu (I) and  $\text{CO}_3^{2-}$  solution with a CN:Cu ratio of 4, a S:Cu ratio of 0.5, and where redox reactions are not considered.

## 2.5 Summary

The recovery of cyanide and copper from gold cyanidation tailings using sulfidisation has seen several commercial successes, and is fast becoming a popular technique to mitigate the environmental and economic problems caused by copper in gold ores. While this is the case, there are also numerous problems with the process such as high reagent consumption and low precipitate grades. A review of the literature on the process shows that there have been limited fundamental studies of the process and only a few impacting factors have been explored.

For most studies on sulfidisation, the key variables explored are pH and sulfide to copper molar ratio. It is well established that for successful operation of sulfidisation processes, the pH should be between 4 and 5. The majority of the literature shows that a sulfide to copper molar ratio just above 0.5 is sufficient for high copper and cyanide recovery. Industrial experience shows, however, that higher sulfide to copper molar ratios of near one are often required for sulfidisation processes. The reason for the difference is unknown and not addressed in the literature.

Other variables which may impact sulfidisation have been explored in a small number of studies. These studies showed that the copper concentration fed to sulfidisation and temperature both have no impact on the process. Studies on volatilisation showed that a hybrid sulfidisation and volatilisation process is not effective due to loss of sulfide as dihydrogen sulfide gas. The variables of cyanide to copper molar ratio and significant residence times have remained unexplored in the available literature.

The review of the available literature combined with thermodynamic modelling shows that different species that appear in gold cyanidation

tailings may respond differently during sulfidisation. Silver sulfide and zinc sulfide are shown to precipitate preferentially to copper sulfide in certain pH ranges for both past studies and thermodynamic modelling. There is, however, a disagreement between the literature and thermodynamic model around zinc recovery at high pH. Gold can form gold sulfide species at low pH, although copper sulfide formation is preferential to this.

Both iron and nickel do not appear to precipitate as sulfides. Iron can, however, produce copper iron cyanide precipitates, although the formation of copper sulfide occurs preferentially when sulfide is present. Nickel does not form a sulfide species during sulfidisation of a cyanide solution.

Cyanate can potentially increase acid consumption during sulfidisation due to its hydrolysis to form bicarbonate and ammonium. The presence of carbonate may also increase acid consumption due to the formation of hydrogen carbonate species. Both the impacts of thiosulfate and chloride remain unstudied with their impact on sulfidisation being unknown.

### **3 METHODS**

This chapter details the standard methods used for experiments and analysis during the course of the research. The results presented and discussed in subsequent chapters will refer to this chapter whenever such a method is used.

The first steps for every experiment was reagent and reactor preparation. After this, batch reactor sulfidisation experiments were performed with varying experimental conditions. Most experiments involved sulfidisation and acidification of cyanide solutions. Solutions were then sampled and analysed before reneutralisation and disposal of any waste.

#### **3.1 Reagents and solution preparation**

All reagents used in this research are shown in Table 3-1. Solutions for use in experiments were made up as shown in Section 3.1.1 to 3.1.5. The preparation of any solutions for use in analytical methods are discussed under their respective method in Section 3.6.

##### ***3.1.1 Distilled and deionised water***

Distilled water was obtained from a centralised distillation unit used at the CSIRO Australian Minerals Research Centre (AMRC) in Waterford, Perth, Western Australia. Deionised water for use in high performance liquid chromatography (HPLC) was generated using a Millipore Simplicity water purification unit.

Table 3-1 Details of metal salts used in experiments

Reagent	Formula	Purity	Supplier
Sodium cyanide	NaCN	>95%	Merck
Copper cyanide	CuCN	LR, >95%	Unilab
Potassium gold cyanide	KAu(CN) <sub>2</sub>	>95%	Johnson Matthey
Potassium silver cyanide	KAg(CN) <sub>2</sub>	>95%	Johnson Matthey
Potassium ferrocyanide	K <sub>4</sub> Fe(CN) <sub>6</sub> ·3H <sub>2</sub> O	AR	Analar
Potassium ferricyanide	K <sub>3</sub> Fe(CN) <sub>6</sub>	AR, >99%	Univar
Zinc sulfate	ZnSO <sub>4</sub> ·7H <sub>2</sub> O	AR, >99.5%	Univar
Nickel sulfate	NiSO <sub>4</sub> ·6H <sub>2</sub> O	LR, >96%	Unilab
Sodium sulfide	Na <sub>2</sub> S·9H <sub>2</sub> O	>98%	Sigma Aldrich
Sulfuric acid	H <sub>2</sub> SO <sub>4</sub>	95%-98%	Fluka Analytical
Potassium chloride	KCl	AR, >99.8%	Univar
Silver nitrate solution	AgNO <sub>3(aq)</sub>	0.1 M volumetric standard	Fluka Analytical
Sodium thiosulfate	Na <sub>2</sub> S <sub>2</sub> O <sub>3</sub> ·5H <sub>2</sub> O	AR, >99%	Riedel-deHaeu
Potassium thiocyanate powder	KSCN	AR, >99%	Analar
Potassium thiocyanate solution	KSCN <sub>(aq)</sub>	0.1 M volumetric standard	Rowe Scientific
Sodium perchlorate	NaClO <sub>4</sub> ·H <sub>2</sub> O	AR, >98%	Fluka Analytical
Sodium hydroxide pellets	NaOH	>97%	Sigma Aldrich
Sodium hydroxide solution	NaOH <sub>(aq)</sub>	50%-52%	Fluka Analytical
Industrial SART feed solution	Cu(CN) <sub>x-x+1</sub> , NaCN	Impure	Newcrest Mining Ltd
Industrial SART sulfide solution	Na <sub>2</sub> S	Impure	Newcrest Mining Ltd

### **3.1.2 Metal cyanide solutions**

For all experiments, metal cyanide solutions were made by weighing the required amount of solid metal salt and sodium cyanide and quantitatively transferring them to either a volumetric flask or a measuring cylinder.

For small reactor (Section 3.3.1.1) experiments, the solutions were always prepared in a volumetric flask and made up to the mark with distilled water. The solution was then transferred to the reactor with a 50 mL pipette. For large reactor (Section 3.3.1.2) experiments, the solutions were prepared in a 2000 mL measuring cylinder and made up to 1500 mL with distilled water. The solution was then poured into the large reactor. The initial solution concentrations were determined using the methods described in Section 3.6.

### **3.1.3 Sulfide solutions**

Sulfide solution was prepared by dissolving sodium sulfide nonahydrate ( $\text{Na}_2\text{S}\cdot 9\text{H}_2\text{O}$ ) in distilled water targeting a 500 mM sulfide solution. The initial solution concentrations were determined using the potentiometric titration with silver nitrate as described in Section 3.6.3.1. Sulfide solutions degraded over time, as shown in Figure 3.1, so a fresh solution was made every day as to limit the error associated with degradation of the sulfide. Since a new sulfide solution was made daily the degradation products were not determined.

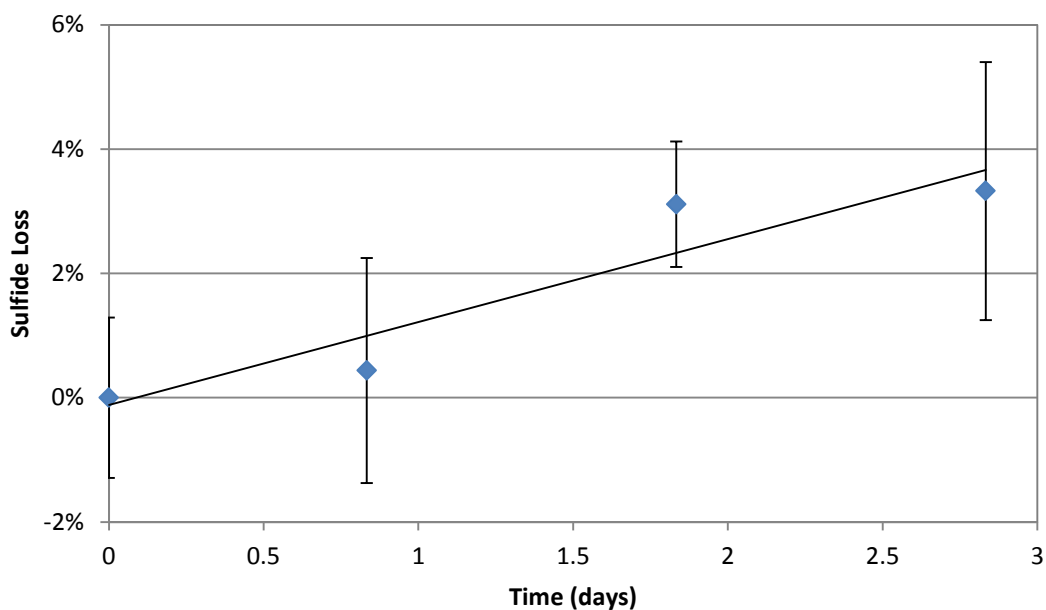


**Figure 3.1 Degradation of a sulfide solution over time starting with 406 mM of sulfide.**  
 Error bars show standard deviation over 3 samples.

### **3.1.4 Diluted sulfuric acid**

Diluted sulfuric acid ( $\text{H}_2\text{SO}_4$ ) solutions were made by first measuring the required amount of distilled water into a beaker. The desired volume of 98% sulfuric acid was then measured in a measuring cylinder and added to the distilled water. This technique was used to prevent any vigorous reaction caused by adding water to acid. The concentration of the acid solution was standardised by titration with a standardised sodium hydroxide solution.

### **3.1.5 Sodium hydroxide solution**

Approximately 1 M sodium hydroxide solution for use in experiments was made by dissolving sodium hydroxide pellets in distilled water. In situations where an exact concentration of sodium hydroxide was required, such as acid standardisation, the hydroxide was standardised with potassium hydrogen phthalate.

### 3.2 Reactor design

The focus of the reactor design was safety due to the potential for experiments to generate toxic hydrogen cyanide ( $\text{HCN}_{(g)}$ ) and dihydrogen sulfide ( $\text{H}_2\text{S}_{(g)}$ ) gasses. A small reactor (100 mL) and a large reactor (2000 mL) were used for these experiments.

The small reactor was made of glass with a plastic screw top lid. The lid had two openings for pH or ORP probes, two dual sided screw fittings for attaching tubes or drippers, and one tube for drawing samples. This design allowed for a cost effective method to safely perform experiments with a variety of different sealed reactor configurations. The small reactor is shown in Figure 3.2.



Figure 3.2 Small reactor.

The large reactor was a glass vessel with multiple “quickfit” openings in a glass lid. The openings were all sealed with glass stoppers during experiments except for one. For this opening, a rubber stopper was made with grooves in the edges to insert sample tubes, drippers, and probes. Every tube or cable that passed into the reactor through the grooves in the rubber stopper was wrapped in Parafilm® to create an airtight seal. The large reactor is shown in Figure 3.3.



**Figure 3.3 Large reactor with funnel in the top section for pouring sodium sulfide solution into the reactor.**

Mixing in both reactor vessels was achieved using a Teflon coated magnetic stirrer bar and magnetic stirrer. To confirm that complete mixing was occurring, solution mixing was tested by adding copper sulfate to an ammonia solution to form dark blue copper tetraamine. Figure 3.4 shows the reaction of one drop of copper sulfate, added at time zero, at 0.24 second intervals for the small reactor. The small reactor is completely mixed in less than one second. The large reactor is completely mixed in approximately three seconds.

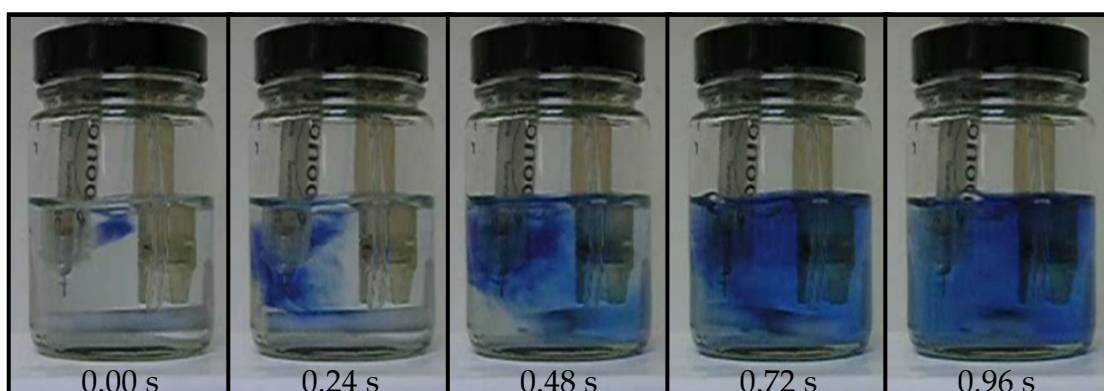


Figure 3.4 Small batch reactor mixing test at 0.24 second intervals.

### 3.3 Pre experiment setup

Each experiment was set up in the small or large batch reactor described in Section 3.2 with test solutions made as described in Section 3.1.

#### 3.3.1 Reactor configuration

##### 3.3.1.1 Small reactor

The general small batch reactor configuration used is shown in Figure 3.5. When setting up the reactor, an acid addition tube was connected to the outside of one of the two dual sided screw fittings on the reactor lid with a

dripper attachment on the other side of the fitting. The acid addition tube was then primed. Acid addition to the reactor is explained in Section 3.3.2. Exactly 50 mL of test solution and a magnetic stirrer bar were added to the reactor before the reactor lid was fastened on. A pH probe (TPS pH electrode model 121207) was calibrated at pH 7 and 4 and inserted into the reactor along with an ORP probe (Ionode Pt electrode model PRFO).

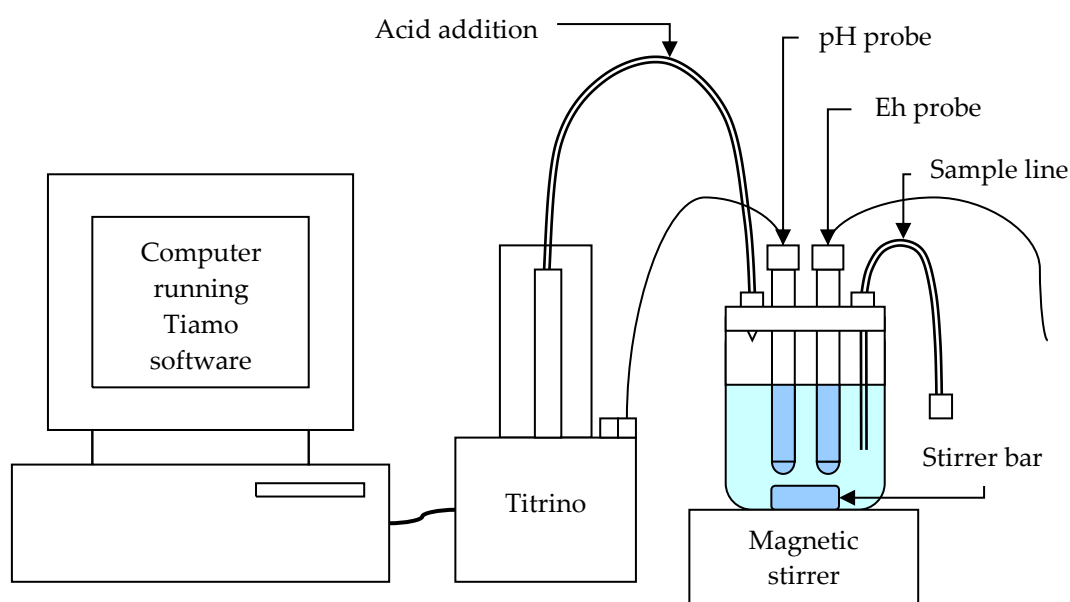


Figure 3.5 Schematic of reactor configuration for the small batch reactor (not to scale).

### 3.3.1.2 Large reactor

To set up the large reactor, 1500 mL of test solution was added to the reactor along with a magnetic stirrer bar. Vacuum grease was then applied to the top lip of the reactor and the lid was attached. The acid addition tube was primed and then inserted through one of the top openings in the reactor lid along with a sample line. Finally, the pH probe (TPS pH electrode model 121207) was calibrated at pH 7 and 4 and inserted into the reactor along with

the ORP probe (Ionode Pt electrode model PRFO). The rubber stopper with grooves was then sealed around the edges with Parafilm®.

Some experiments required the addition of oxygen to the reactor headspace before the experiment began. For these experiments, one of the glass stoppers was removed from one of the reactor lid openings and an oxygen tube was inserted. The reactor headspace was then purged with oxygen for five minutes before the pipe was removed and the glass stopper replaced.

### **3.3.2 Acid control and measurement**

For accurate control of pH, acid addition into the reactor was controlled using a Metrohm 716 DMS Titrino operated by Tiamo software. The use of the Titrino also allowed pH to be recorded at various stages during the reaction. A TPS pH electrode (model 121207) was used to measure pH.

The Tiamo software was configured so the acid addition rate was high initially ( $5 \text{ mL min}^{-1}$ ) until the solution pH was within two units of the target pH. From that point, acid addition was slowed from  $5 \text{ mL min}^{-1}$  to  $25 \text{ }\mu\text{L min}^{-1}$  as the endpoint was approached. This method limits overshooting of the target pH. Before a pH value was accepted, the system was allowed to equilibrate for 30 seconds to allow for any increases in pH due to solution buffering.

Even though the slow addition of acid helped prevent endpoint overshooting, acid addition was still problematic due to small droplets of acid forming on the acid addition dripper tip. This often resulted in overdosing when using concentrated acid. To overcome this issue, an acid addition tube that extended into the solution was trialled. Nevertheless, this was unsuccessful as precipitates would form on the tube tip causing pressure

build up and seal failure at the tube joining points. Ultimately, it was found that using the dripper with low concentrations of acid (~0.125 M) resulted in less overshooting of the target endpoint. Dilution due to acid addition was then accounted for when processing the results.

### **3.3.3 Oxidation/reduction potential (ORP) measurement**

Oxidation/reduction potential (ORP) was measured using an Ionode platinum electrode (model PRFO) with a Ag/AgCl reference. The probe was connected to a TPS WP-80 pH, mV, and temperature metre which gave the ORP reading in mV. An ORP reading was taken and recorded whenever samples were taken.

## **3.4 Main experimental procedures**

Three generic experimental procedures were used over the duration of the research. These procedures allowed for various scenarios to be tested during sulfidisation. Experiments were set up as shown previously in Section 3.3.

### **3.4.1 Staged sulfide addition experiments**

Experiments to determine the impact of changing sulfide addition at a fixed pH were performed as shown in Figure 3.6. Experiments started by titrating the solution with acid until a desired pH was achieved. Sulfide was then added to the reactor, which in turn causes a slight pH increase. To counteract this, the slurry was then titrated with acid back to the target pH before solution sampling was done as described in Section 3.5.1. At this point more sulfide could be added with the slurry once again being titrated with acid back to the target pH. Another sample could then be taken. This process was repeated for the number of sulfide addition samples required. At the end of the experiment either a solid sample was taken (Section 3.5.2) or sodium

hydroxide was added to the reactor to bring the pH up to 11 for safe disposal of the solution.

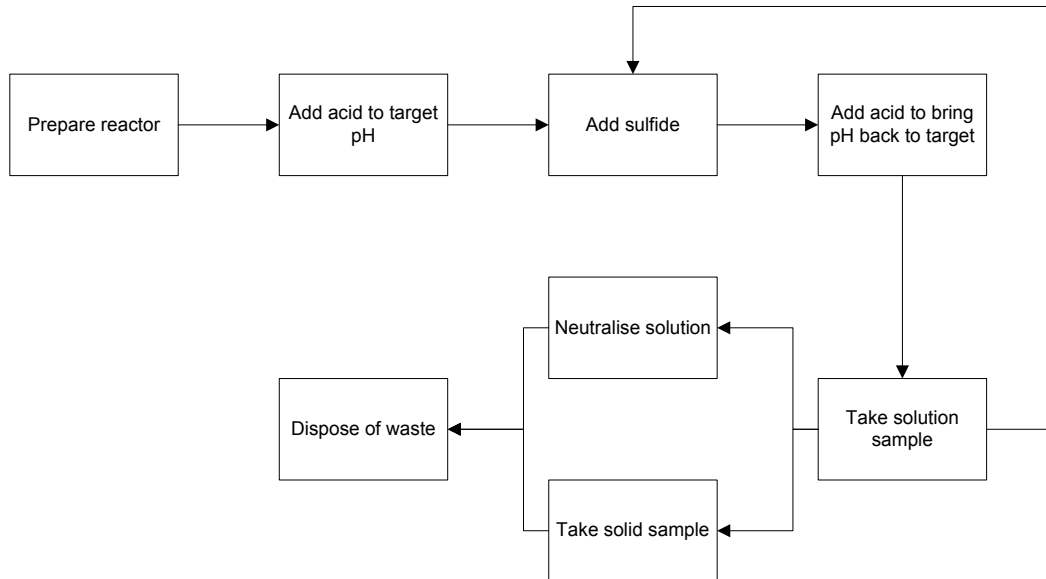


Figure 3.6 Staged sulfide addition experiment procedure.

### 3.4.2 Acid titration experiments

The method to determine the effect of pH on sulfidisation at a fixed sulfide addition is shown in Figure 3.7. Acid titrations were performed by initially adding sulfide to the reactor discussed in Section 3.3.1. Acid was added until the desired pH for solution sampling was achieved. The solution was sampled as described in Section 3.5.1. After sampling, the pH could then be reduced to a lower value and the solution sampled again. This could be repeated for as many pH values as required. Once all solution samples had been taken at the appropriate pH values, the solution could be dealt with in one of two ways. Either a solid sample was taken using the method described in Section 3.5.2, or sodium hydroxide was added to the reactor to bring the pH up to 11 for safe disposal of the solution.

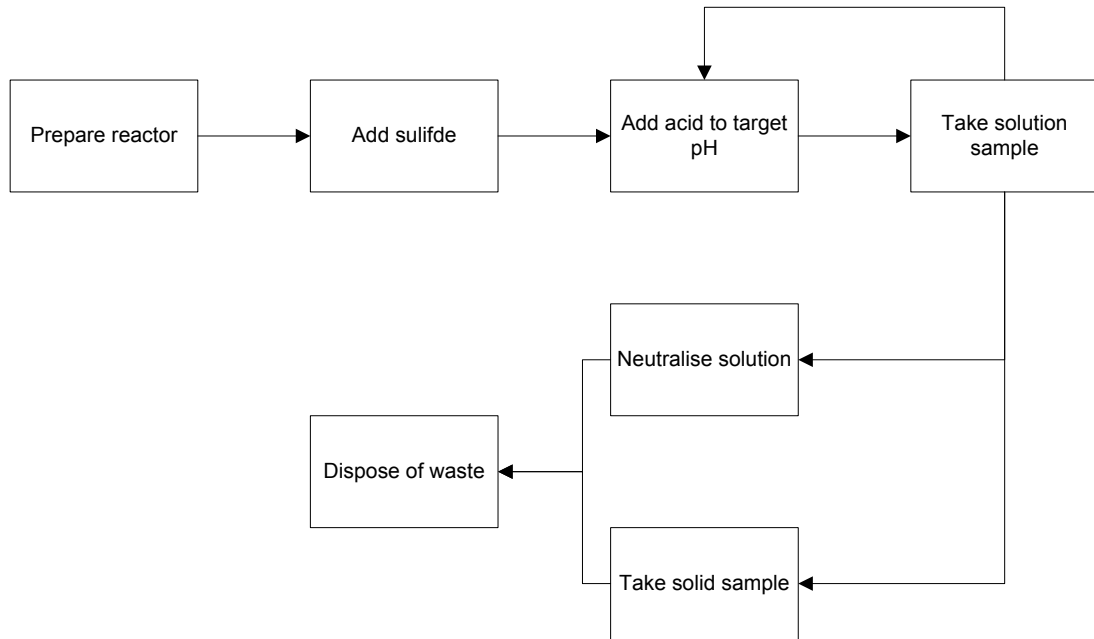
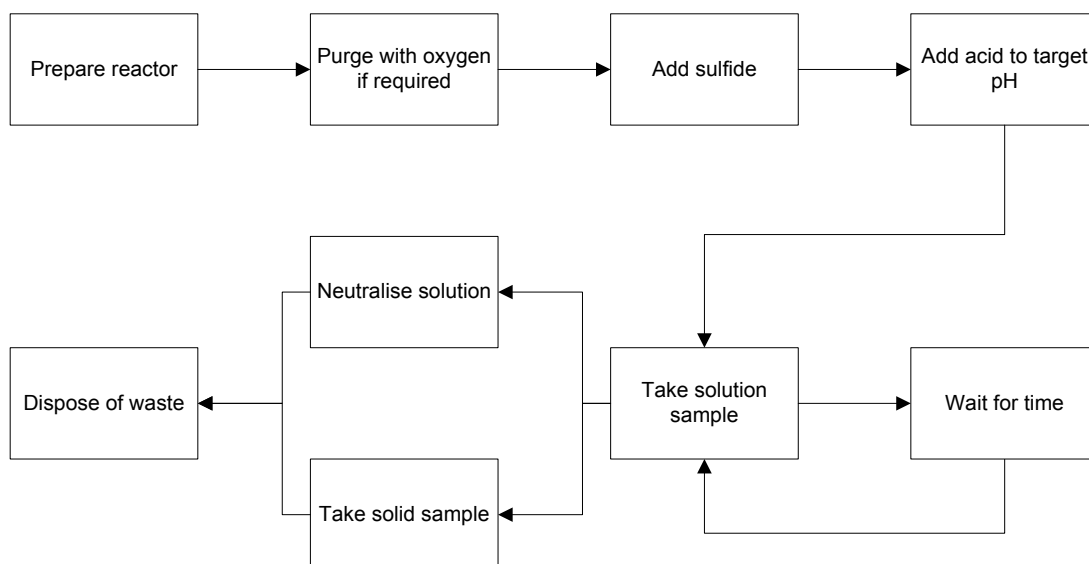


Figure 3.7 Acid titration experiment procedure.

### 3.4.3 Residence time experiments

Experiments to determine the impact of residence time on sulfidisation were performed as shown in Figure 3.8. To begin with, sulfide solution was added to the reactor which was prepared with the desired test solution as discussed in Section 3.3.1. The solution with sulfide was then titrated with acid to the desired pH. Once at the target pH the solution was left in the reactor with continuous agitation. Samples were taken at the desired time intervals as described in Section 3.5.1. During this time the Tiamo software continued to monitor pH. At the end of the time period either a solid sample was taken using the method described in Section 3.5.2 or sodium hydroxide was added to the reactor to bring the pH up to 11 for safe disposal of the solution.



**Figure 3.8 Residence time experiment procedure.**

For most of the residence time experiments, the pH changed over time. While this was acceptable for some experiments, some required the pH to be maintained within a certain range. To do this, an acid or base addition system was set up on the titrator depending on which way the pH moved. Sulfuric acid or sodium hydroxide was then added whenever the pH moved outside of the acceptable pH range for the experiment.

## **3.5 Sampling**

### **3.5.1 Solution sampling**

Solution sampling was performed by drawing just over 5 mL of slurry from the reactor through the sample line with a syringe. The sample was passed through a 0.45  $\mu\text{m}$  nylon syringe filter to remove the precipitate. Visual inspection showed that all precipitates were removed. Exactly 5 mL of filtered sample was taken and dispensed into a volumetric flask (10 mL) containing approximately 2 mL of 1 M sodium hydroxide. The sodium hydroxide converts dissolved hydrogen cyanide ( $\text{HCN}_{(\text{aq})}$ ) and dihydrogen sulfide ( $\text{H}_2\text{S}_{(\text{aq})}$ ) back to cyanide ( $\text{CN}^-$ ) and hydrogen sulfide ( $\text{HS}^-$ )

respectively, preventing loss of the two species as gasses. The high pH conditions also result in the solutions remaining stable for the period before analysis. Samples were then diluted by different factors depending on the analysis technique required and analysed using the methods described in Section 3.6.

### **3.5.2 Solids sampling**

Sampling of solids was only possible at the final pH and sulfide values in an experiment. This is due to the small amount of solids generated during the experiments requiring the whole volume of solids generated to be used in analysis. To sample the solids, the entire reactor contents were poured into a vacuum flask and filtered through Whatman type 42 ashless filter paper. The receiver of the vacuum flask contained caustic to reneutralise the solution and convert any hydrogen cyanide and dihydrogen sulfide back to their aqueous ions. The flask was also connected to the vacuum system, through a caustic scrubber, to capture any excess hydrogen cyanide or dihydrogen sulfide gas.

Solids were washed with distilled water and dried for 18 hours at 50 °C before being analysed. This temperature was selected as it would limit the likelihood of any oxidation of the precipitate. The solids were then analysed using methods described in Section 3.6.

## **3.6 Analytical techniques**

This section describes the different methods used to determine the concentrations of various species in the solutions and solids from experiments.

### **3.6.1 Atomic absorption spectrometry (AAS)**

Atomic absorption spectrometry (AAS) was used for the determination of copper concentration when there was no requirement to determine sulfide or other metal concentrations. The settings used were: acetylene flame with air as an oxidant; a wavelength of 327.4 nm; a slit width 0.5 nm; and standards of 2, 5, 10, and 20 mg L<sup>-1</sup> of copper. AAS standards were made by quantitative dilution of a 1 g L<sup>-1</sup> copper sulfate stock solution with 1 g L<sup>-1</sup> sodium cyanide solution. The large excess of cyanide during dilution converts copper (II) sulfates in the stock to copper (I) cyanides.

### **3.6.2 Inductively coupled plasma optical emission spectrometry (ICP-OES)**

Solutions containing mixed metals were analysed for copper, gold, silver, iron, zinc, and nickel or combinations of these using a Varian 735-ES inductively coupled plasma optical emission spectrometer (ICP-OES). The analysis was performed by the analytical support service staff at CSIRO Australian Minerals Research Centre (AMRC) in Waterford, Perth, Western Australia.

### **3.6.3 Potentiometric titration**

Potentiometric titration was performed by measuring the potential of a silver wire in solution while being titrated with standardised silver nitrate. This method was useful for the determination of sulfide and free cyanide concentration.

The silver nitrate used for titration was made up as a 1 mM or a 10 mM solution by quantitatively diluting a 0.1 M silver nitrate volumetric standard. Due to the possibility of the silver nitrate being degraded over time, the

concentration of the diluted solution was standardised using potassium thiocyanate volumetric standard (Equation 3.1). This was done by titrating potassium thiocyanate with the silver nitrate using the potential of a silver wire for endpoint detection.



### 3.6.3.1 Sulfide concentration

Potentiometric titration was used for the determination of sulfide concentration in solutions used for sulfide dosing during experiments. This is due to sulfide reacting with silver to form silver sulfide (Equation 3.2). Sulfide concentration was determined by titrating three 0.1 mL aliquots of sulfide solution with 0.01 M silver nitrate. This method, however, was not suitable for quantifying the often small amounts of sulfide in solutions sampled from experiments with other methods used for this purpose (Section 3.6.4.1). It should be noted here, that the sulfide value reported is for sulfur in the species  $\text{H}_2\text{S}_{(aq)}$ ,  $\text{HS}^-$ , and  $\text{S}^{2-}$ , which are present in varied quantities depending on pH (Section 2.3.1).



### 3.6.3.2 Cyanide concentration

Free cyanide concentration was determined using potentiometric titration with silver as free cyanide reacts to form silver cyanide (Equation 3.3). If copper cyanide is present, the fourth cyanide on copper will also titrate with silver at the same time as free cyanide (Equation 3.4). For this reason, the fourth cyanide associated with copper cyanide is also considered free. As the titration proceeds the third cyanide in the copper tricyanide ( $\text{Cu}(\text{CN})_3^{2-}$ )

complex reacts with silver (Equation 3.5). If sulfide is in the solution it will react before any cyanide (Equation 3.2).



Provided each species concentration is large enough, the inflection points for sulfide, free cyanide, and the third cyanide from copper cyanide are distinct in the titration. The solutions obtained from experiments, however, often had low sulfide and copper concentrations making separation of endpoints difficult. Hence, to measure cyanide concentration, the total amount of silver consumed for the reactions in Equations 3.2 to 3.5 was determined. As copper and sulfide concentrations can be ascertained with other methods (Section 3.6.1, 3.6.2, and 3.6.4.1), the amount of silver consumed by sulfide and cyanide associated with copper was then subtracted from the total silver consumed value. This method then gives the amount of silver consumed by free cyanide only, allowing the concentration of free cyanide to be determined. The calculation steps are shown in the Appendices (Section 10.2).

The presence of thiosulfate in the samples may reduce the sensitivity of the determination through the formation of silver thiosulfate complexes (Breuer, Sutcliffe, and Meakin 2011). The authors showed, however, that thiosulfate does not interfere with the determination of cyanide concentration. Breuer, Sutcliffe, and Meakin (2011) also show that thiocyanate and cyanate have no impact on the technique.

### 3.6.4 High performance liquid chromatography (HPLC)

#### 3.6.4.1 Mixed species quantification

High performance liquid chromatography (HPLC) was used for the determination of sulfide, chloride, thiocyanate, thiosulfate, copper, and iron. A Waters 2695 Separation Module was used with Dionex IonPac AS16 analytical column and the elution gradient shown in Table 3-2. Species detection was done with a Waters 2996 Photodiode Array Detector which measured UV absorbance across the range 190 nm to 400 nm with a resolution of 1.2 nm. Single point calibrations were then used to quantify sulfide, chloride, thiocyanate, thiosulfate concentrations along with copper and iron. The time, wavelength at maximum absorbance, and standard concentration for analysis is shown in Table 3-3.

**Table 3-2 HPLC elution gradient for sulfide quantification.**

Time	Water	100 mM NaClO <sub>4</sub> + 10 mM NaCN	10 mM NaOH	500 mM NaClO <sub>4</sub>
0	89%	2%	1%	8%
15	52%	2%	1%	45%

**Table 3-3 HPLC residence time, wavelength, and standard concentration for sulfide, thiocyanate, thiosulfate, copper, and iron quantification.**

Species	S <sup>2-</sup>	SCN <sup>-</sup>	S <sub>2</sub> O <sub>3</sub> <sup>2-</sup>	Cu	Fe
Time (min)	3.9	5.9	9.1	14.2	17.9
Wavelength (nm)	230	192	214	230	214
Standard concentration	Varied (~10 mM)	9.8 mM	10 mM	100 ppm	100 ppm

HPLC eluents containing sodium perchlorate and sodium hydroxide were made from sodium perchlorate powder (Table 3.1) and sodium hydroxide solution respectively. Sodium cyanide in eluents was added as sodium cyanide powder.

Thiocyanate standards were made by quantitative dilution of sodium thiocyanate volumetric standard. Thiosulfate and chloride standards were made by weighing the appropriate amount of their respective solid powders (Table 3-1) and quantitatively transferring it to a volumetric flask. The solutions were then made up to the mark using distilled water.

Sulfide standards were made by quantitative dilution of more concentrated sulfide solutions described in Section 3.1.3. These sulfide solutions had known concentrations obtained from potentiometric titration with silver nitrate as described in Section 3.6.3. As previously mentioned, the sulfide value reported is for the species  $\text{H}_2\text{S}_{(\text{aq})}$ ,  $\text{HS}^-$ , and  $\text{S}^{2-}$ , which are present in varied quantities depending on pH.

A  $100 \text{ mg L}^{-1}$  copper and iron standard solution was made by weighing the appropriate amount of copper cyanide and potassium ferrocyanide powder and quantitatively transferring it to a volumetric flask. The solution was then made up to the mark using approximately  $1 \text{ g L}^{-1}$  sodium cyanide solution.

#### *3.6.4.2 Cyanide quantification*

Quantification of cyanide was also trialled using high performance liquid chromatography (HPLC). The method trialled used a Dionex IonPac AS17-C analytical column with a Waters 2465 Electrochemical Detector (amperometric detector). A guard column was also used to prevent copper cyanides entering the analytical column. Cyanide was easily quantified in

solutions which contained no sulfide. Trace amounts of sulfide, however, significantly impacted the results due to the sulfide eluting at the same speed as cyanide and amperometric detection being highly sensitive to sulfide.

Attempts were made to separate sulfide and cyanide in the analytical column so they did not interfere with each other during detection. Changes to the technique had limited success and separation was only achievable with longer retention times which resulted in significant peak broadening. The poor success of separating sulfide and cyanide with the available columns meant a HPLC method for cyanide detection was rejected. It should be noted, however, that sulfide and cyanide are separable using HPLC with other column types (DIONEX Corporation 2008).

Sulfate could also be detected during the cyanide detection method development. This may have been useful to detect sulfate generated during experiments. Nevertheless, due to the use of sulphuric acid in the experiments, any sulfate generated would be difficult to detect in the large background concentration of sulfate from the acid.

### **3.6.5 *Ion selective electrode***

Quantification of sulfide and cyanide was trialled using a TPS uniPROBE ion selective electrode. The module allowed for the tip of the unit to be changed for selective determination of either species. It was found, however, that both species interfered with one another during detection. Hence, ion selective electrodes were not used in this study.

### **3.6.6 *Carbon and sulfur analysis in solids***

Solids were analysed for sulfur and carbon using a Labfit Pty Ltd CS-2000 Carbon and Sulfur Analyser. The analysis was performed by the analytical

support service staff at CSIRO Australian Minerals Research Centre (AMRC) in Waterford, Perth, Western Australia.

### **3.6.7 X-ray diffraction (XRD)**

X-ray diffraction (XRD) was used to determine the minerals in the precipitate. A PANalytical Empyrean X-ray Diffractometer system was used for this purpose with the following settings: scanning range from 5 °2θ to 90 °2θ, a step size of 0.026 °2θ, a scan time of 90 minutes, a fixed divergence slit at 0.5°, a cobalt Kα source, and use of a secondary monochromator. The XRD patterns were analysed using PANalytical HighScore Plus version 3.0.5 with the databases ICSD 2011-1 and PDF-2 2000. When matching XRD patterns to the database the search was narrowed to minerals containing copper, sulfide, carbon, nitrogen, and combinations of these.

### **3.6.8 Scanning electron microscopy (SEM)**

A JEOL JSM-7001F field emission scanning electron microscope (SEM) was used to determine the elemental ratios in the precipitate. Of particular interest was the amount of sulfide, copper, carbon, and nitrogen.

Before SEM, the precipitates were carbon coated to provide a conductive surface. The SEM was then used at magnifications of around 20000x with working distances between 10 and 10.5 mm. High quality images were captured at magnifications of 25000x.

Due to carbon coating of the precipitate, it was not possible to determine the amount of carbon in the precipitate meaning any cyanide in the precipitate would result in the mass fractions of elements in the material being measured incorrectly. Platinum coating was also trialled, but the peak caused by platinum also masked any carbon present.

To overcome the inability to detect carbon, the assumption was made that for any nitrogen present there must be a similar amount of carbon. This is due to nitrogen in the sample being likely to only be present as cyanide. The elemental mass percentages for any precipitates with nitrogen were then rebalanced to take the missing carbon into account.

## 4 MODELLING SULFIDISATION CHEMISTRY

### 4.1 Introduction

A fundamental model of sulfidisation for cyanide and copper recovery has never been reported. This is presumably due to sulfide to copper molar ratio (S:Cu ratio) and pH being considered the key variables in the process, with their individual impact on the process being well understood. Nonetheless, with no fundamental model of the process, there is limited understanding of how process variables interact and the impact of process variables when they are not set at their respective optimums. In addition, modelling of sulfidisation may help to elucidate some of the problems experienced in some industrial sulfidisation processes, such as formation of CuS in the process instead of Cu<sub>2</sub>S (Guzman et al. 2010). Finally, as such a model would also provide a useful benchmark to compare impurity studies to, the building of a fundamental model of sulfidisation for cyanide and copper recovery was considered the best starting point for this research. It should be noted here that as the kinetics of the primary sulfidisation reaction are fast, the model developed is for when the system is at equilibrium with respect to Equation 1.3.

Factorial experimentation is an excellent way to create mathematical models of systems, as it delivers a model that considers both the individual effect of factors and the effect of interacting factors (Bas and Boyaci 2007). Hence, a factorial design was selected to study sulfidisation of copper cyanide solutions. There are a large variety of factorial designs which are available for modelling systems and the selection of the most appropriate one is often based on a trade-off between accuracy and number of experiments required. Due to this, determination of important factors in sulfidisation was the first stage completed in modelling the system.

## **4.2 Determination of important model factors**

Before conducting factorial design experiments examining sulfidisation, screening experiments were performed to determine which variables are most important to sulfidisation processes. Screening was also used to determine the range of values which the optimum is likely to fall within and hence increase the accuracy of the model (Bas and Boyaci 2007). The factors which appeared to have the largest impact on sulfidisation were then chosen for use in the factorial design with the reasoning for each selection explained with the screening results. Based off the literature review (Section 2.3), the factors screened were pH, sulfide to copper molar ratio (S:Cu ratio), cyanide to copper molar ratio (CN:Cu ratio), initial copper concentration, and residence time.

### **4.2.1 Experimental Methods**

Copper cyanide solutions for the screening experiments were made using the method described in Section 3.1.2. Experiments were then set up using the small reactor (Section 3.2) as per Section 3.3.1.1. Finally, all screening experiments were performed using the method in Section 3.4.2, except when determining the effect of sulfide to copper ratio which used the method in Section 3.4.1.

During the screening experiments, solutions were sampled (Section 3.5.1) and analysed for copper using AAS (Section 3.6.1). Copper concentration and acid addition were the only responses examined during screening as these responses give a good indication of a factors impact on sulfidisation.

#### 4.2.2 Effect of pH

The effect of pH on sulfidisation of copper cyanide solutions is well known and mentioned in many SART papers (Barter et al. 2001; Dreisinger et al. 2008; Ford, Fleming, and Henderson 2008). As selection of pH for sulfidisation is driven by maximising recovery of cyanide and copper, whilst minimising the acid consumption, pH is an obvious parameter to include as a factor in the factorial design.

Although pH can be selected as a factor without the requirement of screening, a screening experiment was performed to determine over what pH range the factorial design should be performed. Figure 4.1 shows the copper recovery at different pH values for a 31.4 mM (~2000 ppm) copper cyanide solution with a CN:Cu ratio of 3 and S:Cu ratio of 0.5.

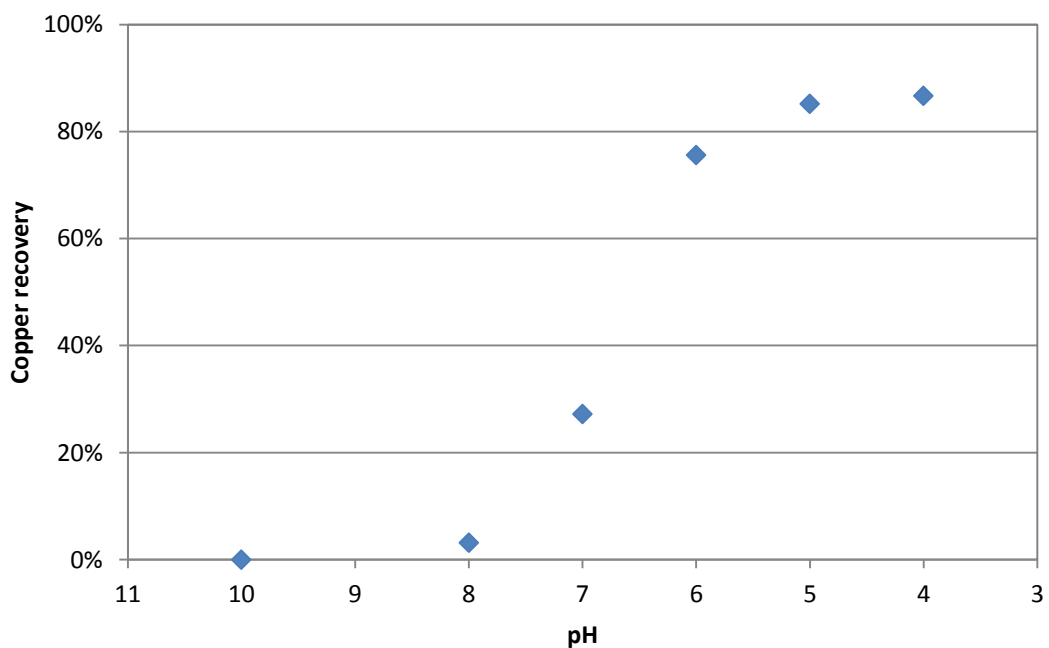


Figure 4.1 Copper recovery at various pH values for a solution initially containing 31.4 mM copper with a CN:Cu ratio of 3 and S:Cu ratio of 0.5.

Copper recovery began to plateau between pH 6 and 5. Hence, based on the screening result the upper pH value selected for the factorial design was pH 5.5 as below this value copper recovery should be high (> 80%). A pH value of four was selected as the lower pH value due to the potential for copper cyanide precipitates to be generated at pH values lower than four if sulfide addition is insufficient to precipitate all of the copper. The generation of copper cyanide precipitate would result in high recoveries and potentially provide misleading results in the factorial design. Also, the generation of copper cyanide precipitate in an industrial scale sulfidisation process may reduce the marketability of the precipitate to copper smelters (MacPhail, Fleming, and Sarbutt 1998) and should be avoided.

#### **4.2.3 Effect of sulfide to copper ratio**

S:Cu ratio directly effects copper and cyanide recovery during sulfidisation as per Equation 1.3. As discussed in Section 2.3.3, however, a slight excess of sulfide compared to the stoichiometric value from Equation 1.3 may be required to achieve complete copper and cyanide recovery. Due to the relationship between copper recovery and sulfide addition from Equation 1.3, S:Cu ratio is an important factor to include in the factorial design. Nonetheless, a screening experiment was still required to determine the range to set for the factorial design.

To determine the impact of S:Cu ratio, sulfide was incrementally added to a 29.8 mM (~2000 ppm) copper solution with a CN:Cu ratio of 3 and pH of 5. Figure 4.2 shows the copper recovery as sulfide was added. The requirement for a slight excess of sulfide is apparent from the results, as at a S:Cu ratio of 0.5, copper recovery is only approximately 85%; whereas, by an S:Cu ratio of 0.62, copper recovery is 98%. These results agree with the laboratory and pilot scale data presented in the literature (Section 2.3.3). A requirement for a

large excess of sulfide, as seen at the Telfer and Yanacocha SART plants, was not observed (Section 2.3.3).

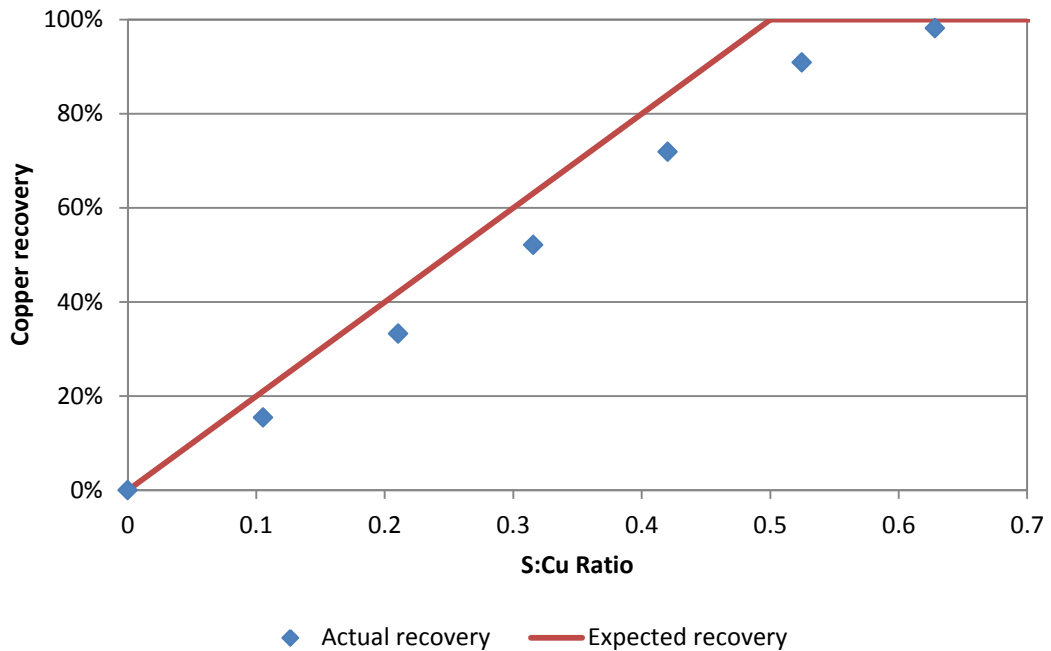


**Figure 4.2** Copper recovery at various S:Cu ratios for a solution initially containing 29.8 mM copper with a CN:Cu ratio of 3 and pH of 5. Expected recovery is based on Equation 1.3.

The range selected for S:Cu ratio in the factorial design was between 0.4 and 0.6. The upper bound of 0.6 was selected as copper recovery should be near 100% by this value. Above this S:Cu ratio recovery changes would become incrementally smaller, resulting in little value of extra recovery compared to the amount of sulfide added. While a higher lower bound (0.45) could be selected, as this would make copper recovery above 80%, the value of 0.4 was chosen because this puts the stoichiometric value of 0.5 in the centre of the design range.

#### 4.2.4 Effect of cyanide to copper ratio

Cyanide to copper molar ratio (CN:Cu ratio) has not been studied in the available literature. This is presumably because cyanide to copper ratio is seen as uncontrollable during sulfidisation due to its value being determined by the cyanide requirements during gold leaching. Figure 4.3 shows the effect of CN:Cu ratio on copper recovery in solutions containing initial targets of 31.4 mM (~2000 ppm) copper with a S:Cu ratio of 0.5 and at varied pH.

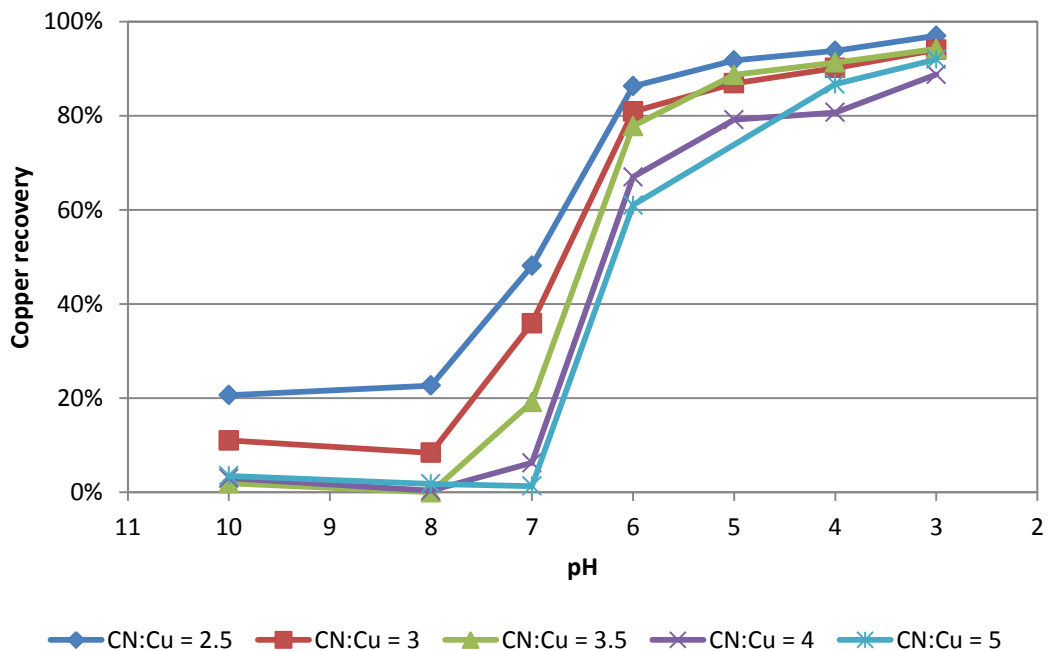
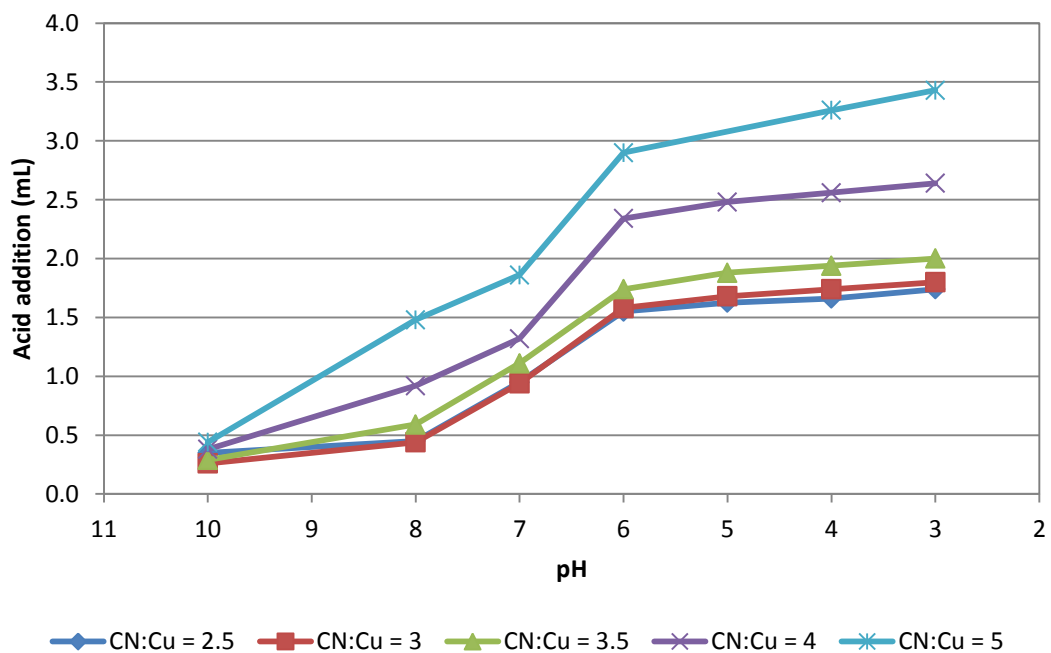


Figure 4.3 Copper recovery at various pH values for solutions initially containing 31.4 mM copper with varied CN:Cu ratios and S:Cu ratios of 0.5.

At high pH it is apparent that CN:Cu ratio can have a significant impact on copper recovery. The impact is also present, but to a lesser degree, at the lower pH values. Figure 4.3 clearly shows that low cyanide to copper ratios maximises copper recovery.

CN:Cu ratio also impacted the acid requirements during the experiments. Figure 4.4 shows the acid addition to the reactor during the same experiments as shown in Figure 4.3. For all data points below pH 10, acid addition is increased when more cyanide is present. This agrees with the primary sulfidisation equation (Equation 1.3). The increased impact of CN:Cu ratio at low pH is due to more cyanide being released from copper and consuming acid at low pH.



**Figure 4.4 Acid addition at various pH values for solutions initially containing 31.4 mM copper with varied CN:Cu ratios and S:Cu ratio of 0.5.**

CN:Cu ratio was included in the factorial design due to the clear impact of CN:Cu ratio on both copper recovery and acid addition. A lower CN:Cu ratio boundary of 3 was selected for the factorial design due to cyanidation typically operated with some free cyanide in the tails (CN:Cu > 3). A CN:Cu ratio of 5 was selected as the upper boundary as most processing operations try to limit the amount of cyanide added to solution to reduce costs.

#### 4.2.5 Effect of initial copper concentration

The impact of copper concentration was screened using four solutions with varied copper concentrations, a CN:Cu ratio of 4, S:Cu ratio of 0.5, and a pH value of 5. The copper concentrations of the initial solutions were 7.9 mM (~500 mg L<sup>-1</sup>), 18.2 mM (~1200 mg L<sup>-1</sup>), 30.3 mM (~1900 mg L<sup>-1</sup>), and 62.9 mM (~4000 mg L<sup>-1</sup>).

Copper concentration had only a small impact on copper recovery during sulfidisation. Copper concentration, however, impacted acid addition as shown in Table 4-1. While copper concentration does impact the acid consumption, the initial copper concentration has no impact on the ratio of acid consumed (mmol) per initial amount of copper (mmol). Hence, initial copper concentration does not need to be included in the factorial design, provided acid consumed is always considered as acid consumed per initial amount of copper. By removing copper concentration as a factor, the amount of experiments required in the factorial design is reduced.

**Table 4-1 Acid addition and copper recovery during sulfidisation for solutions (50 mL) containing varied amounts of copper with a CN:Cu ratio of 4, S:Cu ratio of 0.50, and a pH of 4.**

Copper concentration (mM)	Copper recovery	Acid addition (mmol)	Acid addition (mmol) / initial copper (mmol)
7.9	No sample	0.83	2.10
18.2	93.6%	2.03	2.22
30.3	94.1%	3.20	2.11
61.0	93.8%	6.57	2.15

An interesting outcome during screening of initial copper concentration is that at a copper concentration of 7.9 mM, the precipitate passes the 0.45  $\mu\text{m}$  filter. This is not an issue with more concentrated solutions. This result indicates that whatever the mechanism of crystallisation, larger precipitate crystals can be formed at higher copper feed concentrations. This result is also apparent through visual inspection of the precipitates in the reactor. While this effect has an impact on seeding and crystallisation reactor selection, it is outside the scope of this research.

#### **4.2.6 Effect of time**

Screening experiments for time showed that, over time, the recovery of copper, pH, and the amount of excess sulfide in solution decreased. The cause of this effect was unknown at the time of this work and not mentioned in the literature. The effect was, however, similar to the problems seen on some industrial SART plants (Section 1.3.5 and Section 2.3.3), where significant amounts of excess sulfide is required to maintain high copper recovery. As residence time may potentially explain the cause of some industrial problems, the effect of residence time is examined in depth in Chapter 6 and subsequently in Chapter 7. Due to the cause of the effect being unknown, residence time was excluded as a factor in the factorial design, with all subsequent investigations in Chapters 4 and 5 conducted to explore sulfidisation chemistry at initial conditions only.

#### **4.2.7 Temperature**

Temperature was not screened as a factor due to the fast kinetics of precipitation making temperature unlikely to impact the process. Temperature can affect volatilisation of hydrogen cyanide gas (Estay et al. 2012), but the use of a sealed reactor in the experiments makes this potential

impact of temperature difficult to study. The use of gas scrubbing on an industrial scale also results in no loss of cyanide from the process by this mechanism.

### **4.3 Response models**

#### **4.3.1 Experimental design**

Based on the factors to be tested, the number of experiments required for different factorial designs were calculated. Most of these designs are similar to that of a full three level factorial design with some design points removed to reduce the number of experiments required (Bezerra et al. 2008). As only three factors had been selected, a full factorial design did not require many more experiments than the reduced factorial designs. The use of a full factorial design also generates a more accurate model. Hence, a full factorial design was selected to model the system. Centre point replication was used in the design as a means of determining experimental error. This gave a total of 31 experiments.

Low, centre, and high values for each factor were set based on the values found during screening (Section 4.2). Figure 4.5 shows a graphical representation of the experimental design where each black dot represents an experiment with the conditions represented on the three axes. The centre point experiment is coloured blue. Copper concentration was maintained at 19.6 mM ( $\sim 1250 \text{ mg L}^{-1}$ ) for the experiments.

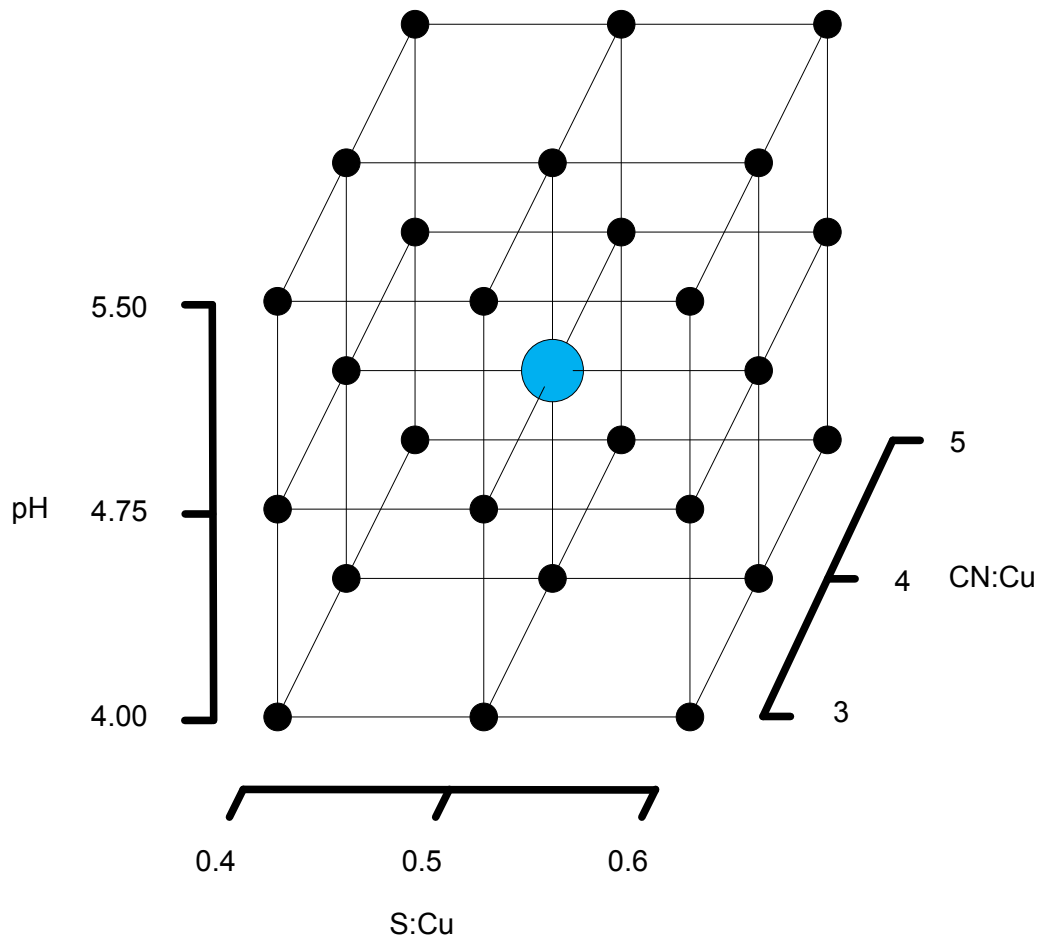


**Figure 4.5 Graphical representation of factor combinations for experiments in the factorial design.**

For calculation of the response models, the factors were coded with CN:Cu ratio, S:Cu ratio, and pH coded to factors A, B, and C respectively. Coding of the variables is required for model fitting, as all variables are changing over the same range of -1 to +1 (Anderson and Whitcomb 2005). For the coded factors, the low values were given a value of -1, the centre values were given a value of 0, and the high values were given a value of +1. An example coding equation for CN:Cu ratio is shown in Equation 4.1.

$$A = \left( \frac{2}{CN:Cu_{high} - CN:Cu_{low}} \right) \left( CN:Cu_{actual} - \frac{CN:Cu_{high} + CN:Cu_{low}}{2} \right) \quad 4.1$$

$$A = \left( \frac{2}{5 - 3} \right) \left( CN:Cu_{actual} - \frac{5 + 3}{2} \right)$$

Four responses were measured, these were: copper recovery, cyanide recovery, acid consumed per initial copper concentration, and oxidation/reduction potential (ORP). The first three of these responses were selected due to their impact on SART efficiency. The last, ORP, was chosen to determine if ORP could be used to monitor and control SART in any way. For every response a variety of models were trialled using the software Design Expert 8 (Stat-Ease Inc 2011). The best fitting model for the response was selected. In every case, this was a four dimensional second order polynomial. The standard response equations for coded and actual responses are shown in Equation 4.2 and Equation 4.3 respectively. In these equations  $c_x$  and  $a_x$  are the coefficients for each term. All statistically insignificant terms were then removed from each response model to simplify the equations.

$$\begin{aligned} Response = c_1 + c_2 \times A + c_3 \times B + c_4 \times C + c_5 \times A \times B + c_6 \\ \times A \times C + c_7 \times B \times C + c_8 \times A^2 + c_9 \times B^2 + c_{10} \\ \times C^2 \end{aligned} \quad 4.2$$

$$\begin{aligned} Response = a_1 + a_2 \times CN:Cu + a_3 \times S:Cu + a_4 \times pH + a_5 \\ \times CN:Cu \times S:Cu + a_6 \times CN:Cu \times pH + a_7 \times S:Cu \\ \times pH + a_8 \times CN:Cu^2 + a_9 \times S:Cu^2 + a_{10} \times pH^2 \end{aligned} \quad 4.3$$

Simplified analysis of how different factors impact the response is possible through examination of the coded response model (Anderson and Whitcomb 2005). Larger values of  $c_x$  in the coded response model indicate a greater impact of that factor on the response. Positive coded  $c_x$  coefficients indicate a

proportional relationship between the factor and the response with negative coded  $c_x$  coefficients indicating an inverse relationship.

Analysis of variance (ANOVA) is also provided with the response models as a way to assess the variation in the model from changing factors compared to variation caused by experimental error (Bezerra et al. 2008). ANOVA was performed using the software Design Expert 8 (Stat-Ease Inc 2011). There are several important values obtained from the ANOVA such as the model and lack of fit significance probability values (p-values) as well as the coefficient of determination ( $R^2$ ). Generally, p-values less than 0.05 are considered as statistically significant while those above 0.1 are insignificant. Each response model should have high significance to show it has an overall good fit.

As well as the p-values, the coefficient of determination also shows how well the data fits the model with values closer to one being better. If the coefficient of determination is multiplied by 100, the number represents the percentage of total variation in the system explained by the model. The actual data points from experiments are shown on the response surface graphs represented by red dots. This gives a visual method of showing the fit of the model to the experimental data. The lack of fit (LoF) value shows if the variation between the model and data points can be explained by experimental error and should be statistically insignificant. If lack of fit is significant, then some other untested or uncontrolled factor may be affecting the system.

#### **4.3.2 Experimental Methods**

Factorial design solutions were prepared using the methods described in Section 3.1.2. The experiments were then performed in the small reactor (Section 3.2) configured as described in Section 3.3.1.1 and with the method

described in Section 3.4.2. A new experiment was performed for every data point to avoid any interference caused by residence time, as seen in the screening experiments.

Samples were taken from the reactor (Section 3.5.1) and analysed for copper using AAS (Section 3.6.1), cyanide using potentiometric titration (Section 3.6.3.2), and sulfide and sulfide degradation products using HPLC (Section 3.6.4.1). Acid addition and ORP measurements are described in Section 3.3.2 and 3.3.3 respectively.

### **4.3.3 Copper recovery model**

The response of copper recovery produced the coded copper recovery model shown in Equation 4.4 and the actual copper recovery model shown by Equation 4.5. ANOVA data for the model is shown in Table 4-2. The model of copper recovery was significant (p-value < 0.001), had insignificant lack of fit (LoF p-value = 0.9997), and a high coefficient of determination ( $R^2 = 0.98772$ ). Figure 4.6, Figure 4.7, and Figure 4.8 show the modelled copper recovery for varied pH and S:Cu ratio, pH and CN:Cu ratio, and S:Cu and CN:Cu ratio respectively.

$$CuRec = 94.56 - 0.7763 \times A + 11.08 \times B - 1.579 \times C + 0.9677 \times B \times C - 6.166 \times B^2 \text{ where } \{A, B, C | -1 \leq A, B, C \leq 1, CuRec | 0 \leq CuRec \leq 100\} \quad 4.4$$

$$CuRec = -71.2 - 0.776 \times CN:Cu + 666 \times S:Cu - 8.56 \times pH + 12.9 \times S:Cu \times pH - 617 \times S:Cu^2 \text{ where } \{CN:Cu | 3 \leq CN:Cu \leq 5, S:Cu | 0.4 \leq S:Cu \leq 0.6, pH | 4 \leq pH \leq 5.5, CuRec | 0 \leq CuRec \leq 100\} \quad 4.5$$

Table 4-2 Copper recovery model ANOVA.

	Sum of squares	Degrees of freedom	Mean square	F Value	p-value
<b>Model</b>	2563.2	5	512.64	402.04	< 0.0001
<b>A-CN:Cu</b>	10.848	1	10.848	8.5078	0.0074
<b>B-S:Cu</b>	2209.3	1	2209.3	1732.6	< 0.0001
<b>C-pH</b>	44.868	1	44.868	35.188	< 0.0001
<b>BC</b>	11.237	1	11.237	8.8126	0.0065
<b>B<sup>2</sup></b>	286.99	1	286.99	225.07	< 0.0001
<b>Residual</b>	31.877	25	1.2751		
<b>Lack of Fit</b>	12.043	21	0.57348	0.11566	0.9997
<b>Pure Error</b>	19.834	4	4.9586		
<b>Total</b>	2595.1	30			

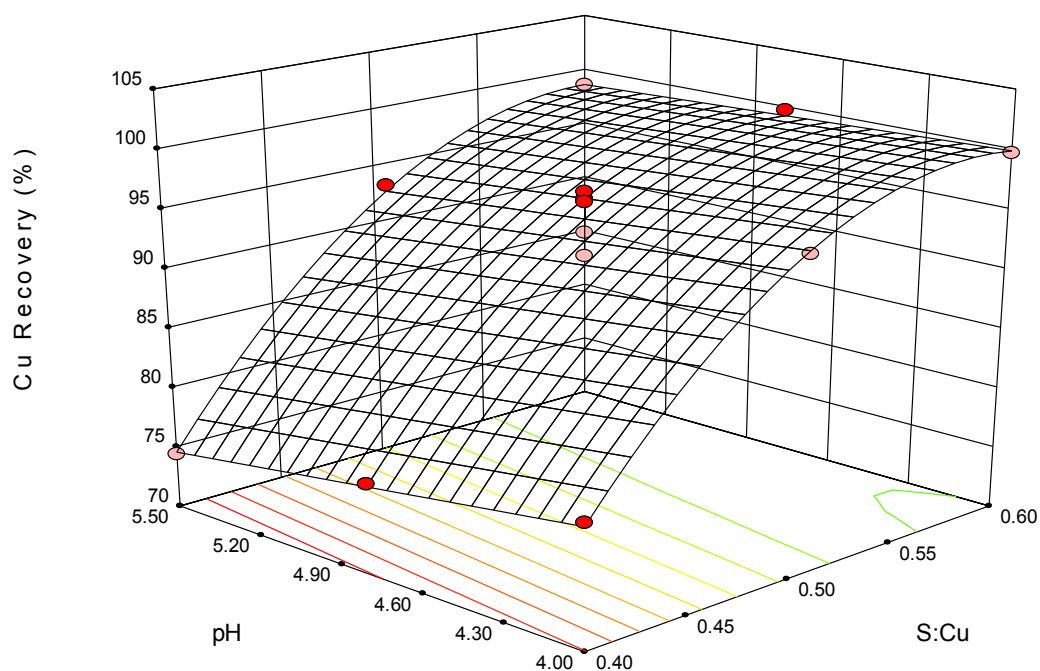


Figure 4.6 Copper recovery model when pH and S:Cu ratio are varied and CN:Cu ratio is

4.

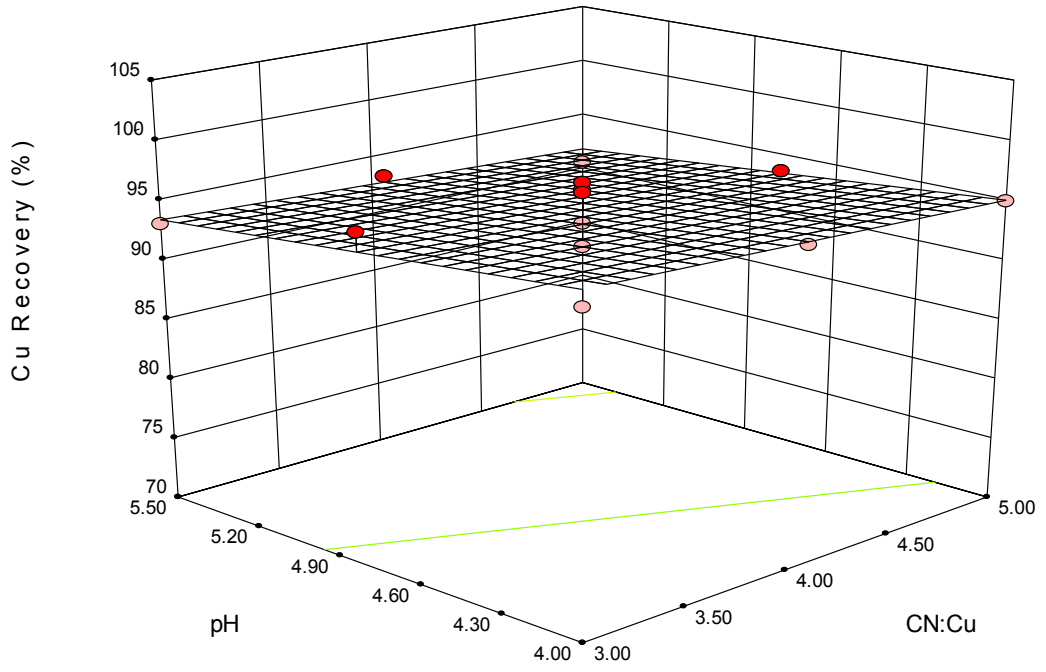


Figure 4.7 Copper recovery model when pH and CN:Cu ratio are varied and S:Cu ratio is 0.5.

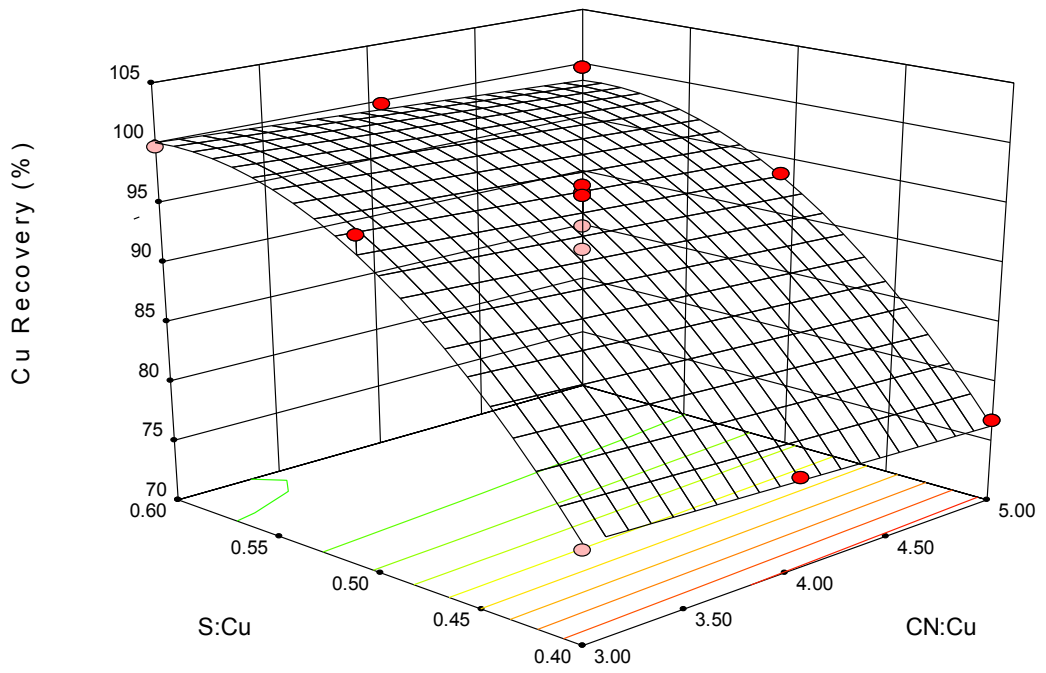


Figure 4.8 Copper recovery model when S:Cu ratio and CN:Cu ratio are varied and pH is 4.75.

From Equation 4.4 it is apparent that S:Cu ratio had the largest impact on copper recovery, with CN:Cu ratio and pH only having a minor impact. Copper recovery is maximised by adding sulfide and lowering pH (Figure 4.6), with lower cyanide to copper ratios (Figure 4.8) also being advantageous. The maximum copper recovery is on the edge of the design region with a S:Cu ratio of 0.6, pH of 4, and CN:Cu ratio of 3.

It was expected from the primary sulfidisation equation (Equation 1.3) that changes in S:Cu ratio would cause large changes in copper recovery until a ratio of 0.5 was achieved, where further addition would only cause very slight recovery increases. Figure 4.6 and Figure 4.8 show, however, that the point at which adding more sulfide only causes small changes is above a ratio of 0.5, lying somewhere around a ratio of 0.55. Small amounts of thiosulfate and thiocyanate were detected during the experiment, so it is likely that the cause of lower than expected recovery at stoichiometry is caused by some oxidation of sulfide. This suggests that not all the sulfide added is available for precipitation of copper.

#### **4.3.4 Cyanide recovery model**

Cyanide recovery data produced the cyanide recovery model in Equation 4.6 (coded) and Equation 4.7 (actual). ANOVA for the cyanide recovery model is shown in Table 4-3. The cyanide recovery model exhibited borderline significant lack of fit (LoF p-value = 0.0538) indicating that experimental error could not account for variation between the data and the model. A similar problem was observed by (Barter et al. 2001) who found it difficult measuring small differences in cyanide recovered compared to the large amount of cyanide present. Furthermore, gas losses during sampling may also cause the results to be inconsistent.

$$CNRec_{(actual)} = 88.98 + 0.9542 \times A + 11.50 \times B - 0.9201 \times C - 3.760 \times A \times B + 0.9583 \times B \times C - 2.0146 \times B^2 \text{ where } \{A, B, C | 1 \leq A, B, C \leq 1, CNRec_{(actual)} | 0 \leq CNRec_{(actual)} \leq 100\}$$
4.6

$$CNRec_{(actual)} = -61.7 + 19.8 \times CN:Cu + 406 \times S:Cu - 7.61 \times pH - 37.6 \times CN:Cu \times S:Cu + 12.8 \times S:Cu \times pH - 201 \times S:Cu^2 \text{ where } \{CN:Cu | 3 \leq CN:Cu \leq 5, S:Cu | 0.4 \leq S:Cu \leq 0.6, pH | 4 \leq pH \leq 5.5, CNRec_{(actual)} | 0 \leq CNRec_{(actual)} \leq 100\}$$
4.7

Table 4-3 Cyanide recovery model ANOVA.

	Sum of squares	Degrees of freedom	Mean square	F Value	p-value
<b>Model</b>	2623.6	21	437.26	125.78	< 0.0001
<b>A-CN:Cu</b>	16.387	22	16.387	4.7143	0.0400
<b>B-S:Cu</b>	2380.7	23	2380.7	684.85	< 0.0001
<b>C-pH</b>	15.239	24	15.239	4.3838	0.0470
<b>AB</b>	169.61	25	169.61	48.793	< 0.0001
<b>BC</b>	11.021	26	11.021	3.1705	0.0876
<b>B<sup>2</sup></b>	30.635	27	30.635	8.8128	0.0067
<b>Residual</b>	83.428	28	3.4761		
<b>Lack of Fit</b>	80.532	29	4.0266	5.5614	0.0538
<b>Pure Error</b>	2.8961	30	0.7240		
<b>Total</b>	2707.0	31			

Due to the cyanide measurements causing lack of fit in the cyanide recovery model, a calculated cyanide recovery for each experiment was instead deduced from copper recovery so that the cyanide recovery data could be

fitted to a model. For the calculation of cyanide recovery, loss of cyanide due to formation of thiocyanate was also incorporated into the equation based on excess sulfide measurements. This effect is not observed during sulfidisation, but occurs once cyanide and sulfide are returned to leaching where catalysts cause cyanide and sulfide to form thiocyanate (Breuer, Jeffrey, and Hewitt 2008; Hewitt et al. 2009). The outcome of the model is not expected to significantly change if this assumption is incorrect and cyanide did not react with 100% of the excess sulfide present.

The calculated cyanide recovery model is shown in Equation 4.8 (coded) and Equation 4.9 (actual) with ANOVA data in Table 4-4. The model was significant (p-value < 0.001), had insignificant lack of fit (LoF p-value = 0.9935), and a high coefficient of determination ( $R^2 = 0.9857$ ). Figure 4.9, Figure 4.10, and Figure 4.11 show the cyanide recovery model for varied pH and S:Cu ratio, pH and CN:Cu ratio, and S:Cu and CN:Cu ratio respectively.

$$\begin{aligned}
 CNRec_{(calc)} &= 94.29 + 2.037 \times A + 11.19 \times B - 1.627 \times C - 2.295 \times A \times B + 1.054 \times B \times C - 0.9969 \times A^2 - 6.683 \times B^2 \\
 &\text{where } \{A, B, C | -1 \leq A, B, C \leq 1, CNRec_{(calc)} | 0 \leq CNRec_{(calc)} \leq 100\}
 \end{aligned}
 \tag{4.8}$$

$$\begin{aligned}
 CNRec_{(calc)} &= -155 + 21.5 \times CN:Cu + 805 \times S:Cu - 9.20 \times pH - 23.0 \times CN:Cu \times S:Cu + 14.1 \times S:Cu \times pH - 0.997 \times CN:Cu^2 - 668 \times S:Cu^2 \\
 &\text{where } \{CN:Cu | 3 \leq CN:Cu \leq 5, S:Cu | 0.4 \leq S:Cu \leq 0.6, pH | 4 \leq pH \leq 5.5, CNRec_{(calc)} | 0 \leq CNRec_{(calc)} \leq 100\}
 \end{aligned}
 \tag{4.9}$$

Table 4-4 Calculated cyanide recovery model ANOVA.

	Sum of squares	Degrees of freedom	Mean square	F Value	p-value
<b>Model</b>	2817.9	7	402.56	226.88	< 0.0001
<b>A-CN:Cu</b>	74.707	1	74.707	42.105	< 0.0001
<b>B-S:Cu</b>	2253.7	1	2253.7	1270.2	< 0.0001
<b>C-pH</b>	47.640	1	47.640	26.850	< 0.0001
<b>AB</b>	63.211	1	63.211	35.626	< 0.0001
<b>BC</b>	13.336	1	13.336	7.5163	0.0116
<b>A^2</b>	7.1855	1	7.1855	4.0498	0.0560
<b>B^2</b>	322.97	1	322.97	182.02	< 0.0001
<b>Residual</b>	40.809	23	1.7743		
<b>Lack of Fit</b>	19.925	19	1.0487	0.20086	0.9935
<b>Pure Error</b>	20.884	4	5.2210		
<b>Total</b>	2858.7	30			

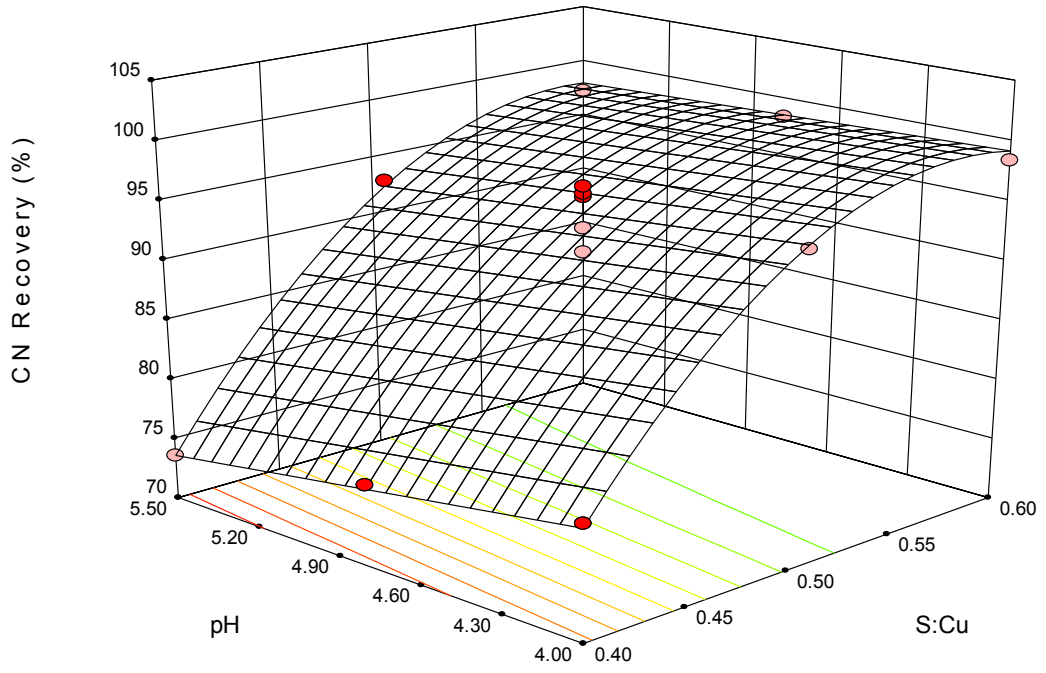


Figure 4.9 Calculated cyanide recovery model when pH and S:Cu ratio are varied and CN:Cu ratio is 4.

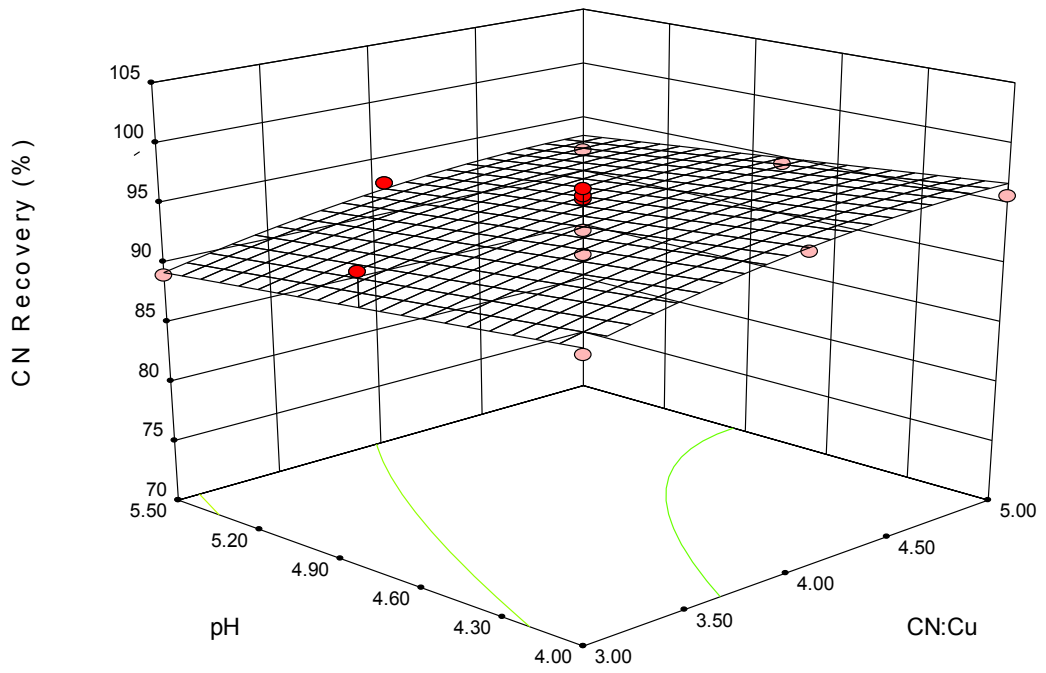
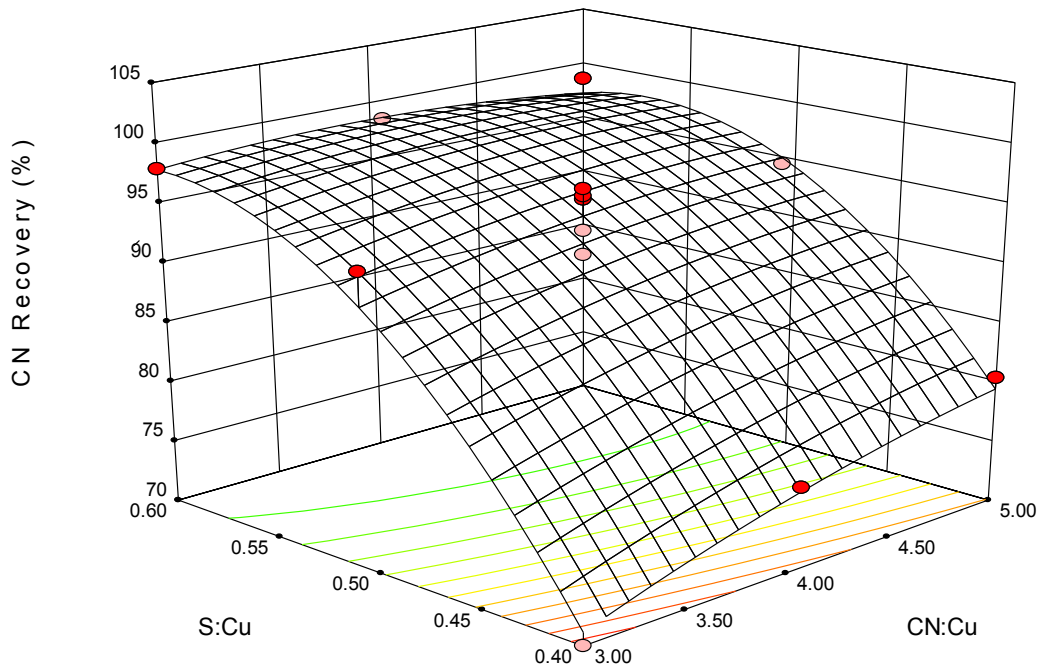


Figure 4.10 Calculated cyanide recovery model when pH and CN:Cu ratio are varied and S:Cu ratio is 0.5.



**Figure 4.11** Calculated cyanide recovery model when S:Cu ratio and CN:Cu ratio are varied and pH is 4.75.

S:Cu ratio has the highest impact on cyanide recovery followed by CN:Cu ratio based on Equation 4.8. The maximum cyanide recovery is found at a pH of 4, S:Cu ratio between 0.55 and 0.60, and CN:Cu ratio of 5. Unlike with the copper recovery model, there are S:Cu ratios within the design region where cyanide recovery is maximised. As the reaction of excess sulfide consuming cyanide is accounted for by the calculated model, this result was expected. What was not expected, however, was that the maximum cyanide recovery did not lie at the stoichiometric (Equation 1.3) S:Cu ratio of 0.5. Instead, the maximum cyanide recovery appears at S:Cu ratios of between 0.55 and 0.6. As discussed with copper recovery (Section 4.3.3), this is likely due to some oxidation of sulfide during precipitation, resulting in the actual S:Cu ratio being less than the calculated S:Cu ratio.

#### 4.3.5 Acid addition model

Equation 4.10 (coded) and Equation 4.11 (actual) show the models for the response of acid addition (mmol) per amount of copper (mmol) with ANOVA data in Table 4-5. The model was significant (p-value < 0.001), had insignificant lack of fit (LoF p-value = 0.9981), and a high coefficient of determination ( $R^2 = 0.9980$ ). Figure 4.12, Figure 4.13, and Figure 4.14 show the modelled acid addition per amount of copper model for varied pH and S:Cu ratio, pH and CN:Cu ratio, and S:Cu and CN:Cu ratio respectively.

$$\begin{aligned} \text{Acid} = & 1.987 + 0.4447 \times A + 0.1904 \times B - 0.03559 \times C + & 4.10 \\ & 0.02526 \times B \times C - 0.04247 \times B^2 \text{ where } \{A, B, C | -1 \leq A, B, C \leq \\ & 1, \text{Acid} | \text{Acid} \geq 0\} \end{aligned}$$

$$\begin{aligned} \text{Acid} = & -0.780 + 0.445 \times \text{CN:Cu} + 4.55 \times \text{S:Cu} - 0.216 \times \\ & \text{pH} + 0.337 \times \text{S:Cu} \times \text{pH} - 4.25 \times \text{S:Cu}^2 \text{ where } \{\text{CN:Cu} | 3 \leq & 4.11 \\ & \text{CN:Cu} \leq 5, \text{S:Cu} | 0.4 \leq \text{S:Cu} \leq 0.6, \text{pH} | 4 \leq \text{pH} \leq 5.5, \text{Acid} | \text{Acid} \geq 0\} \end{aligned}$$

Table 4-5 Acid addition per amount of copper model ANOVA.

	Sum of squares	Degrees of freedom	Mean square	F Value	p-value
<b>Model</b>	4.2558	5	0.85115	2439.5	< 0.0001
<b>A-CN:Cu</b>	3.5592	1	3.5592	10200	< 0.0001
<b>B-S:Cu</b>	0.65248	1	0.65248	1870.0	< 0.0001
<b>C-pH</b>	0.022801	1	0.022801	65.349	< 0.0001
<b>BC</b>	0.007654	1	0.007654	21.937	< 0.0001
<b>B<sup>2</sup></b>	0.013614	1	0.013614	39.020	< 0.0001
<b>Residual</b>	0.008723	25	0.000349		
<b>Lack of Fit</b>	0.004003	21	0.000191	0.16154	0.9981
<b>Pure Error</b>	0.00472	4	0.00118		
<b>Total</b>	4.2645	30			

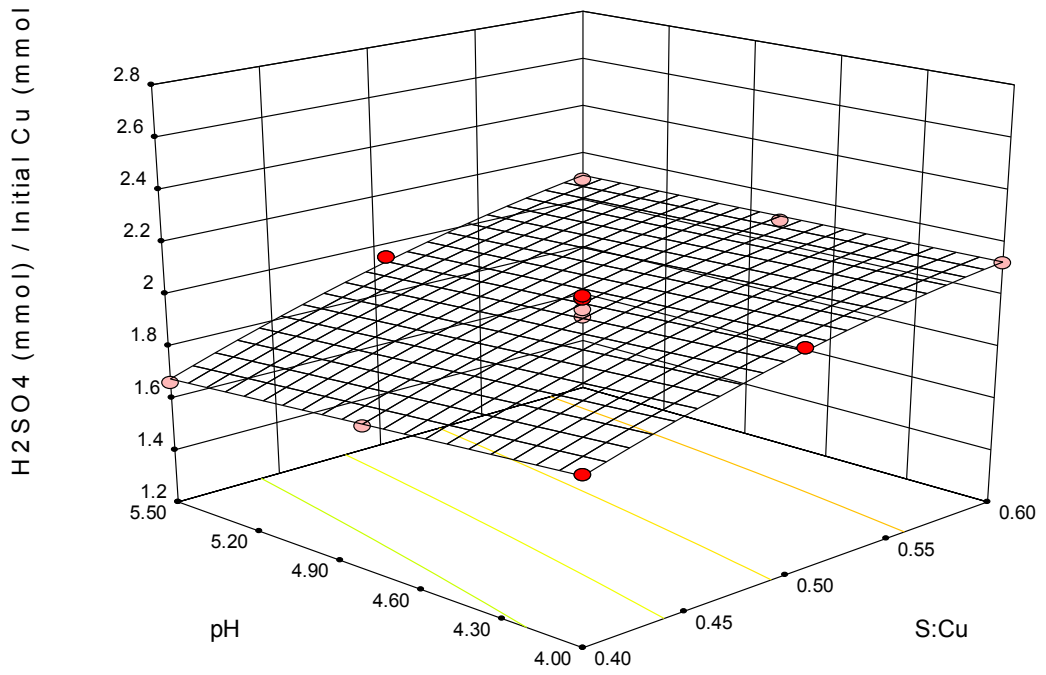


Figure 4.12 Acid addition per copper model when pH and S:Cu ratio are varied and CN:Cu ratio is 4.

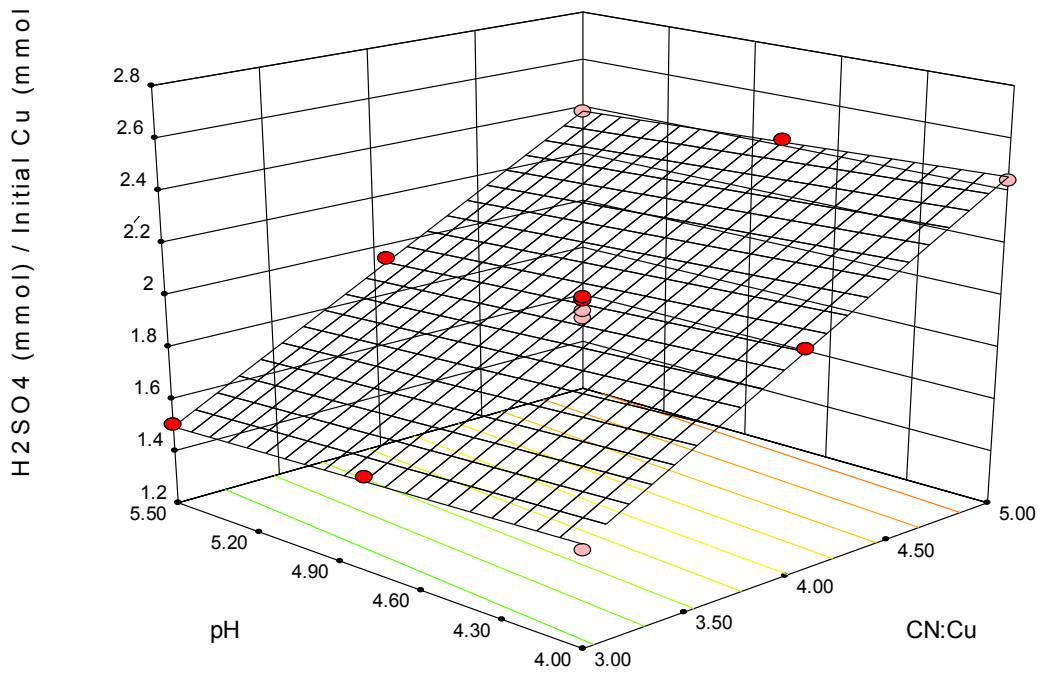
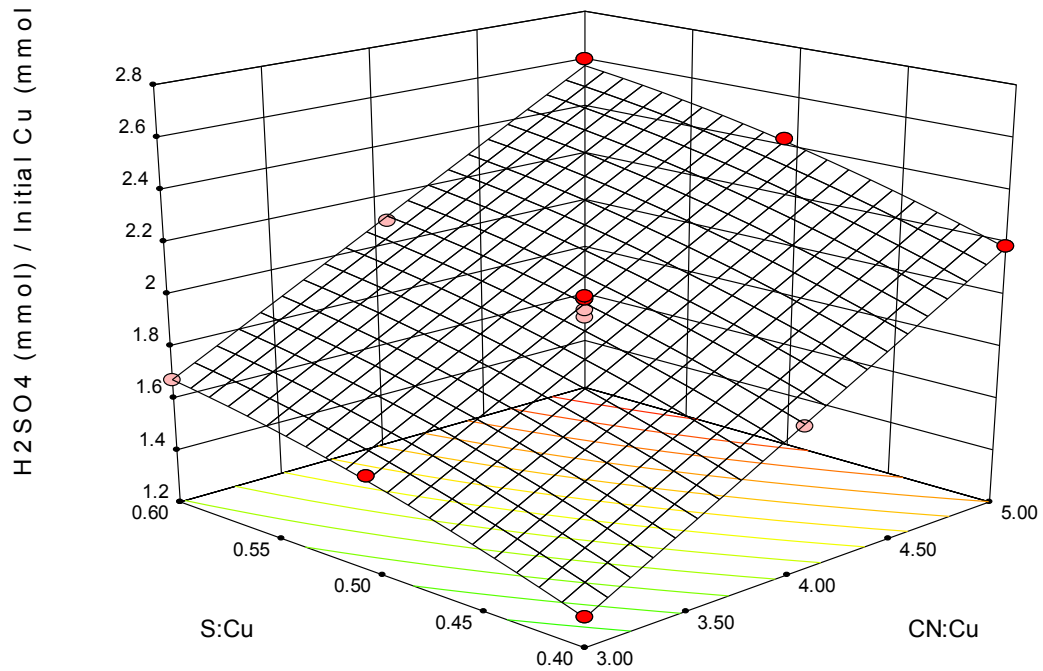


Figure 4.13 Acid addition per copper model when pH and CN:Cu ratio are varied and S:Cu ratio is 0.5.



**Figure 4.14 Acid addition per copper model when S:Cu ratio and CN:Cu ratio are varied and pH is 4.75.**

According to Equation 4.10, CN:Cu ratio and S:Cu ratio have the largest impact on acid addition. Interestingly, pH has only a small impact in comparison. The response for acid consumption is in good agreement with the primary sulfidisation equation (Equation 1.3) showing that most of the acid is consumed by cyanide in forming aqueous hydrogen cyanide. For example, at a S:Cu ratio of 0.55 and CN:Cu ratio of 5, roughly 2.5 mol of sulphuric acid is consumed per mole of copper. At this S:Cu ratio, cyanide recovery is high indicating the amount of cyanide recovered is near 5 moles per mole of copper. Hence, roughly one mole of hydrogen ions is consumed per mole of cyanide recovered as per the primary sulfidisation equation (Equation 1.3). The minimum acid consumed per amount of copper is 1.25, which lies on the boundary of the design range with a pH of 5.5, a S:Cu ratio of 0.4, and a CN:Cu ratio of 3.

### 4.3.6 Oxidation/reduction potential (ORP) model

The model for oxidation/reduction potential (ORP) is shown in Equation 4.12 (coded) and Equation 4.13 (actual) with ANOVA data in Table 4-6. The model was significant (p-value < 0.001), had insignificant lack of fit (LoF p-value = 0.6396), and a high coefficient of determination ( $R^2 = 0.9458$ ). Figure 4.15, Figure 4.16, and Figure 4.17 show the ORP model for pH and S:Cu ratio, pH and CN:Cu ratio, and S:Cu and CN:Cu ratio respectively.

$$ORP = -276.4 - 58.81 \times B - 63.61 \times C + 21.49 \times B \times C \text{ where} \quad 4.12$$

$$\{A, B, C | -1 \leq A, B, C \leq 1\}$$

$$ORP = 1101 - 1949 \times S:Cu - 228.1 \times pH + 286.6 \times S:Cu \times pH$$

$$\text{where } \{CN:Cu | 3 \leq CN:Cu \leq 5, S:Cu | 0.4 \leq S:Cu \leq 0.6, pH | 4 \leq pH \leq 5.5\} \quad 4.13$$

Table 4-6 ORP model ANOVA.

	Sum of squares	Degrees of freedom	Mean square	F Value	p-value
<b>Model</b>	14062	3	4687.4	157.16	< 0.0001
<b>B-S:Cu</b>	62257	1	62257	208.73	< 0.0001
<b>C-pH</b>	72822	1	72822	244.15	< 0.0001
<b>BC</b>	5542.7	1	5542.7	18.583	0.0002
<b>Residual</b>	8053.1	27	298.26		
<b>Lack of Fit</b>	6715.6	23	291.98	0.87318	0.6396
<b>Pure Error</b>	1337.6	4	334.39		
<b>Total</b>	14868	30			

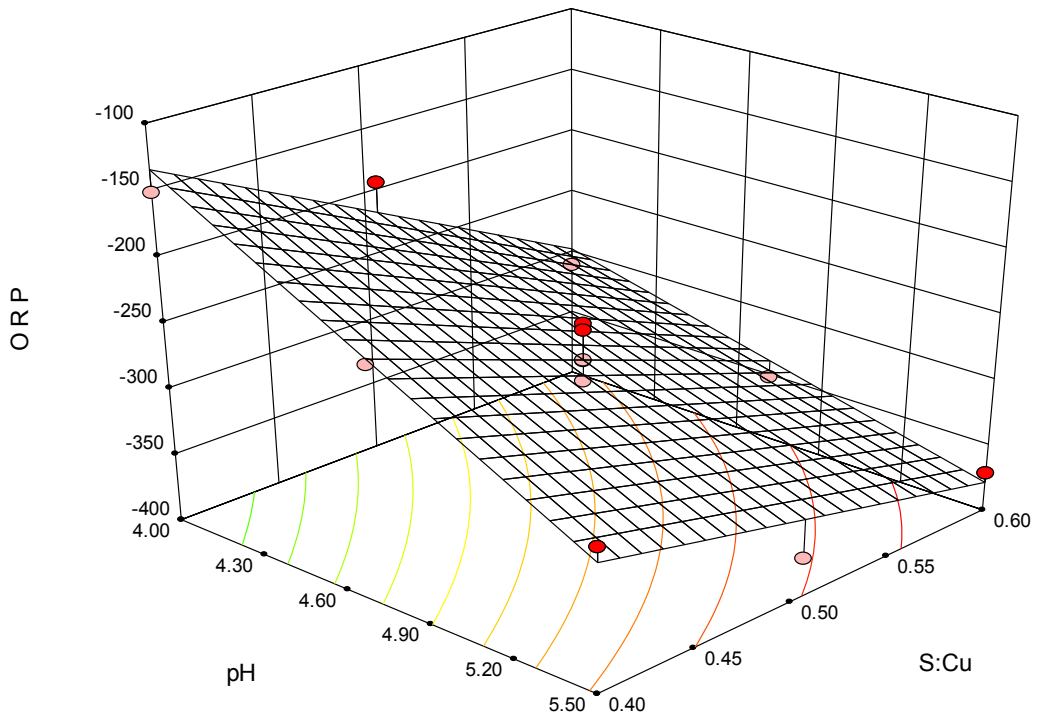


Figure 4.15 ORP model when pH and S:Cu ratio are varied and CN:Cu ratio is 4. NB: pH axis has been reversed.

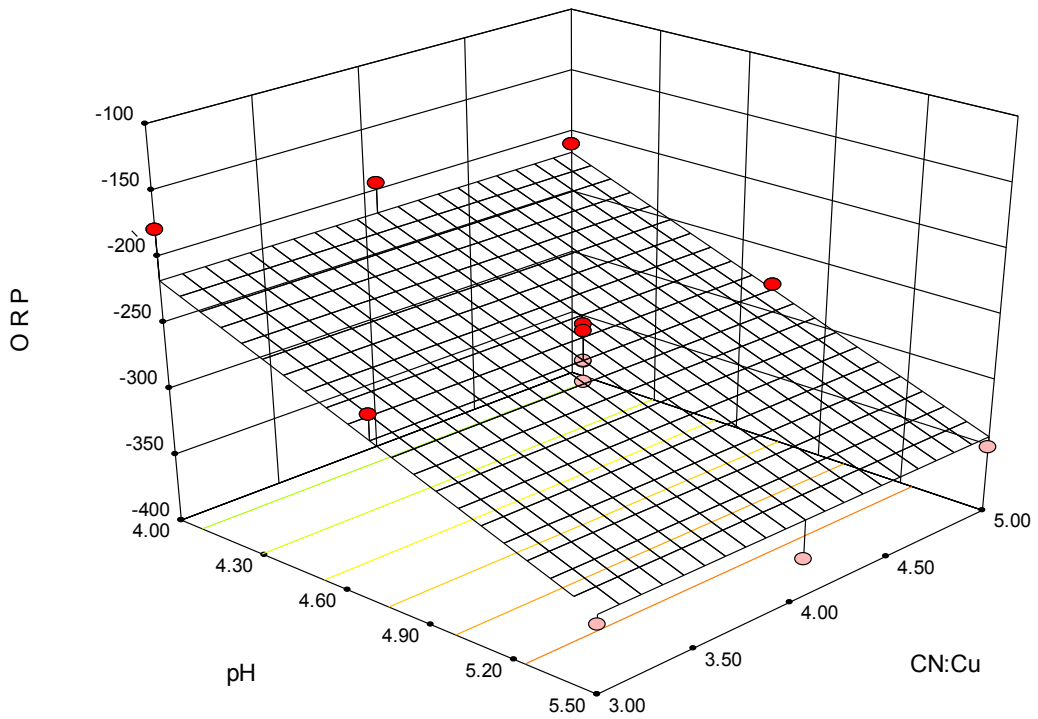
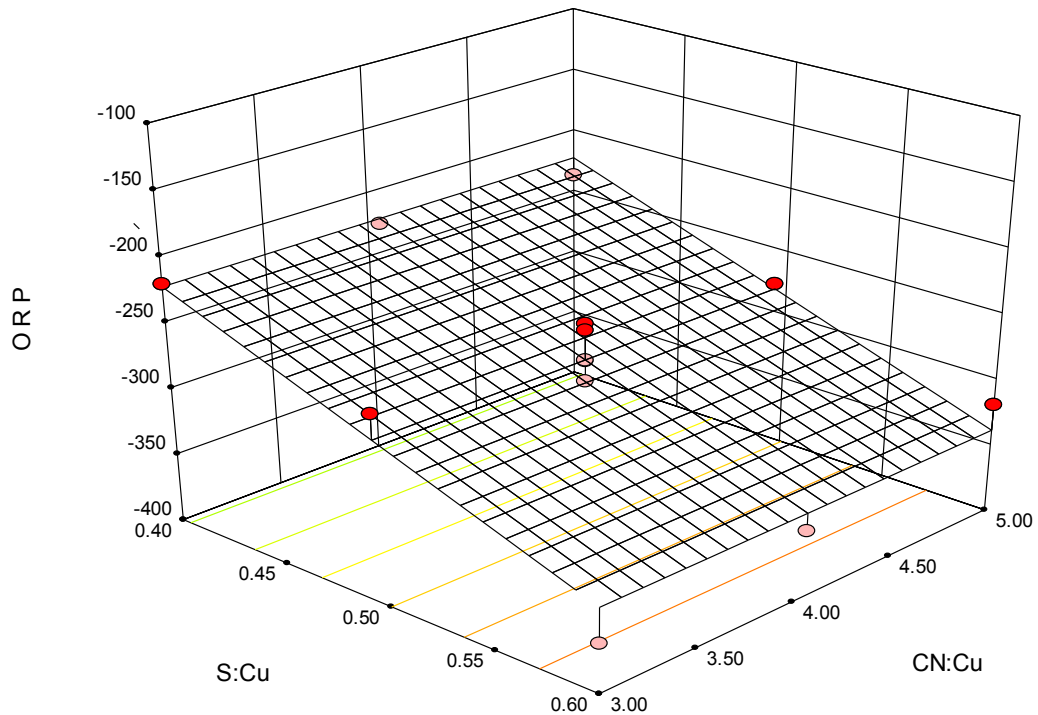


Figure 4.16 ORP model when pH and CN:Cu ratio are varied and S:Cu ratio is 0.5. NB: pH axis has been reversed.



**Figure 4.17 ORP model when S:Cu ratio and CN:Cu ratio are varied and pH is 4.75. NB: S:Cu ratio axis has been reversed.**

ORP was measured during experiments to determine if it could be used as a technique to control sulfide addition at the optimum value in an industrial process. This is needed as optimum sulfide addition is relative to copper concentration (Section 4.3.3, 4.3.4, and 4.4.2), a value which may constantly change in a sulfidation process feed solution. While the model for ORP fit well, visual inspection of the response model (Figure 4.15, Figure 4.16, and Figure 4.17) shows large variation between the experimental results (red dots) and the model (coloured surface). The model of ORP also failed to show any obvious indicators of the S:Cu ratio to maximise cyanide recovery. While it does appear possible to control sulfide addition using an ORP value at a given pH (Figure 4.15), this technique may suffer from problems when dealing with industrial solutions which contain other species that affect ORP. Hence, the ORP model developed here does not appear to be a useful model to control sulfide dosing during sulfidation.

The failure of the model shown here to act as an acceptable indicator to control sulfide addition does not rule out the possibility that a higher order model of ORP would not achieve that outcome (Bas and Boyaci 2007). This may also explain how sulfide dosing is successfully controlled using ORP at some industrial SART plants (Kratochvil, Chan, and Hall 2013). Specific details of the control strategy used by Kratochvil, Chan, and Hall (2013) are not available. The development of a control process for sulfidisation was outside the scope of this research and was not explored further.

#### **4.4 Economic impacts**

As the copper recovery, cyanide recovery, and acid addition per copper models suggest different optimums and impacting factors for each response, an objective function must be created to find the whole system's optimum. A desirability equation (Derringer and Suich 1980) can be used to achieve this goal, but has the inherent flaw that the person determining the optimum must decide which responses are more important than others.

To overcome this problem, an economic model was used to find the optimum for this system. An economic model was chosen as the best technique to find the optimum as all of the responses could be re-written in terms of revenue or loss to create a profit equation (Equation 4.14) where  $P$  is profit,  $R_{Cu}$  is the revenue from copper recovered,  $L_{CN}$  is the loss from cyanide not recovered,  $L_A$  is the loss from acid consumed,  $L_B$  is the loss from base consumed, and  $L_S$  is the loss from sulfide consumed.

$$P = R_{Cu} - L_{CN} - L_A - L_B - L_S \quad 4.14$$

Note that cyanide has been treated as cyanide lost from failure to recover cyanide rather than revenue from cyanide recovered. This is because there is

a cost associated with purchasing the cyanide entering sulfidisation and thus cyanide recovered is not truly a revenue stream. If cyanide recovered were to be treated as revenue, the economic model would suggest that operations should put in more cyanide to make more profit from sulfidisation which is illogical.

In the case presented here, the term profit does not take into account costs that are not influenced by sulfidisation operating conditions, such as power, labour, maintenance, and so forth. Hence, the profit value is not a true profit value, but rather a good way to combine the responses from the factorial design into one objective function to find the optimum conditions of the process.

#### 4.4.1 Equations

Based on the output from the factorial design, Equation 4.15 to Equation 4.21 can be deduced, where [Cu] is the initial copper concentration ( $\text{mmol m}^{-3}$ ) and  $V_{\text{Cu}}$ ,  $V_{\text{CN}}$ ,  $V_A$ ,  $V_B$ , and  $V_S$  are the dollar values of pure copper, sodium cyanide, acid, base, and sulfide in  $\$ \text{mmol}^{-1}$  respectively. Each of these equations give a value in  $\$ \text{m}^{-3}$  of feed, ultimately giving profit (Equation 4.14) in the same units.

$$\text{Copper revenue equation: } R_{\text{Cu}} = V_{\text{Cu}} \times [\text{Cu}] \times \frac{\text{CuRec}}{100} \quad 4.15$$

$$\text{Cyanide loss equation: } L_{\text{CN}} = V_{\text{CN}} \times [\text{Cu}] \times \text{CN:Cu} \times \frac{100 - \text{CNRec}}{100} \quad 4.16$$

$$\text{Acid consumed if using Na}_2\text{S: } L_A = V_A \times [\text{Cu}] \times \text{Acid} \quad 4.17$$

$$\text{Acid consumed if using NaSH: } L_A = V_A \times \frac{(2 \times [\text{Cu}] \times \text{Acid} - [\text{Cu}] \times \text{S:Cu})}{2} \quad 4.18$$

$$\text{Base consumed if using CaO: } L_B = V_B \times [\text{Cu}] \times \text{Acid} \quad 4.19$$

$$\text{Base consumed if using NaOH: } L_B = 2 \times V_B \times [Cu] \times \text{Acid} \quad 4.20$$

$$\text{Sulfide consumed: } L_S = V_S \times [Cu] \times S:Cu \quad 4.21$$

#### 4.4.2 System optimum and sensitivity

The objective of the economic model was not to find the best economic situation for SART, but to find the optimum SART operating conditions in different economic situations. Doing this requires optimisation of the profit equation (Equation 4.14). Optimisation was trialled by determining the stationary points of the profit equation using partial differentiation with respect to S:Cu ratio, CN:Cu ratio, and pH. Before this could be done, the copper recovery (Equation 4.5), cyanide recovery (Equation 4.9), and acid consumption (Equation 4.11) model equations were substituted into Equations 4.15 to 4.21. Equations 4.15 to 4.21 were, in turn, substituted into the profit equation (Equation 4.14) to give the profit equation in terms of S:Cu ratio, CN:Cu ratio, and pH (Equation 4.22). The coefficients  $b_x$  are shown in the Appendices (Section 10.3) for when Na<sub>2</sub>S is used as the sulfide source and CaO is used for base.

$$\begin{aligned} P = & b_1 + b_2 \times \text{CN:Cu} + b_3 \times \text{S:Cu} + b_4 \times \text{pH} + b_5 \times \text{CN:Cu} \times \text{S:Cu} \\ & + b_6 \times \text{CN:Cu} \times \text{pH} + b_7 \times \text{S:Cu} \times \text{pH} + b_8 \times \text{CN:Cu}^2 \\ & + b_9 \times \text{S:Cu}^2 + b_{10} \times \text{CN:Cu} \times \text{S:Cu}^2 + b_{11} \times \text{CN:Cu}^2 \\ & \times \text{S:Cu} + b_{12} \times \text{CN:Cu} \times \text{S:Cu} \times \text{pH} + b_{13} \times \text{CN:Cu}^3 \end{aligned} \quad 4.22$$

Partial differentiation of Equation 4.22 yields a set of non-linear equations (Equations 4.23, 4.24, and 4.25) which are difficult to solve while the reagent prices are left as variables. In addition, the results would yield optimum equations which may not show useful system optimums as there are no constraints on the cost and revenue values.

$$\begin{aligned} \frac{\partial P}{\partial CN:Cu} = & b_2 + b_5 \times S:Cu + b_6 \times pH + 2 \times b_8 \times CN:Cu + b_{10} \\ & \times S:Cu^2 + 2 \times b_{11} \times CN:Cu \times S:Cu + b_{12} \times S:Cu \times pH \\ & + 3 \times b_{13} \times CN:Cu^2 \end{aligned} \quad 4.23$$

$$\begin{aligned} \frac{\partial P}{\partial S:Cu} = & b_3 + b_5 \times CN:Cu + b_7 \times pH + 2 \times b_9 \times S:Cu + 2 \times b_{10} \\ & \times CN:Cu \times S:Cu + b_{11} \times CN:Cu^2 + b_{12} \times CN:Cu \times pH \end{aligned} \quad 4.24$$

$$\frac{\partial P}{\partial pH} = b_4 + b_6 \times CN:Cu + b_7 \times S:Cu + b_{12} \times CN:Cu \times S:Cu \quad 4.25$$

Due to the problems associated with using a calculus method, a graphical approach was selected as the best way to determine both the system optimums and sensitivity in a variety of economic situations. This was done by randomly generating 100 economic situations with reagent and product prices between the maximum and minimum values shown in Table 4-7. These numbers were based on reagent values used by Adams and Lloyd (2008). Copper concentrations between 3 and 30 mM (~200-2000 ppm) were also randomly generated along with random selection of sulfide (Na<sub>2</sub>S or NaHS) and base (CaO or NaOH) reagents. The economic situations were then used with Equation 4.14 to Equation 4.21 to give profit equations and to find the optimum operating conditions for each economic situation.

**Table 4-7 Value ranges of reagents and products for the sensitivity analysis of the profit model.**

Item	Min (US\$/t)	Max (US\$/t)
Cu	4000	8000
NaCN	1000	2000
H <sub>2</sub> SO <sub>4</sub>	100	500
CaO	500	1500
NaOH	500	1500
Na <sub>2</sub> S	500	1500
NaSH	500	1500

Figure 4.18, Figure 4.19, and Figure 4.20 show the profit using one of the random economic situations for pH and S:Cu ratio, pH and CN:Cu ratio, and S:Cu and CN:Cu ratio respectively. For this economic situation, the value of copper, sodium cyanide, sodium sulfide, sulphuric acid, and lime is 6000 US\$ t<sup>-1</sup>, 1250 US\$ t<sup>-1</sup>, 1000 US\$ t<sup>-1</sup>, 250 US\$ t<sup>-1</sup>, and 1000 US\$ t<sup>-1</sup> respectively with 1250 ppm of copper in the feed.

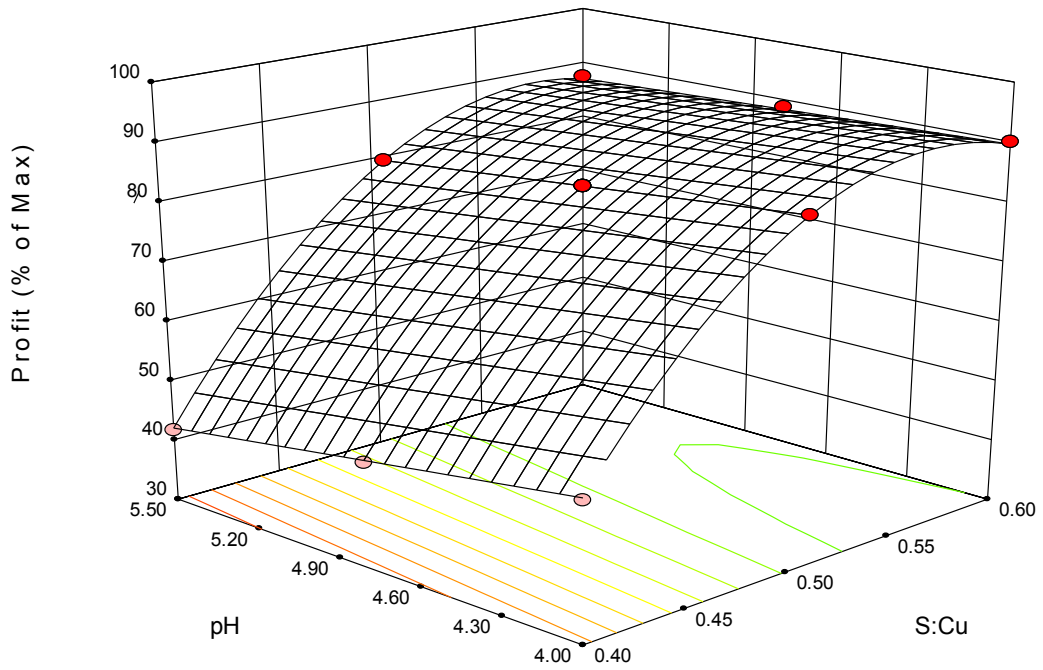


**Figure 4.18** Example profit model when pH and S:Cu ratio are varied and CN:Cu ratio = 4. Reagent and product values used are Cu– 6000 US\$/t, NaCN – 1250 US\$/t, Na<sub>2</sub>S – 1000 US\$/t, H<sub>2</sub>SO<sub>4</sub> – 250 US\$/t. Initial Cu concentration used was 1250 mg L<sup>-1</sup>.

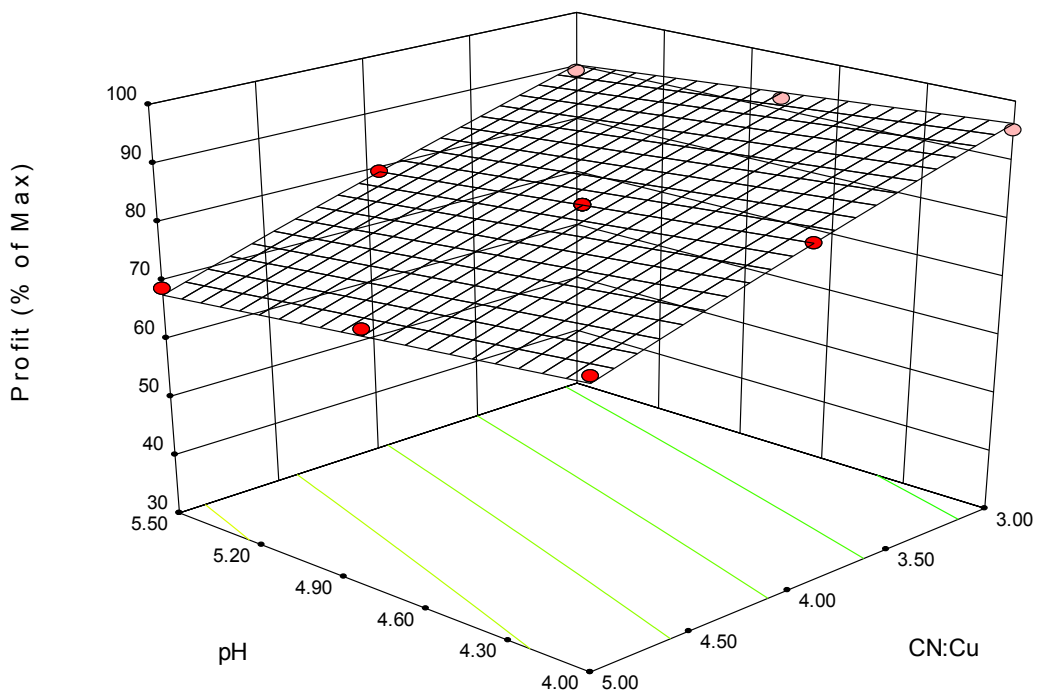


**Figure 4.19** Example profit model when pH and CN:Cu ratio are varied and S:Cu ratio = 0.56. NB: CN:Cu axis has been reversed. Reagent and product values used are Cu– 6000 US\$/t, NaCN – 1250 US\$/t, Na<sub>2</sub>S – 1000 US\$/t, H<sub>2</sub>SO<sub>4</sub> – 250 US\$/t. Initial Cu concentration used was 1250 mg L<sup>-1</sup>.

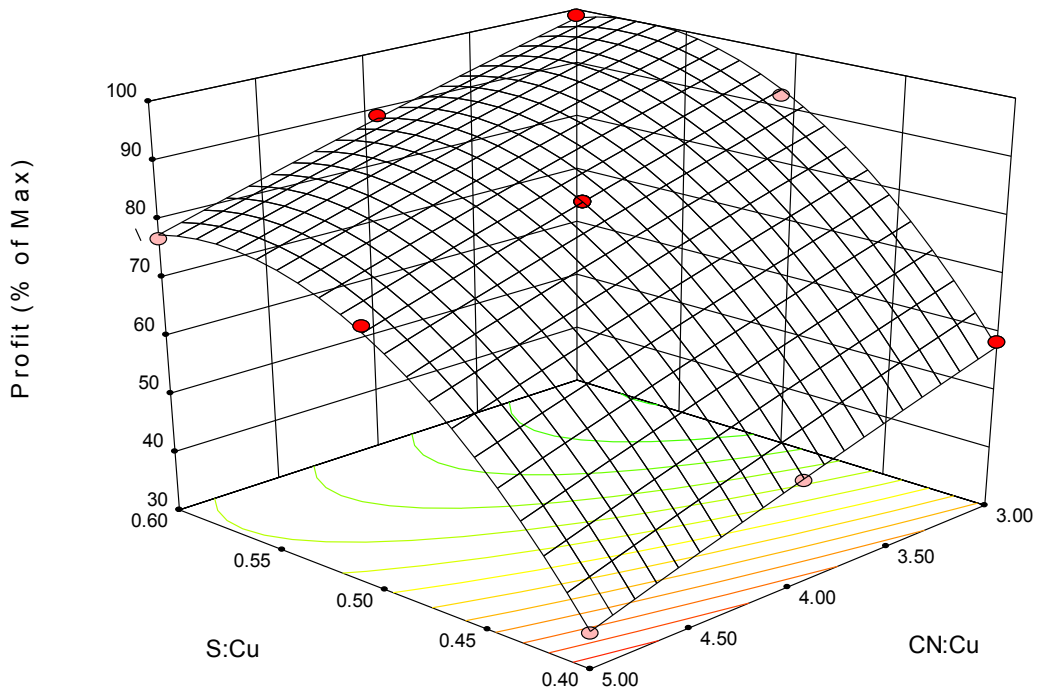


**Figure 4.20 Example profit model when S:Cu ratio and CN:Cu ratio are varied and pH = 3.**

**NB: CN:Cu ratio axis has been reversed. Reagent and product values used are Cu – 6000 US\$/t, NaCN – 1250 US\$/t, Na<sub>2</sub>S – 1000 US\$/t, H<sub>2</sub>SO<sub>4</sub> – 250 US\$/t. Initial Cu concentration used was 1250 mg L<sup>-1</sup>.**

Interestingly, for every economic situation, the optimum pH and CN:Cu ratio was calculated as 4 and 3 respectively. Optimum S:Cu ratio was, on average, 0.56 with a standard deviation of only 1.7%. These results indicate that the optimum conditions for sulfidisation are insensitive to price variation within the range set out in Table 4-7.

Although the optimum conditions are the same for different economic situations, the shape of the model in four dimensional space is not. This indicates that the impact on profit when operating away from the optimum varies significantly under different economic situations. In the following subsections, the response curves are discussed for a single factor in each economic situation, where the other two factors are set at their optimum value. This provides a simple way of showing a single factor's impact on profit when operating away from the process economic optimum.

The graphs in the following subsections (Figure 4.21, Figure 4.22, and Figure 4.23) show what the effect of varying a single factor (horizontal axis) on each of the 100 economic situations does to maximum profit for each economic situation (vertical axis). Mathematically, this is the equivalent to looking at a two dimensional plane cut through the four dimensional model for each of the 100 economic situations.

#### *4.4.2.1 Effect of varying cyanide to copper ratio on the model optimum*

Figure 4.21 shows the effect that changing CN:Cu ratio has on profit when S:Cu ratio (0.56) and pH (4) are held at their optimum values for each of the 100 economic situations. If CN:Cu ratio is not kept at its optimum, profit can be significantly less than profit at the optimum of 3. The reason that high CN:Cu ratio causes a drop in profit is due to more acid and base being consumed when more cyanide is present for the same copper concentration. The higher the acid and base costs are, the steeper the change in profit.

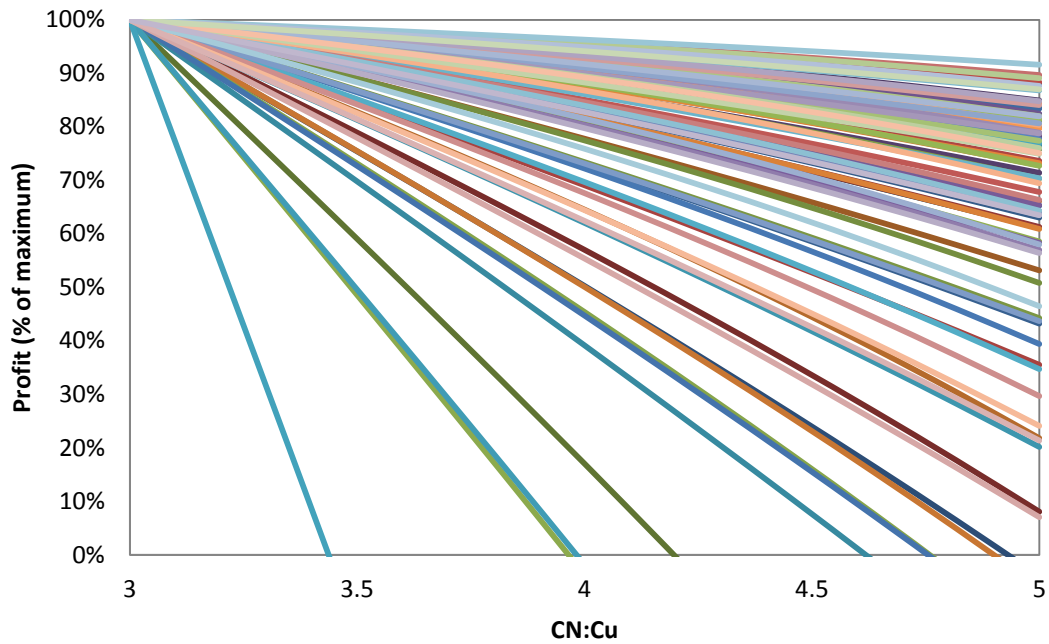


**Figure 4.21 Profit (% of maximum) for different economic situations when CN:Cu is varied and S:Cu and pH are held constant at 0.56 and 4 respectively.**

The problem this would cause for industrial sulfidisation processes is that CN:Cu ratios greater than the optimum of 3 are typically observed in the discharge from cyanidation. This is due to low CN:Cu ratios causing copper cyanide to load onto activated carbon during gold adsorption, in turn reducing gold recovery and causing downstream gold processing issues (Fleming and Nicol 1984; Dai and Breuer 2009). Hence, the CN:Cu ratio during gold leaching needs to be optimised to limit adsorption of copper cyanide species on carbon during gold recovery, whilst minimising free cyanide in the cyanidation discharge which is detrimental to sulfidisation economics. This is not an issue for processes using sulfidisation to remove copper before carbon adsorption of gold (Kratochvil, Chan, and Hall 2013). For the subsequent graphs, where S:Cu ratio and pH are varied (Figure 4.22 and Figure 4.23), a CN:Cu ratio of 4 was adopted as the optimum to reflect the typical CN:Cu ratio of operating gold plants.

#### 4.4.2.2 Effect of varying sulfide to copper ratio on the model optimum

Figure 4.22 shows the effect changing S:Cu ratio has on profit when CN:Cu ratio is 4 and pH is held at its optimum of 4. Like CN:Cu ratio, economic variation has a large effect on profit variation when operating with the S:Cu ratio away from its optimum value. The reduction in profit at low S:Cu ratios are mainly caused by lower copper and cyanide recovery compared to the optimum. The reduction in profit at high S:Cu ratio, however, is caused by both cyanide loss, due to the assumed formation of thiocyanate in downstream processes (Section 2.3.3 and 4.3.4), and increased acid and base consumption. High acid, base, and sulfide costs coupled with low copper values appeared to cause a more drastic reduction in profit when operating at suboptimal conditions.

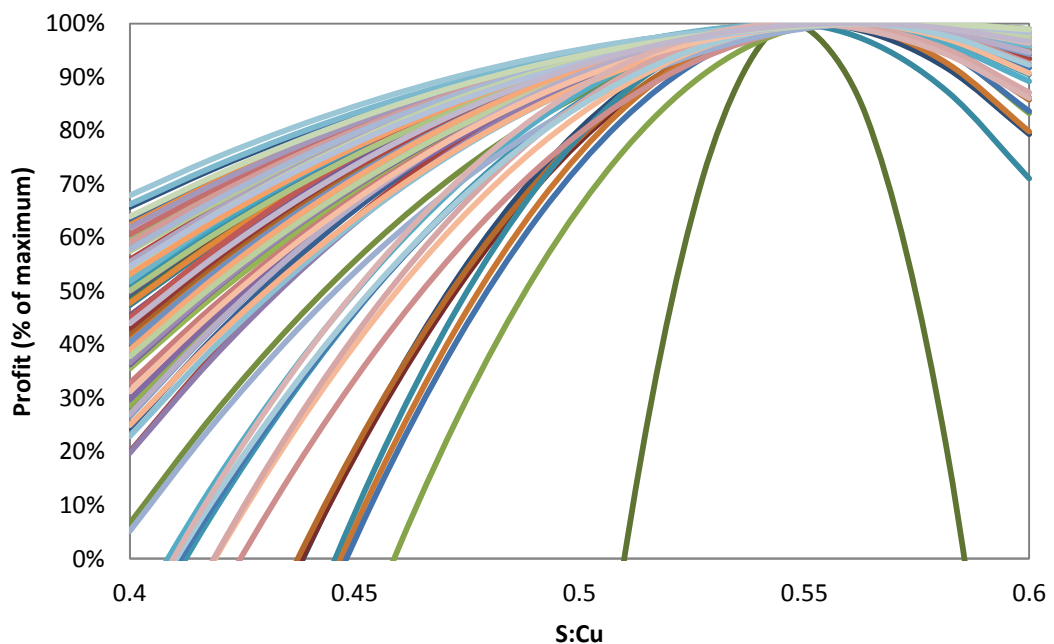


**Figure 4.22 Profit (% of maximum) for different economic situations when S:Cu is varied and CN:Cu and pH are held constant at 4 and 4 respectively.**

Figure 4.22 highlights the importance of operating sulfidisation processes at the optimal S:Cu ratio. Operational experience with the SART process (Guzman et al. 2010) shows that S:Cu ratio is often not controlled well, although this is becoming better in recent times (Kratochvil, Chan, and Hall 2013). The result of the modelling coupled with the industrial experience suggests that more importance should be placed on controlling sulfide addition during sulfidisation to maximise profit.

#### *4.4.2.3 Effect of varying pH on the model optimum*

The effect changing pH has on profit when CN:Cu ratio is 4 and the S:Cu is held at its optimum of 0.56 is shown in Figure 4.23. Overall, pH has only a minor effect on profit compared to the other factors, showing less than 20 % change in profit for most of the economic situations tested. The low optimum for pH is caused by the fact that pH changes only consume a small amount of acid which is of low cost but yield slightly more copper and cyanide which is of higher value. This result is interesting as many papers on the SART process, as discussed in Section 2.3.2, suggest that pH targets closer to 5 are beneficial to reduce acid consumptions and in turn reduce costs. While this is true (Section 4.3.5), none of these studies considered that the extra profit from higher copper and cyanide recovery at low pH can offset this cost, causing low pH to be more profitable.

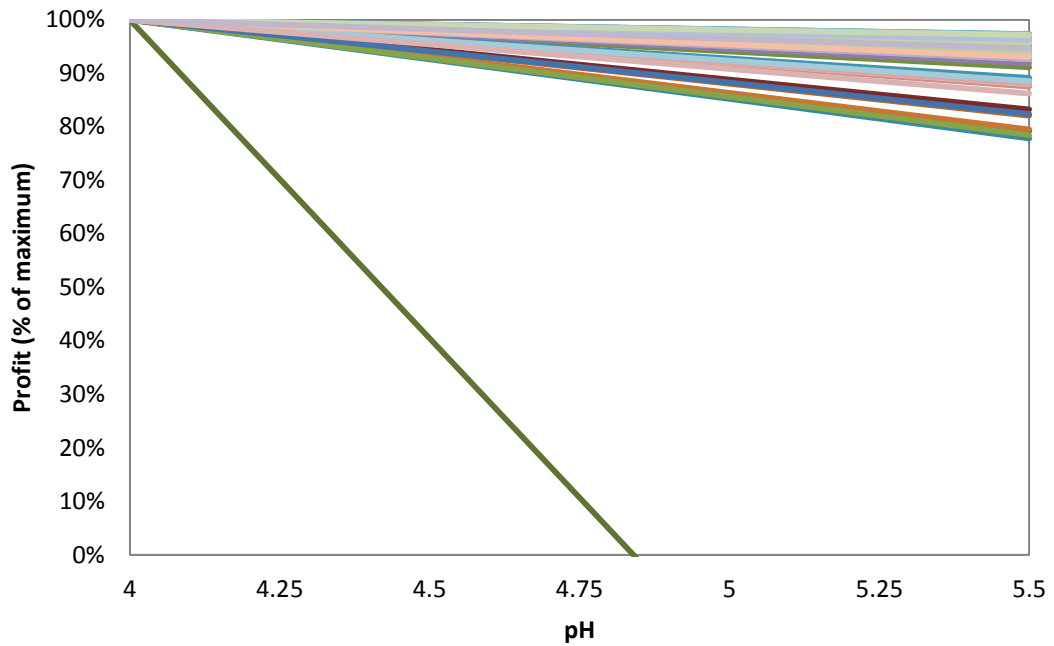


**Figure 4.23 Profit (% of maximum) for different economic situations when pH is varied and CN:Cu and S:Cu are held constant at 4 and 0.56 respectively.**

As the optimum lies on the design boundary of the factorial design, the optimum pH may be lower than a value of 4. The use of lower pH in sulfidisation, however, increases the chances of copper cyanide precipitates forming, especially if control of S:Cu ratio is poor. As copper cyanide may reduce the marketability of the precipitate (MacPhail, Fleming, and Sarbutt 1998), a pH lower than 4 is not recommended for industrial sulfidisation plants.

#### **4.5 Conclusions**

A full three-level factorial design was performed to determine the effect of key factors on sulfidisation process performance and how these factors interact. It also creates a baseline model for comparing results of future experiments. Four-dimensional, second-order polynomials were used to

model the response of copper recovery, cyanide recovery, acid consumption, and ORP.

The maximum copper recovery was on the boundary of the design region with a S:Cu ratio of 0.6, a CN:Cu ratio of 3, and a pH of 4. Actual cyanide recovery data did not model well due to problems with measuring small changes in cyanide concentration in high concentration solutions. A calculated cyanide recovery model was created instead which gave a maximum cyanide recovery at a S:Cu ratio between 0.55 and 0.60, a CN:Cu ratio of 5, and pH of 4. For the calculated cyanide recovery, the CN:Cu ratio and pH for maximum recovery was on the boundary of the design region. Acid addition per initial amount of copper was at its minimum on the design boundary at a S:Cu ratio of 0.4, CN:Cu ratio of 3, and pH of 5.5. The ORP model was not useful for determining sulfide addition to a sulfidisation process, but does not rule out the possibility of using ORP for this purpose.

As the different responses had different optimums, an economic model was created to show the economic optimum for the whole process. It was found using the economic model that, within the reagent and product value ranges specified, sulfidisation processes should be operated with S:Cu ratios slightly above stoichiometric (~0.56), at a pH of 4, and with CN:Cu ratios that are as low as possible. The model also showed that, of the factors tested, the S:Cu ratio and the CN:Cu ratio have the largest impacts on sulfidisation economic performance.

The outcome of the economic model, and surrounding sensitivity analysis, has several implications for operation of a sulfidisation process. Firstly, the S:Cu ratio is a critical parameter and should be tightly controlled if profit is to be kept at its optimum. Secondly, a balance needs to be struck with CN:Cu

ratio, with the ratio being kept high enough to minimise copper interfering with gold processing, while also being kept low enough to minimise its impact on sulfidisation profitability. Finally, the pH should be kept low to maximise profit from cyanide and copper recovered.

The modelling of sulfidisation also showed two other interesting occurrences. The first is that a small amount of sulfide is oxidised during sulfidisation. Due to this, the optimum S:Cu ratio (~0.56) is above reaction stoichiometry (0.50) of the primary sulfidisation equation (Equation 1.3). The second was that residence time appears to impact sulfidisation performance, which has been explored in more detail in Chapter 6 and Chapter 7.

## **5 IMPACT OF IMPURITIES ON SULFIDISATION**

### **5.1 Introduction**

There are a limited number of studies focused on impurities in sulfidisation, with most being a result of the use of industrial solutions (Dymov, Ferron, and Fleming 1997; Dreisinger et al. 2008; Guzman et al. 2010; Littlejohn, Kratochvil, and Hall 2013) and few being the result of fundamental studies (Milosavljevic, Solujic, and Kravetz 2004). A better understanding of how impurities impact sulfidisation is important as impurities in sulfidisation may increase reagent consumption, reduce precipitate grades, and result in cyanide species being present in the precipitate which may in turn reduce the precipitate marketability (MacPhail, Fleming, and Sarbutt 1998).

The objective of this chapter is to determine the impact of common species found in gold cyanidation tailings on sulfidisation. The focus of the studies was to determine how the impurities affect reagent consumption and the viability of selective metal precipitation. This was done by individually studying the impacts of silver, gold, iron, nickel, zinc, thiocyanate, thiosulfate, and chloride during sulfidisation of a copper cyanide solution. To determine how various impurities interact in a complex system, mixed impurity solutions containing silver, gold, copper, iron, nickel, and zinc with varying amounts of sulfide were also studied.

As residence time has been shown to impact sulfidisation (Section 4.2.6), the impurity study was focused on the impact of impurities under initial sulfidisation conditions. This was done so the impact of each impurity on sulfidisation was clearly related to the initial impurity concentration.

## **5.2 Single impurity experiments**

Single impurity experiments were performed to determine how various impurities individually impact reagent consumption and selective precipitation during sulfidisation of a copper cyanide solution.

### **5.2.1 Experimental methods**

For each experiment, test solutions were made as described in Section 3.1.2, targeting a copper concentration of 16 mM (~1000 mg/L). The impurity concentration target was half (8 mM) of the copper concentration with the exception of gold and chloride. High impurity concentrations were selected so any impact the impurity had on sulfidisation was able to be clearly detected in the results. The gold impurity target concentration was one tenth (1.6 mM) of the copper concentration, because gold is usually not found in high concentrations in the gold processing tailings. Chloride concentration was set at 1.0 M as this experiment was designed to test the feasibility of sulfidisation on copper cyanide eluted from ion exchange resin using chloride ions as an eluent (Section 2.4.9).

The cyanide to metal molar ratio for every metal, except for iron, was set at 4 moles of cyanide per mole of metal. For iron, the ratio was 6 moles of cyanide per mole of metal. This is due to iron forming  $\text{Fe}(\text{CN})_6^{4-}$  and  $\text{Fe}(\text{CN})_6^{3-}$  species. For the anionic species tested (thiocyanate, thiosulfate, and chloride), the cyanide to copper molar ratio was set at 4. Excess cyanide was not added for the anionic species as they are not known to form cyanide complexes.

For each metal impurity, two experiments were carried out. Both were done using the large reactor described in Section 3.2 which was prepared as described in Section 3.3.1.2. The experiments for each metal impurity were

then performed using the method described in Section 3.4.2 with a sulfide to copper molar ratio (S:Cu ratio) of 0.5. Samples were taken at pH 10 through to a pH of 3 using the sampling method in Section 3.5.1. An initial sample was also taken to determine initial conditions. For each metal impurity the experiment was then repeated using a S:Cu ratio of 1.0.

The solution samples from the experiments were analysed to determine the concentration of metals (Section 3.6.2) and the concentration of sulfide and sulfide degradation products (Section 3.6.4.1). All graphs have been shown from high pH to low pH as this was how pH was changed during the experiments. Cyanide analysis was not performed because of difficulty in clearly determining cyanide concentration in solution (Section 4.3.4). Hence, metal precipitation and acid consumption are used as an indicator of cyanide recovery. Due to the copper sulfide precipitates formed being black, precipitate colour could not be used as an indicator of other precipitates formed.

### **5.2.2 Baseline Experiment**

Before impurity experiments were conducted, two baseline experiments were performed, one at a S:Cu ratio of 0.5 and one at a S:Cu ratio of 1.0. This was done so the impact of any impurity is clearly visible in the results. While the model from Chapter 4 would also be suitable for this purpose, the model was only constructed over a small pH range ( $4 \leq \text{pH} \leq 5.5$ ) and S:Cu ratio region ( $0.4 \leq \text{S:Cu ratio} \leq 0.6$ ). The baseline results are shown in every impurity graph for this section so that the impact of the impurity can be easily compared to the baseline data.

### **5.2.3 Silver**

The impact of silver on sulfidisation at a sulfide to copper ratio of 0.5 is shown in Figure 5.1. Silver precipitates from solution as soon as sulfide is added with a recovery greater than 99% for every pH value tested. This precipitation of silver at high pH causes 49% of the sulfide in solution (at pH 10) to be consumed as per Equation 1.3.

A small amount of copper is also lost from solution (3% to 6%) at values between pH 10 and 7. This loss of copper may be due to either co-precipitation, via formation of a distinct phase or substitution of copper into the crystal lattice (Mullin 2004; Demopoulos 2009), or by adsorption of copper cyanide on the silver sulfide surface as gold cyanide does with sulfide minerals (Venter, Chryssoulis, and Mulpeter 2004). Study of the mechanism causing the loss of copper is outside of the scope of this research, with similar effects seen throughout the rest of this thesis labelled as co-precipitation / adsorption.

Significant precipitation of copper begins below pH 7 with a recovery of 47% by a pH of 6. The consumption of sulfide at high pH by silver results in only approximately half the initial amount of sulfide being available for precipitation of copper. This causes both a lower pH for significant copper precipitation to begin and recoveries lower than the baseline. An increase of copper recovery to 92% occurs at pH 3, which is due to the precipitation of the remaining soluble copper as copper cyanide (CuCN) (reverse of Equation 2.3).

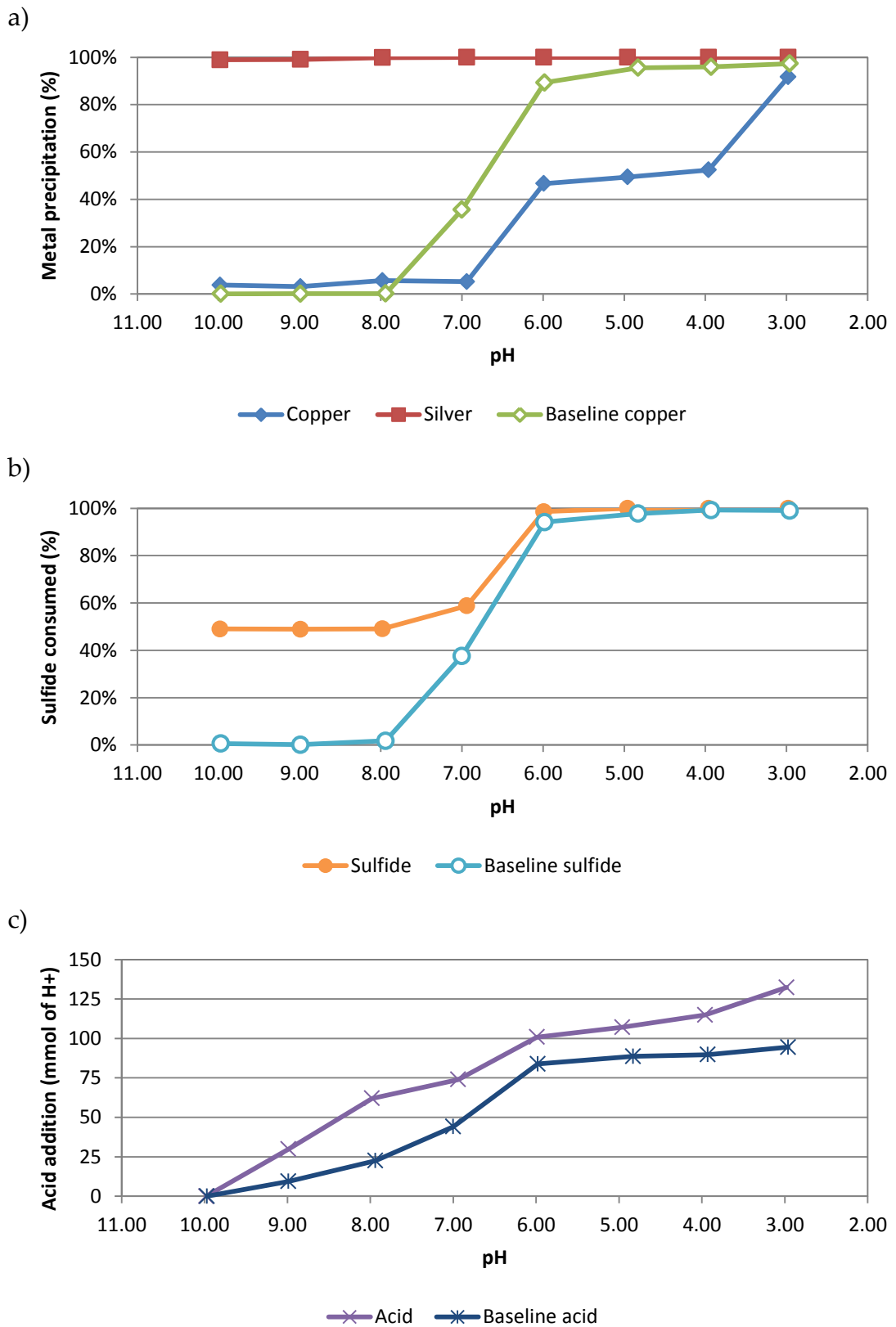


Figure 5.1 a) Metal precipitation, b) sulfide consumption, and c) acid addition when changing the pH from 10 to 3 on a solution containing: 18.0 mM Cu, 8.0 mM Ag, CN:metal ratio of 4, and a S:Cu ratio of 0.5.

Acid consumption was higher for the silver impurity test than it was for the baseline test. This is caused by the high pH precipitation of silver releasing cyanide. Cyanide that is released from the silver then requires one mole of acid for every mole of cyanide as the pH is reduced (Equation 2.1). The acid consumption increase compared to the baseline test between pH 4 and 3 is caused by the release of cyanide from copper cyanide complexes ( $\text{Cu}(\text{CN})_{x^{1-x}}$ ) until copper cyanide ( $\text{CuCN}$ ) precipitates (reverse of Equation 2.5, 2.4, and 2.3).

Figure 5.2 shows the impact of silver on sulfidisation when the sulfide to copper molar ratio is 1.0. As for a sulfide to copper ratio of 0.5, silver recovery is high (>99%) for every pH value sampled. The higher sulfide addition results in 77% of sulfide remaining in solution once silver precipitates. The amount of sulfide remaining in solution after silver precipitation causes copper precipitation over similar pH values to the baseline experiments. Sulfide consumption, while higher due to silver sulfide formation, follows a similar trend to the baseline.

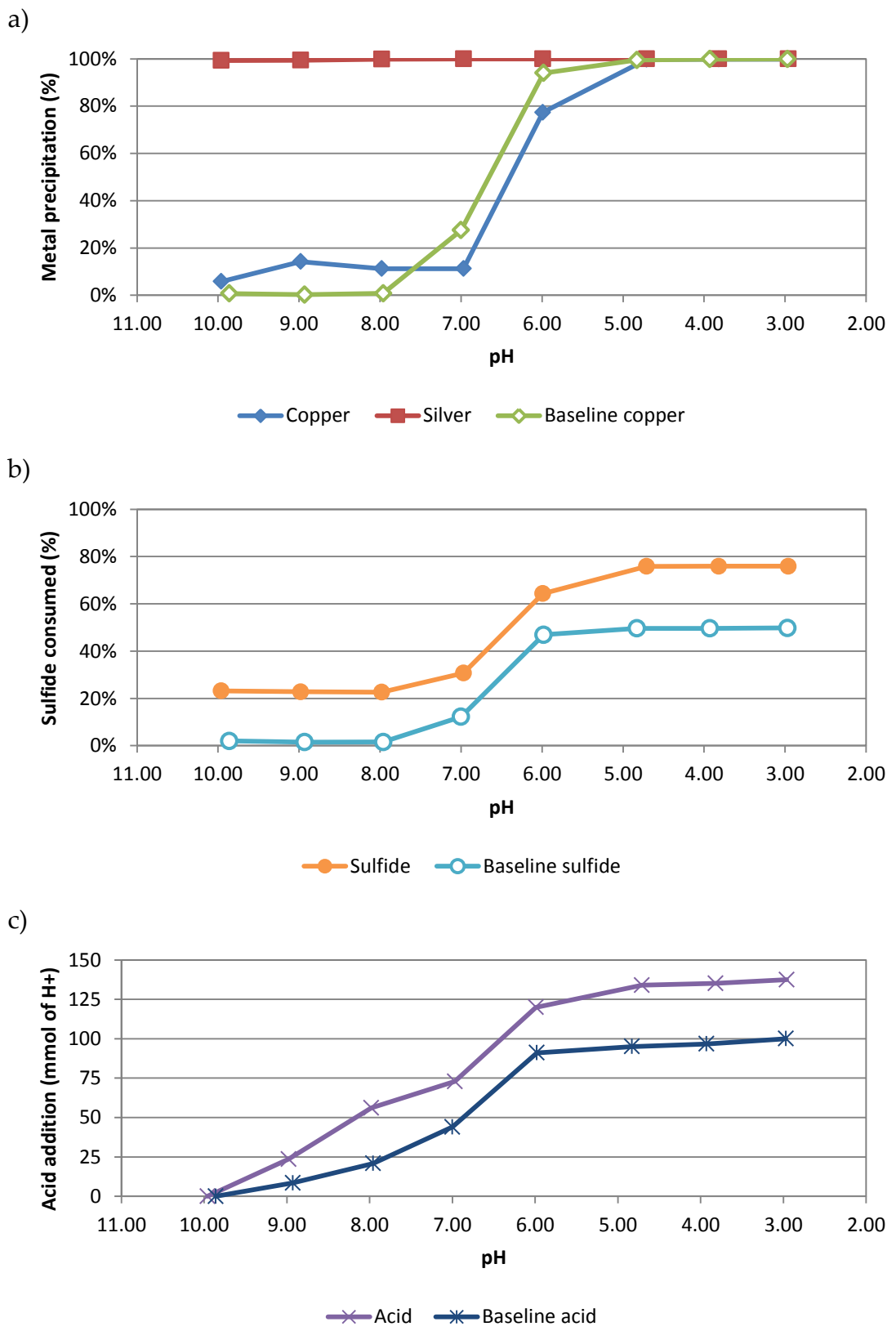


Figure 5.2 a) Metal precipitation, b) sulfide consumption, and c) acid addition when changing the pH from 10 to 3 on a solution containing: 16.2 mM Cu, 8.2 mM Ag, CN:metal ratio of 4, and a S:Cu ratio of 1.0.

Copper co-precipitation / adsorption also occurs at a S:Cu ratio of 1.0 as it did with the S:Cu ratio of 0.5. The copper co-precipitated / adsorbed with silver when the S:Cu ratio was 1.0 is between 6% and 14% when the pH is at 7 or above. These co-precipitation / adsorption values are higher than when the S:Cu ratio is 0.5. Interestingly, the larger amount of co-precipitated / adsorbed copper does not cause an increase in sulfide consumption in this pH range. The total sulfide consumption at pH 4, however, is consistent with all the copper having formed copper sulfide. This suggests that copper loss above pH 7 is not due to the formation of copper sulfide but more likely adsorption of copper cyanide. The cause of why larger sulfide concentrations cause more co-precipitation / adsorption is outside of the scope of the research. Hence, the effect was not investigated further.

The results of the experiments largely agree with the literature and thermodynamic modelling discussed in Section 2.4.1, showing that silver could easily be selectively precipitated from copper, ignoring some copper loss due to copper co-precipitation / adsorption. The loss of copper co-precipitated with silver is unmentioned in the majority of the relevant papers on silver in sulfidisation (Potter, Bergmann, and Haidlen 1986; Guzman et al. 2010). Milosavljevic, Solujic, and Kravetz (2004) do note that complete separation is not possible, but do not detail the reasons. As larger S:Cu ratios seem to cause more co-precipitation / adsorption of copper, it may be necessary to control sulfide dosing during silver precipitation in an industrial separation process to limit copper co-precipitation / adsorption.

#### **5.2.4 Gold**

Figure 5.3 shows the impact of gold on sulfidisation at a S:Cu ratio of 0.5. The figure shows no major changes in copper recovery or sulfide consumption compared to the baseline when gold is present during sulfidisation, except

for a slight decrease in copper recovery and sulfide consumption at pH 7. This difference can be attributed to experimental error caused by slight pH variation between individual experiments at the target pH. While the effect occurs at all pH values, it is noticeable around pH 6-7 as small changes in pH result in large changes in copper recovery in this pH region (Figure 2.10). Further, the difference is accentuated by the linear lines joining the experimental points, which are shown for ease of viewing the change between pH points and not to indicate the course of the pH profile between sample points.

Acid addition is slightly higher than the baseline when gold is present during sulfidisation. This is particularly obvious below pH 9. The cause of higher acid consumption is due to the initial solution having four moles of cyanide per mole of gold. As gold only forms a complex with two moles of cyanide per mole of gold ( $\text{Au}(\text{CN})_2^-$ ), there are two additional cyanide molecules free in solution per gold atom. Each molecule of free cyanide will consume one proton below pH 9.2, therefore increasing acid consumption.

Although gold has no obvious impact on the efficiency of sulfidisation to recover copper, the amount of gold in solution does decrease with a gold recovery between 9% and 11% in the pH range from 6 to 3. The slight recovery of gold is associated with the recovery of copper, suggesting that gold recovery is caused by co-precipitation / adsorption of gold rather than precipitation of gold as a sulfide or another species. This is also consistent with what was seen when copper co-precipitated with silver in Section 5.2.3.

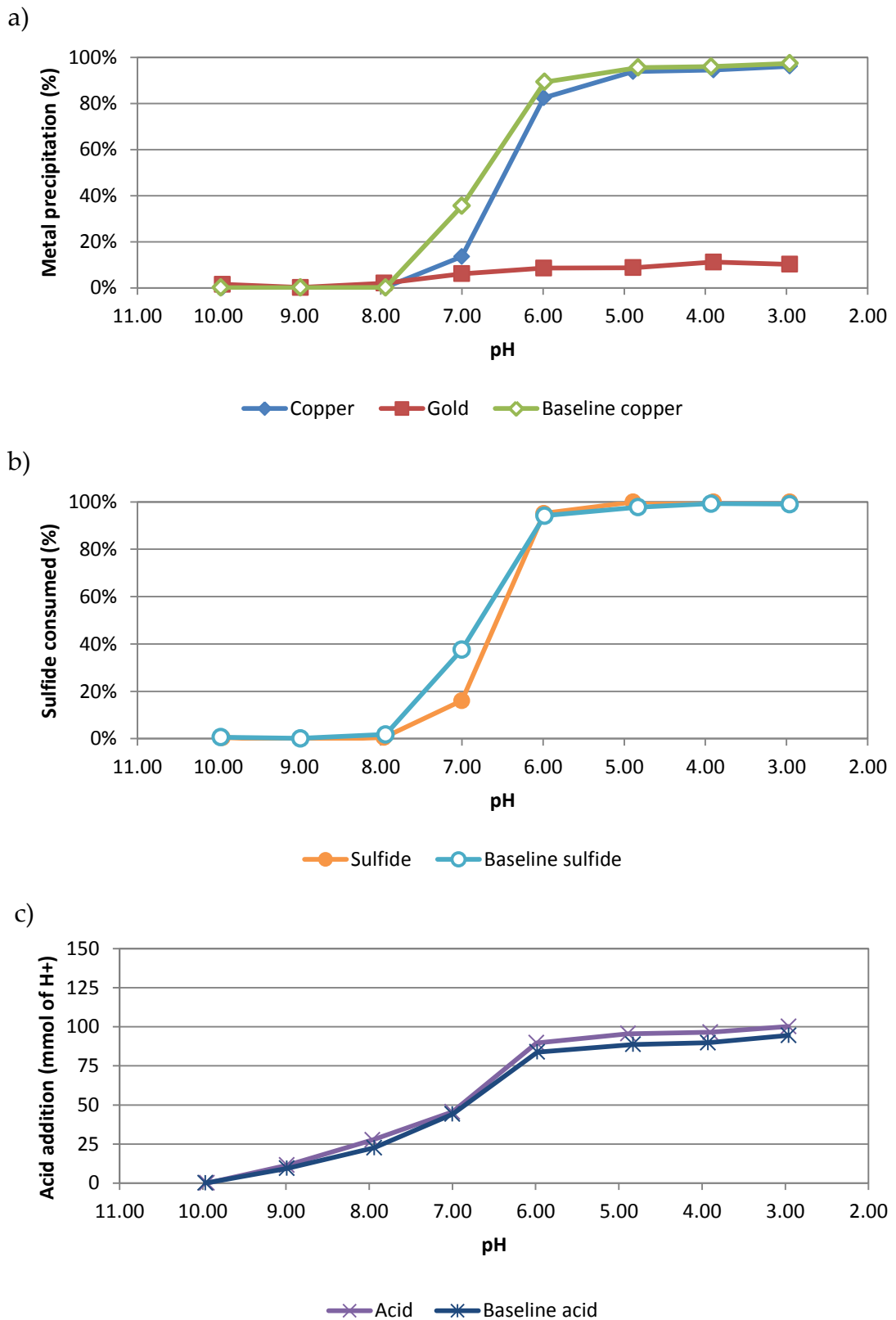


Figure 5.3 a) Metal precipitation, b) sulfide consumption, and c) acid addition when changing the pH from 10 to 3 on a solution containing: 18.1 mM Cu, 1.7 mM Au, CN:metal ratio of 4, and a S:Cu ratio of 0.5.

Figure 5.4 shows the impact of gold on sulfidisation at a S:Cu ratio of 1.0. As with a S:Cu ratio of 0.5, there is no notable impact of gold on copper recovery at any pH. Gold recovery is between 10% and 12% from pH 7 to 5, which is also similar to gold recovered when the S:Cu ratio is 0.5. Gold recovery is, however, notably higher at low pH rising to 16% at a pH of 3.6 and 27% at a pH of 2.9. The low pH gold precipitation at a S:Cu ratio of 1.0 suggests copper precipitation occurs preferentially to gold precipitation.

While the slight recovery of gold from pH 7 to 5 is related to co-precipitation, the increased recovery seen at the lowest two pH sample points is more likely to be caused by the precipitation of gold as gold sulfide. This is consistent with the thermodynamic modelling done in Section 2.4.2. The thermodynamic model, however, predicts higher gold recovery at pH 3. This kind of variation can be expected as the thermodynamic data for some sulfide minerals is difficult to determine and results can be unreliable (Osadchii and Rappo 2004).

Unfortunately, the composition of the gold precipitate could not be verified by examining the sulfide consumption data. This is because the gold concentration in solution was low and only a small portion of that was recovered. This, coupled with the fact that two gold atoms are required to react with one sulfide atom to form gold sulfide, results in sulfide consumption within experimental error if this reaction is occurring. Acid addition for a S:Cu ratio of 1.0 is slightly higher than the baseline. This is caused by the same reasons as seen at a S:Cu ratio of 0.5.

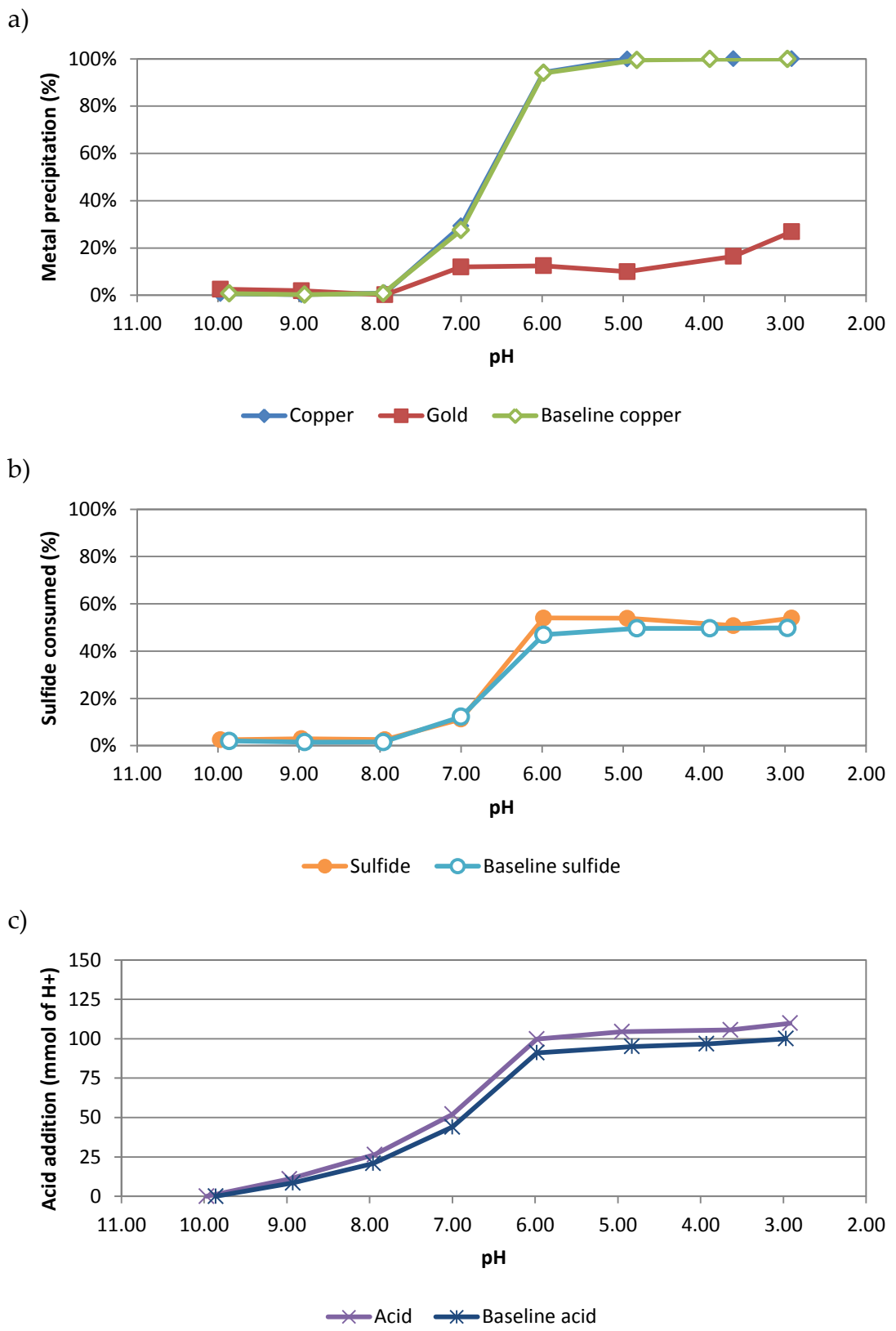


Figure 5.4 a) Metal precipitation, b) sulfide consumption, and c) acid addition when changing the pH from 10 to 3 on a solution containing: 17.7 mM Cu, 1.8 mM Au, CN:metal ratio of 4, and a S:Cu ratio of 1.0.

The precipitation of gold at low pH when excess sulfide is present is consistent with the results of Guzman et al. (2010). Guzman et al. (2010) did not note if gold co-precipitation / adsorption also occurred as copper precipitated. The results are also in agreement with Littlejohn, Kratochvil, and Hall (2013) who showed only small gold recoveries (<1.5%) during sulfidisation at pH 4.5. The increased gold co-precipitation in this study is due to the far higher gold concentration used (1.6 mM) compared to Littlejohn, Kratochvil, and Hall (2013) (0.2 mM). While the results of the experiments are consistent with Guzman et al. (2010) and Littlejohn, Kratochvil, and Hall (2013), they are in disagreement with Dreisinger et al. (2008) who recorded 20% to 30% gold recovery with just over stoichiometric sulfide additions and a pH between 4 and 5. The difference is potentially caused by more complex precipitates forming in the work by Dreisinger et al. (2008) due to more impurities being present in their solution. This is discussed further in the mixed metal experiment results (Section 5.3).

As discussed in Section 2.4.2, minimal gold recovery during sulfidisation is preferable in cases where sulfidisation is used on solutions which have not undergone gold recovery processes such as carbon adsorption. Hence, these results show that sulfidisation would be an acceptable way to recover copper with minimal loss of gold from solution, provided there is not a large excess of sulfide present.

### **5.2.5 Iron (II)**

The impact of iron (II) on sulfidisation at a S:Cu ratio of 0.5 is shown in Figure 5.5. Iron (II) appears to have no major impact on sulfidisation until the pH is less than 4, ignoring the co-precipitation / adsorption of between 4% and 6% iron with copper from pH 7 to 4. Below pH 4 there is an increase in iron recovery from 6% to 12%. This increase is accompanied by an increase in

acid consumption above the baseline and a slight increase in copper recovery.

The increased recovery of iron (II) and copper below pH 4 can be attributed to the formation of a copper iron cyanide salt similar to the one shown in Equation 2.11.  $\text{Cu}_4\text{Fe}(\text{CN})_6$  would be the expected species formed if copper was in the +1 oxidation state and iron was in the +2 oxidation state. The change from pH 3.9 to 3.0 resulted in a precipitate with a copper to iron molar ratio of approximately 2 based on the change of copper and iron concentration in solution. This ratio is half of that expected if  $\text{Cu}_4\text{Fe}(\text{CN})_6$  were forming. Due to the complexity of copper iron cyanide chemistry it is difficult to determine why the lower than expected ratio occurs.

The precipitation of copper and iron below pH 4 is accompanied by an acid addition of 12.57 mmol. While some of this acid is required to react with cyanide released from copper as it precipitates, the acid consumption is high considering the amount of copper recovered. Instead, it is likely that some protonated iron cyanide species are forming as shown in the thermodynamic model discussed in Section 2.4.3.

Figure 5.6 shows the impact of iron (II) on sulfidisation when the S:Cu ratio is 1.0. As with the S:Cu ratio of 0.5, iron (II) appears to have little impact on sulfidisation except for a small amount of iron co-precipitation / adsorption with copper and an increase in acid consumption when the pH is reduced below 4. As with previous impurity experiments, co-precipitation / adsorption of iron from pH 7 to 4 is higher (11% to 13%) when the S:Cu ratio is 1.0 compared to a S:Cu ratio of 0.5. The difference between the baseline reading and experiment results at pH 7 is due to experimental error as discussed in Section 5.2.4.

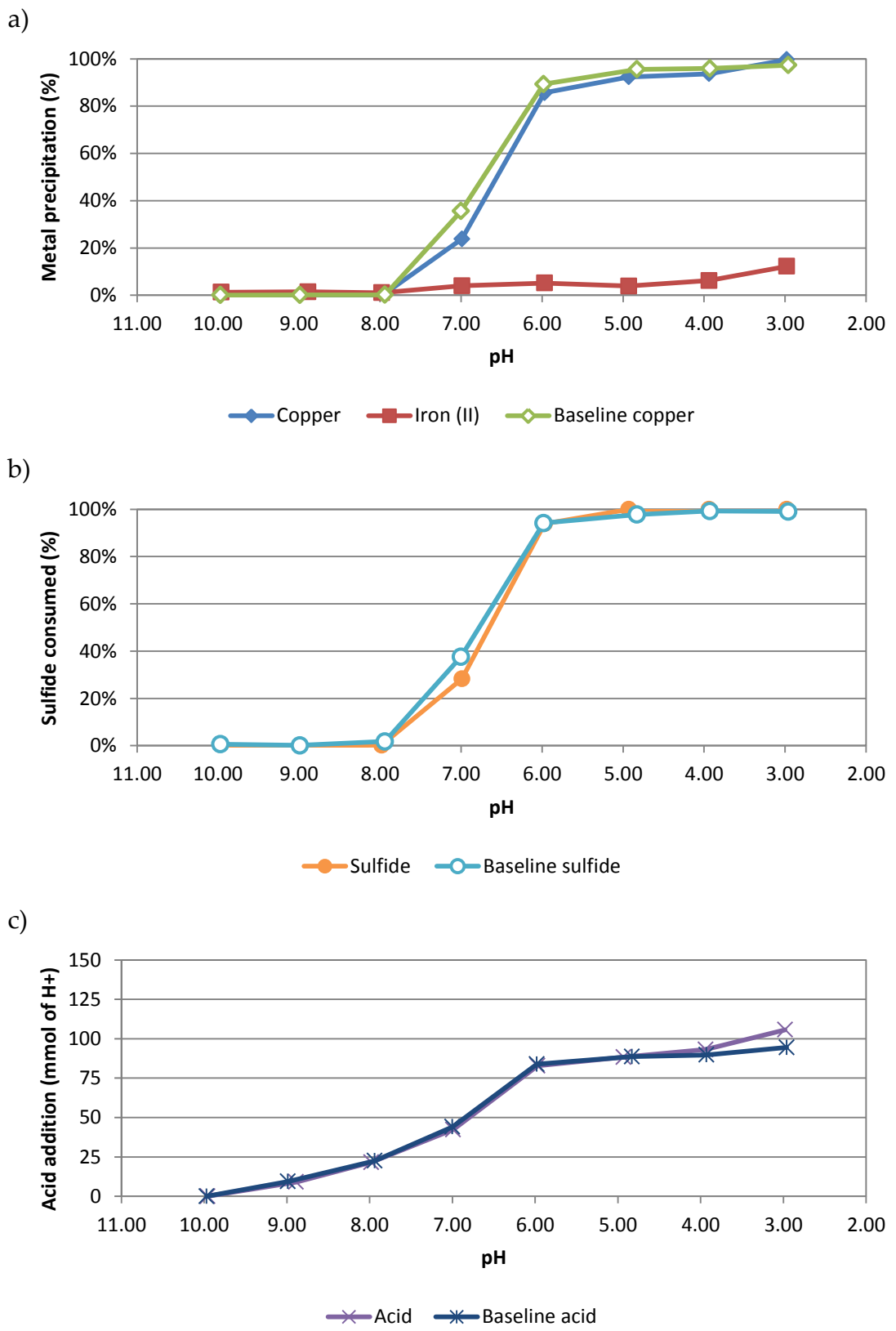


Figure 5.5 a) Metal precipitation, b) sulfide consumption, and c) acid addition when changing the pH from 10 to 3 on a solution containing: 18.3 mM Cu, 9.1 mM Fe(II), CN:metal ratio of 4 for Cu and 6 for Fe, and a S:Cu ratio of 0.5.

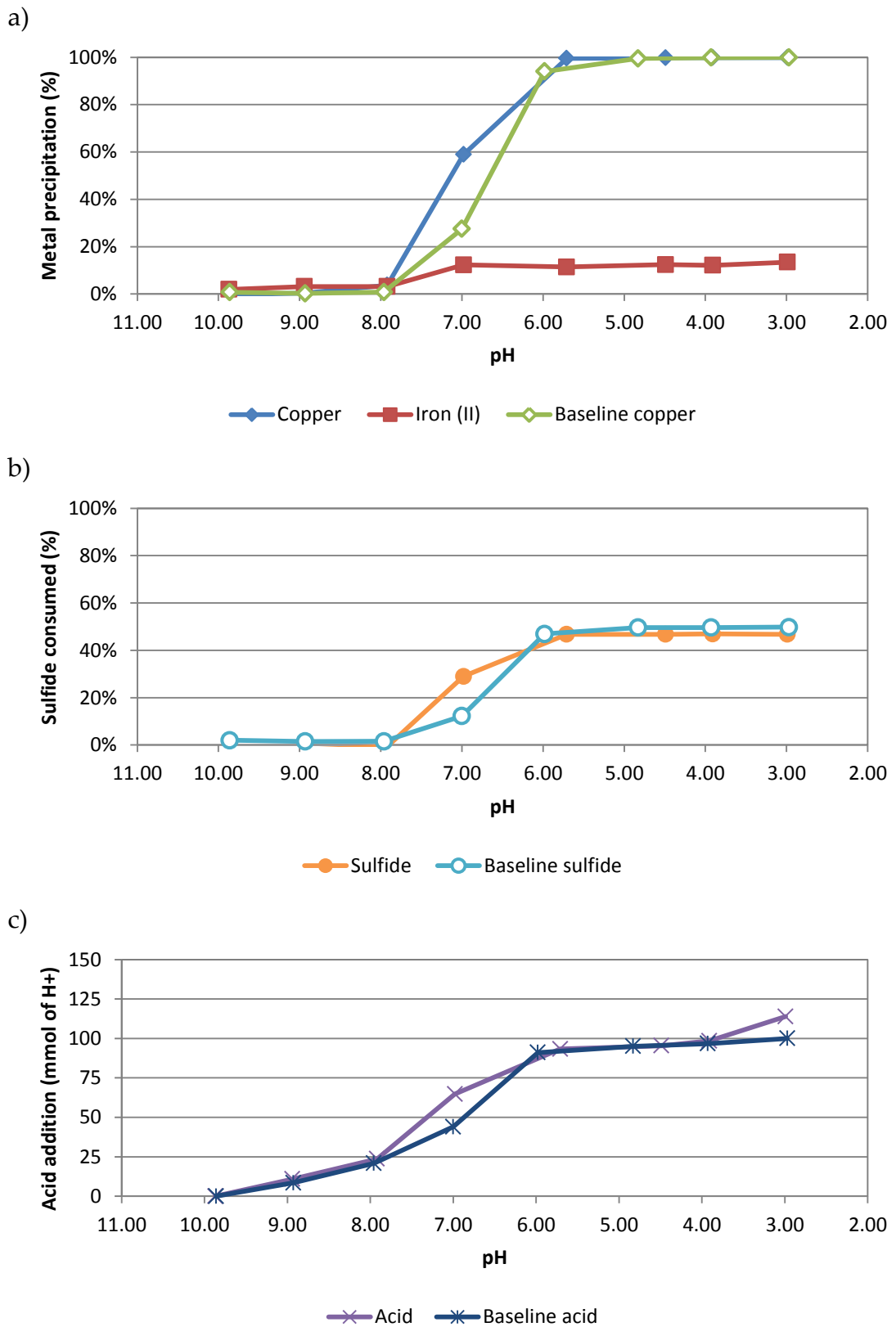


Figure 5.6 a) Metal precipitation, b) sulfide consumption, and c) acid addition when changing the pH from 10 to 3 on a solution containing: 15.6 mM Cu, 7.9 mM Fe(II), CN:metal ratio of 4 for Cu and 6 for Fe, and a S:Cu ratio of 1.0.

An increase in acid consumption is observed below pH 4 compared to the baseline. This is similar to when the S:Cu ratio is 0.5. Nevertheless, as copper recovery is high, the acid consumption increase is not caused by release of cyanide from unrecovered copper as in the S:Cu ratio of 0.5 experiment. No change in iron recovery is observed in this region either. This confirms that acid consumption in the iron (II) impurity experiments is likely caused by the formation of protonated iron cyanide complexes (Section 2.4.3).

The lack of extra iron precipitation below pH 4 when the S:Cu ratio is 1.0, compared to when the S:Cu ratio is 0.5, also confirms that copper iron cyanide double salts will not form unless there is copper available in solution that has not reacted with any sulfide. This is consistent with the thermodynamic model in Section 2.4.3. The consumption of extra acid compared to the baseline at low pH suggests that, when iron (II) is present during sulfidisation, the pH used should not be less than 4 as to minimise acid consumption.

### **5.2.6 Iron (III)**

The impact of iron (III) on sulfidisation at a S:Cu ratio of 0.5 is shown in Figure 5.7. As with iron (II), there is little impact of iron (III) on sulfidisation down to a pH of 4, except for slight co-precipitation / adsorption of iron (III) (5-8%) with copper from pH 7 to 4.

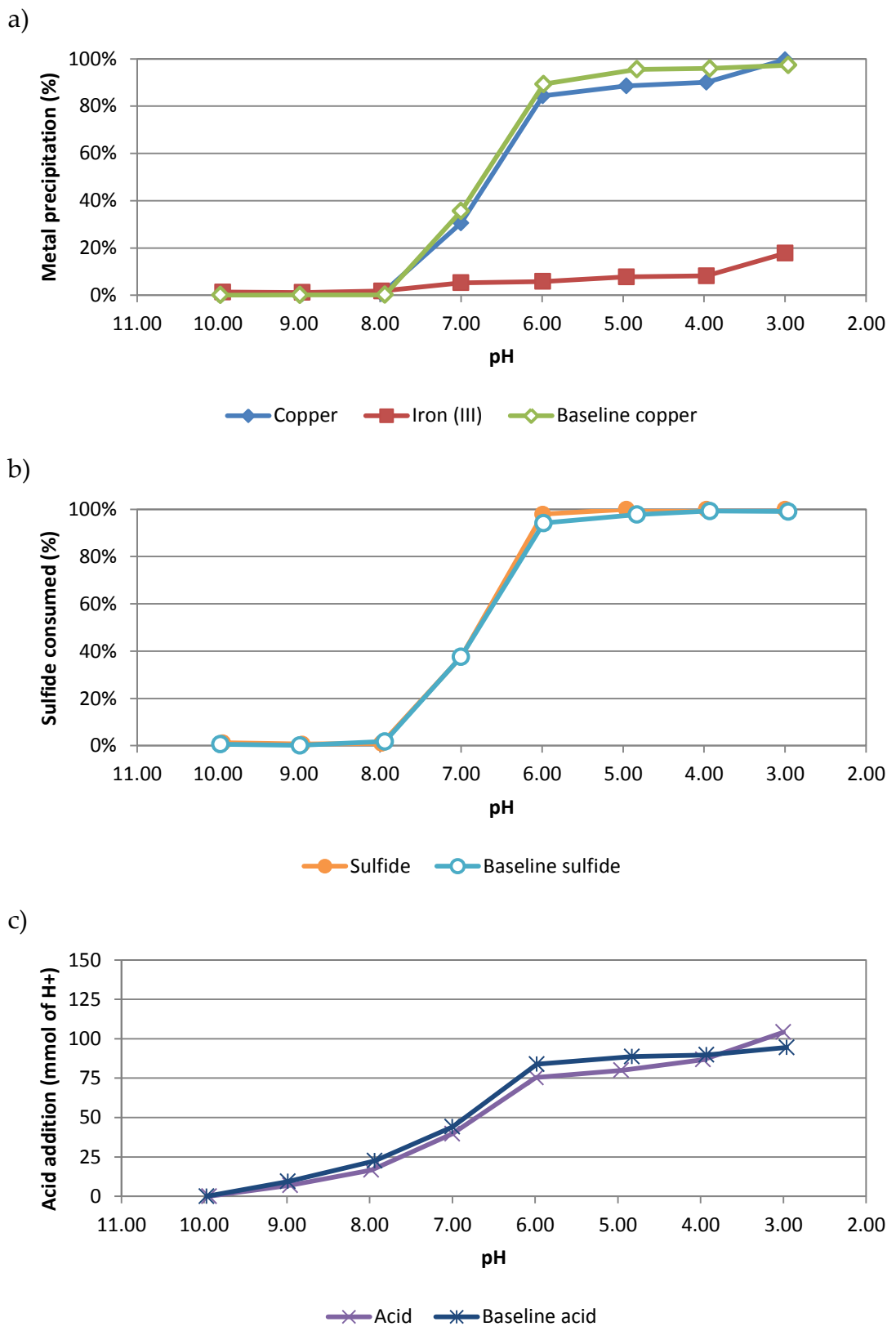


Figure 5.7 a) Metal precipitation, b) sulfide consumption, and c) acid addition when changing the pH from 10 to 3 on a solution containing: 18.2 mM Cu, 9.2 mM Fe(III), CN:metal ratio of 4 for Cu and 6 for Fe, and a S:Cu ratio of 0.5.

Below pH 4 there is an increase in copper recovery and acid consumption compared to the baseline. This is accompanied by an increase in iron precipitation. Like with iron (II) (Section 5.2.5), the increase in copper and iron recovery suggests the formation of a copper iron cyanide double salt. The change in copper and iron concentration between pH 4 and pH 3 suggests a copper to iron molar ratio of 2 in the precipitate. This is similar to that seen in the iron (II) experiment and indicates that iron (II) and (III) may be forming a similar precipitate. As iron (III) can oxidise copper (I) to copper (II), it was not possible to determine an expected molar ratio of copper to iron in this experiment.

Acid addition when iron (III) is present as an impurity at a S:Cu or 0.5 is slightly less than the baseline from pH 10 to 5. The acid addition trend over this region was, however, the same as the baseline with the deviation likely due to experimental error. The increase in acid addition between pH 4 and 3 is caused by the release of cyanide from copper when copper iron cyanide double salts precipitate. The increased acid consumption could also be due to iron cyanide protonation like with iron (II) (Section 5.2.5), although this is not expected based on the thermodynamic modelling (Section 2.4.3).

Figure 5.8 shows the impact of iron (III) on sulfidisation at a S:Cu ratio of 1.0. As with other impurities at a S:Cu ratio of 1.0, the co-precipitation / adsorption of iron with the copper precipitate is higher than at a S:Cu ratio of 0.5. Also, like iron (II), the complete precipitation of copper due to excess sulfide results in no increase in iron precipitation below pH 4.

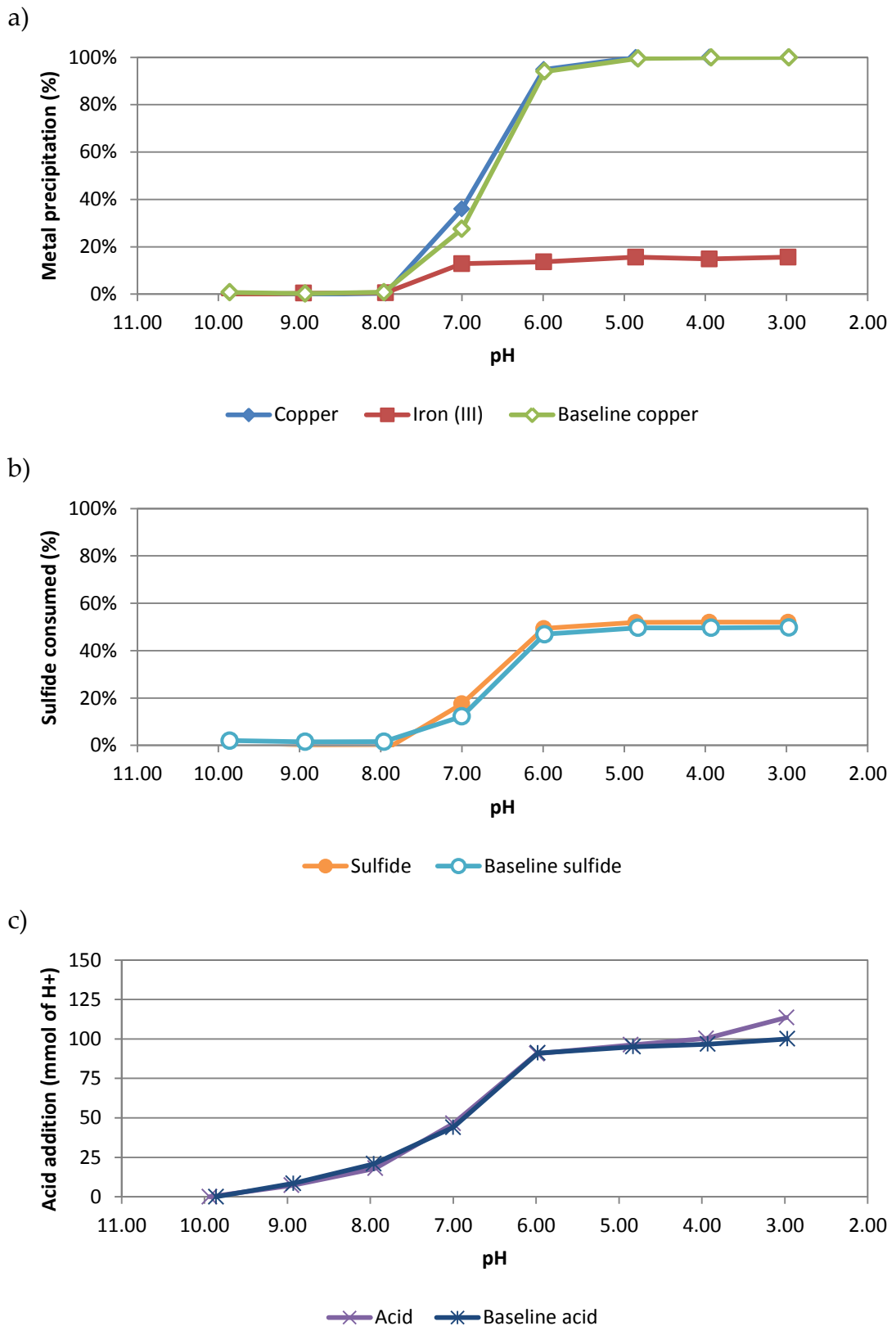


Figure 5.8 a) Metal precipitation, b) sulfide consumption, and c) acid addition when changing the pH from 10 to 3 on a solution containing: 17.1 mM Cu, 10.0 mM Fe, CN:metal ratio of 4 for Cu and 6 for Fe, and a S:Cu ratio of 1.0.

Interestingly, an increase in acid consumption compared to the baseline occurs for iron (III) at a S:Cu ratio of 1.0 when the pH is below 4. This was unexpected as thermodynamic modelling did not predict increased acid consumption caused by iron (III). Also, at the S:Cu ratio of 1.0, the increase cannot be attributed to copper iron cyanide double salt formation as all the copper is precipitated with sulfide. The cause of the increased acid consumption could be due to iron cyanide protonation like in the iron (II) experiment (Section 5.2.5). This, however, could not be verified and detailed examination of iron cyanide chemistry at low pH is outside of the scope of research. Although the cause of the acid consumption is unknown, the result does suggest that when iron is present during sulfidisation, the pH should be kept above 4 to minimise acid consumption.

### **5.2.7 Nickel**

Figure 5.9 shows the impact of nickel on sulfidisation when the S:Cu ratio is 0.5. Copper recovery for the experiment was slightly lower than the baseline. This, however, is due to a slightly lower dosing of sulfide in the experiment. Nickel has no impact on sulfidisation except for co-precipitation / adsorption of between 4% and 7% of the nickel with copper. Figure 5.10 shows that at a S:Cu ratio of 1.0, nickel has no impact on sulfidisation except for co-precipitation / adsorption (16% to 18%).

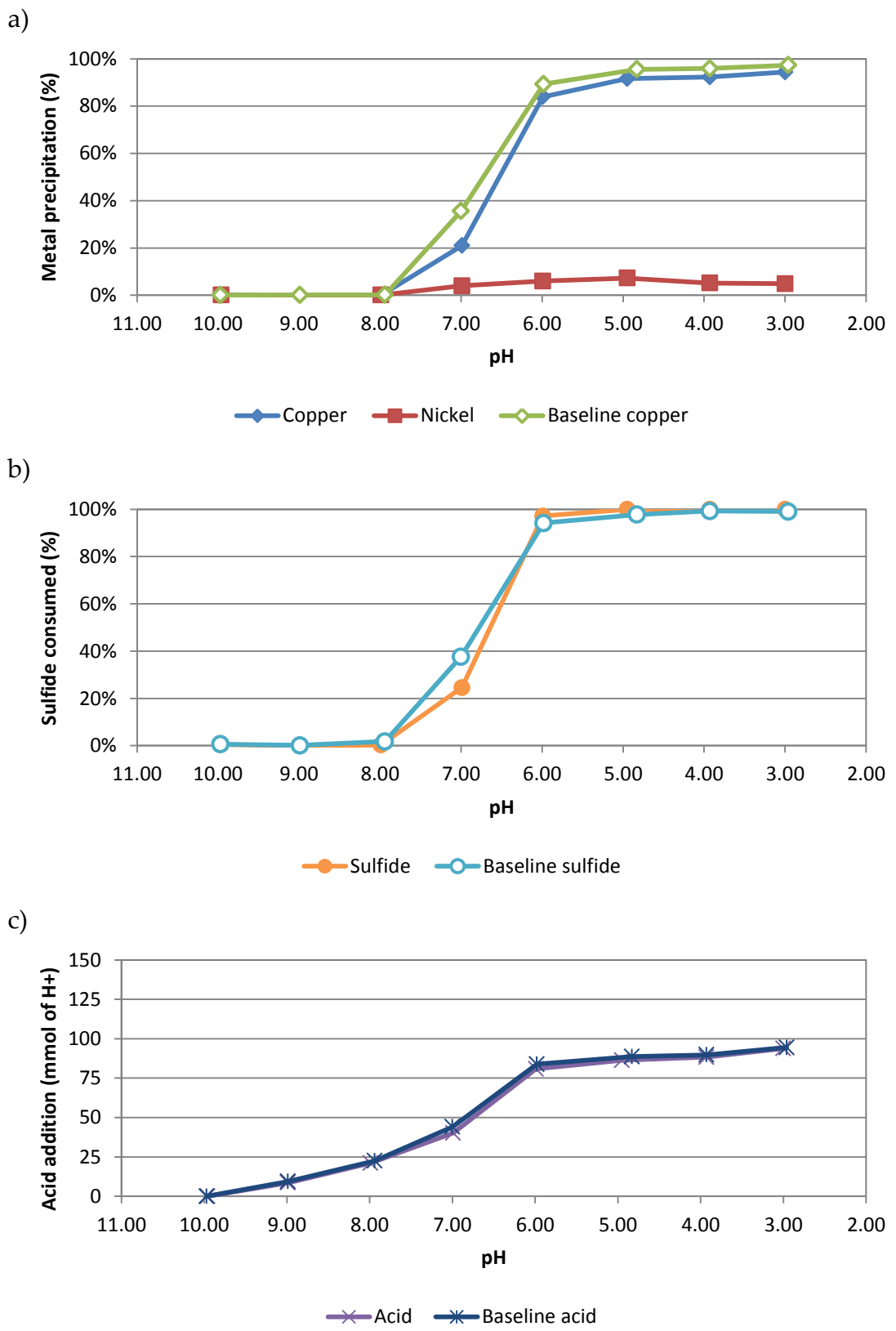


Figure 5.9 a) Metal precipitation, b) sulfide consumption, and c) acid addition when changing the pH from 10 to 3 on a solution containing: 18.1 mM Cu, 8.6 mM Ni, CN:metal ratio of 4, and a S:Cu ratio of 0.5.

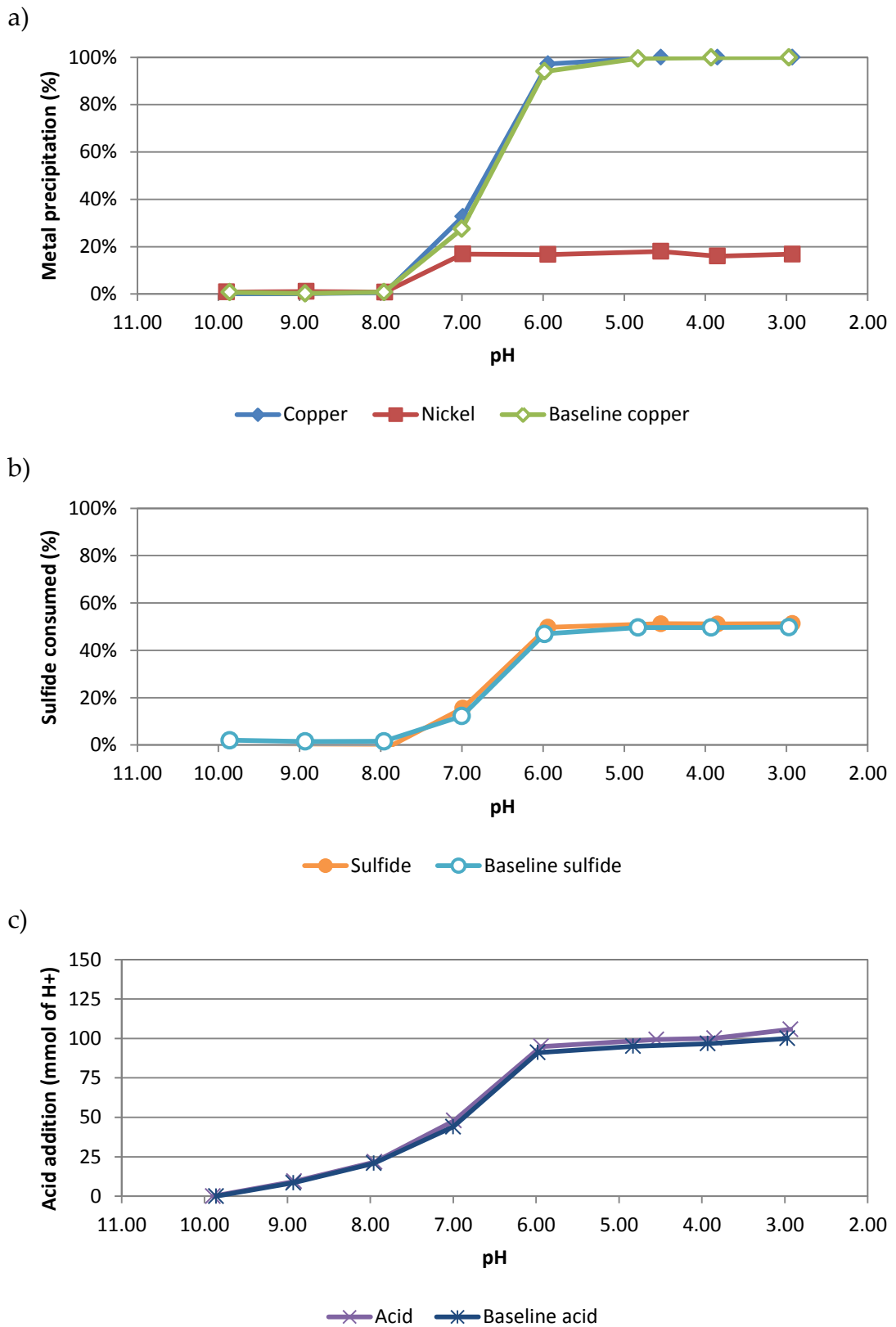


Figure 5.10 a) Metal precipitation, b) sulfide consumption, and c) acid addition when changing the pH from 10 to 3 on a solution containing: 16.9 mM Cu, 8.8 mM Ni, CN:metal ratio of 4, and a S:Cu ratio of 1.0.

### 5.2.8 Zinc

Zinc responded differently during sulfidisation than the other metals tested. When sulfide was dosed to the solution in either S:Cu ratio, a fine white precipitate formed. For samples between pH 8 and 10, a second white precipitate formed after filtering and making alkaline when using the standard sampling method in Section 3.5.1. Under the presumption that the precipitate formed on making the sample alkaline was a zinc sulfide, the experiments were repeated at both S:Cu ratios (0.5 and 1.0), but with 1 M cyanide solution in the neutralising solution, in an attempt to prevent the formation of zinc sulfide. This technique, however, did not stop the formation of the white precipitate on making the sample alkaline.

In a final effort to determine the zinc concentration at the sample pH, the experiment was repeated with all samples treated with lead (II) nitrate to remove sulfide from solution as lead sulfide (Mudder, Botz, and Smith 2001b). The lead sulfide formed was then filtered from the solution to leave a clear solution. After a few hours a second precipitate, which was yellow in colour, had formed in the solution. This was also filtered off before analysis. The results from this technique, however, were inconclusive.

Figure 5.11 shows the impact of zinc on sulfidisation when the S:Cu ratio is 0.5. The first available datum is at pH 7. Between pH 7 and 5 zinc precipitates preferentially to copper, with a small amount of copper co-precipitation / adsorption. As the pH was reduced to less than 5, zinc redissolution occurred with copper precipitating. This result is consistent with the thermodynamic modelling (Section 2.4.5) which shows zinc redissolves as  $Zn^{2+}$  ions as per Equation 5.1. The redissolution of zinc causes sulfide to be released into solution in turn causing copper to precipitate (Equation 1.3).

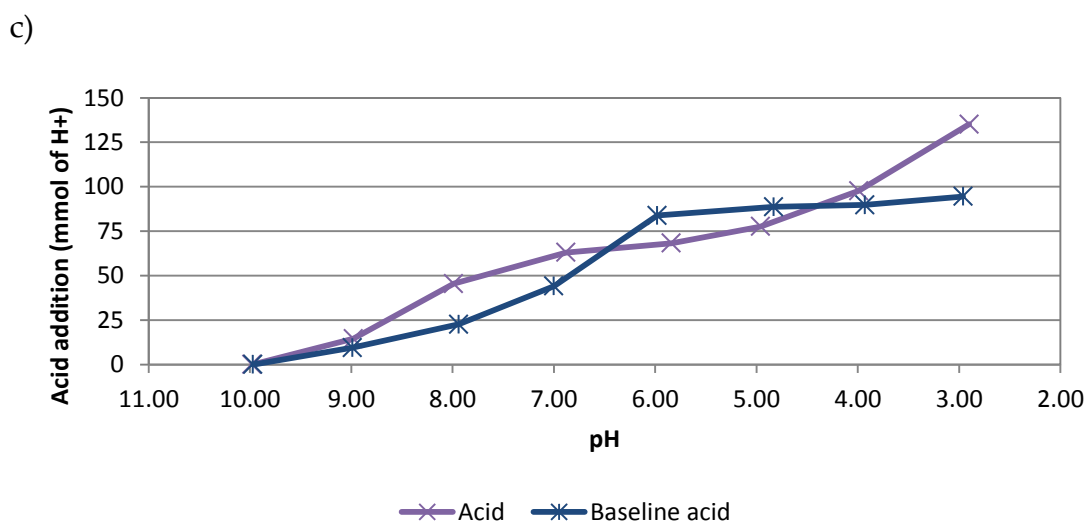
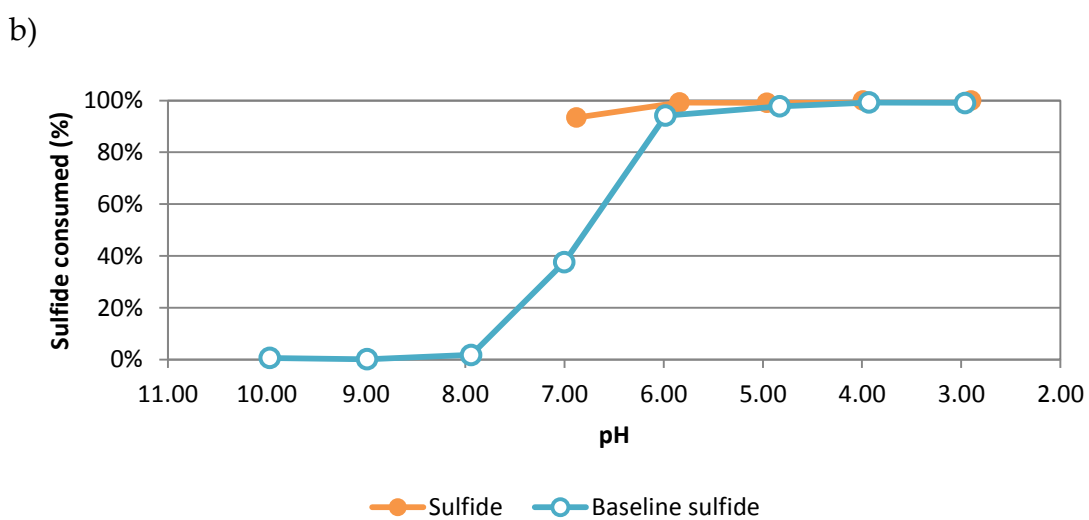
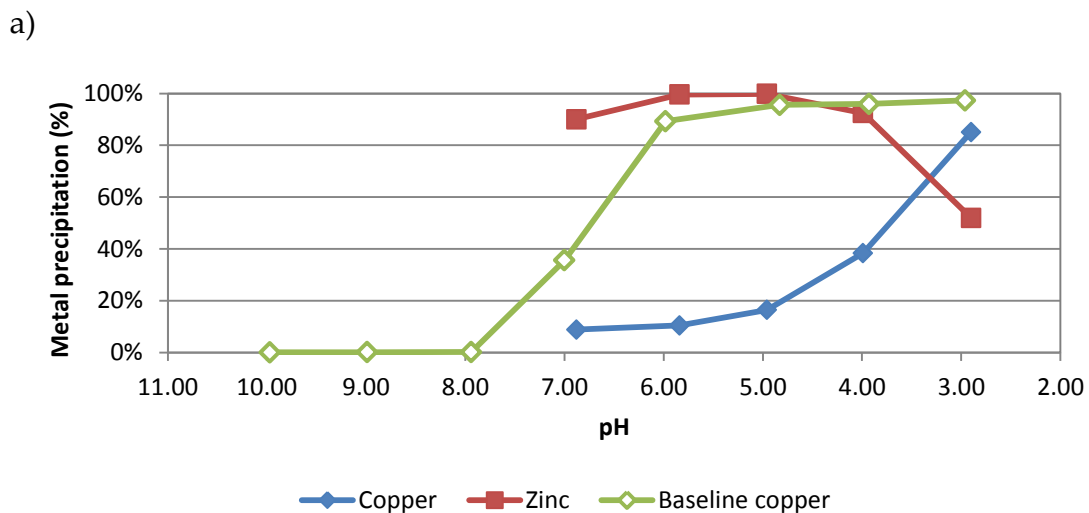
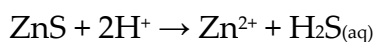


Figure 5.11 a) Metal precipitation, b) sulfide consumption, and c) acid addition when changing the pH from 10 to 3 on a solution containing: 15.7 mM Cu, 9.4 mM Zn, CN:metal ratio of 4, and a S:Cu ratio of 0.5.



5.1

Acid addition during the experiment is consistent with the metal recovery results, with acid addition greater than the baseline between pH 9 and approximately 6.5 due to cyanide released from zinc during zinc sulfide precipitation. The acid addition is then less than the baseline from a pH of approximately 6.5 to 4.5 due to cyanide not being released from copper cyanide species as there is no sulfide available to precipitate the copper. Finally, below pH 4.5 the acid addition rises above the baseline due to copper precipitation as both copper sulfide and copper cyanide releasing cyanide.

The impact of zinc on sulfidisation at a S:Cu ratio of 1.0 is shown in Figure 5.12. Due to the large sulfide concentration in solution zinc recovery from pH 7 down to 4 is greater than 99%. There is a slight dip in recovery below pH 4 due to the redissolution of zinc as  $\text{Zn}^{2+}$  ions (Equation 5.1). Copper recovery is slightly less than baseline copper recovery, but is similar to the baseline copper for a S:Cu ratio of 0.5 (Figure 5.11). This is due to sulfide being present in excess in the S:Cu ratio of 1.0 baseline experiment, whereas it is consumed by zinc in this experiment (Figure 5.12 b).

Acid addition is greater than the baseline for the entire pH range tested. This is due to zinc releasing cyanide during precipitation (pH 10 to ~7) followed by copper releasing cyanide as it precipitates (pH ~7 to ~3). This is consistent with the reactions that were expected.

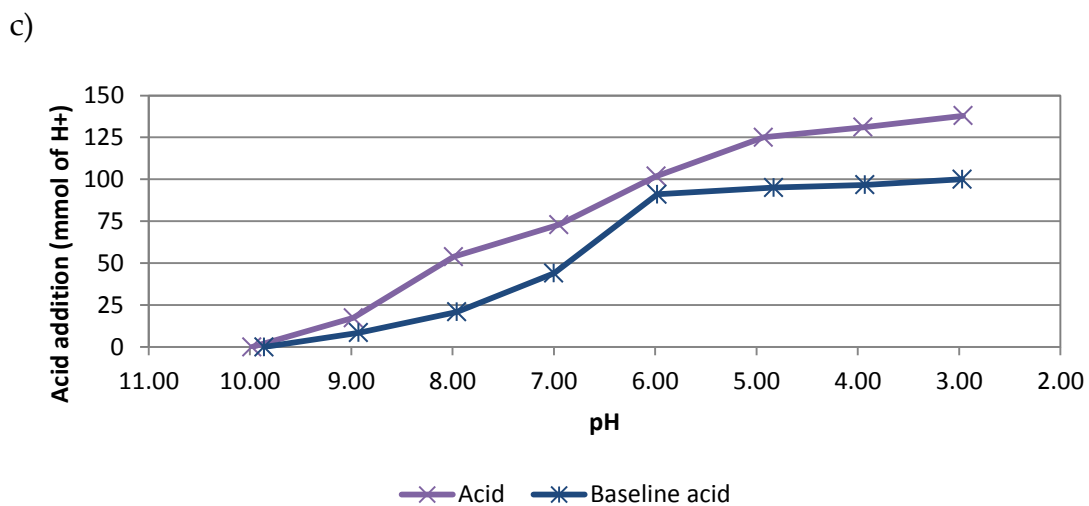
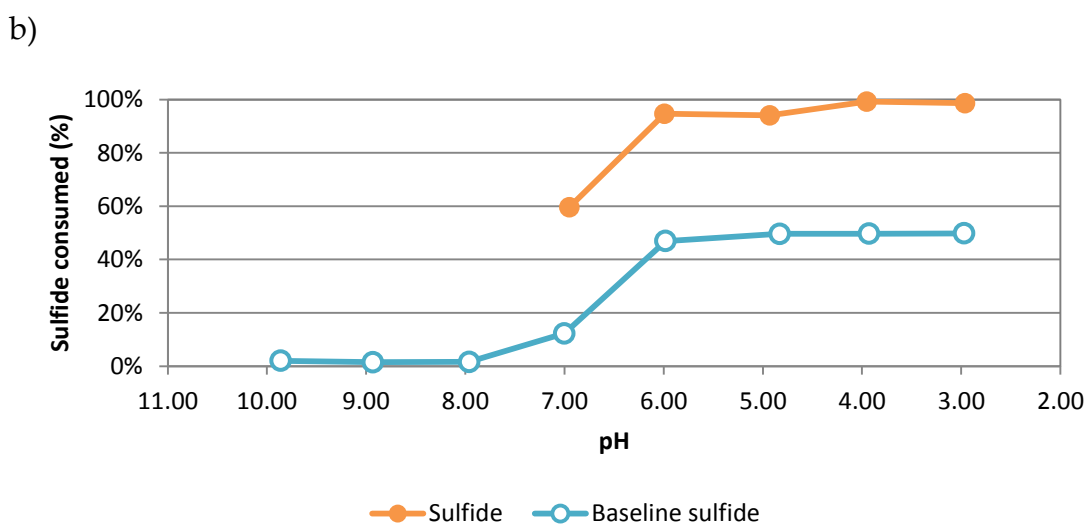
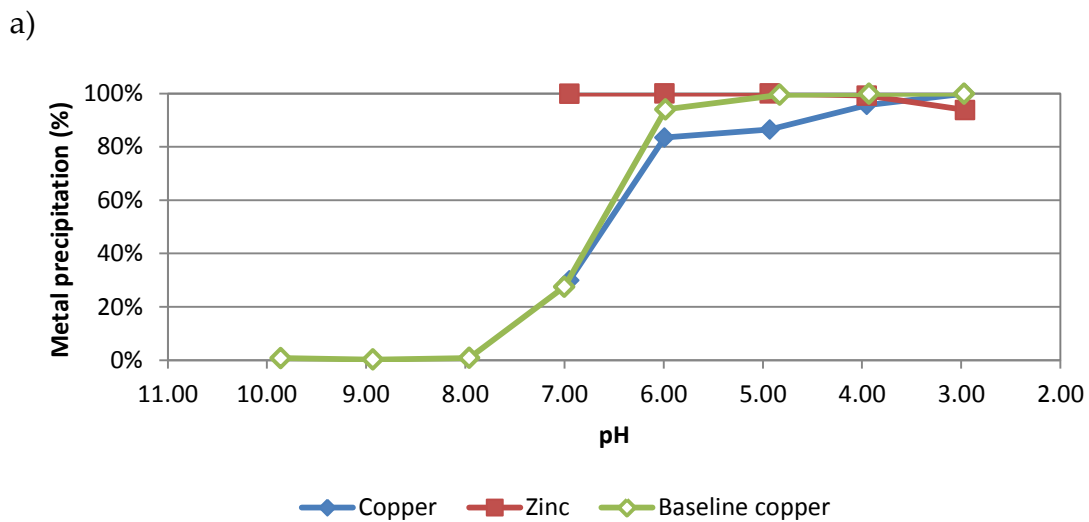


Figure 5.12 a) Metal precipitation, b) sulfide consumption, and c) acid addition when changing the pH from 10 to 3 on a solution containing: 15.7 mM Cu, 9.5 mM Zn, CN:metal ratio of 4, and a S:Cu ratio of 1.0.

The results of the two experiments show that zinc can be selectively recovered from solution with only minor copper co-precipitation / adsorption at pH above 6 provided only enough sulfide is present to react with zinc (Equation 2.14). If more sulfide is available then copper precipitation will also occur in this pH region. This suggests that sulfide addition should be carefully controlled if selective precipitation is required in this pH region. Although there are no data points above pH 7 in Figure 5.12, it is apparent that separate recovery of zinc is achievable above pH 7 when sulfide dosing is not controlled as copper recovery is trending back towards zero. This is consistent with the results of Littlejohn, Kratochvil, and Hall (2013) who selectively recovered zinc from solution at pH 7.5 when excess sulfide was available. Due to the lack of data available above pH 7, the upper pH limit for high zinc recovery could not be established.

### **5.2.9 Thiocyanate**

The impact of thiocyanate on sulfidisation at a S:Cu ratio of 0.5 is shown in Figure 5.13. Thiocyanate has no impact on copper recovery, sulfide consumption, or acid addition in sulfidisation over the pH range tested. The sulfide consumption is less than the baseline once copper precipitates due to accidental makeup of low copper concentration in the initial solution.

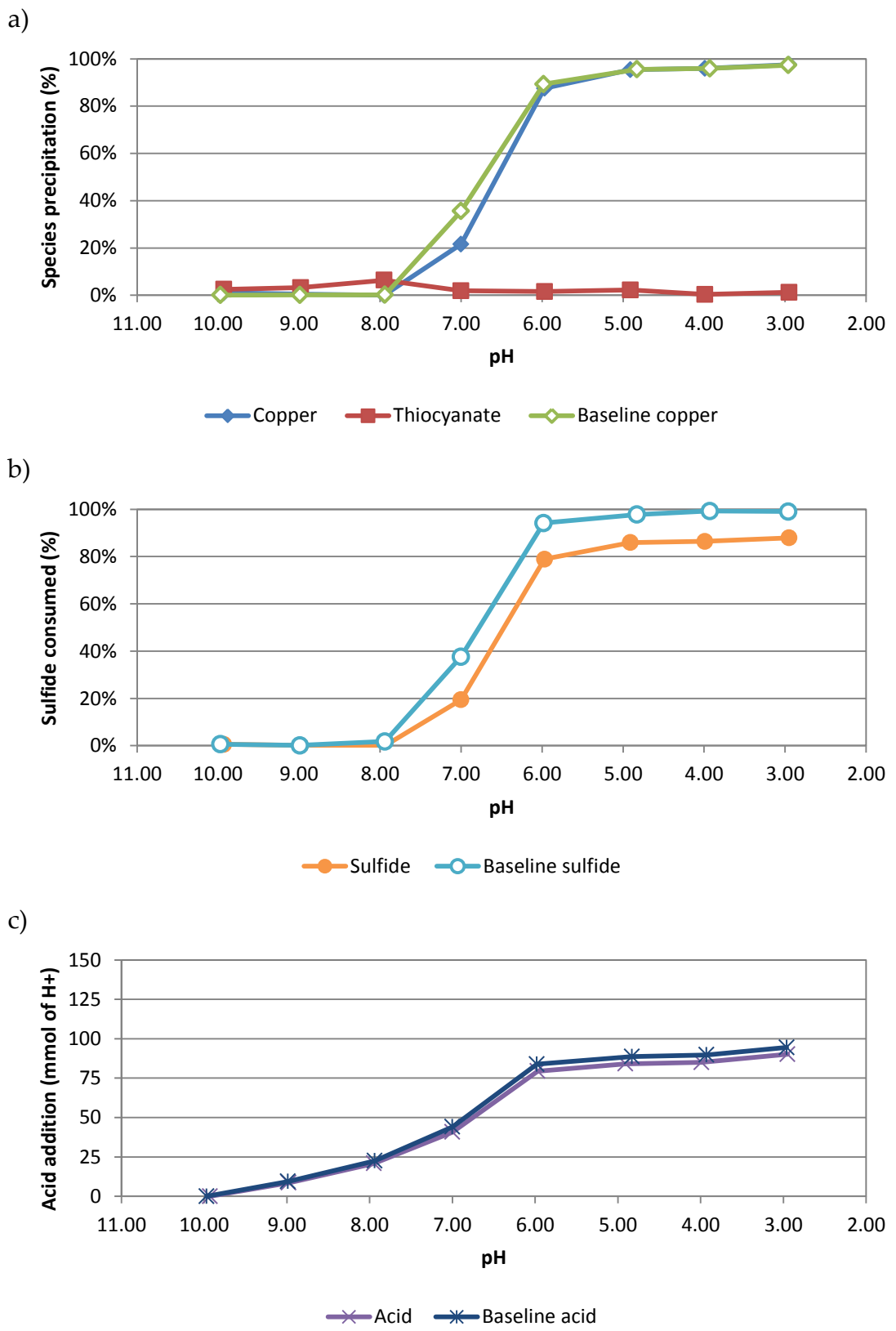


Figure 5.13 a) Species precipitation, b) sulfide consumption, and c) acid addition when changing the pH from 10 to 3 on a solution containing: 14.3 mM Cu, 8.1 mM SCN<sup>-</sup>, CN:metal ratio of 4, and a S:Cu ratio of 0.5.

Interestingly, unlike the metal cation impurities, there is no notable co-precipitation / adsorption of thiocyanate when copper sulfide precipitated from solution. This could be related to generation of thiocyanate during sulfidisation (Section 4.3.3), although the generation of thiocyanate is expected to be small compared to the amount of thiocyanate available in solution. Instead, it is likely that thiocyanate simply does not co-precipitate / adsorb as seen with the metal impurities. The cause of the small increase in thiocyanate recovery around pH 8 is unknown, and is potentially due to error. No experiment with a S:Cu ratio of 1.0 was performed as thiocyanate is not expected to consume sulfide or acid when sulfide is in excess.

#### **5.2.10 Thiosulfate**

The impact of thiosulfate on sulfidisation when the S:Cu ratio is 0.5 is shown in Figure 5.14. It is evident from Figure 5.14 that thiosulfate, like thiocyanate, has no impact on sulfidisation. The slight dip in copper recovery and sulfide consumption at pH 7 and 6 is due to experimental error as discussed in Section 5.2.4. Sulfide consumption follows a similar trend in this region, supporting this idea. Again, like thiocyanate, there is no observable co-precipitation / adsorption of thiosulfate in the copper sulfide precipitate. No experiment with a S:Cu ratio of 1.0 was performed as thiosulfate is not expected to consume sulfide or acid when sulfide is in excess.

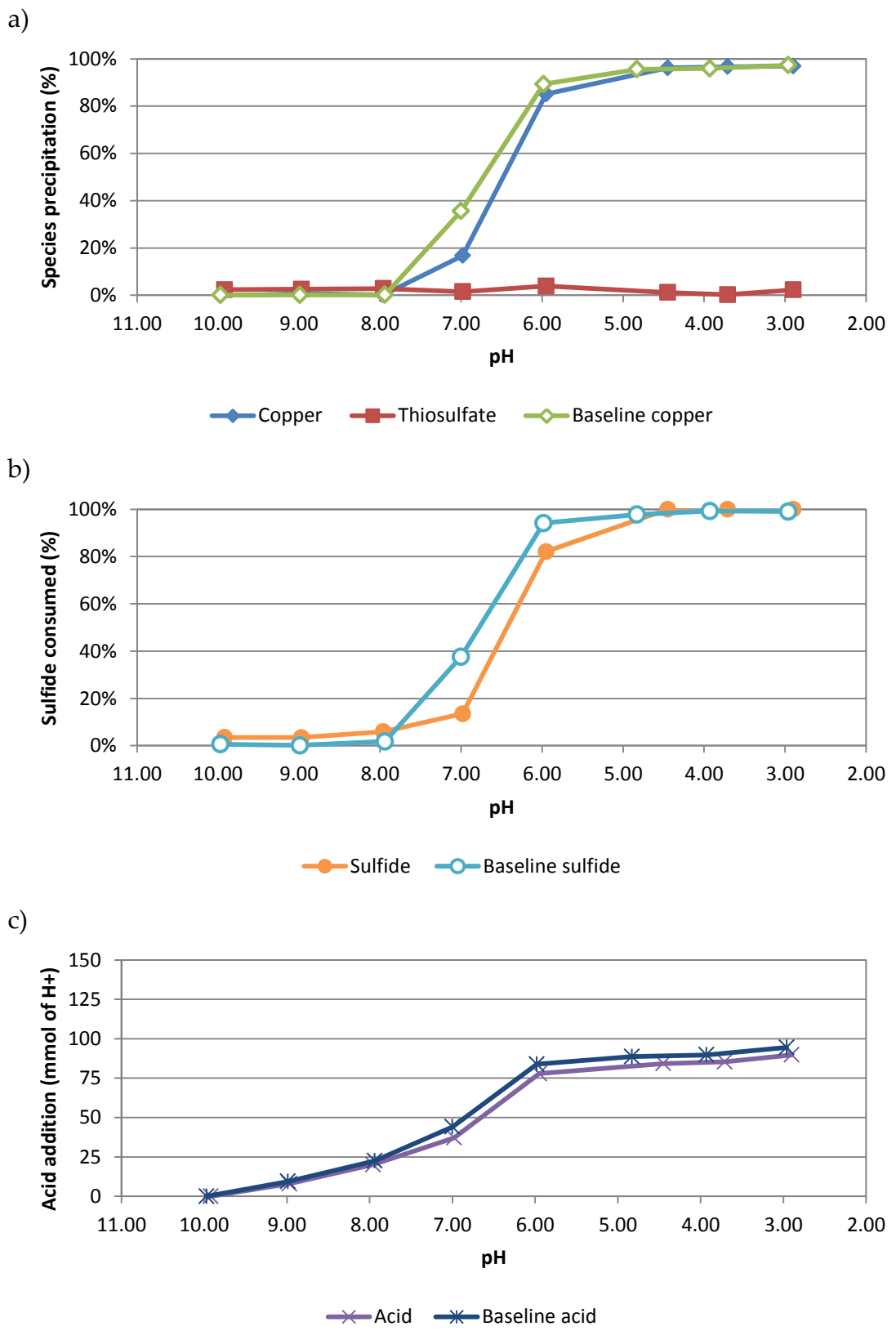


Figure 5.14 a) Species precipitation, b) sulfide consumption, and c) acid addition when changing the pH from 10 to 3 on a solution containing: 14.3 mM Cu, 8.3 mM S<sub>2</sub>O<sub>3</sub><sup>2-</sup>, CN:metal ratio of 4, and a S:Cu ratio of 0.5.

### **5.2.11 Chloride**

Chloride was selected as an impurity to study due to the potential to use sulfidisation on copper cyanide solutions generated from stripping ion exchange resins. This was discussed in detail in Section 2.4.9. Figure 5.15 shows the impact of having a 1.0 M chloride concentration in solution during sulfidisation when the S:Cu ratio is 0.5. When chloride is present copper recovery begins at a lower pH than when there is no chloride present.

Although chloride affects copper recovery at some pH values, copper recovery is still high by pH 5. As sulfidisation is usually done between pH 5 and 4 (Section 2.3.2), with 4 being the optimum suggested by modelling in Chapter 4, chloride would have little impact on sulfidisation when done under these conditions. Sulfide consumption and acid addition both vary from their baselines due to the shift in pH for copper precipitation.

A small amount of chloride co-precipitation / adsorption occurs during sulfidisation. While this has little impact on sulfidisation itself, the loss of chloride from solution may impact the ion exchange elution process as the solution is recycled. As copper recovery is high and acid consumption is unchanged in the usual sulfidisation operating pH range, using sulfidisation to recover cyanide and copper from a resin strip solution appears feasible.

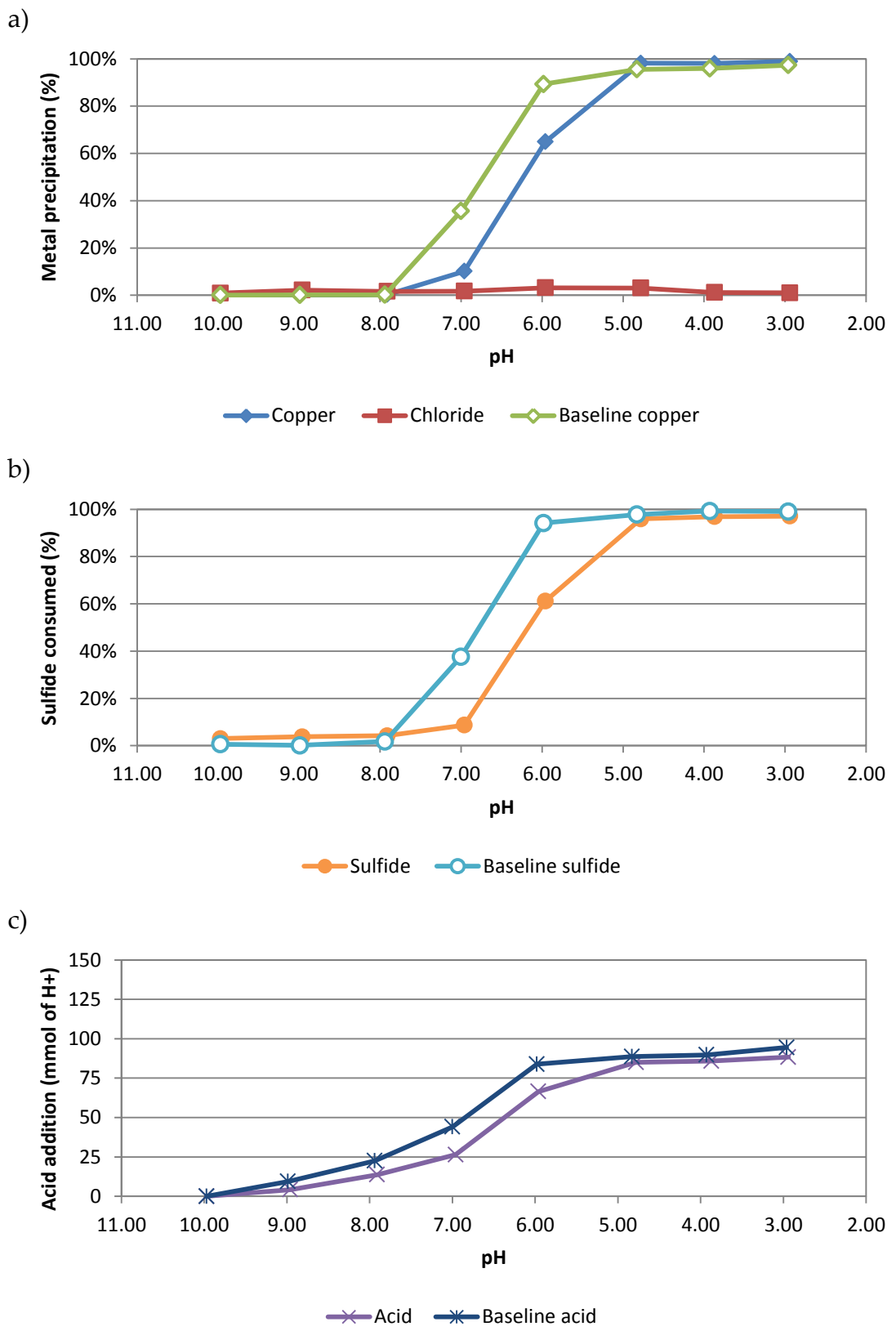


Figure 5.15 a) Species precipitation, b) sulfide consumption, and c) acid addition when changing the pH from 10 to 3 on a solution containing: 15.3 mM Cu, 2 M Cl<sup>-</sup>, CN:metal ratio of 4, and a S:Cu ratio of 0.5.

### **5.3 Mixed metal experiments**

Mixed metal experiments were performed to determine if multiple impurities in solution affect sulfidisation differently to when only one impurity is present. It also gives an opportunity to determine the feasibility of selective precipitation between the metal impurities.

#### **5.3.1 Experimental methods**

For each mixed metal experiment, mixed metal cyanide solutions were made as described in Section 3.1.2, targeting a copper concentration of 16 mM (~1000 mg L<sup>-1</sup>). The impurity concentration target was half (8 mM) of the copper concentration target for all impurities (iron, nickel, silver, zinc) excluding gold. As with the single impurity experiments, the gold target concentration was one tenth (1.6 mM) of the copper concentration as gold is usually not found in high concentrations in the gold processing tailings. Iron was made up as 50% iron (II) and 50% iron (III).

The cyanide to metal molar ratio (CN:metal ratio) for every metal except for iron was set at 4 moles of cyanide per mole of metal. For iron, the CN:metal ratio was 6 moles of cyanide per mole of metal due to iron forming Fe(CN)<sub>6</sub><sup>4-</sup> and Fe(CN)<sub>6</sub><sup>3-</sup>.

Five experiments were carried out on the mixed metal cyanide solution using the large reactor described in Section 3.2, prepared as described in Section 3.3.1.2. Each experiment was performed using the method described in Section 3.4.2 with different amounts of sulfide added to the mixture for each experiment. The sulfide addition was 0, 10, 20, 30, and 40 mmol of sulfide which corresponded to sulfide to metal molar ratios (S:metal ratio) of approximately 0, 0.2, 0.4, 0.6, and 0.8 for each experiment, respectively.

Samples for each experiment were taken at pH 10 through to 2 as per the sampling method in Section 3.5.1. An initial sample was also taken to determine the initial concentration of each metal in solution. The samples were analysed to determine the concentration of each metal using the method described in Section 3.6.2. Cyanide analysis was not performed because of difficulty in clearly determining cyanide concentration in solution. Hence, metal precipitation is used as an indicator of cyanide recovery.

### **5.3.2 No sulfide addition**

Metal precipitation when adjusting pH from 10 to 2 on a mixed metal cyanide solution with no sulfide present is shown in Figure 5.16. Above pH 8, there is no precipitation of any of the metals. Between pH 8 and 6 there is precipitation of both zinc and iron. The precipitation of these two species over the same pH range suggests the formation of a zinc iron cyanide double salt (Equation 2.13). Zinc and iron precipitated in a zinc to iron molar ratio of 1.42.

As the zinc and iron precipitate, there is a slight recovery of all metals while the pH is reduced. These small recoveries of all the other metals is likely related to co-precipitation / adsorption of the metals in the formed precipitates as seen in the single impurity experiments (Section 5.2).

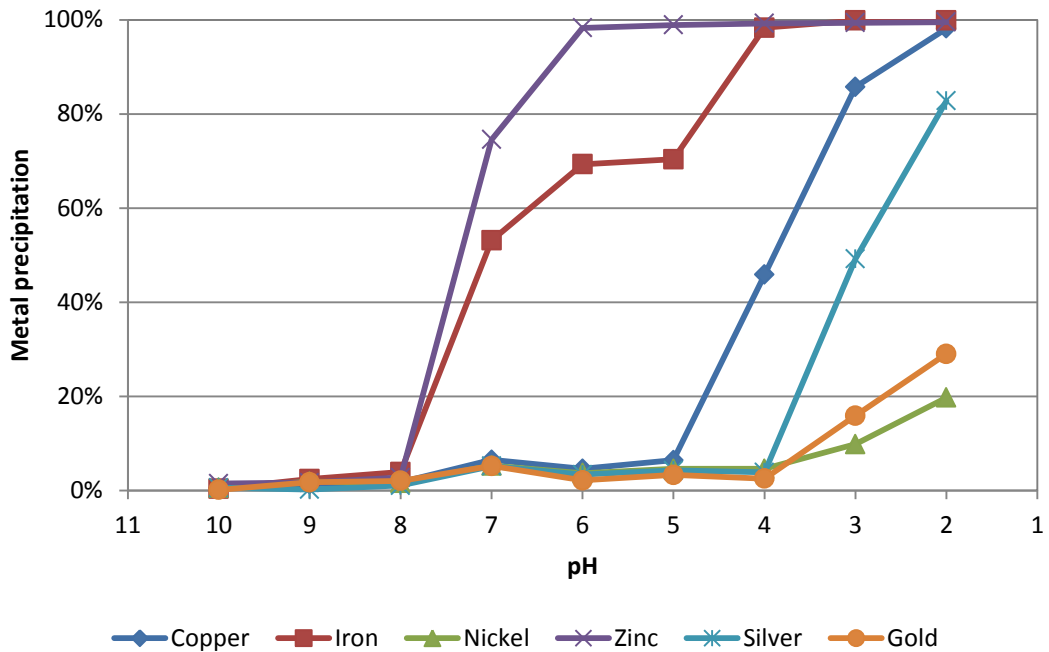
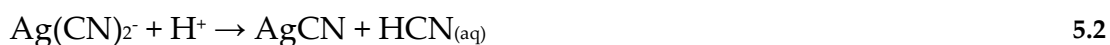


**Figure 5.16 Metal precipitation when changing the pH from 10 to 2 for a solution containing 12.8 mM Cu, 8.2 mM Fe, 7.1 mM Ni, 8.9 mM Zn, 8.1 mM Ag, 1.8 mM Au, CN:metal ratio of 6 for Fe and 4 for all other metals, and no sulfide addition.**

The remaining iron in solution then precipitates between pH 5 and 4 with copper precipitating at the same time. This is due to the formation of a copper iron cyanide double salt (Equation 2.11). The copper to iron ratio in the solid formed is 2.8 calculated from the change in copper and iron concentrations between pH 5 and 4. Due to the mixture of iron (II) and iron (III) in solution, coupled with the potential for oxidation and reduction to occur, it is not possible to determine the exact form of the precipitate based on the solution analysis data.

Below pH 4, copper recovery continues to increase due to the formation of a copper cyanide precipitate (reverse of Equation 2.3). Silver recovery also increases below pH 4 due to the formation of a silver cyanide precipitate (Equation 5.2). Silver and copper are not known to form silver copper

cyanide precipitates so there precipitation over the same range is not likely to be caused by co-precipitation.



The increase in nickel and gold precipitation at pH values less than 4 is potentially related to co-precipitation. Nonetheless, the exact cause of the precipitation is unknown, with the determination of the precipitate formed being outside the scope of the research.

### **5.3.3 Sulfide to metal molar ratio of 0.2**

The effect of changing pH from 10 to 2 on metal precipitation for a mixed metal cyanide solution with 10 mmol of sulfide (S:metal ratio of 0.2) is shown in Figure 5.17. As with the single impurity experiment for silver (Section 5.2.3), the precipitation of silver occurs over the entire pH range with recoveries greater than 98%. Silver should be precipitating as  $\text{Ag}_2\text{S}$  (Equation 2.10); hence, the precipitation of silver should only result in consumption of 6 mmol of the 10 mmol of sulfide added. This leaves approximately 4 mmol of sulfide in solution. The high pH recovery of silver results in co-precipitation / adsorption of all the other metals over the entire pH range. Except for co-precipitation / adsorption, the high pH recovery of silver shows that silver can easily be selectively precipitated from all the other species in the solution at pH 10.

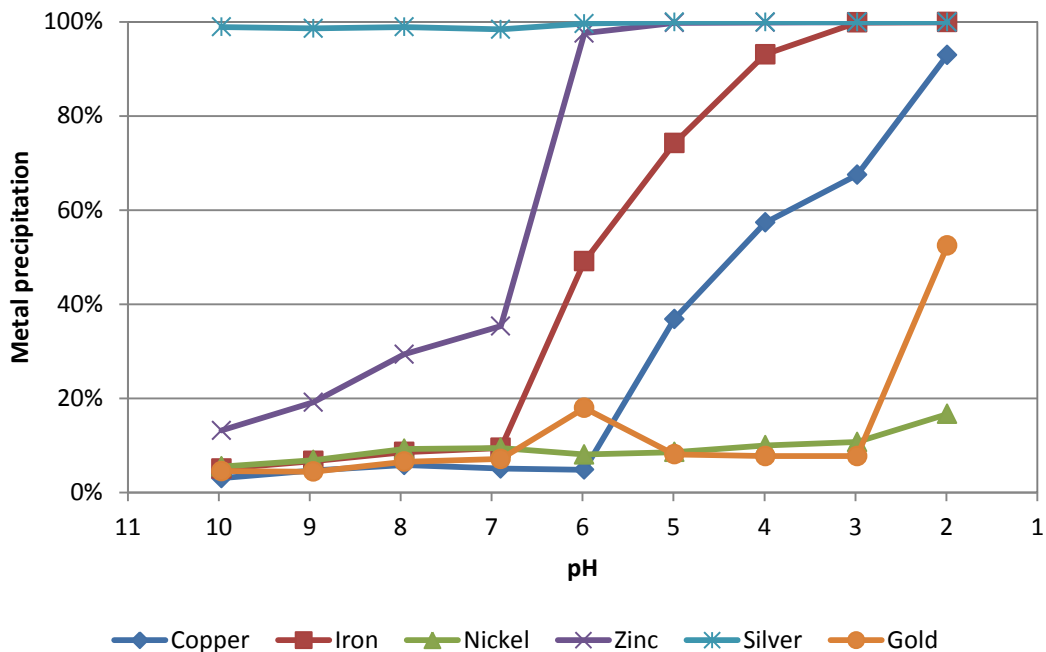


Figure 5.17 Metal precipitation when changing the pH from 10 to 2 for a solution containing 14.8 mM Cu, 8.0 mM Fe, 6.8 mM Ni, 7.2 mM Zn, 7.5 mM Ag, 1.6 mM Au, CN:metal ratio of 6 for Fe and 4 for all other metals, and an initial S concentration of 6.7 mM.

The next metal to precipitate as the pH is reduced is zinc, which has between 13% and 35% recovery over the pH range 10 to 7. The 35% recovery of zinc by pH 7 corresponds to a zinc loss from solution of 3.8 mmol. As zinc precipitates with sulfide as ZnS (Equation 2.14), the precipitation of zinc corresponds to reaction with the remaining sulfide in solution after silver is precipitated. The result agrees with Milosavljevic, Solujic, and Kravetz (2004) who show that, using organo-sulfur reagents, silver and zinc are separable, as silver precipitates as a sulfide preferentially to zinc. By pH 6, the zinc recovery increases to 97% with iron recovery also increasing to 49%. As with the no sulfide addition experiment (Section 5.3.2), a zinc iron cyanide double salt is most likely formed when no excess sulfide is present for zinc precipitation. The zinc to iron ratio in the precipitate is 1.57.

Iron continues to precipitate from pH 6 through to pH 3. Copper also precipitates over this region again likely due to the formation of a copper iron cyanide double salt. The ratio of copper to iron precipitated over this range is 2.46, based on solution concentration. This is less than the ratio seen in the experiment with no sulfide addition (Section 5.3.2).

Due to the ability for zinc to release sulfide from the zinc sulfide precipitate at low pH (Equation 5.1), it is possible that copper sulfide is also forming. This reaction would release iron cyanide into solution which can react with zinc ions and form a zinc iron cyanide double salt (Equation 2.13). Hence, if this were occurring, no drop in zinc recovery at low pH would be observed as seen in the single impurity experiments (Section 5.2.8). Equation 5.3 shows the overall equation for this proposed reaction, where  $\text{Cu}_3\text{Fe}(\text{CN})_6$  is an example of one of the possible copper iron cyanide double salts that may have precipitated.



As the formation of either copper iron cyanide double salts with zinc sulfide or copper sulfide with zinc iron cyanide double salts will give the same species concentrations in solution, it was not possible to determine which precipitates are forming. Nonetheless, as either reaction affects the process in the same way in terms of metal and cyanide recovery, determination of the precipitates formed is outside the scope of research.

Gold was not expected to form any precipitates due to the consumption of sulfide by silver and zinc at high pH. Interestingly, gold recovery increased from 8% to 53% between pH 3 and 2. In an attempt to understand why gold was precipitating, thermodynamic modelling was performed on the system

using MEDUSA thermodynamic software as described in Section 2.1. The model showed that gold can precipitate as a gold silver sulfide (Equation 5.4) and that the sulfide could be provided to gold from the release of sulfide from the zinc sulfide precipitate (Equation 5.1). Further work is required to confirm if this is occurring. As with copper, the presence of iron prevents an increase in zinc concentration in solution due to the formation of a zinc iron cyanide double salt (Equation 2.13).



#### **5.3.4 Sulfide to metal molar ratio of 0.4**

Metal precipitation when lowering pH from 10 to 2 on a mixed metal cyanide solution and 20 mmol of sulfide (S:metal ratio of 0.4) is shown in Figure 5.18. Both silver and zinc have high recoveries of above 99% and 93% respectively for every pH value tested. This is due to enough sulfide being present that both metals can form their respective sulfide precipitates at pH 10. There is slight recovery of all metals at every pH due to co-precipitation / adsorption.

By comparing the silver and zinc results from the 0.2 S:metal mixed metal solution experiment (Section 5.3.3), it can be observed that the ability to separate silver and zinc is dependent on the availability of sulfide. Hence, to separate silver from zinc in an industrial sulfidisation process, sulfide dosing would need to be controlled to limit zinc precipitation during silver precipitation. After silver sulfide has been separated from the solution, more sulfide could be added to precipitate zinc. This technique, however, may be difficult to operate continuously on an industrial scale due the changing nature of industrial solutions and a need to accurately dose sulfide.

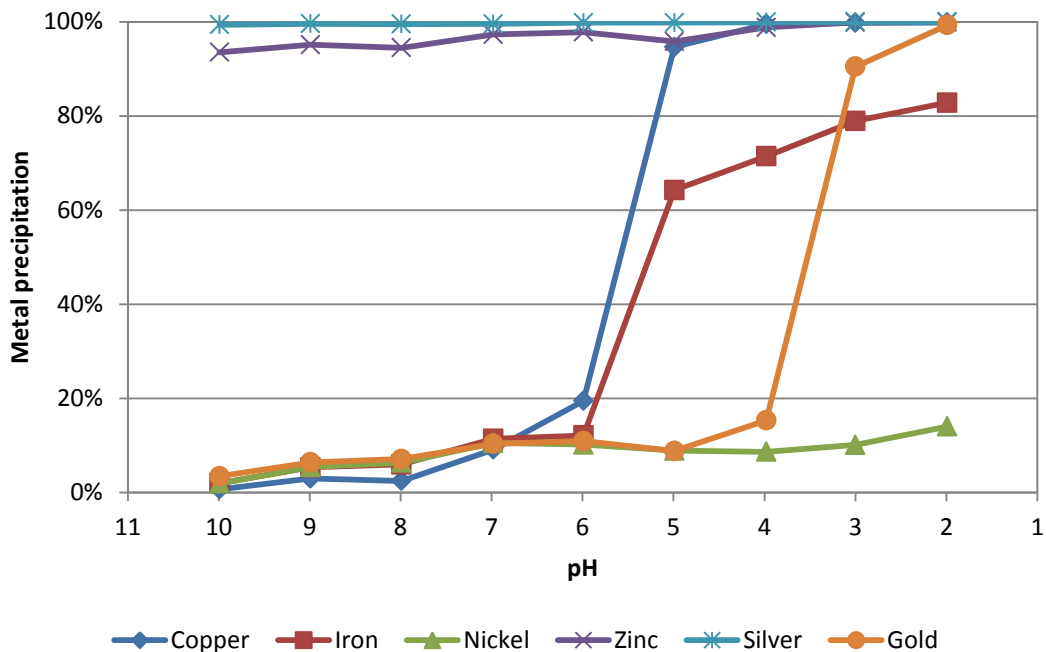


**Figure 5.18 Metal precipitation when changing the pH from 10 to 2 for a solution containing 14.7 mM Cu, 7.9 mM Fe, 6.7 mM Ni, 7.1 mM Zn, 7.4 mM Ag, 1.6 mM Au, CN:metal ratio of 6 for Fe and 4 for all other metals, and an initial S concentration of 13.3 mM.**

With a sulphide to metal molar ratio of 0.4, the consumption of sulfide by silver and zinc leaves approximately 4 mmol of sulfide in solution. This small amount of sulfide results in copper recovery of 20% by pH 6. Below pH 6, both copper and iron precipitate with high copper recovery (>94%) shown at pH 5. As discussed in Section 5.3.3, this could be due to the formation of a copper iron cyanide double salt, or a copper sulfide precipitate and zinc iron cyanide double salt caused by zinc sulfide releasing sulfide ions (Equation 5.3) as the pH is reduced. As with the results in Section 5.3.3, it is not possible to elucidate which is occurring from the data available.

Like the mixed metal experiment with a S:metal ratio of 0.2 (Section 5.3.3), gold precipitation occurs at low pH (<4). This precipitation of gold results in a gold recovery of 99% by pH 2. In this experiment, all sulfide in solution is

consumed by silver, zinc, and copper as the pH is reduced. Due to the consumption of sulfide ions in the solution, the precipitation of gold is likely caused by zinc sulfide releasing sulfide as discussed in Section 5.3.3. Zinc redissolution is not seen as an increase in zinc in solution due to the ability for zinc and iron to form zinc iron cyanide double salts (Equation 2.13). This mechanism also explains the continued iron precipitation as pH is reduced.

The precipitation of gold between pH 4 and 3 supports the conclusion from Section 5.3.3 that gold is potentially forming a gold silver sulfide precipitate rather than gold sulfide. This becomes evident when compared to the single impurity experiment with gold when the S:Cu ratio is 1.0 (Section 5.2.4), where only minor gold precipitation was observed between pH 4 and 3.

### **5.3.5 Sulfide to metal molar ratio of 0.6**

The effect of lowering pH from 10 to 2 on metal precipitation from a mixed metal cyanide solution with 30 mmol of sulfide (S:metal ratio of 0.6) is shown in Figure 5.19. As with the previous experiment (Section 5.3.4), the recoveries of both silver and zinc are high over the entire pH range tested. The high pH precipitation of these two metals again resulted in a small amount of co-precipitation / adsorption of all other species. The precipitation of silver and zinc results in approximately 9 mmol of sulfide being available in solution as the pH is reduced.

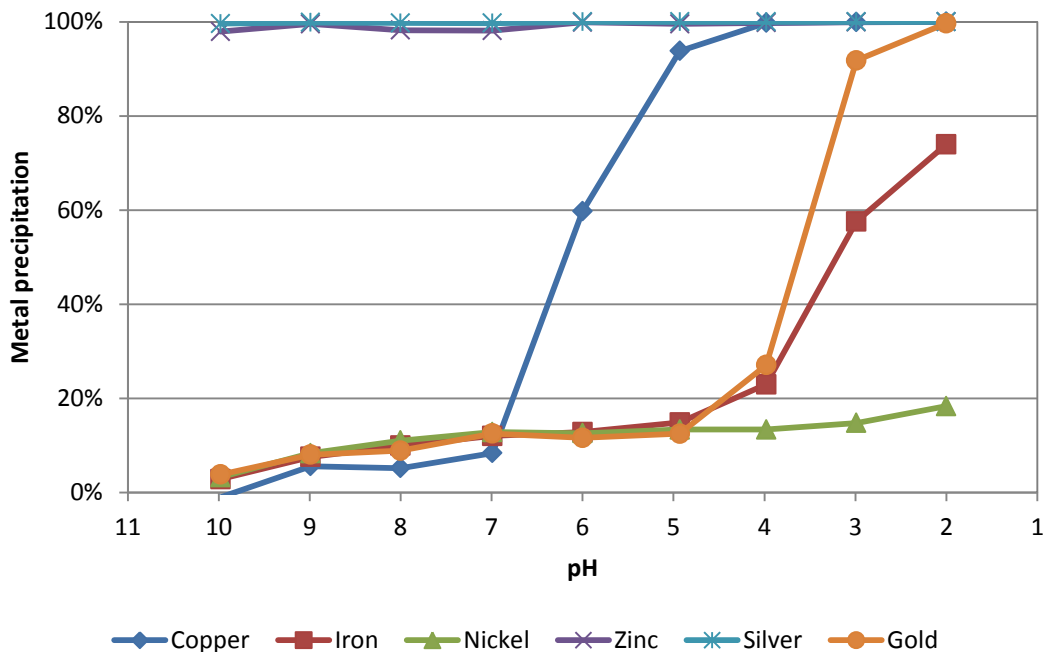


**Figure 5.19 Metal precipitation when changing the pH from 10 to 2 for a solution containing 14.5 mM Cu, 10.0 mM Fe, 8.1 mM Ni, 9.9 mM Zn, 8.8 mM Ag, 1.6 mM Au, CN:metal ratio of 6 for Fe and 4 for all other metals, and an initial S concentration of 20 mM.**

Copper precipitation occurs between pH 7 and 5 with 94% of copper recovered at pH 5. With the high level of sulfide in solution, most of the copper is precipitated as  $\text{Cu}_2\text{S}$  before pH 5. This is apparent due to the lack of significant iron precipitation with copper above pH 5 as seen when less sulfide is present (Section 5.3.4). Between pH 5 and pH 4, there is a slight increase in iron precipitation with the precipitation of the remaining copper.

Again, as discussed in Section 5.3.3 and Section 5.3.4, the precipitation of copper and iron together could be due to the formation of a copper iron cyanide double salt, or a copper sulfide precipitate and zinc iron cyanide double salt caused by zinc sulfide releasing sulfide (Equation 5.3). It is not possible to elucidate what precipitates are occurring from the data available.

The results show that copper can be selectively removed from the remaining gold, nickel, and iron in solution in the vicinity of pH 4 with sufficient sulfide present. Unlike separating silver and zinc, however, a more precise pH value and sulfide addition would be required to achieve selective copper recovery.

With the near complete precipitation of silver, zinc, and copper below pH 4, there is no sulfide expected to be remaining in solution. As pH is reduced below 4 there is, however, still precipitation of iron and gold. This is likely to be caused by the same mechanism discussed in Section 5.3.3. That is, sulfide is released from zinc to allow gold to precipitate as a gold sulfide or silver gold sulfide while zinc and iron react to give a zinc iron double salt.

The continued precipitation of iron below pH 3 is potentially caused by a number of reactions. This includes the continued release of sulfide from zinc sulfide and subsequent formation of a zinc iron cyanide double salt. It is also possible that iron cyanide double salts or haematite are forming as discussed in Section 2.4.3. Thermodynamic modelling also suggests that the formation of mixed iron (II) and iron (III) sulfides is possible. Due to the focus of this section not being on the complexity of iron cyanide chemistry, the nature of the precipitate is not explored further.

### **5.3.6 Sulfide to metal molar ratio of 0.8**

The effect of lowering pH from 10 to 2 on metal precipitation from a mixed metal cyanide solution with 40 mmol of sulfide (S:metal ratio of 0.8) is shown in Figure 5.20. As there is a large amount of sulfide available in the system, the precipitation of silver and zinc is complete at every pH value sampled. The amount of sulfide present also results in high copper recovery (>99%) by pH 5 and gold precipitation occurring at higher pH values.

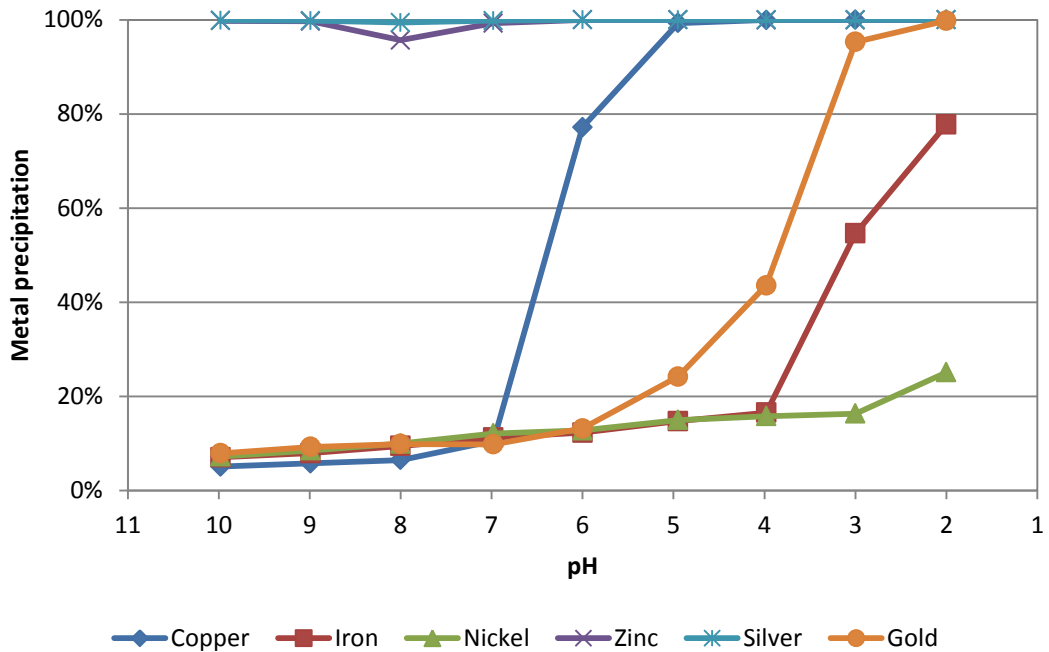


**Figure 5.20 Metal precipitation when changing the pH from 10 to 2 for a solution containing 14.7 mM Cu, 10.1 mM Fe, 8.2 mM Ni, 10.0 mM Zn, 8.9 mM Ag, 1.6 mM Au, CN:metal ratio of 6 for Fe and 4 for all other metals, and an initial S concentration of 26.7 mM.**

Gold recovery was between 24% and 44% between pH 5 and 4, which is potentially due to the formation of gold silver sulfide precipitates as discussed in Section 5.3.3. Significant gold precipitation above pH 4 had not been observed in previous experiments, and may potentially explain the recovery of 20% to 30% of gold during sulfidation seen by Dreisinger et al. (2008) which was not seen in other work where gold was present (Guzman et al. 2010; Littlejohn, Kratochvil, and Hall 2013).

As discussed in Section 2.4.2, the recovery of gold may or may not be advantageous depending on the process flow sheet in which sulfidation is applied. The results of the mixed metal experiments, coupled with thermodynamic modelling, shows that, when silver and gold are present during sulfidation, and enough sulfide is available, high gold recovery is

achievable at pH 3 and below. Increasing sulfide concentration increases the pH at which gold precipitation occurs. Hence, if both silver and gold are present during sulfidisation, control of sulfide addition and pH during sulfidisation may be critical if gold precipitation, or lack thereof, is an important factor in the process.

Iron precipitation also occurs below pH 4. As discussed in Section 5.3.5, iron precipitation could be the result of numerous reactions and is not explored further.

#### **5.4 Conclusions**

The impact of impurities in sulfidisation is a complex area due to the ability for different metals to form combinations of sulfide and cyanide precipitates and the potential for some metals to exchange between these forms. For this reason, the impact of various impurities on sulfidisation of a copper cyanide solution were studied separately to elucidate their individual impacts. It was found that:

- When sulfide precipitates form, co-precipitation / adsorption of other species occurs. The level of co-precipitation / adsorption increases with sulfide dosing. For this reason, dosing of sulfide should be controlled to limit co-precipitation / adsorption of unwanted metals during sulfidisation.
- Silver can be selectively recovered from copper due to it forming a sulfide precipitate over the entire pH range tested from 10 to 2. The formation of silver sulfide occurs preferentially to copper sulfide.
- Gold will form sulfide precipitates at low pH (< 3.5), but requires excess sulfide and results in low gold recovery (< 30%). This is beneficial if sulfidisation is used to remove copper before a gold

recovery process such as carbon adsorption. Control of pH and sulfide addition determines gold recovery.

- Iron (II) and iron (III) do not interfere with the precipitation of copper sulfide and are not recovered unless there is copper that is not precipitated by sulfide. Iron does, however, cause increases in acid consumption at low pH ( $< 4$ ). For this reason, if iron is present in solution, the control point for pH should be above four to minimise unnecessary acid consumption.
- Nickel had no impact on sulfidisation except for co-precipitation / adsorption.
- Zinc can be selectively recovered from copper at pH values above 7 due to the formation of zinc sulfide. If zinc sulfide is not separately precipitated and removed, it will release sulfide at low pH ( $< 5$ ) resulting in zinc redissolution. Excess sulfide aids in the stabilisation of zinc sulfide at low pH.
- Thiocyanate and thiosulfate have no impact on sulfidisation.
- Chloride reduces the maximum pH for sulfidisation of copper, but otherwise has no effect on the process. Due to co-precipitation / adsorption of chloride, if sulfidisation was integrated into a resin recovery process for copper cyanide, more chloride may need to be added for each eluent cycle.

Solutions of mixed impurities were also studied to determine how complex systems of multiple impurities respond to sulfidisation. It was found that:

- Silver can be selectively recovered from all other metals at high pH with stoichiometric sulfide addition. Silver is also the most stable precipitate, forming preferentially to the other precipitates at all pH values.

- Zinc can be selectively recovered at high pH once silver is removed from the reactor. If iron is present, zinc may form zinc iron cyanide double salts below pH eight when no sulfide is present. Zinc sulfide is, however, more stable than zinc iron cyanide double salts at neutral pH values, with zinc iron cyanide double salts becoming more stable at low pH values (< 5).
- Copper can be selectively recovered from the other metals but would require tight control of pH and sulfide addition.
- The presence of silver, if not selectively removed, may result in gold forming gold silver sulfide at pH values higher than required to form gold sulfide (pH 5 – 3). Further work is required to verify this interaction. Gold recoveries between 52.5% and 95.3% at pH 3 were observed as sulfide dosing is increased.
- Recovery or rejection of gold to the precipitate when performing sulfidisation in mixed metal solution may require tight control of pH and sulfide addition.
- Iron will form double salts with copper below pH five when copper has not been precipitated with sulfide. Iron will also form double salts with zinc at pH values less than eight when zinc has not been precipitated with sulfide or at low pH (< 5) as zinc sulfide is less stable in this region.
- Low pH iron chemistry is complex and a number of precipitates may be potentially forming at pH values less than 4. The chemistry of iron cyanide solutions needs to be explored further.

While this work shows the ranges in which different metals precipitate during sulfidisation, variation in metal concentration and cyanide concentration may cause these ranges to change. Due to the complexity of

some of the metal interactions, it may be necessary to study specific systems individually to determine the metal precipitation ranges.

## **6 IMPACT OF RESIDENCE TIME ON SULFIDISATION**

### **6.1 Introduction**

The factorial design screening experiments from Chapter 4 showed that long residence times during sulfidisation cause decreases in copper and cyanide recovery unless excess sulfide is present. This apparent impact of residence time may be related to problems seen at some industrial SART plants, such as high sulfide consumption (Turton-White, personal communication, 2010), and precipitates that are composed of covellite (CuS) rather than chalcocite (Cu<sub>2</sub>S) (Guzman et al. 2010).

This chapter, on a laboratory scale, explores the impact of residence time on sulfidisation. The primary objective is to elucidate the factors which influence copper recovery and sulfide consumption changes over time during sulfidisation. Secondary to this is to determine if residence time is causing changes in precipitate structure over time producing the precipitate observed in some industrial sulfidisation processes.

### **6.2 Factorial design screening**

The impact of residence time on sulfidisation was first observed during the factorial design screening experiments in Section 4.2.6. The effects, however, were not reported in Chapter 4 due to their relevance to this chapter. Hence, the results of the screening experiments from Section 4.2.6 are discussed here in Section 6.2, with further research on this topic reported and discussed in the subsequent sections of Chapter 6.

#### **6.2.1 *Experimental methods***

The screening experiments to determine the impact of residence time were performed using the small reactor described in Section 3.2 and prepared as

described in Section 3.3.1.1. Experiments were performed using the method described in Section 3.4.3.

Solutions were sampled as described in Section 3.5.1 and analysed for copper, sulfide, and sulfide degradation products using high performance liquid chromatography (Section 3.6.4.1). At the end of each experiment a solid sample was taken using the method described in Section 3.5.2. The solid sample from experiments was analysed for sulfide content using a sulfur and carbon analyser (Section 3.6.6). While it would have been useful, dissolved oxygen was not measured during this test work as hydrogen cyanide and dihydrogen sulfide interfere with dissolved oxygen meters.

### **6.2.2 Results**

The first residence time screening experiment indicated that copper redissolved from the sulfidisation precipitate over time. Nonetheless, this experiment did not generate enough precipitate for analysis due to the small volume (50 mL) and initial copper concentration of 15.7 mM (~1000 mg L<sup>-1</sup>). To generate a larger amount of precipitate, the experiment was repeated with an initial copper concentration of 62.9 mM (~4000 mg L<sup>-1</sup>). Figure 6.1 shows the change in copper concentration, sulfide concentration, and pH over time for the solution which had a CN:Cu ratio of 4, a S:Cu ratio of 0.6, and initial pH of 5. The time zero sample was taken as soon as the target pH of 5 was reached. The recovery of copper at time zero was greater than 99%.

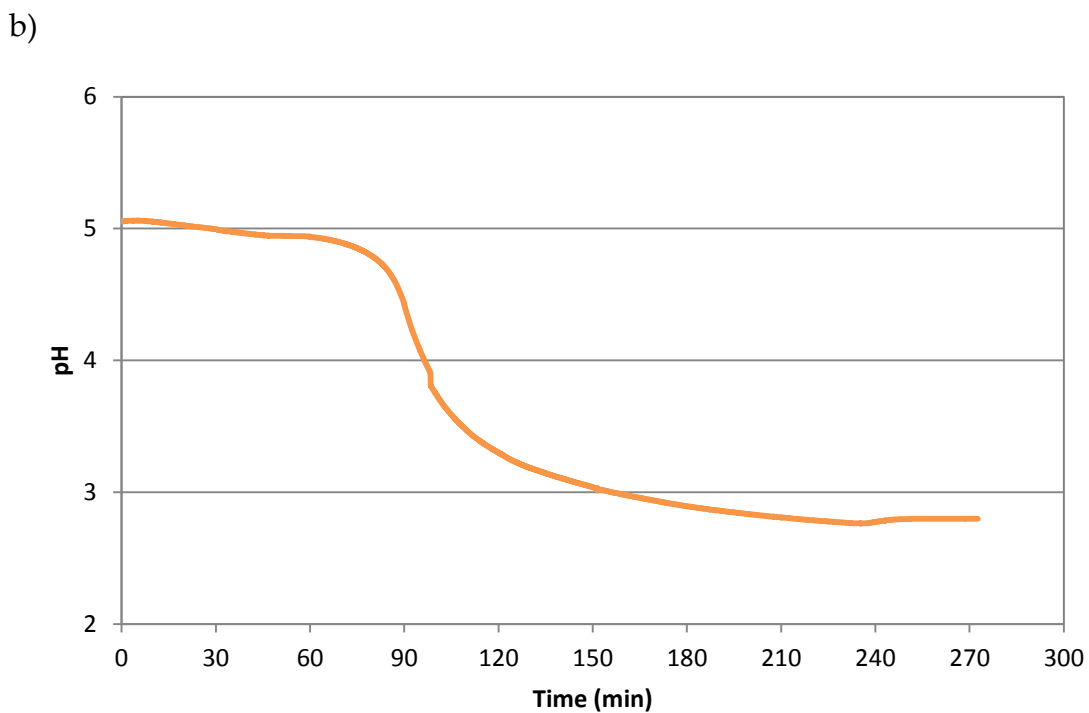
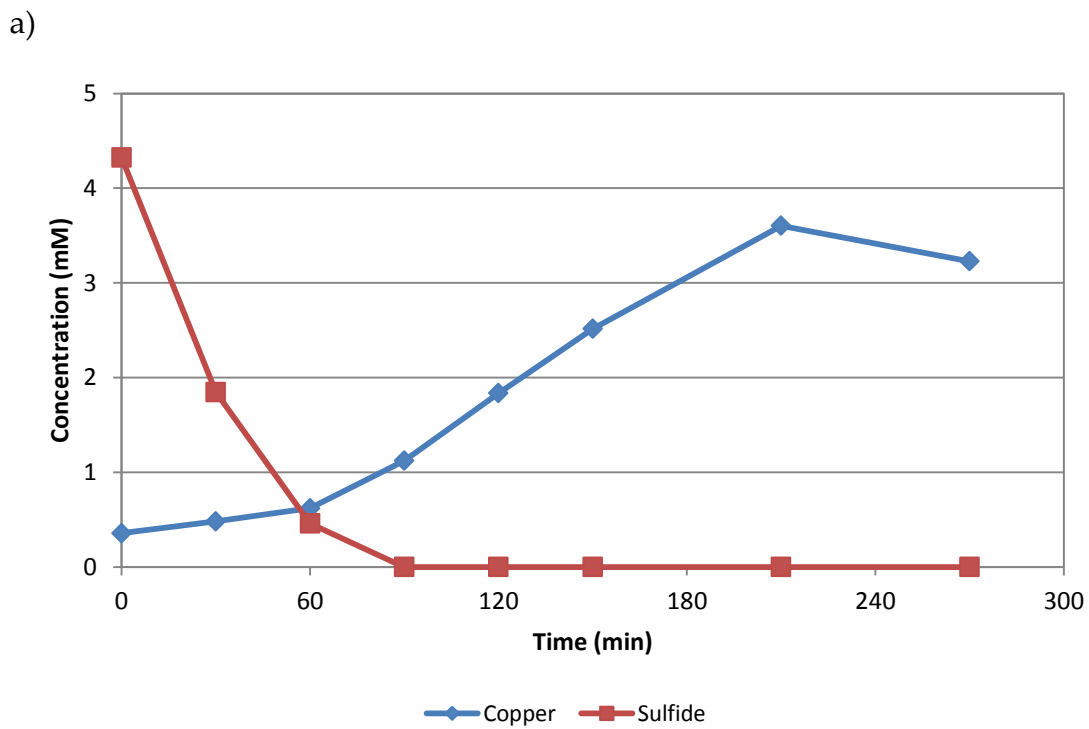


Figure 6.1 a) Species concentration in solution and b) pH over time during sulfidation for a solution initially containing 62.9 mM copper with a CN:Cu ratio of 4, S:Cu ratio of 0.6, and pH of 5.

Figure 6.1 can be divided into three distinct regions: from 0 to 90 minutes, 90 to 240 minutes, and greater than 240 minutes. In the first 90 minutes, there is a reduction in sulfide concentration to zero. Copper concentration and pH do not change significantly in this time period. Between 90 and 210 minutes, there is redissolution of the copper from the precipitate and a decrease in pH. After 210 minutes, the pH becomes constant and copper concentration appears to decrease. As the last two samples are taken an hour apart, it is not certain whether the copper concentration has stopped changing or is decreasing over time. The total change in copper concentration from time 0 to 270 minutes corresponds to a copper recovery change from 99% to 95%. During the experiment there was no change in thiocyanate or thiosulfate concentration in solution.

The first two regions of Figure 6.1 can both be potentially explained by consumption of sulfide over time. In the first region (0 to 90 min), the concentration of sulfide decreases over time. Once excess sulfide is depleted (90 minutes onwards), it is possible that the primary sulfidation equation (Equation 1.3) is reversed to provide a source of sulfide ions. If this is occurring, it would explain the redissolution of copper over time. A number of mechanisms could explain the loss of sulfide ions from solution including loss of sulfide from the reactor as dihydrogen sulfide gas, oxidation of copper sulfide towards a sulfide rich structure, or adsorption of sulfide on the precipitate surfaces.

To determine whether the decrease in sulfide concentration in solution was caused by the sulfide becoming incorporated into the solids or escaping the reactor as dihydrogen sulfide gas, two more experiments were performed to obtain precipitates for analysis of sulfur (sulfide) content. The initial solutions both had target copper concentration of 62.9 mM ( $\sim 4000 \text{ mg L}^{-1}$ ),

CN:Cu ratio of 4, S:Cu ratio of 1.0, and an initial pH of 5. For the first experiment, a solids sample was taken at time zero (when pH reached 5). For the second experiment, a solids sample was taken once there was no excess sulfide measured in solution. Analysis of the solids by a sulfur and carbon analyser gave 22 wt% sulfide in the time zero solids sample compared to 30 wt% from the solids sample taken when the excess sulfide in solution was depleted.

The change in sulfide percentage in the precipitate is equivalent to the precipitate changing structure from  $\text{Cu}_{1.8}\text{S}$  to  $\text{Cu}_{1.2}\text{S}$ . This indicates that the excess sulfide in solution is becoming incorporated into the precipitate over time. Interestingly, the increase of sulfide in the precipitate is similar to that observed in mineralogical analysis of SART precipitate from Newmont Mining Corporation's Yanacocha SART plant (Guzman et al. 2010). Guzman et al. (2010) found that, at Yanacocha, the final precipitate was largely  $\text{CuS}$  rather than  $\text{Cu}_2\text{S}$  as expected from Equation 1.3. Hence, the observations from the screening experiments may be related to what has been observed at Yanacocha.

While the screening experiments show that residence time has an impact on sulfidisation, the work did not indicate a cause for this observation. Hence, further investigation of this system was performed using larger scale experiments to determine the cause of the residence time impact on sulfidisation.

### **6.3 Large scale residence time tests**

To further explore the impact of residence time on sulfidisation, experiments were performed using the large reactor described in Section 3.2. The large reactor was used primarily to generate a larger mass of solids for analysis.

The larger scale also allowed more samples to be taken with less volume change impact on the experiment.

### **6.3.1 Experimental methods**

Large scale residence time experiments were conducted using the large reactor described in Section 3.2 and prepared as described in Section 3.3.1.2. Experiments were then performed using the methods described in Section 3.4.3. All experiments were performed with an air headspace unless otherwise stated.

Solutions were sampled at various time intervals using the solution sampling technique (Section 3.5.1) and analysed for copper, sulfide, thiocyanate, and thiosulfate using high performance liquid chromatography (Section 3.6.4.1). For some experiments, precipitate samples were taken at the end of the experiment (Section 3.5.2) and analysed using X-ray diffraction (Section 3.6.7) and scanning electron microscopy (Section 3.6.8).

Cyanide concentration was determined using potentiometric titration as discussed in Section 3.6.3.2. It was found, however, that the small changes of cyanide concentration which may occur in the experiments were difficult to detect and are also impacted by the possibility of hydrogen cyanide gas loss during sampling. This was similarly observed when building the sulfidisation model in Section 4.3.4. For this reason, cyanide measurements are not used as part of the solution analysis, with copper recovery used as an indicator for cyanide recovery.

### **6.3.2 Initial precipitate structure**

To determine the composition of the precipitate initially produced during sulfidisation, XRD and SEM analysis was performed on a precipitate

obtained at time zero. Figure 6.2 shows the XRD pattern from a precipitate produced using a 15.7 mM ( $\sim 1000 \text{ mg L}^{-1}$ ) copper solution with a CN:Cu ratio of 4 and a S:Cu ratio of 0.5. The precipitate was recovered from the slurry as soon as the target pH of 4.75 was achieved. The qualification of the mineral formed in the precipitate using XRD showed that it was roxbyite ( $\text{Cu}_7\text{S}_4$ ). This gives a S:Cu ratio in the precipitate of 0.57 which is close to the expected S:Cu of 0.5 based on the primary sulfidisation equation (Equation 1.3).

Elemental quantification of nine random points in the precipitate using SEM gives a S:Cu ratio of 0.44 in the precipitate. The lower than expected value from the SEM analysis is caused by difficulty in analysing the fine precipitate produced from the experiment. The fine nature of the precipitate is highlighted in Figure 6.3, which shows an SEM image of the precipitate. Due to the potential for error when using SEM, the results of SEM analysis are only used as a guide throughout this chapter.

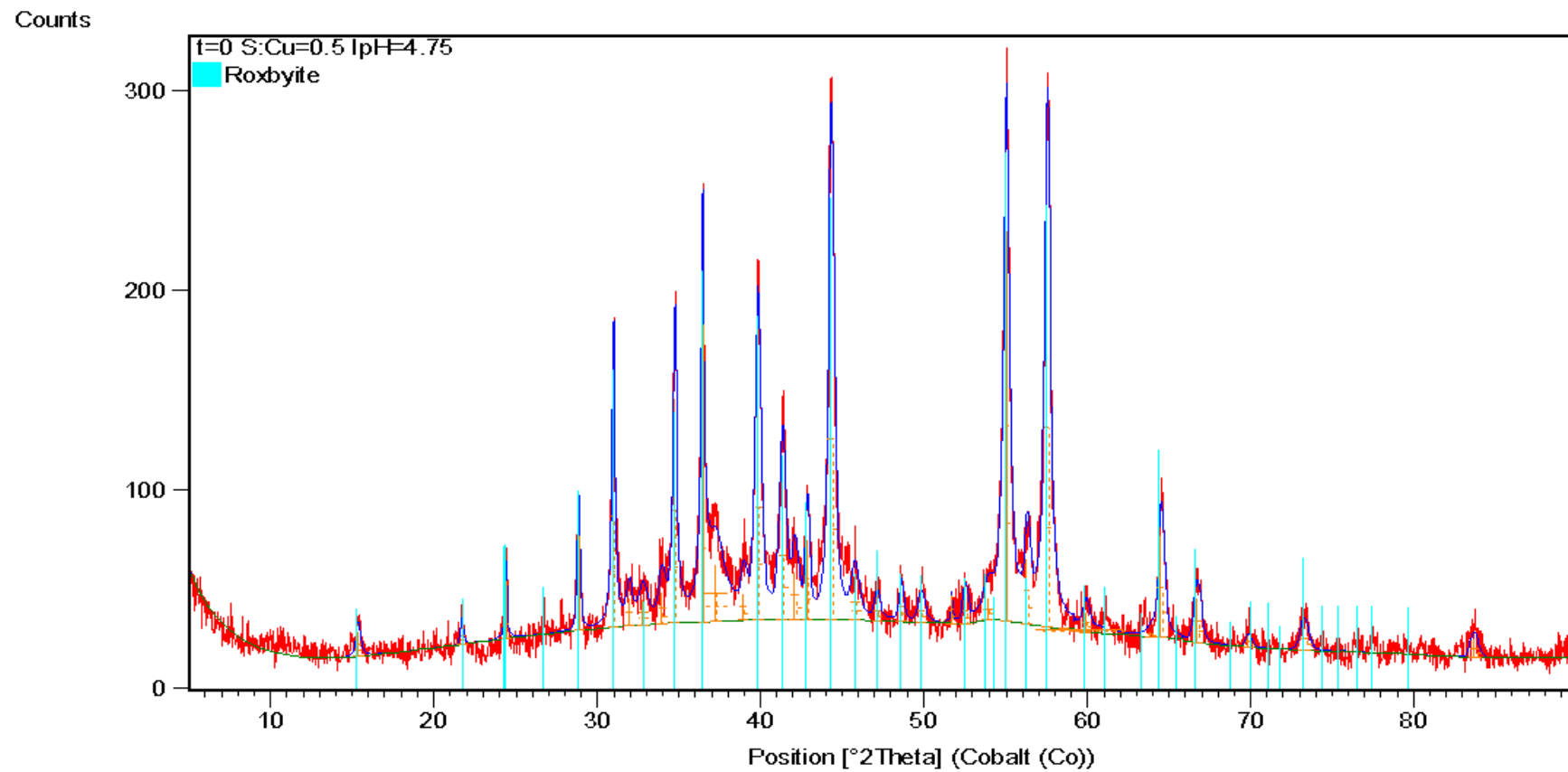


Figure 6.2 XRD pattern of a sulfidation precipitate at time zero from a solution initially containing 15.7 mM Cu, a CN:Cu of 4, a S:Cu of 0.5, and a pH of 4.75. The precipitate was prepared for XRD using powder packing.

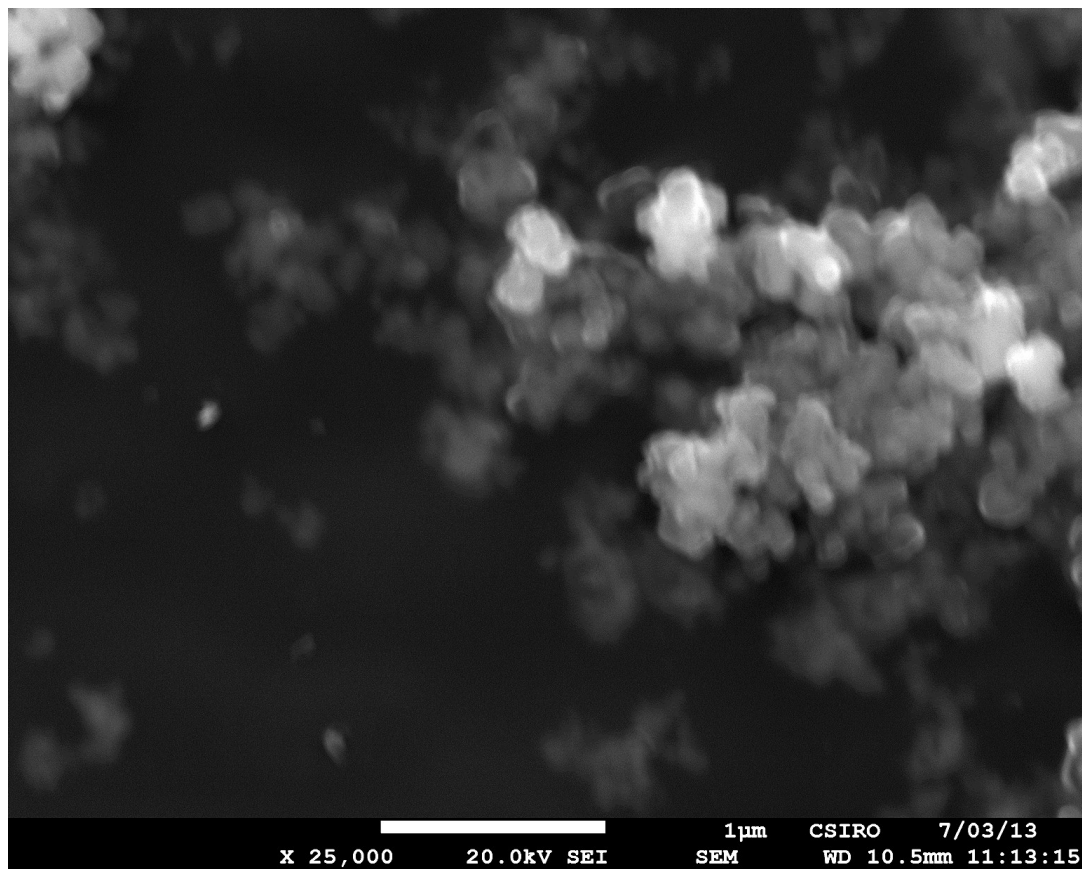


Figure 6.3 SEM image of a sulfidisation precipitate at time zero from a solution initially containing 15.7 mM Cu, a CN:Cu of 4, a S:Cu of 0.5, and a pH of 4.75.

### **6.3.3 Effect of sulfide to copper ratio**

As the screening experiments for residence time (Section 6.2) show distinct regions related to the amount of sulfide in solution, the impact of residence time on sulfidisation was explored at various S:Cu ratios. Three experiments were performed with target copper concentrations of 15.7 mM (1000 mg L<sup>-1</sup>); CN:Cu ratios of 4; pH of 4.75; and with S:Cu ratios of 1.0, 0.5, and 0.25 respectively.

### 6.3.3.1 Sulfide to copper molar ratio of 1.0

Figure 6.4 shows the change in species concentration and pH for the S:Cu ratio of 1.0 experiment. When excess sulfide is present, a decrease in the concentration of sulfide in solution can be observed. There is no change in copper (thiocyanate points overlay copper), thiocyanate, or thiosulfate (not shown) concentration during the five hours the experiment was performed. There is a change in pH over time, although the change is small. As there was no measurable copper redissolution, copper recovery remained greater than 99% for the duration of the experiment.

Interestingly, the loss of sulfide from solution occurred at a significantly slower rate than what was seen during the screening experiments (section 6.2.2). During screening there was a sulfide concentration change of 4.3 mM in 1.5 hours, whereas, in the large reactor experiment, the sulfide concentration only changed by 1 mM in 5 hours. The possible causes of this slower reaction rate are discussed in Section 6.3.3.4. A solid sample was not analysed due to the small concentration changes in solution.

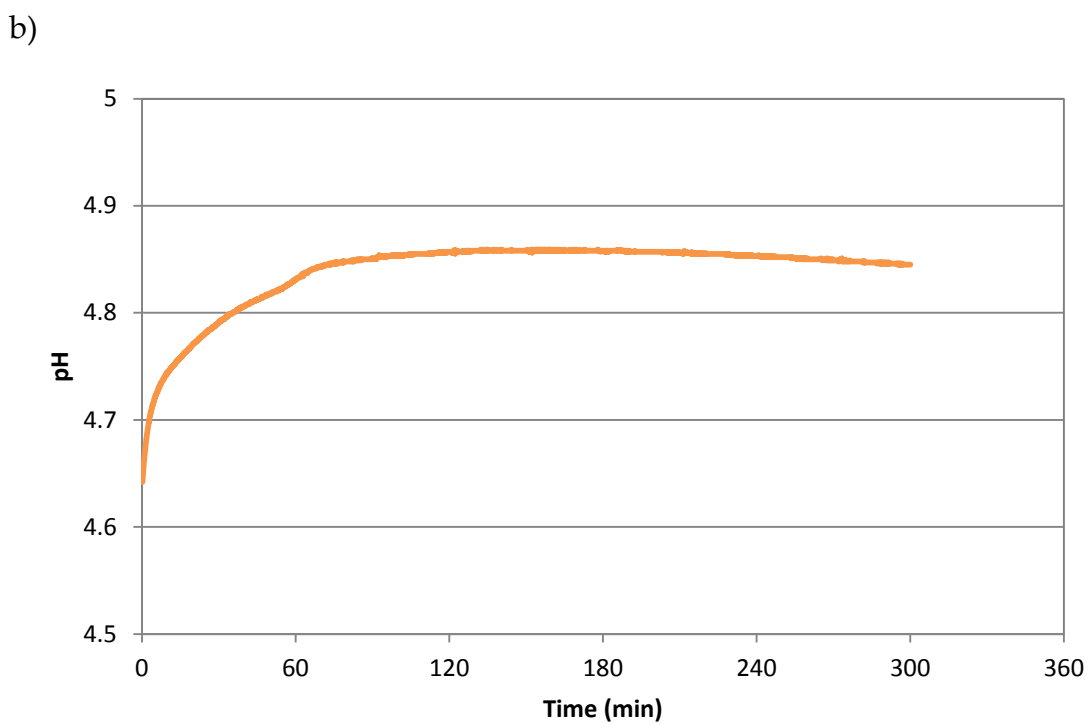
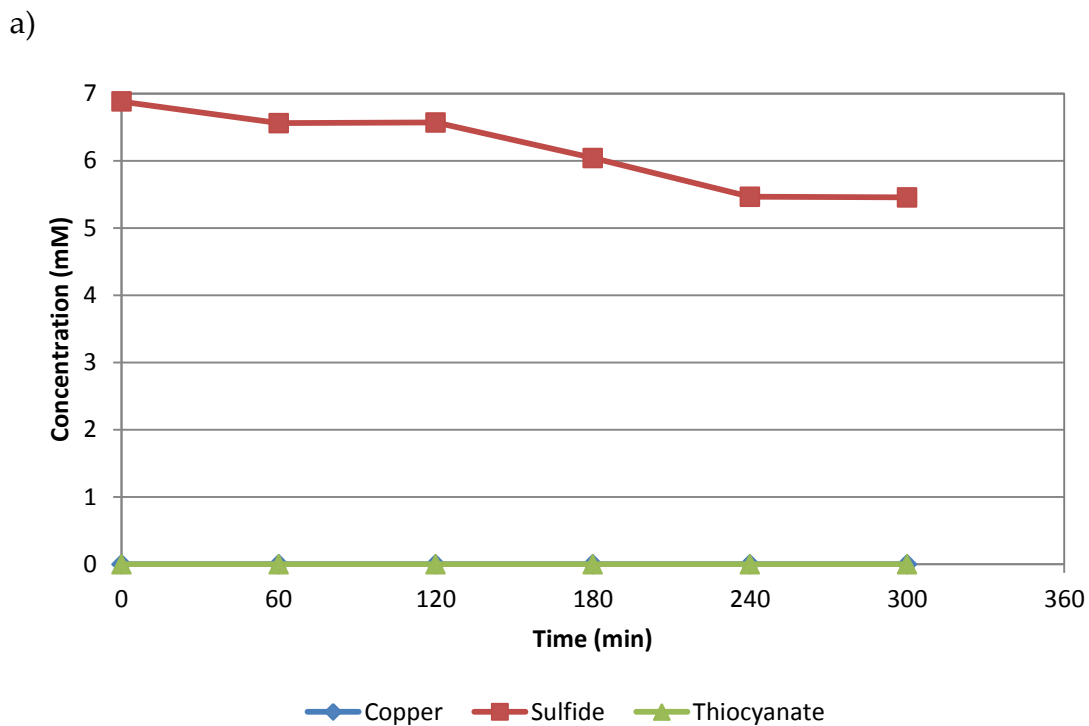


Figure 6.4 a) Species concentration and b) pH over time during sulfidisation for a solution initially containing 13.8 mM copper with a CN:Cu ratio of 4, S:Cu ratio of 1, and pH of 4.65.

### 6.3.3.2 Sulfide to copper molar ratio of 0.5

Figure 6.5 shows the change in species concentration and pH over time for the S:Cu ratio of 0.5 experiment. There was no sulfide detected in solution at any point during the experiment with all sulfide being initially consumed by copper as per the primary sulfidisation equation (Equation 1.3). Over five hours, copper and thiocyanate concentrations increased in solution with copper recovery decreasing from 92.4% to 83.4%. The pH of the solution decreased over the entire time period.

The rate of copper redissolution in this large reactor experiment was significantly less than the rate seen in the screening experiments (Section 6.2.2). The possible causes of this are discussed in Section 6.3.3.4. Again, due to the small change in solution concentration, a solids sample was not analysed.

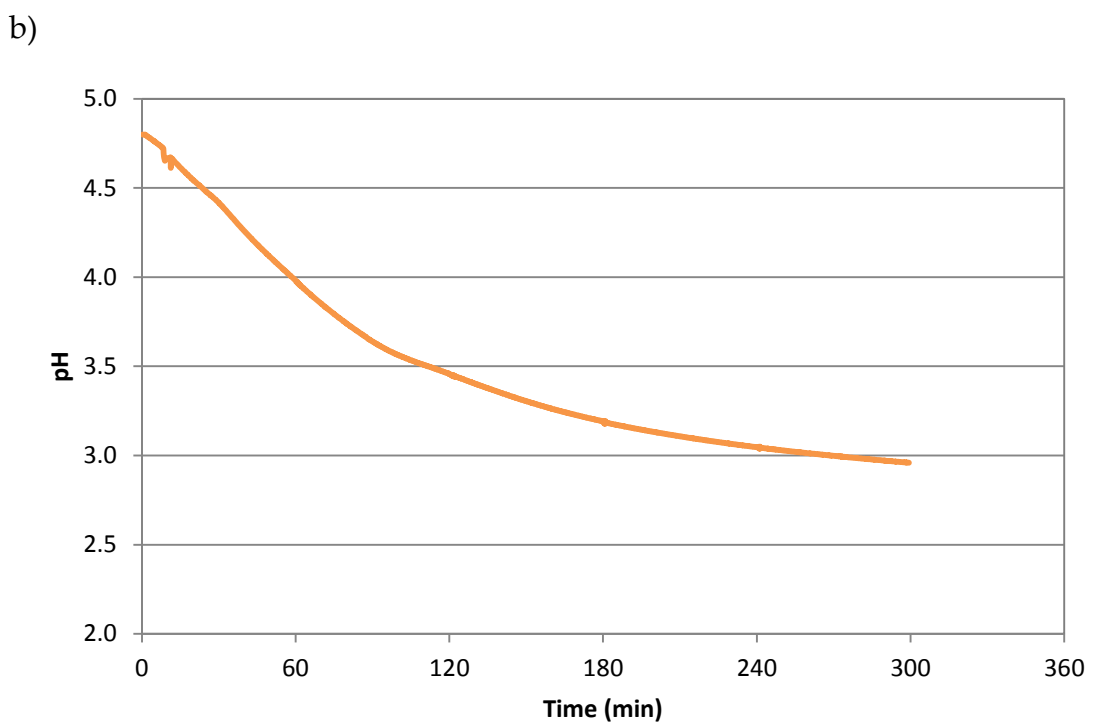
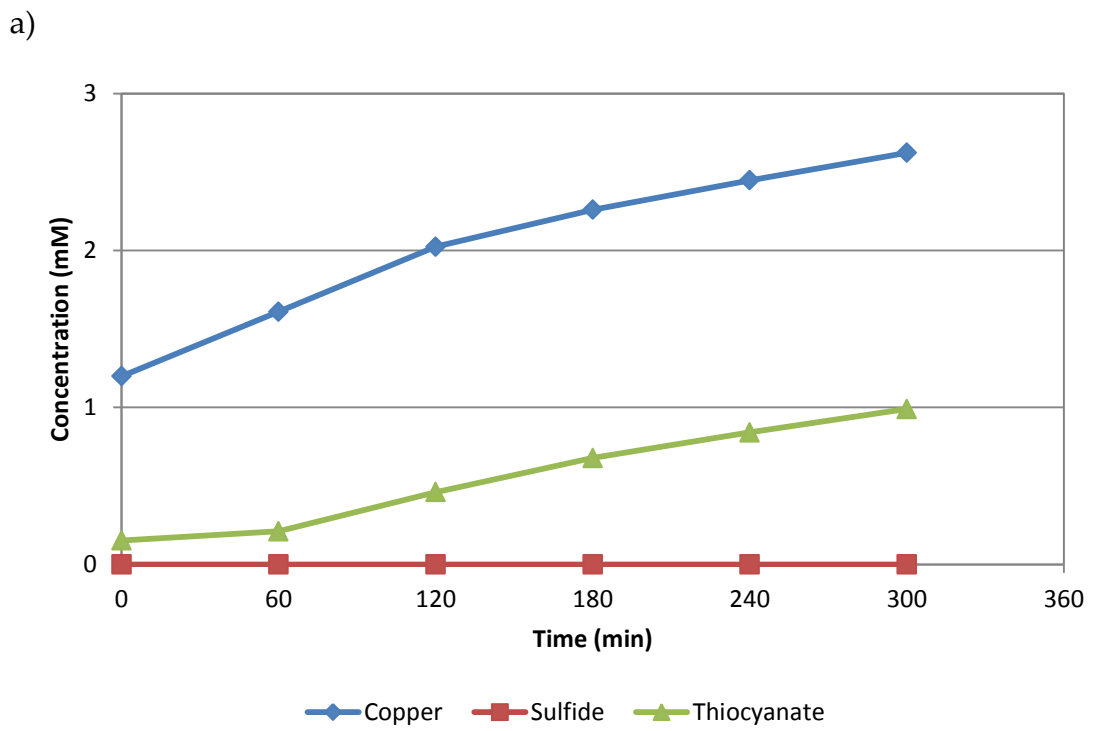


Figure 6.5 a) Species concentration and b) pH over time during sulfidisation for a solution initially containing 15.9 mM copper with a CN:Cu ratio of 4, S:Cu ratio of 0.5, and pH of 4.8.

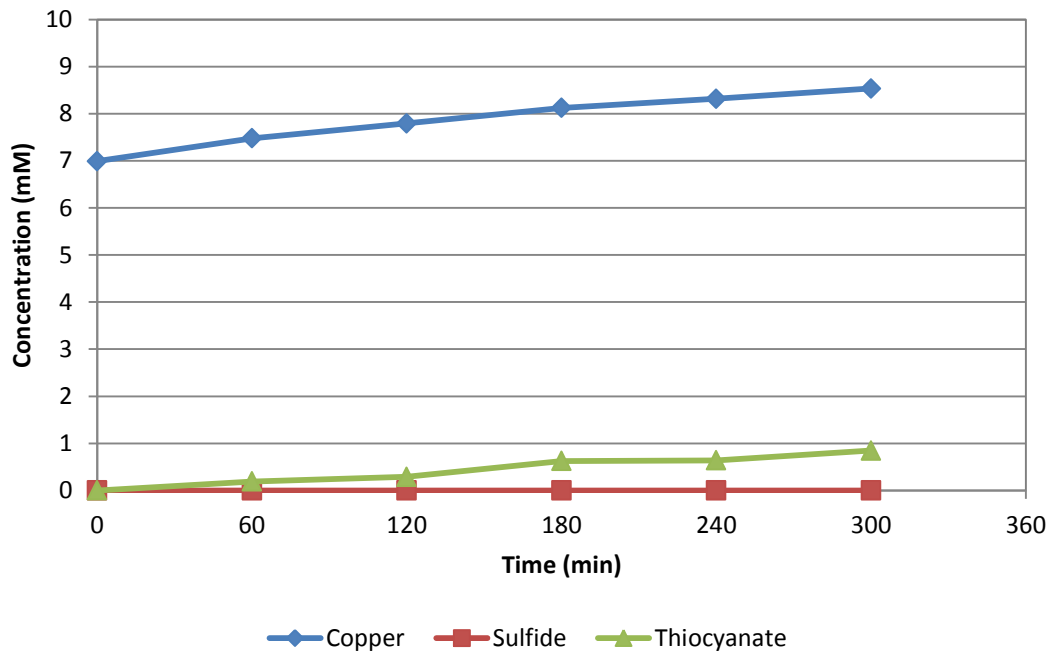
### 6.3.3.3 Sulfide to copper molar ratio of 0.25

Figure 6.6 shows the change in species concentration and pH over time for the S:Cu ratio of 0.25 experiment. As with a S:Cu ratio of 0.5, copper and thiocyanate concentration in solution increase over time. Redissolution of copper resulted in a recovery decrease from 49.9% to 39.1% over five hours. A decrease in pH is also observed over the time period.

The lower S:Cu ratio of 0.25 has no effect on the rate of copper redissolution when compared to the S:Cu ratio of 0.5 experiment. Nonetheless, like the previous two experiments, the rate at which residence time impacted the dissolution of copper was less than that seen for the screening experiments. The possible causes of this are discussed in Section 6.3.3.4. As with an S:Cu ratio of 1.0 and 0.5, a precipitate sample was not analysed due to the small change observed in the solution chemistry.

The results of varying S:Cu ratio clearly show that residence time has two different impacts on sulfidisation depending on if excess sulfide is present in solution or not. When excess sulfide is present, it is depleted from solution over time with no copper dissolution, pH change, or thiocyanate generation. When excess sulfide is not present, copper redissolution occurs, which is accompanied by a decrease in pH over time and generation of thiocyanate.

a)



b)

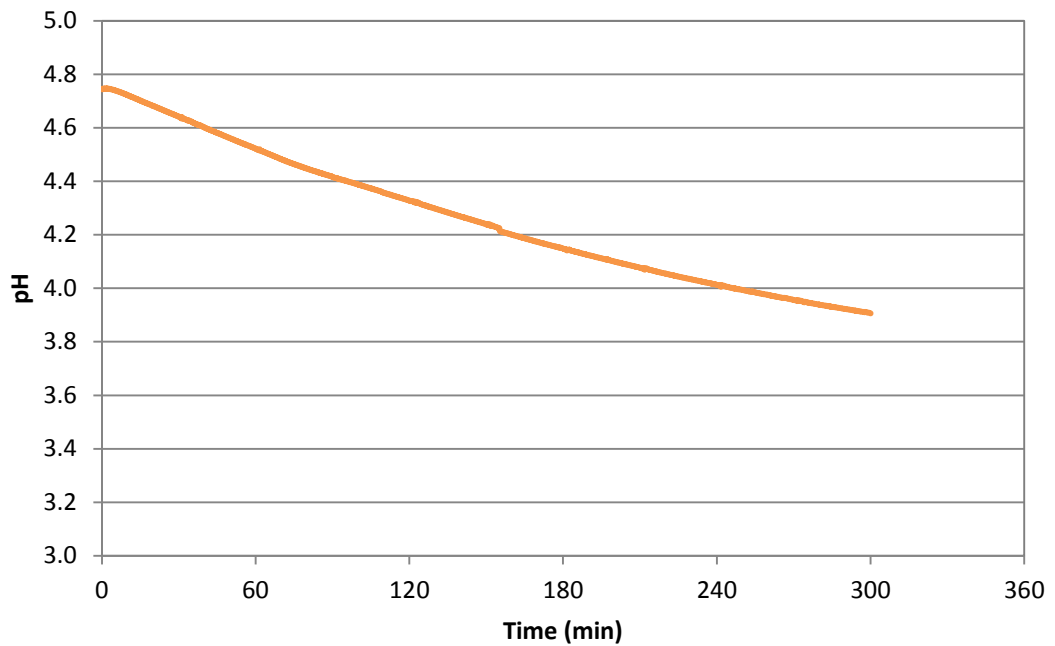


Figure 6.6 a) Species concentration and b) pH over time during sulfidisation for a solution initially containing 14.0 mM copper with a CN:Cu ratio of 4, S:Cu ratio of 0.25, and pH of 4.74.

#### 6.3.3.4 Comparison of reaction rates

Figure 6.7 shows the change in copper concentration of the screening experiment compared to the two S:Cu ratio variation experiments where copper redissolution occurred. It is apparent from Figure 6.7 that copper redissolution occurred significantly faster in the screening experiment than it did in the large reactor experiments. Also notable in Figure 6.7 is that the S:Cu ratio had no impact on the rate at which the copper redissolution occurred in the large reactor.

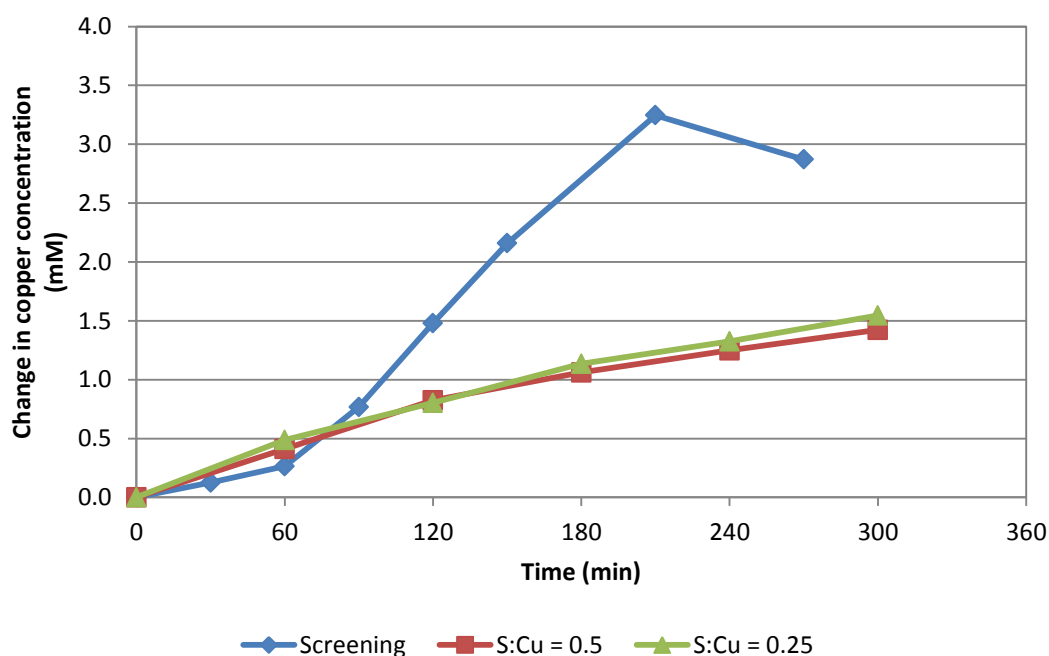


Figure 6.7 Change in copper concentration over time during sulfidisation for the screening experiment (initial solution containing 62.9 mM copper with a CN:Cu ratio of 4, S:Cu ratio of 0.6, and pH of 5) compared to the large reactor experiments (initial solutions targeting 15.7 mM copper with CN:Cu ratios of 4, initial pH of 4.75, and varied S:Cu ratios).

The two key differences between the screening and large reactor S:Cu ratio experiments were the initial copper concentration and the reactor used. The impact of residence time on sulfidisation at different copper concentrations is

discussed in section 6.3.4. The difference in reactor configuration and how this influences the impact of residence time during sulfidisation is developed further in section 6.3.5.

#### **6.3.4 Effect of copper concentration**

Copper concentration may explain the differences in the rates of sulfide consumption and copper redissolution over time between experiments shown in Section 6.2.2 and Section 6.3.3. Hence, the impact of residence time on sulfidisation was studied at various copper concentrations in the large reactor. Figure 6.8 shows the effect of different initial copper concentration on copper redissolution from the precipitate. Initial copper concentration of the solutions were 15.8 mM (~1000 mg L<sup>-1</sup>), 31.5 mM (~2000 mg L<sup>-1</sup>), and 61.9 mM (~4000 mg L<sup>-1</sup>). Each solution had a CN:Cu ratio of 4, S:Cu ratio of 0.5, and a time zero target pH of 4.75.

To allow for an easy comparison between the rates of dissolution, Figure 6.8 shows the change in solution copper concentration rather than the actual copper concentration. Both the 31.5 mM and 61.9 mM copper concentration solutions had a slight excess of sulfide at time zero. Hence, the results in Figure 6.8 are shown from 60 minutes at which time the excess sulfide had been consumed.

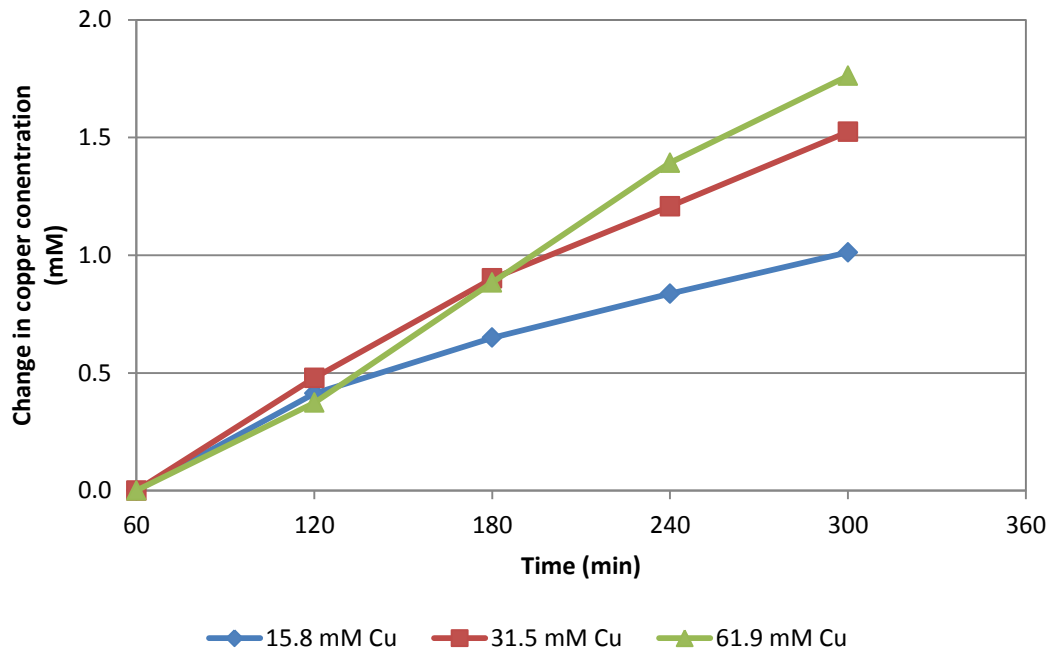


**Figure 6.8 Change in copper concentration over time during sulfidisation for copper cyanide solutions with CN:Cu ratios of 4, S:Cu ratios of 0.5, target pH of 4.75, and different initial copper concentrations.**

Interpretation of the results in Figure 6.8 indicate that the initial rate of copper redissolution from the precipitate during sulfidisation is independent of the copper concentration. A subsequent decrease in the copper dissolution rate is observed which commences earlier as a function of decreasing copper concentration. As the rate is similar for different copper concentrations, the impact of residence time at different copper concentrations is not the same when considered in terms of the decrease in copper recovery. Figure 6.9 shows the reduction in copper recovery during sulfidisation compared with the recovery at 60 minutes. It is apparent from Figure 6.9 that the percentage drop in copper recovery is greater at lower initial copper concentrations.

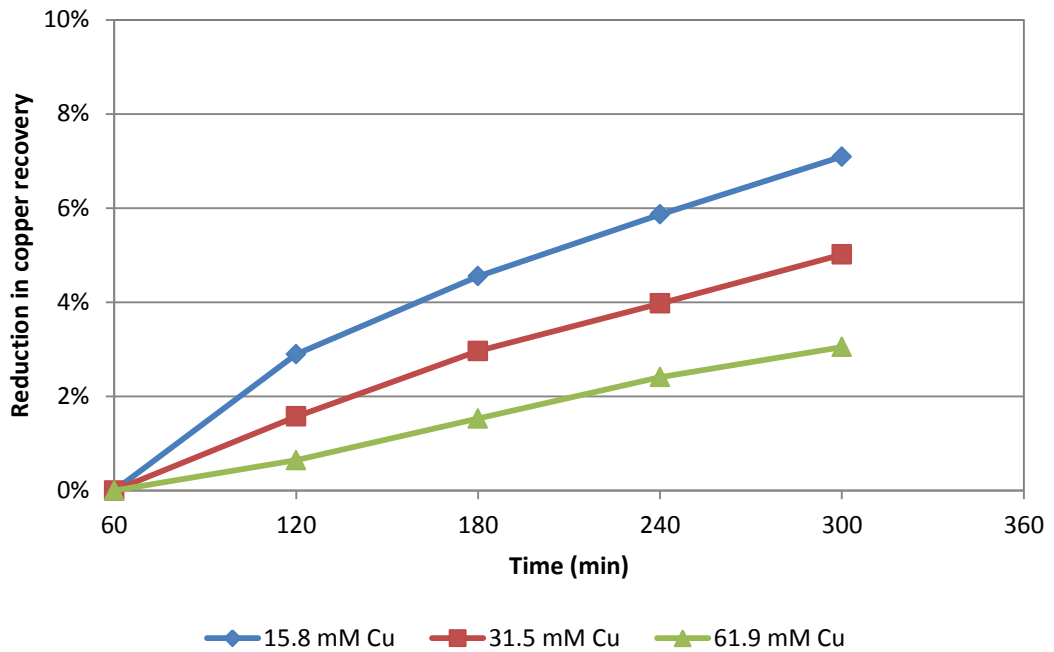


**Figure 6.9 Reduction in copper recovery over time during sulfidisation for copper cyanide solutions with initial CN:Cu ratios of 4, S:Cu ratios of 0.5, target pH of 4.75, and with different initial copper concentrations.**

As with the experiments on S:Cu ratio (Section 6.3.3), thiocyanate was generated over time during these experiments. Figure 6.10 shows the generation of thiocyanate for the solutions with different copper concentrations. Interestingly, thiocyanate generation does not begin immediately, with longer delay periods for solutions with larger initial copper concentrations. Presuming that the precipitate structure is changing, as shown in the screening experiments (Section 6.2), the delay in thiocyanate generation may be related to a requirement for a certain percentage of the precipitate structure to change. This is indicated by the order that the reduction in copper recovery reaches a certain percentage (Figure 6.9) when compared to the order that thiocyanate starts being generated (Figure 6.10). Ultimately, this suggests thiocyanate generation is caused by a secondary reaction to that causing copper redissolution.

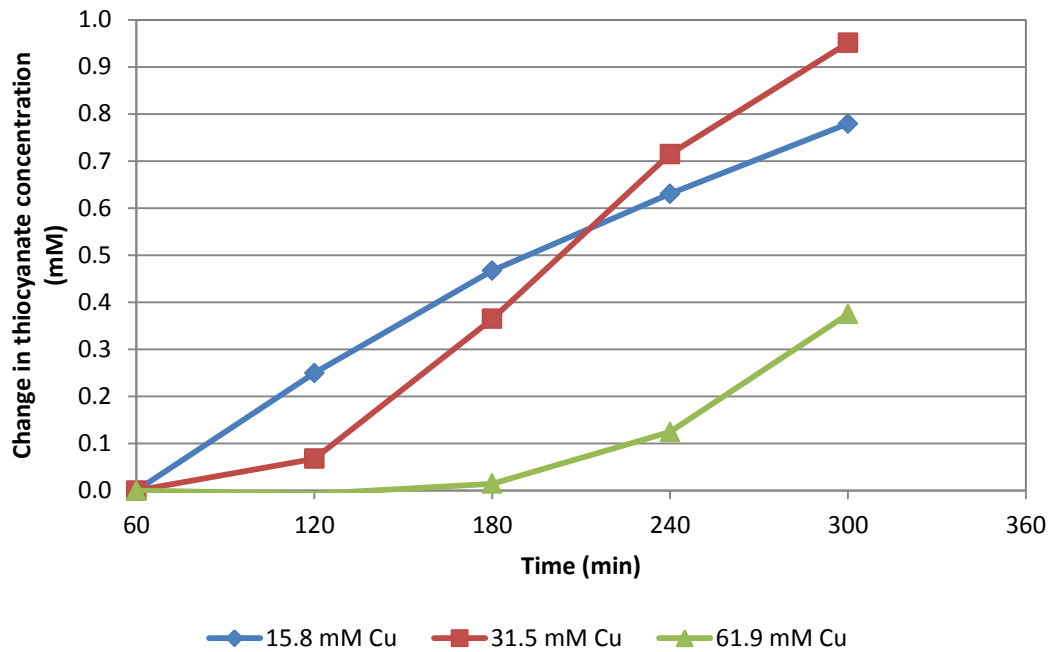


**Figure 6.10 Change in thiocyanate concentration over time during sulfidisation for copper cyanide solutions with initial CN:Cu ratios of 4, S:Cu ratios of 0.5, target pH of 4.75, and different initial copper concentrations.**

The pH in every experiment decreased from 4.75 to approximately 3. Due to the excess sulfide in two of the experiments, however, the pH responses cannot be directly compared as a response to residence time. As with the S:Cu experiments, no solids samples were taken due to the small change in the solution concentrations.

While increasing the concentration of copper in the initial solution did increase the rate of copper redissolution over the time period, the concentration change was still less (1.8 mM after 5 hours) than observed in the screening experiment (3.2 mM after 3.5 hours) for the same initial copper concentration. Hence, a larger initial copper concentration was not the cause of the higher copper redissolution rate in the screening experiment. Thus, it is likely that the difference is caused by differences in the reactors used in the two experiments.

The key difference between the two reactors used in the experiments, apart from the volume of reactor and solution, is the ratio of the solution surface area to volume. In the small reactor there is 50 mL of solution with 19.6 cm<sup>2</sup> of surface area. This gives a surface area to volume ratio of 0.39 cm<sup>-1</sup> in the small reactor. In the large reactor there is 1500 mL of solution with 314 cm<sup>2</sup> of surface area. This gives a surface area to volume ratio of 0.21 cm<sup>-1</sup> in the large reactor. Hence, the small reactor has nearly twice as much surface area per solution volume for diffusion of gases, such as oxygen, from the headspace into the solution or vice versa. Thus, if gas diffusion is involved, then this may explain the faster reaction rate seen in the small reactor compared to the large reactor. As oxygen may play a role in the copper redissolution (oxidation of sulfide), the interaction of residence time and oxygen availability was studied.

#### **6.3.5 Effect of oxygen**

The difference between the rate of copper redissolution in the screening experiments in the small reactor, compared to those done in the large reactor, suggests that oxygen may have an important impact on the rate of copper redissolution from the precipitate generated during sulfidisation. This, coupled with the apparent structure change of the precipitate (Section 6.2.2), also suggest that the cause of the copper redissolution may be related to an oxidation reaction occurring. If this is the case, then the addition of oxygen to the reactor headspace is expected to increase the rate of copper redissolution from the sulfidisation precipitate. As Section 6.3.3 shows a difference between the reactions when there is excess sulfide compared to when there is not (different S:Cu ratios), the impact of oxygen was studied in the large reactor for both sulfide dosing situations.

### 6.3.5.1 Sulfide to copper molar ratio of 1.0

Figure 6.11 shows the consumption of sulfide with both an oxygenated and non-oxygenated headspace (Section 6.3.3.1) for a S:Cu ratio of 1.0. Both solutions had target initial values of 15.7 mM copper, a CN:Cu ratio of 4, a S:Cu ratio of 1.0, and pH of 4.75. It is clear from Figure 6.11 that oxygen increases the rate of sulfide consumption. The outcome supports the hypothesis that consumption of excess sulfide over time is caused by an oxidation reaction.

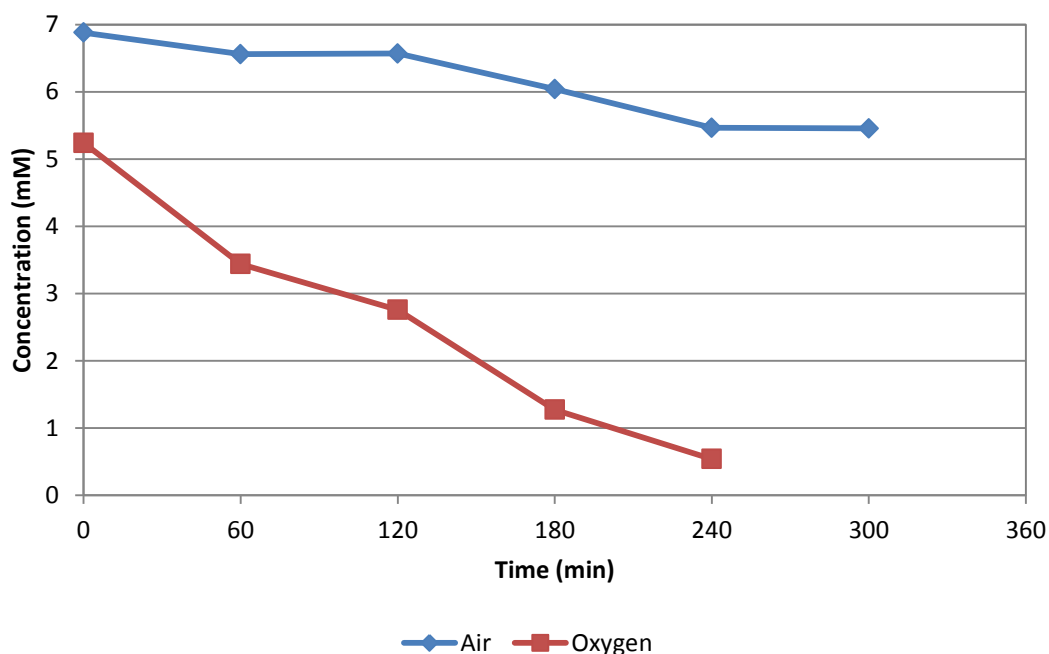


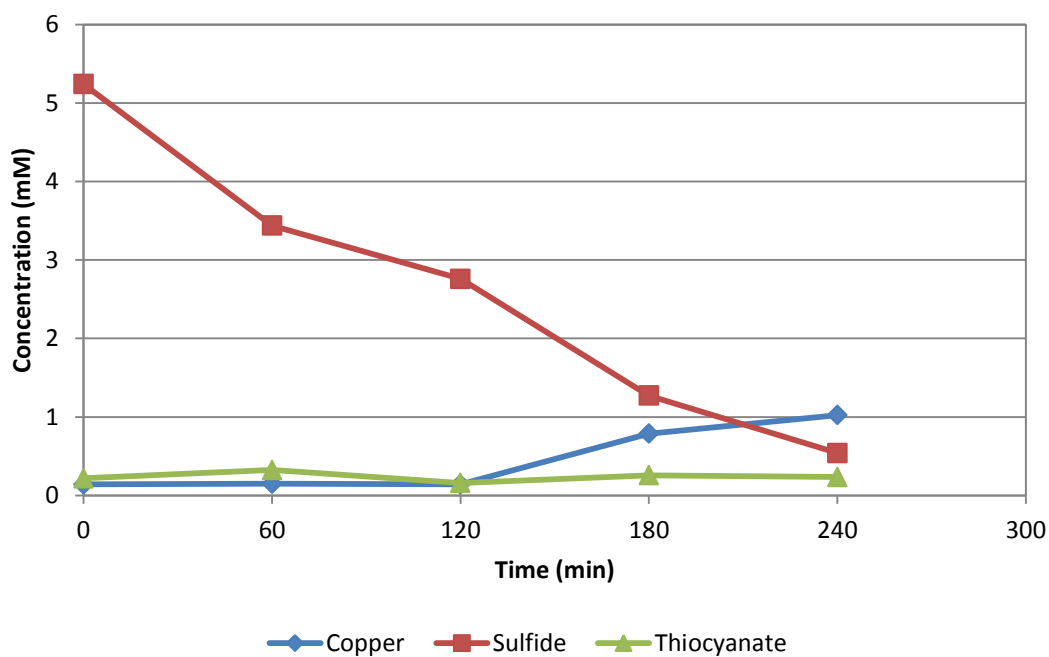
**Figure 6.11 Sulfide concentration over time during sulfidisation for solutions initially containing target values of 15.7 mM copper with a CN:Cu ratio of 4, S:Cu ratio of 1.0, pH of 4.75, and different headspace gas.**

In the experiment with an oxygenated head space, the target initial copper concentration was 15.7 mM (~1000 ppm), but due to an error in solution makeup, it was only measured as 13.3 mM. The target S:Cu concentration in the reactor was 1.0. Nevertheless, the initial sulfide measurement was

slightly lower than expected, with a concentration of 5.2 mM compared to an expected concentration of 7.9 mM. It is likely that due to the higher oxygen concentration in the experiment, oxidation of sulfide during acidification occurred. The lower than target copper concentration resulted in the effective S:Cu ratio in the reactor at time zero (when the target pH was achieved) remaining near the target ratio of 1.0.

Figure 6.12 shows copper, sulfide, and thiocyanate concentration in solution and pH during the experiment with an oxygenated headspace and S:Cu ratio of 1.0. As sulfide concentration approaches zero, copper redissolution began. This is similar to what was seen in the screening experiments once sulfide was consumed (Section 6.2). The lack of thiocyanate and thiosulfate (not shown) generation verifies that the loss of sulfide is not caused by oxidation to these species. A slight change in pH over time is observed, which is similar to that observed when initial S:Cu ratio is 1.0 in an air headspace.

a)



b)

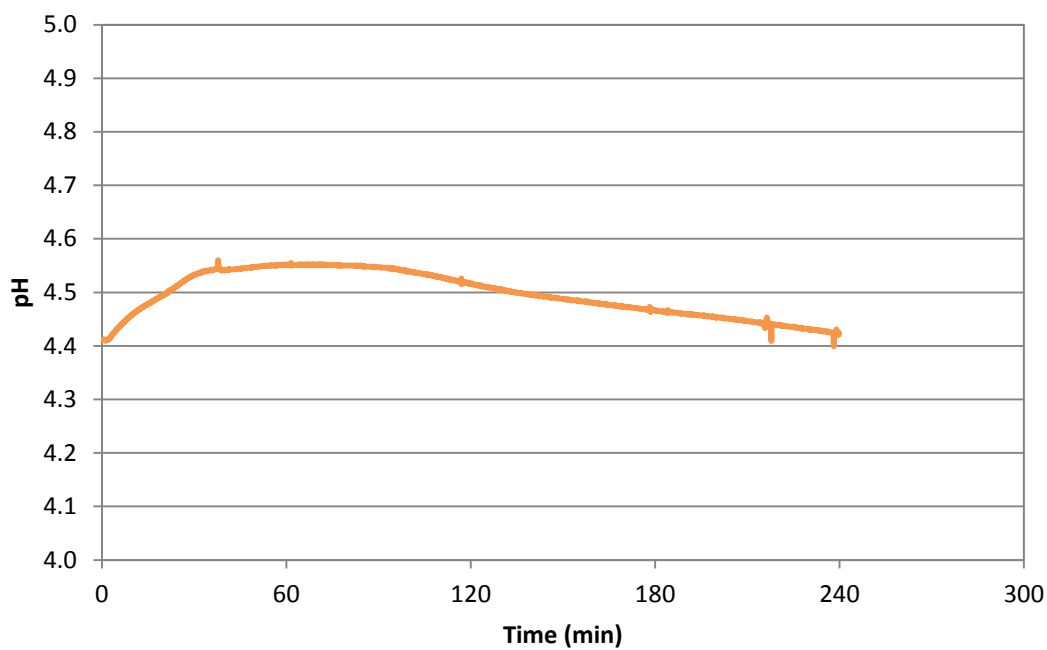


Figure 6.12 a) Species concentration and b) pH over time during sulfidisation for a solution initially containing 13.3 mM copper with a CN:Cu ratio of 4, S:Cu ratio of 1, and pH of 4.41, and an oxygenated headspace.

A solids sample was taken after four hours and analysed using XRD and SEM. Figure 6.13 shows the XRD pattern of the precipitate recovered at the end of the experiment. XRD analysis suggests that the predominant mineral in the solids is covellite ( $\text{CuS}$ ), with some brochantite ( $\text{Cu}_4(\text{SO}_4)(\text{OH})_6$ ). Depending on the amount of brochantite present, the result gives a S:Cu ratio of approximately one in the precipitate. This indicates a change in precipitate structure from the time zero precipitate (Section 6.3.2) and confirms the earlier observation (Section 6.2) that sulfide is consumed due to its incorporation in the precipitate. A S:Cu ratio of 0.96 in the precipitate was predicted from the solution results, agreeing with the outcome of XRD analysis.

SEM analysis of nine randomly selected points in the precipitate yielded a S:Cu ratio of 0.65. This is less than the S:Cu ratio of approximately one suggested by XRD analysis. As discussed earlier (Section 6.3.2), SEM data may be erroneous due to the fine structure of the precipitates being analysed. For this reason, coupled with the agreement between the solution data and XRD pattern, the XRD results should take precedent over the SEM data for this experiment.

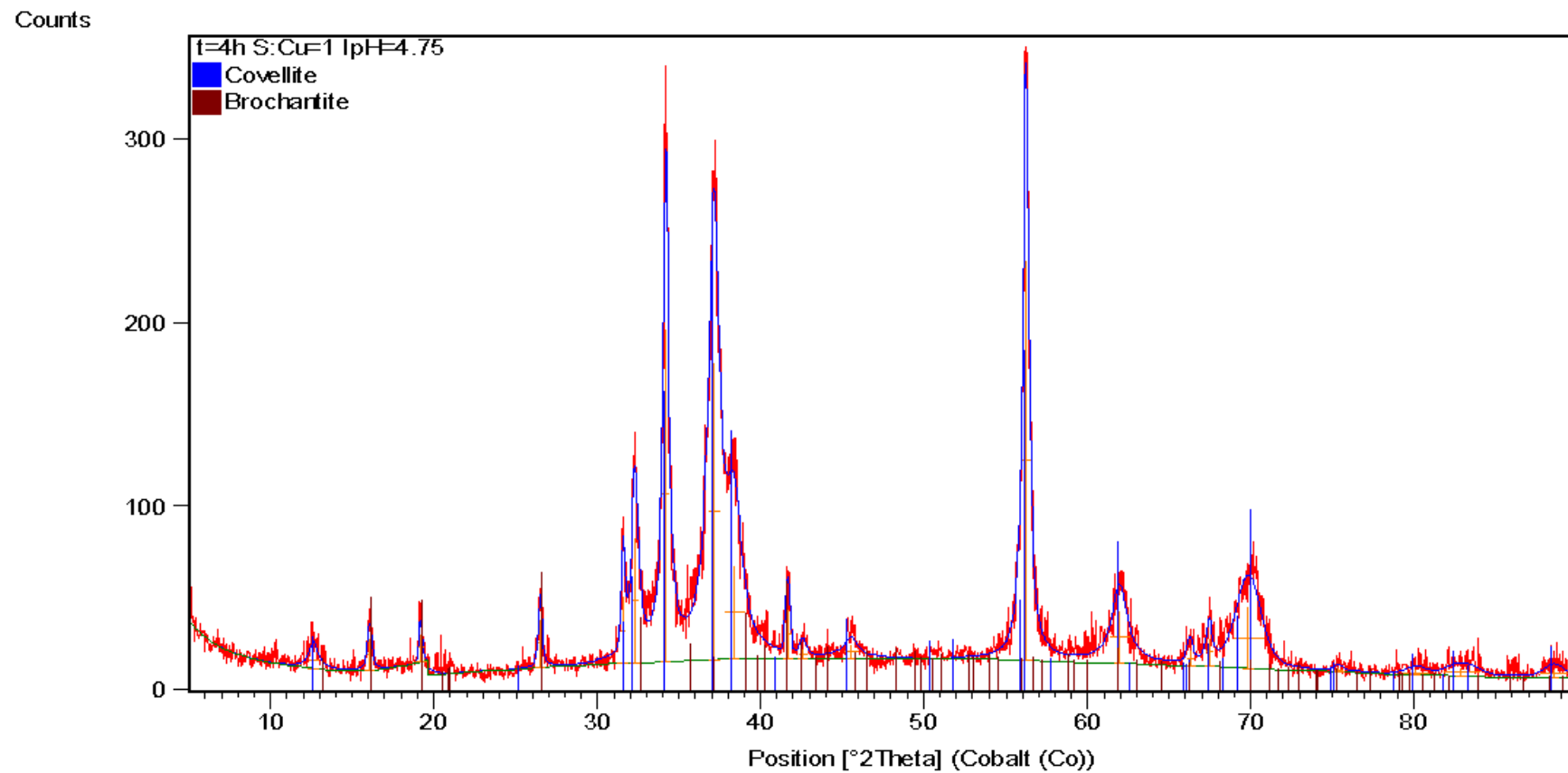


Figure 6.13 XRD pattern of a sulfidisation precipitate after 4 hours from a solution initially containing 13.3 mM Cu, a CN:Cu of 4, a S:Cu of 1.0, and a pH of 4.41. The precipitate was prepared for XRD using powder packing.

#### *6.3.5.2 Sulfide to copper molar ratio of 0.5*

The copper, sulfide, and thiocyanate concentrations in solution and pH during the experiment with an oxygenated headspace and S:Cu ratio of 0.5 is shown in Figure 6.14. The solutions initially contained 15.8 mM copper with a CN:Cu ratio of 4. Initial copper recovery from solution was 78%, which is lower than expected. As discussed with the previous experiment (Section 6.3.5.1), in an oxygenated headspace, this is likely due to increased sulfide oxidation during acidification.

During the experiment, copper concentration in solution increased over a period of approximately one hour, but then decreases for the remainder of the experiment. The region where copper redissolution occurs gives a copper recovery change from 78% down to 71% in one hour. This is faster than in the non-oxygen purged experiments in the large reactor (Section 6.3.3.2) where a copper recovery decrease from 92.4% to 83.4% over 5 hours occurred with no evidence of the copper redissolution stopping. During the final three hours copper re-precipitation occurred, increasing copper recovery from 71% to 79%.

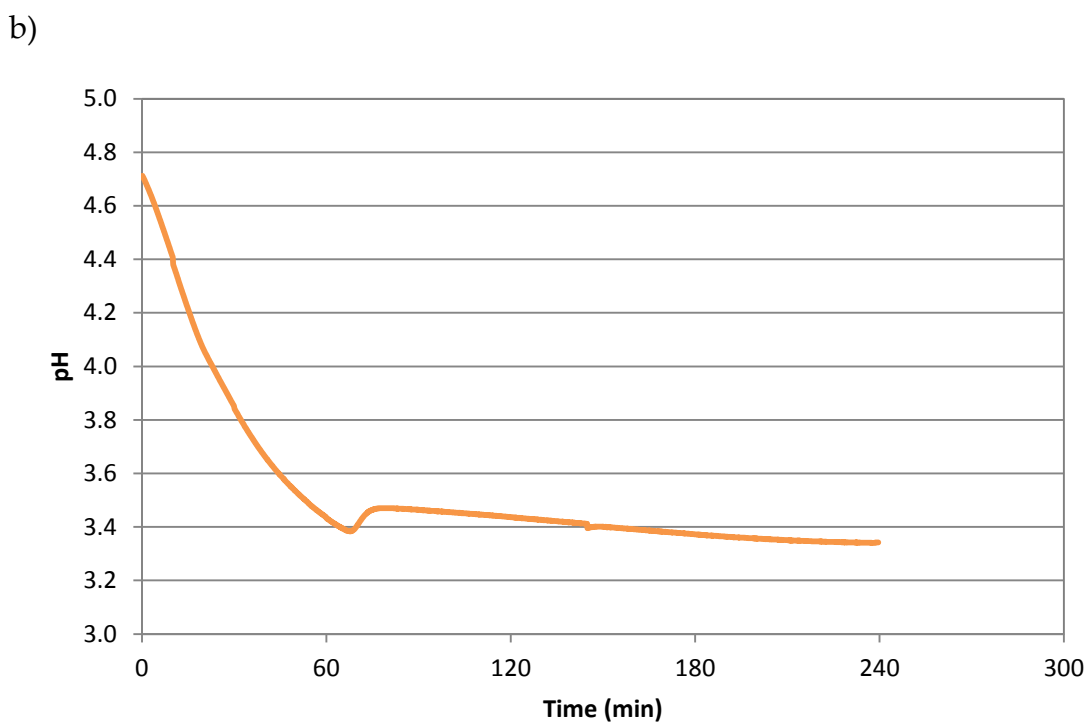
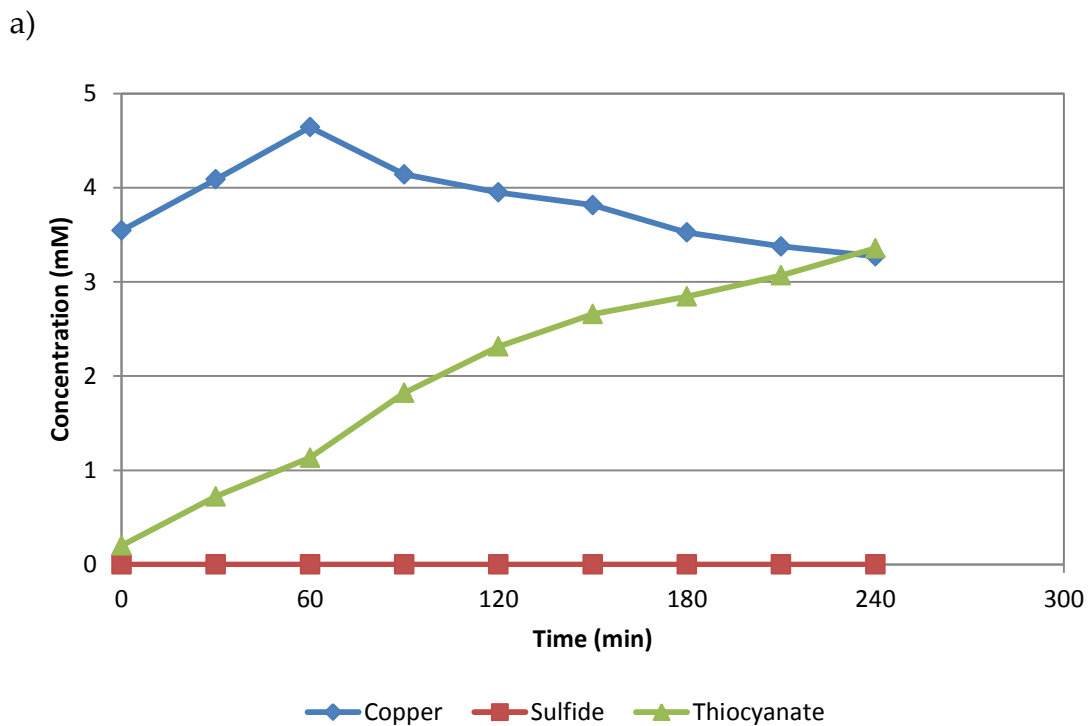
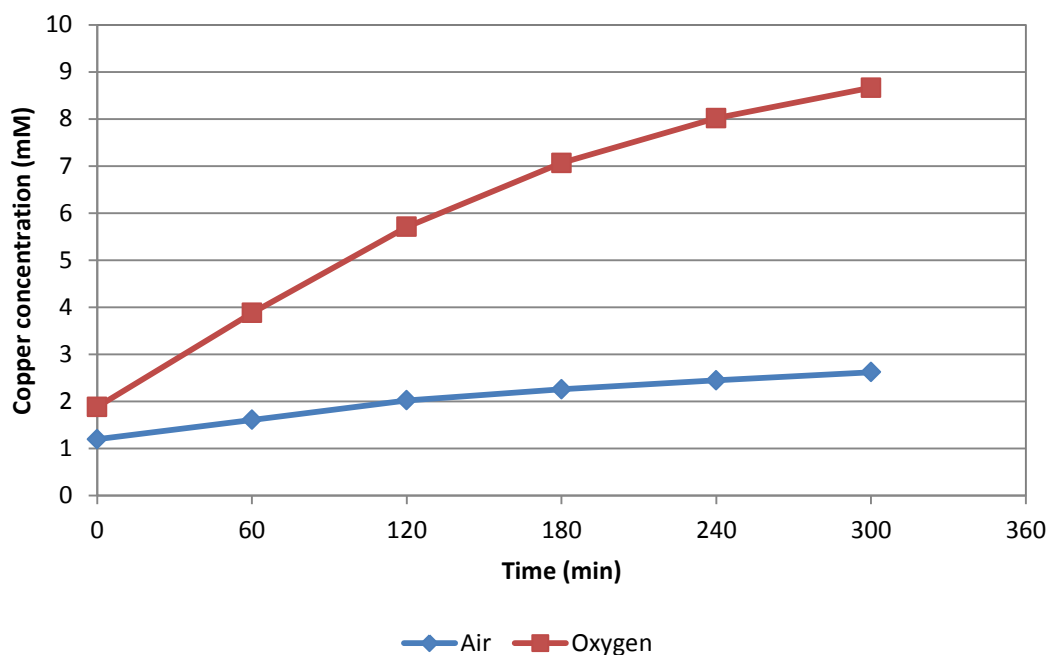


Figure 6.14 a) Species concentration and b) pH over time during sulfidisation for a solution initially containing 15.8 mM copper with a CN:Cu ratio of 4, S:Cu ratio of 0.5, pH of 4.74, and an oxygenated headspace.

During the time period where copper redissolution occurred, the solution pH decreased. At just over one hour the pH of the solution then ceased decreasing (at a similar point in time to the copper re-dissolution stopping), rose slightly, and then continued to decrease at a far slower rate than what was seen in the first hour. This change in the behaviour of the pH and copper concentration was also seen in the screening experiments (Section 6.2). Thiocyanate and thiosulfate (not shown) generation did not appear to be influenced by the change in copper and pH behaviour.

The change in the behaviour of copper redissolution and pH could potentially be explained by the pH of the solution becoming low enough that copper re-precipitates as copper cyanide or copper thiocyanate. Section 6.3.6 explores the effect of pH and residence time on copper behaviour.

As there was a change in reactions occurring during the experiment, the solids from the experiment were not analysed. Instead, the experiment was repeated with the pH controlled using sodium hydroxide (Section 3.4.3). Sodium hydroxide was added to the reactor to bring the pH back up to 4.75 whenever the pH reached 4, or a sample was required. The repeat experiment had an initial copper concentration of 14.7 mM with a CN:Cu ratio of 4, a S:Cu ratio of 0.5, initial pH of 4.7 and an oxygen rich headspace. Figure 6.15 shows the change in copper concentration over time for the pH controlled oxygenated headspace experiment compared to the similar experiment with an air headspace (Section 6.3.3.2). It is clear that oxygen significantly accelerates the rate of redissolution of copper from the precipitate over time.



**Figure 6.15 Copper concentration over time during sulfidisation for solutions initially containing target values of 15.7 mM copper with a CN:Cu ratio of 4, S:Cu ratio of 0.5, pH of 4.75, and different headspace gas.**

Figure 6.16 shows the generation of thiocyanate from the pH controlled oxygenated headspace experiment compared to the similar experiment with an air headspace (Section 6.3.3.2). Again, the impact of oxygen is apparent for the generation of thiocyanate over time, with oxygen causing an increase in the rate of thiocyanate generation. The increased rate of thiocyanate generation in the oxygen headspace, however, was far less than the increased rate of copper redissolution that oxygen caused. Once again, this suggests (Section 6.3.4) that the reaction causing thiocyanate generation is likely to be occurring separately to the one causing copper redissolution. The delay in thiocyanate generation observed in Section 6.3.4 is not seen in these results as the effect is less prominent at lower copper concentrations.

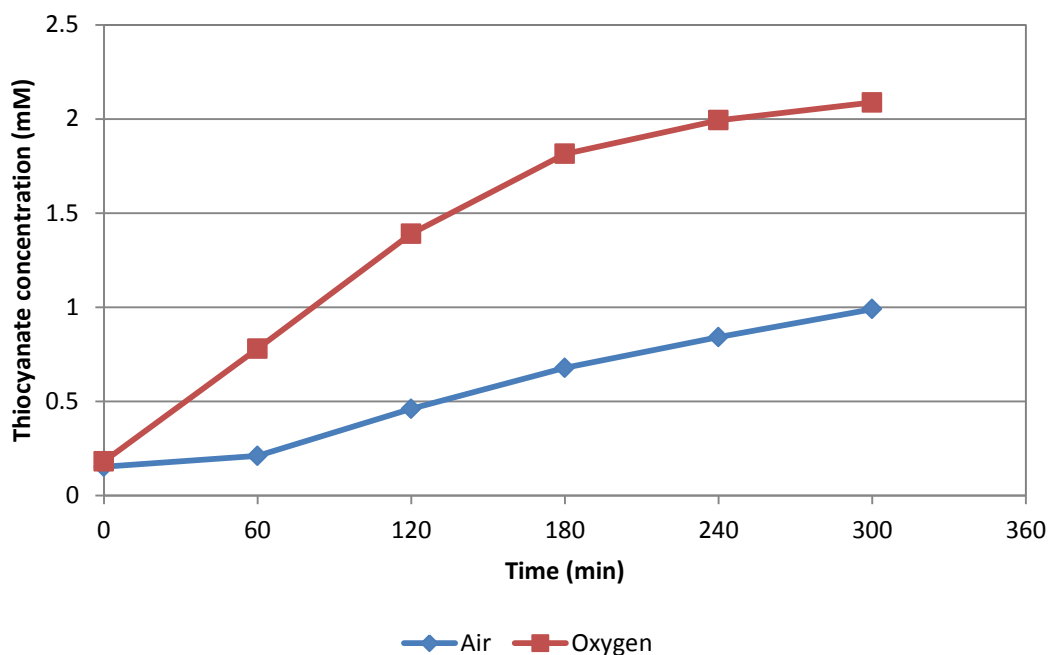


**Figure 6.16 Thiocyanate concentration over time during sulfidisation for solutions initially containing target values of 15.7 mM copper with a CN:Cu ratio of 4, S:Cu ratio of 0.5, pH of 4.75, and different headspace gas.**

Figure 6.17 shows the XRD pattern of the precipitate generated from the pH controlled experiment. The predominant mineral detected from the XRD analysis is covellite (CuS), with some chalcantite (CuSO<sub>4</sub>·5H<sub>2</sub>O). This suggests the S:Cu ratio in the precipitate is 1.0, which is the same as that seen when excess sulfide was present in solution (Section 6.3.5.1). SEM analysis of 18 random points on the precipitate shows a precipitate S:Cu ratio of 0.87, which is in reasonable agreement with the XRD results.

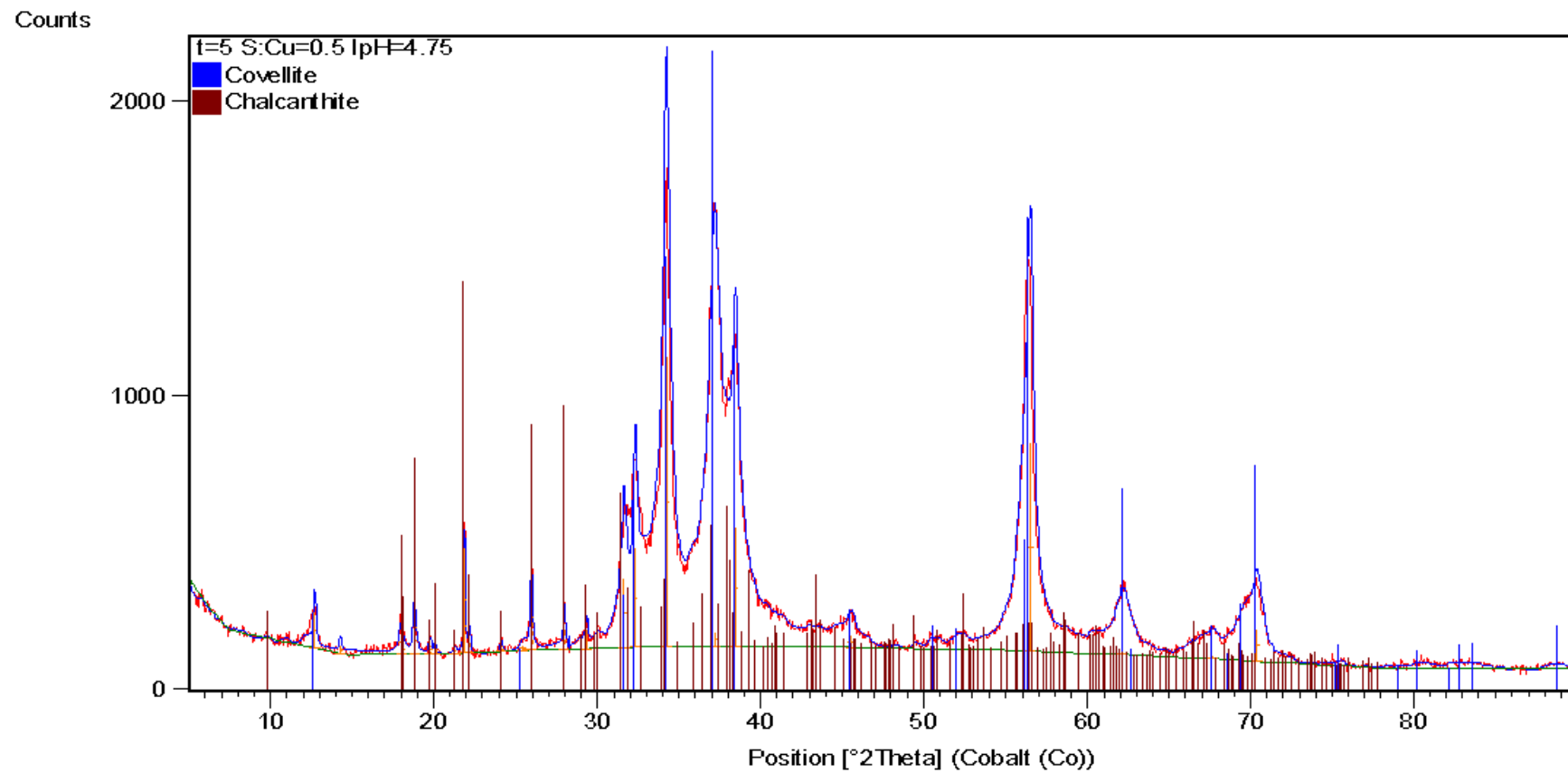


Figure 6.17 XRD pattern of a sulfidisation precipitate after 5 hours from a solution initially containing 14.7 mM Cu, a CN:Cu of 4, a S:Cu of 0.5, and a pH of 4.7. The precipitate was prepared for XRD using a zero background plate.

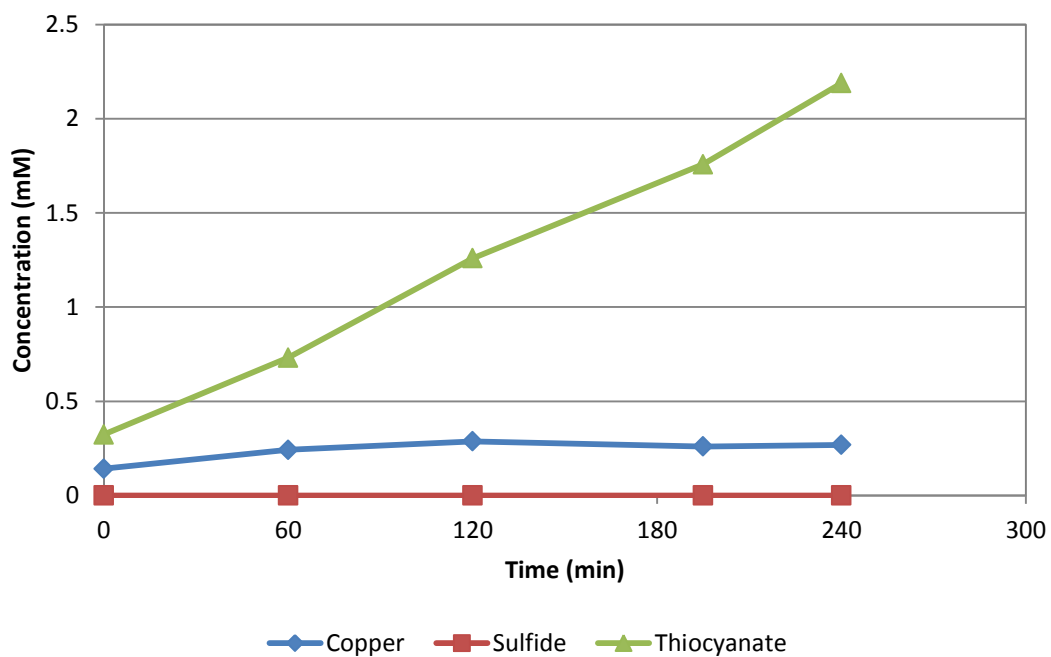
### **6.3.6 Effect of pH**

The previous experiments investigating the impact of oxygen on copper redissolution over time suggests that, at low pH, copper redissolution is overtaken by copper re-precipitation reducing the net copper in solution (Section 6.3.5, Figure 6.14). There is also a noticeable change in the pH response in the solution. To investigate if low pH is the cause of the re-precipitation of copper and the change in pH response over time, the impact of residence time at low pH was investigated.

Figure 6.18 shows the change in species concentration over time for an initial solution containing 15.1 mM copper with a CN:Cu ratio of 4, a S:Cu ratio of 0.5, and an oxygenated headspace. The pH of the solution at time zero was 2.1. An oxygen rich headspace was used for the experiment to accelerate the rate of any reactions as this would result in larger precipitate structure changes, simplifying analysis.

Figure 6.18 shows that, under low pH conditions, copper concentration does not change significantly, while thiocyanate is generated and pH slowly decreases. This result for thiocyanate and pH is similar to that seen in Figure 6.14 after 60 minutes. Unlike in Figure 6.14, no copper re-precipitation is observed in Figure 6.18 due to the high recovery of copper in the experiment initially. Nonetheless, the low rate of pH change over time and the generation of thiocyanate with no copper redissolution in Figure 6.18 suggest that the region where copper re-precipitation occurs in Figure 6.14 (after 60 minutes) is caused by the low pH of the solution.

a)



b)

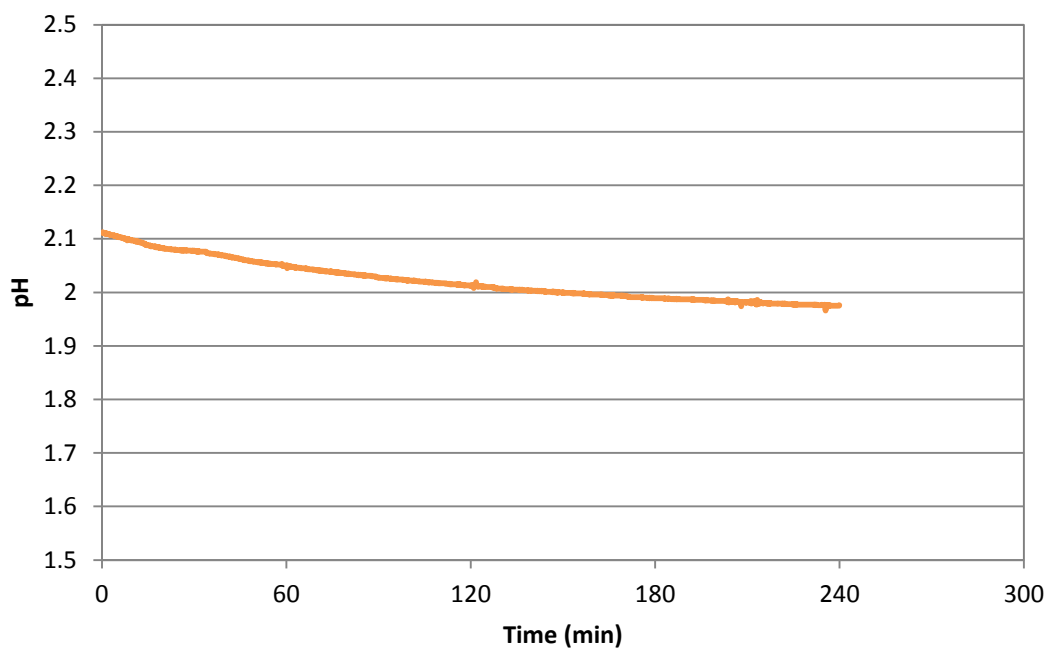


Figure 6.18 a) Species concentration and b) pH over time during sulfidation of a solution initially containing 15.1 mM copper with a CN:Cu ratio of 4, S:Cu ratio of 0.5, pH of 2.1, and an oxygenated headspace.

Figure 6.19 shows the XRD pattern of the precipitate produced from the low pH experiment. Roxbyite ( $\text{Cu}_7\text{S}_4$ ), covellite ( $\text{CuS}$ ), copper thiocyanate ( $\text{CuSCN}$ ), and tenorite ( $\text{CuO}$ ) were detected in the precipitate. The detection of roxbyite and covellite suggest that the change from roxbyite to covellite (Section 6.3.5) is still occurring at low pH even though copper concentration in solution does not increase. Copper thiocyanate and tenorite had not been detected in previous XRD analysis and the generation of these species potentially explain the apparent lack of copper redissolution at low pH. The appearance of tenorite may be due to oxidation of the precipitate between taking the sample and XRD analysis, rather than tenorite being formed during sulfidisation. This is due to tenorite not being thermodynamically stable at the pH used in the experiment (Marani, Patterson, and Anderson 1995). An unassigned peak was also detected at approximately  $34.5^\circ 2\theta$ .

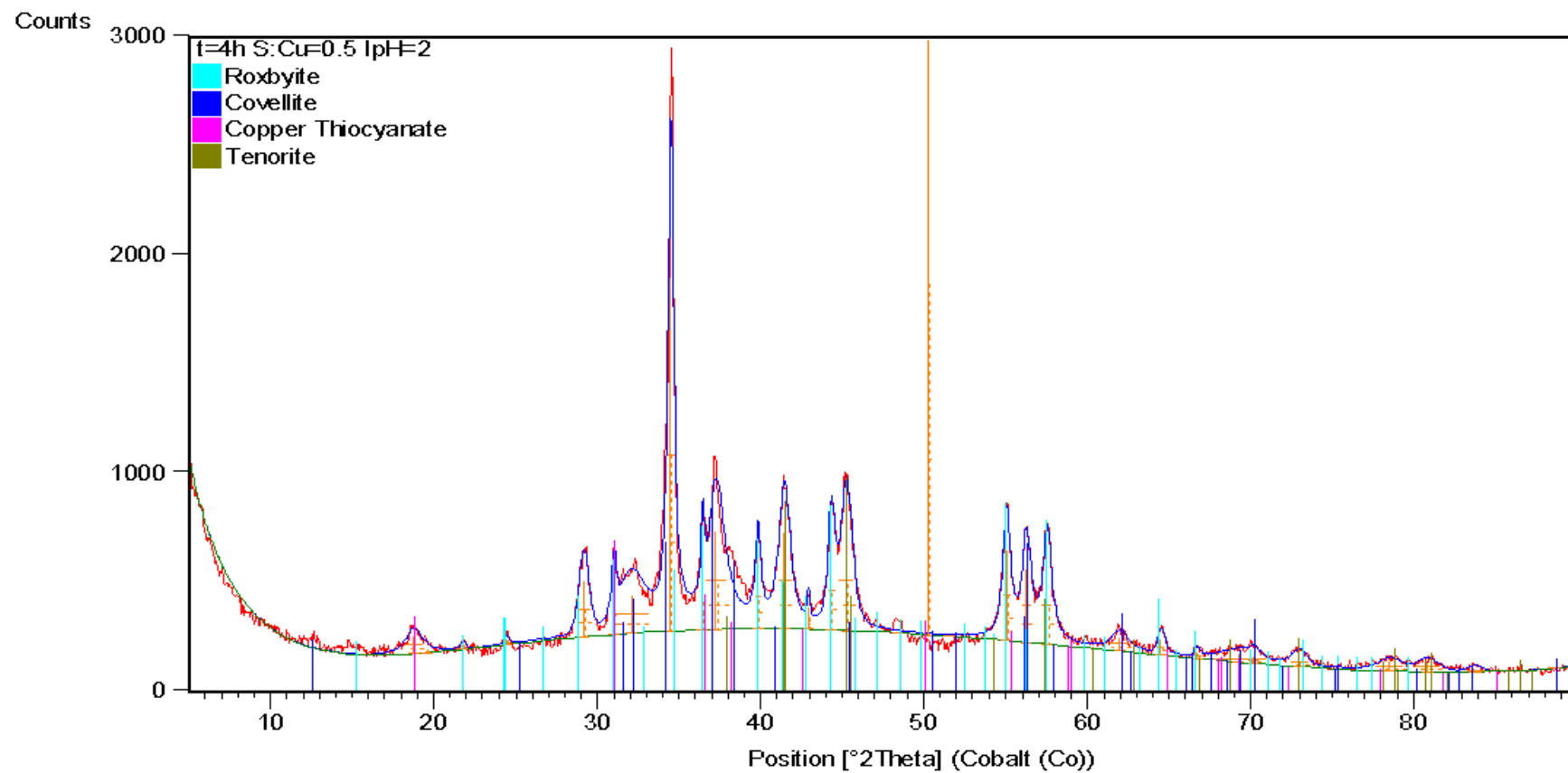


Figure 6.19 XRD pattern of a sulfidisation precipitate after 4 hours from a solution initially containing 15.1 mM Cu, a CN:Cu of 4, a S:Cu of 0.5, and a pH of 2.1 in an oxygen headspace. The precipitate was prepared for XRD using a zero background plate.

SEM analysis of 16 random points in the precipitate showed that nitrogen was present in the sample which could be present as cyanide or thiocyanate precipitates. The amount of nitrogen found varied considerably between the points measured with a standard deviation of 96% of the mean. This shows that the formation of copper thiocyanate or copper cyanide is not homogeneous across the precipitate. Due to the large variation in nitrogen concentration, the amount of copper thiocyanate or copper cyanide present in the precipitate could not be quantified. Carbon is not quantified due to the samples being carbon coated for the SEM analysis (explained in Section 3.6.8).

Although XRD analysis suggests copper thiocyanate is the species forming in the precipitate, which is causing the lack of copper redissolution over time, copper cyanide was also expected to be forming. Nonetheless, no copper cyanide was detected in the XRD pattern. Hence, to confirm that copper cyanide can be detected in the precipitate, if present, a precipitate containing 50% copper sulfide and 50% copper cyanide was prepared for XRD analysis. This precipitate was taken from a solution containing 15.7 mM of copper with a CN:Cu ratio of 4, a S:Cu ratio 0.25, and at a pH of 2. The S:Cu ratio coupled with the pH of 2 causes copper cyanide to precipitate.

Figure 6.20 shows the XRD analysis of the copper sulfide and copper cyanide mixed precipitate. Copper cyanide is clearly detectable in the precipitate along with roxbyite and copper thiocyanate. This confirms the copper re-precipitation observed at low pH (Figure 6.19) is not caused by formation of copper cyanide to any appreciable extent. Due to a low amount of sample being available, the sample had to be prepared using a zero background plate instead of standard powder packing causing a slight shift in the beta copper cyanide peaks compared to the reference pattern.

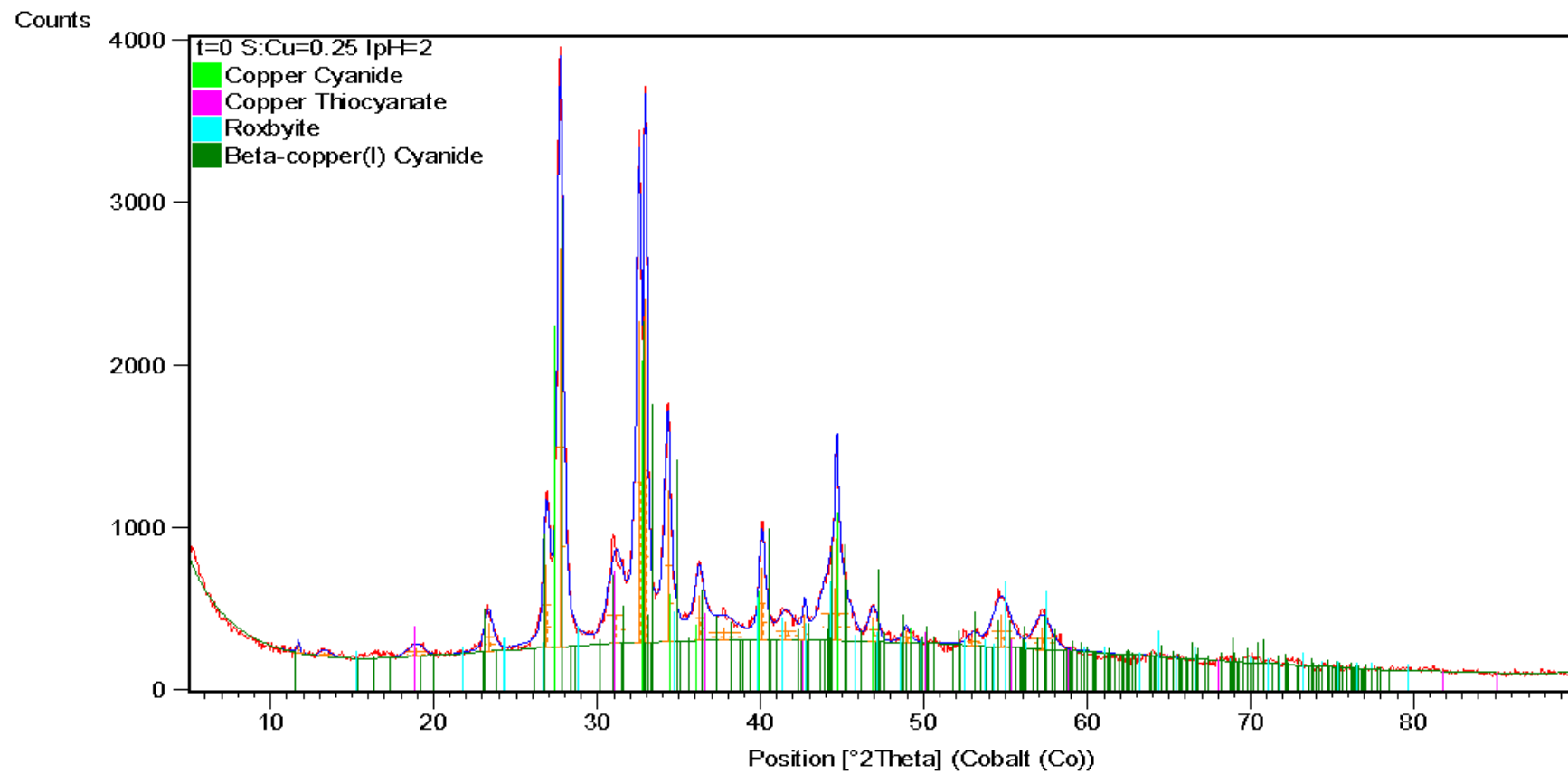
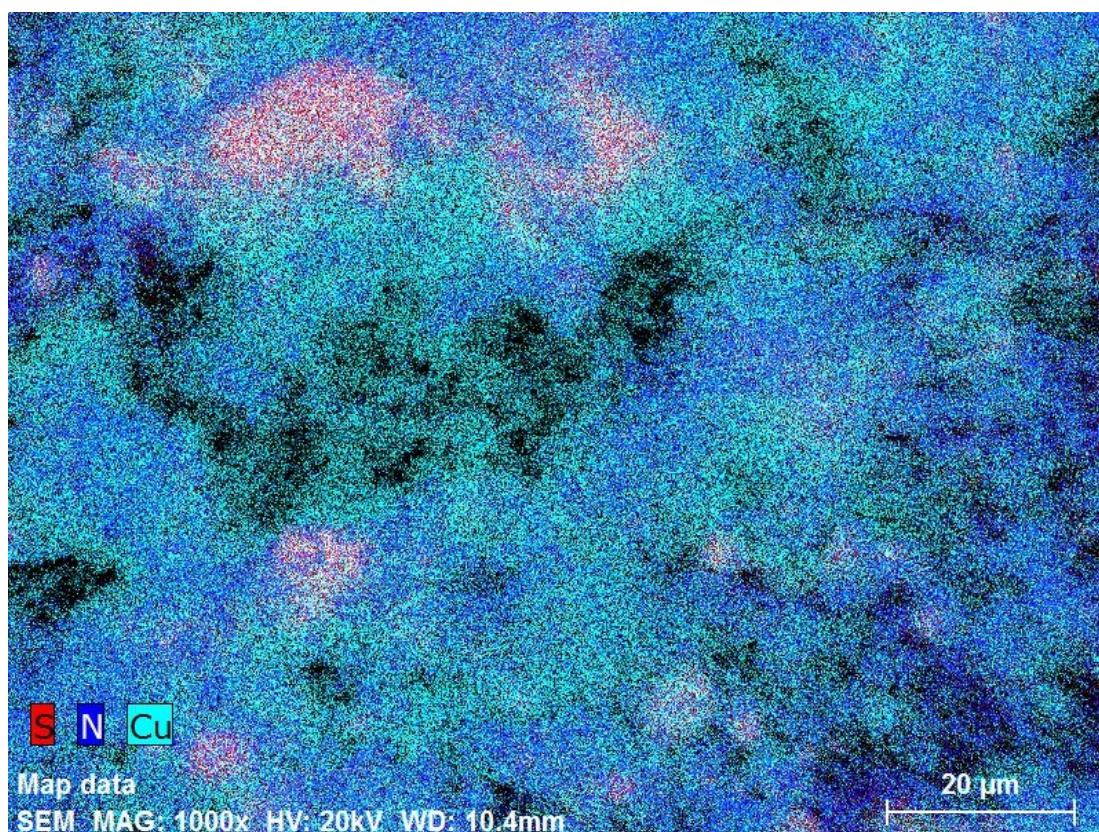


Figure 6.20 XRD pattern of a sulfidisation precipitate from a solution initially containing 15.7 mM Cu, a CN:Cu of 4, a S:Cu of 0.25, and a pH of 2. The precipitate was prepared for XRD using a zero background plate.

SEM analysis of 12 points of the low pH, S:Cu ratio of 0.25 precipitate show a large standard deviation (56%) from the mean for nitrogen. Once more, this suggests that copper thiocyanate and copper cyanide are not homogeneously mixed in the copper sulfide precipitate. To verify this, a species map of a small area of the precipitate was made using the SEM. Figure 6.21 shows the species map which has distinct regions of copper sulfide and copper cyanide. This confirms that SEM is not an accurate technique to determine the cyanide or thiocyanate quantity present in the precipitate without a large set of analysis points.



**Figure 6.21** Map of sulfide, nitrogen, and copper detected with SEM on a region of precipitate from a solution initially containing 15.7 mM Cu, a CN:Cu of 4, a S:Cu of 0.25, and a pH of 2.

### 6.3.7 Effect of cyanide to copper ratio

The effect of CN:Cu ratio on copper redissolution from sulfidisation precipitates is shown in Figure 6.22. All solutions had an initial target concentration of 15.7 mM copper with a S:Cu of 0.5 and pH of 4.75. As CN:Cu ratio is increased, the rate of copper redissolution increases. For a CN:Cu ratio of 3, however, there is a decrease in copper in solution after 240 minutes.

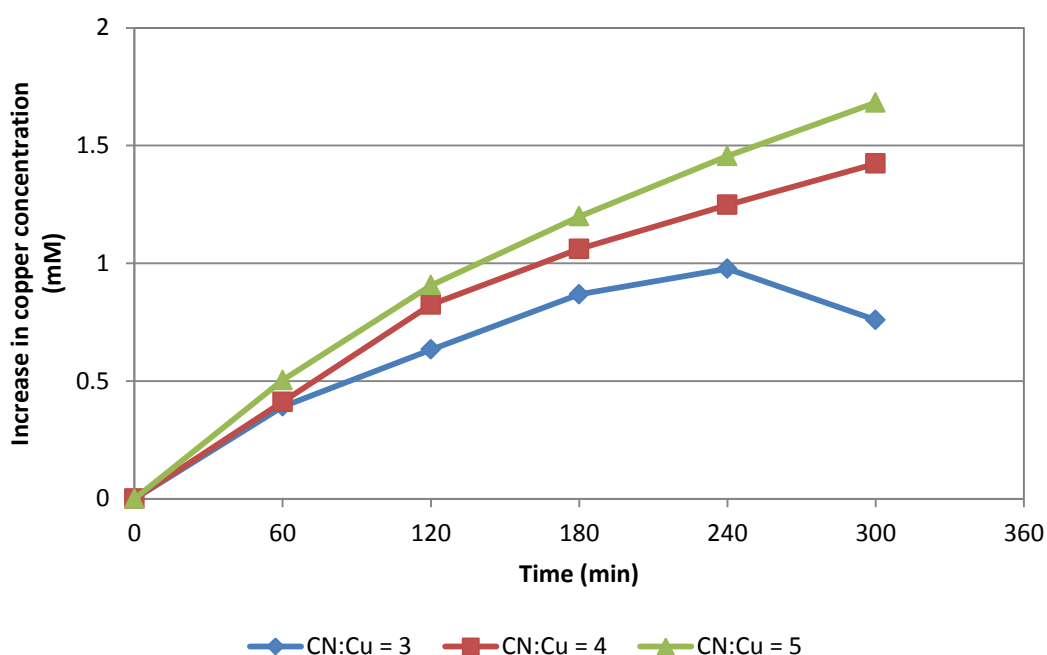
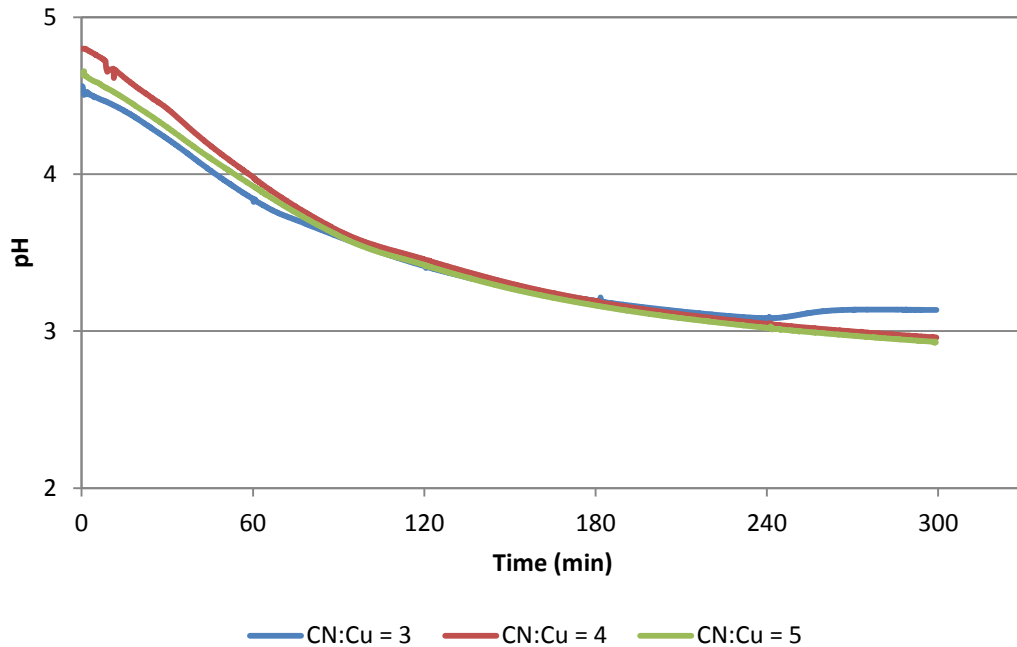


Figure 6.22 Change in copper concentration over time during sulfidisation for solutions initially containing target values of 15.7 mM copper with S:Cu ratios of 0.5, pH of 4.75, and different CN:Cu ratios.

Figure 6.23 shows the pH during the three CN:Cu ratio variation experiments. The pH response is similar for all the CN:Cu ratios up to four hours into the experiment. After approximately four hours, the experiment with a CN:Cu ratio of 3 shows the characteristic pH change associated with the region where copper re-precipitation commences (Figure 6.22). This

shows that the pH below which copper begins re-precipitating as copper thiocyanate (Section 6.3.6) is affected by CN:Cu ratio. Due to only a small amount of copper redissolution, solids samples were not taken for analysis.



**Figure 6.23** pH over time during sulfidisation for solutions initially containing target values of 15.7 mM copper with S:Cu ratios of 0.5, pH of 4.75, and different CN:Cu ratios.

Thiocyanate generation for the three experiments is shown in Figure 6.24. Increasing the CN:Cu ratio causes a slight increase in the rate of thiocyanate generation over time. The rate change, however, is not large compared to the change in cyanide in solution and would result in the impact on cyanide recovery being less for more concentrated cyanide solutions. The characteristic delay time before thiocyanate generation occurs (Section 6.3.4 and 6.3.5.2) is visible, with cyanide concentration appearing to have little impact on the delay time.

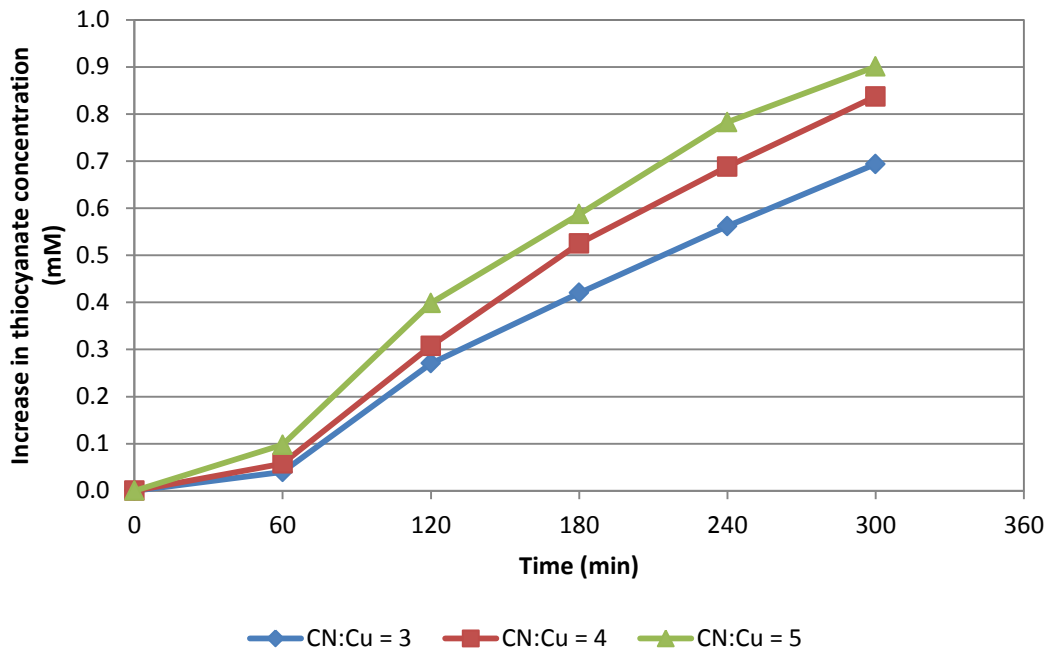


Figure 6.24 Change in thiocyanate concentration over time during sulfidisation for solutions initially containing target values of 15.7 mM copper with S:Cu ratios of 0.5, pH of 4.75, and different CN:Cu ratios.

#### 6.4 Proposed reactions occurring

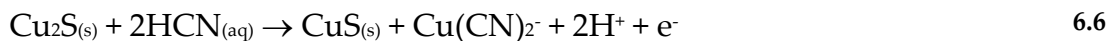
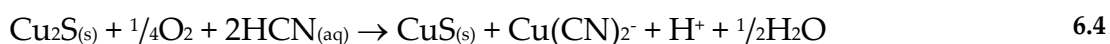
The residence time experiments clearly show that, in the acidic conditions used for sulfidisation, there are reactions occurring over time which either consume excess sulfide when present or cause redissolution of copper from the precipitate. In both cases, the initial precipitate composition of  $\text{Cu}_7\text{S}_4$ , which is similar to the expected composition of  $\text{Cu}_2\text{S}$  (Equation 1.3), is changed to  $\text{CuS}$  over time. The experiments also showed that the rate at which these reactions occur is increased in the presence of oxygen suggesting oxidation of the precipitate formed during sulfidisation.

Such a change in precipitate structure is consistent with the acid leaching of chalcocite ( $\text{Cu}_2\text{S}$ ). Fisher, Flores, and Henderson (1992) showed that chalcocite is leached in sulfuric acid via two stages, the first of which

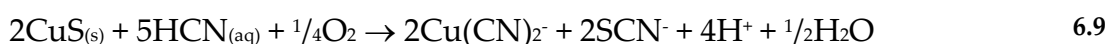
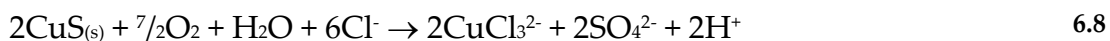
involves the conversion of chalcocite ( $\text{Cu}_2\text{S}$ ) to covellite ( $\text{CuS}$ ) (Equation 6.1). The authors also showed that, when chloride was present, copper released from the chalcocite into solution stayed in a +1 valency state via complexation with chloride (Equation 6.2). This both decreases the oxygen demand for leaching copper and increases the rate of copper dissolution. Fisher (1994) later showed that ammonia has the same effect as chloride (Equation 6.3).



As cyanide is able to form complexes with copper in a +1 valence state, it is feasible that a similar acidic chalcocite leaching reaction to the ones with chloride and ammonia is occurring when hydrogen cyanide is present. This proposed reaction is shown in Equation 6.4, and is consistent with the results seen when no excess sulfide is present in solution and pH has not dipped below the region where copper thiocyanate generation occurs. When excess sulfide is present, copper cyanide released (Equation 6.4) will re-precipitate as  $\text{Cu}_2\text{S}$  as per the primary sulfidisation equation (Equation 1.3). Combining Equation 6.4 and Equation 1.3 gives an oxidation reaction for when excess sulfide is present in solution (Equation 6.5). Equation 6.5 agrees with the experimental results of this chapter that show, when excess sulfide is in solution, it is consumed with no copper redissolution occurring. Oxidation half reactions for Equation 6.4 and Equation 6.5 are shown in Equation 6.6 and Equation 6.7 respectively.



The generation of thiocyanate when copper redissolution occurs appears to be a secondary reaction to Equation 6.4. This is postulated due to the delay period before thiocyanate generation begins and the fact that thiocyanate generation was not influenced to the same degree as copper redissolution when using an oxygenated headspace. Fisher, Flores, and Henderson (1992) show that, when covellite (CuS) is acid leached in the presence of chloride, the sulfide in the CuS is oxidised to sulfate and copper complexes with chloride (Equation 6.8). The authors also showed oxygen pressure to have little impact on the rate of reaction for Equation 6.8. It is possible that a similar reaction is occurring between aqueous hydrogen cyanide and CuS formed from oxidation of Cu<sub>2</sub>S. The presence of cyanide during such a reaction may then result in thiocyanate forming rather than sulfate. A proposed reaction is shown in Equation 6.9.



While Equation 6.9 may potentially explain the generation of thiocyanate over time, it does not account for the lack of thiocyanate generation when there is excess sulfide present in solution even though CuS is still generated over time. Nonetheless, the small amounts of thiocyanate generated and the

lack of oxygen impact signify that whatever reaction is causing thiocyanate generation is minor in comparison to those converting chalcocite to covellite (Equation 6.6). For this reason, the generation of thiocyanate was not explored further.

Interestingly, when the solution pH is low enough, there is a change in the reactions occurring with copper re-precipitation occurring due to the generation of a copper thiocyanate precipitate. A reaction for the formation of the precipitate could not be determined from the data available and was not explored further due to the sulfidisation pH optimum being four (Section 4.4.2).

## **6.5 Industrial implications**

The laboratory scale studies in this chapter show a requirement for excess sulfide, with respect to the primary sulfidisation equation (Equation 1.3), to prevent copper redissolution and a drop in cyanide recovery over time during sulfidisation. As mentioned earlier, the requirement for excess sulfide during sulfidisation is similar to the problems observed in the Newcrest Mining Limited's Telfer SART plant (Turton-White, personal communication, 2010). This indicates that the problems reported at Telfer may be related to oxidation of the precipitate over time.

The results of precipitate analysis in this chapter are also similar to the analysis of precipitates from Newmont Mining Corporation's Yanacocha SART plant (Guzman et al. 2010). Guzman et al. (2010) showed that the precipitate generated in the Yanacocha SART plant contained largely covellite (44% to 90%) with large amounts of copper thiocyanate (10% to 27%). Only small amounts of digenite ( $\text{Cu}_{1.8}\text{S}$ ) ( $\leq 30\%$ ), which is similar to the expected reaction product (Equation 1.3), were detected. Hence, the close

relationship between the precipitates generated in the laboratory scale work of this chapter and the Yanacocha SART plant suggest that, oxidation of the precipitate over time may be the cause of the precipitate structure at Yanacocha.

Although the laboratory results appear to explain the problems experienced at the Telfer and Yanacocha SART plants, the availability of oxygen in the laboratory scale experiments makes direct comparisons difficult. This is due to the considerably larger surface area to volume ratio on the laboratory scale, resulting in faster oxygen transfer to the solution. To determine if the laboratory results are indicative of what is occurring on an industrial scale, the impact of residence time in an industrial SART process is studied in Chapter 7.

## **6.6 Conclusions**

Laboratory scale investigation of the effect of residence time on sulfidisation processes show that, over time, the sulfidisation precipitate undergoes an oxidation reaction transforming it from roxbyite ( $\text{Cu}_7\text{S}_4$ ) to covellite ( $\text{CuS}$ ). It has been shown that the oxidation reaction causes consumption of sulfide with the presence of excess sulfide in solution. When no excess sulfide is present in solution, the oxidation of the precipitate causes copper redissolution to occur. Copper redissolution is accompanied by a decrease in pH over time. A secondary reaction which generates thiocyanate also commences, which is likely caused due to oxidation of covellite formed. The redissolution of copper results in a drop in copper recovery and, by association, cyanide recovery.

Logically, it has been shown that the rate of precipitate oxidation is heavily influenced by the presence of oxygen. The precipitate oxidation rate is

largely dependent on oxygen availability and essentially independent of initial copper concentrations and the presence of more cyanide. Generation of thiocyanate is also increased largely dependent on the oxygen availability and independent of initial copper and cyanide concentrations. Nonetheless, the reaction generating thiocyanate was less influenced by oxygen availability than the initial precipitate oxidation reaction.

It was also found that, when pH becomes low enough, copper re-precipitation occurs due to the formation of a copper thiocyanate precipitate. The pH where this occurs appears to be influenced by the amount of cyanide present in solution. A reaction explaining the region where thiocyanate is generated could not be elucidated from the data available.

The results seen in the laboratory residence time experiments are very similar to precipitate analysis from Newcrest Mining Corporation's Yanacocha SART plant. This suggests that the problems seen on some industrial scale sulfidisation plants are likely caused by the oxidation of the generated precipitate over time during the acidified step of the process. Chapter 7 explores the potential for precipitate oxidation over time to impact industrial scale sulfidisation processes.

## **7 INDUSTRIAL IMPLICATIONS OF RESIDENCE TIME ON SULFIDISATION**

### **7.1 Introduction**

The result of the work on residence time thus far (Chapter 6) clearly indicates that over time the precipitate produced during sulfidisation is subject to oxidation and a resultant drop in precipitate grade (copper to sulfide ratio). The consequence of this is a requirement for higher sulfide addition to maintain high copper and cyanide recoveries on the laboratory scale. This effect may explain similar problems observed in industrial sulfidisation processes, such as high sulfide consumption at Newcrest Mining Limited's Telfer SART plant (Turton-White, personal communication, 2010) and formation of covellite (CuS) instead of chalcocite (Cu<sub>2</sub>S) at Newmont Mining Corporation's Yanacocha SART plant (Guzman et al. 2010). Nonetheless, due to the large surface area to volume ratio in the laboratory experiments, oxygen transfer on the laboratory scale is expected to be significantly higher than what would be expect on an industrial scale. Hence, it is difficult to draw direct comparisons between the problems experienced on an industrial scale and the oxidation of the precipitate at the laboratory scale.

The aim of this chapter is to show that oxidation of the sulfide precipitate formed in sulfidisation does occur on the industrial scale over time. Secondary to this is to establish the relationship between the reactions of industrial solutions and synthetic copper cyanide solutions. This was done through conducting plant surveys on the SART plant at Newcrest Mining Limited's Telfer Gold Mine and followed up with laboratory scale experiments on Telfer SART solutions.

## 7.2 Newcrest Mining Limited's Telfer Gold Mine

Newcrest Mining Limited's Telfer Gold Mine is a 2,600 t h<sup>-1</sup> copper-gold mine with a processing plant that uses flotation to generate a copper concentrate and a pyrite concentrate. The copper concentrate, which also contains a significant portion of gold, is shipped for smelting with credits given for any contained gold value. The pyrite concentrate is treated on site by cyanidation to recover gold associated with pyrite.

While the objective of flotation is to minimise the amount of copper in the pyrite concentrate, the concentrate can still contain significant amounts of cyanide soluble copper. To mitigate the environmental problems caused by cyanide soluble copper (Section 1.2.3), and to reduce reagent cost from high cyanide consumption, Telfer uses leach tails washing with counter current decantation (CCD) followed by the SART process (Section 1.3.5).

The Telfer SART plant follows the standard stages of the SART process (Section 1.3.5) as shown in Figure 7.1. The cyanidation tails solution is fed to the SART plant along with recycled seed (copper sulfide precipitate), sodium sulfide, and sulfuric acid. Two inline mixers are used to mix the cyanidation tails solution and reagents causing the primary sulfidisation reaction (Equation 1.3) to occur. The resultant acidified mixture of copper sulfide precipitate and hydrogen cyanide solution is then fed to a nucleation tank which has a residence time of approximately two hours. The nucleation tank is designed to allow time for precipitates to nucleate and grow.

After nucleation, the slurry is sent to a thickener for the separation of the copper sulfide precipitate from the solution. The copper sulfide thickener residence time can vary greatly depending on the feed flow rate, but is generally between 5 and 15 hours. The copper sulfide thickener overflow is



thickening several times before leaving the SART circuit. The bleed stream is sent to a holding tank where caustic is added to bring the slurry pH back up to 10.5. As there is cyanide present in the solution, some of the precipitate is re-leached by the cyanide. Loss of copper from the precipitate, however, is small compared to the amount recovered. Finally, the copper sulfide slurry is combined with the copper concentrate from the flotation plant and which is then dried and trucked to Port Hedland for shipment to customer's smelting operations.

Although the Telfer SART plant has been effective in recovering cyanide from the Telfer tailings, the plant has suffered from unusually high sulfide consumption (Turton-White, personal communication, 2010). Sulfide dosing in the Telfer SART plant is controlled by taking samples from the SART cyanide return stream and analysing for copper. A target copper concentration of less than 70 ppm in the cyanide return stream has been adopted at Telfer as an "optimum" between sulfide dosing and cyanide recovery. Average copper recovery for the Telfer SART plant from the 1<sup>st</sup> of October 2010 through to the 30<sup>th</sup> of September 2012 was 89.8% with a sulfide to copper molar ratio (S:Cu ratio) of 1.21. This was determined by averaging flow rates and the difference in copper concentration of the SART feed and cyanide recycle stream over the time period. A sulfide solution concentration of 1.86 M was used for the calculation, based on the mixing of solid sodium sulfide and process water as per the procedure used on-site. The S:Cu ratio at Telfer is more than double the sulfide dosing which is expected based on the primary sulfidisation reaction (Equation 1.3) and modelling work in Chapter 4. Newcrest Mining Limited has not been able to identify the reason for high sulfide addition.

Newcrest Mining Limited was interested in the oxidation findings of this PhD research and agreed to support a series of surveys of the Telfer SART plant. The focus was to determine if the high sulfide dosing seen on the Telfer SART plant is related to the oxidation of the sulfidisation precipitate observed during laboratory scale experiments (Chapter 6). During the surveys, Telfer solutions were also collected for confirmatory laboratory scale experiments.

### **7.3 Surveying the Telfer SART plant**

Three surveys were carried out on the Telfer SART plant, the first in August 2011 and the last two in October 2012. Each survey was conducted when the plant was operating with different sulfide to copper ratios and therefore provided useful data to show if changes in copper concentration, sulfide concentration, and pH were occurring over time on an industrial scale sulfidisation process as seen on the laboratory scale (Chapter 6).

#### **7.3.1 Surveying methods**

##### **7.3.1.1 Sampling**

Before surveying, SART flow rates for the 24 hours before the survey were checked to confirm that the plant had been operating in a steady state. The purpose of this was to eliminate generation of misleading survey data caused by process fluctuations. Variables of particular importance were the SART feed rate and copper concentration, sulfide dosing rate, and nucleation tank pH. Periodic dumping of copper eluent from carbon washing into the CCD circuit was also stopped before the surveys to prevent spikes in SART feed copper concentration. Process flow rates, tank levels, and pH values were determined from the Telfer control system using OSIsoft® PI.

Seven sample points around the Telfer SART plant were used for sampling during the survey. The sample points and flow measurements for the survey are shown in Figure 7.1, and will be referenced by their alphabetic (sample points) or numeric (flow measurement) designation shown in Figure 7.1 for the remainder of this chapter.

A sample from each sample point was taken every hour over three hours during each survey. This resulted in four samples per sample point over the duration of the survey. Each sample point had a valve with a hose connection for collecting samples. Samples were taken by opening the specific sample point valve and allowing the solution or slurry to run out of the sample hose for 30 seconds. This cleared the hose of any material left from previous sampling. A plastic container (1 L) was then placed at the end of the sample line and filled to the top before being sealed with a screw cap lid. Once a sample from each of the seven sample points was collected, they were taken to the metallurgical lab on site for treatment before the next set of samples was collected.

In the metallurgical lab, acidic samples (sample points C, D, and F) were treated immediately to prevent any potential precipitate oxidation as discussed in Chapter 6. Acidic samples were filtered using a filter press with Holligsworth and Vose Grade B Wet Strength filter paper. Filtrate from the acidic samples was delivered into a sealed bucket containing a known mass of sodium hydroxide solution. This converted any hydrogen cyanide into free cyanide ions (Equation 1.5). The solids from filtration were washed with plant water, re-filtered, and dried at 80°C overnight. While there should be no solids in sample point D, a small amount of fine blue precipitate was filtered from the solution. Nonetheless, the mass of the sample D precipitate was negligible.

Basic samples (sample points A, B, E, and G) were expected to remain stable and were not treated until the end of each respective survey. At the end of the survey, solutions from sample points A, B, and E were combined into a single composite sample for each respective sample point. The copper product slurry (sample G) was also combined and then filtered. Sample G filtrate was collected and the sample G solids were washed with plant water before being dried at 80°C overnight.

At the end of each survey, 250 mL of each solution sample from all the sample points was taken and refrigerated. The remainder of each solution sample was then discarded. The following day, all solids samples (sample points C, D, F, G) from the survey were combined with solids from the same sample point. The four combined solids samples were then dried, bagged, and placed in a freezer. When transport was available, the solid and solution samples were removed from refrigeration and placed in a cooler with freezer blocks. The samples were then transported to CSIRO Process Science and Engineering's Waterford site for analysis.

#### *7.3.1.2 Analysis*

Solutions were analysed for copper, iron, sulfide, thiocyanate, and thiosulfate, using high performance liquid chromatography (HPLC) as described in Section 3.6.4.1. Free cyanide quantification was attempted using potentiometric titration with silver nitrate (Section 3.6.3.2). The determination of free cyanide concentration, however, was difficult in the feed solution due to problems in successfully determining the endpoint of the titration. This is caused by the low CN:Cu ratio of the Telfer solutions and reduction of sensitivity in detection of the endpoint due to the presence of thiosulfate in the solution (Breuer, Sutcliffe, and Meakin 2011). For this

reason, free cyanide measurements are not included in this section, with copper recovery being used as an indicator for cyanide recovery.

Solids from survey two and three were digested using aqua regia and then analysed for copper, iron, zinc, silver, and gold using inductively coupled plasma optical emission spectrometry (ICP-OES) as described in Section 3.6.2. Sulfur and carbon in the solids from survey two and three were quantified using a Labfit carbon and sulfur analyser (Section 3.6.6).

### **7.3.1.3 Calculations**

Survey flow measurements were obtained by averaging stream flow data over the duration of the survey obtained using OSIssoft® PI software. The average flow rates for the duration of the survey were then used with the survey analysis data to determine the amounts of species moving through SART over time. The Telfer copper sulfide thickener volume (374 m<sup>3</sup>) was determined from plant specifications.

### **7.3.2 Sulfide addition rate**

As mentioned in Section 7.2, the Telfer SART plant had a S:Cu dosing ratio of 1.21 based on the calculated sulfide concentration of 1.86 M sulfide. This calculation assumes that the sodium sulfide is pure and there is no degradation of sulfide in the solution makeup process. Nevertheless, the three surveys of the Telfer SART plant showed that the sulfide concentration in the sulfide feed was lower than the calculated value of 1.86 M. The sulfide values measured were 1.17 M, 1.14 M, and 1.40 M for survey one, two, and three respectively. Degradation of the sodium sulfide used, as well as the possibility of other sulfide reactions occurring because of poor make up

water quality, are the likely cause of the difference between measured and calculated values.

Using the average sulfide concentration of the three surveys (1.24 M), the S:Cu ratio was re-calculated as 0.81, which is still an excess of 60% of sulfide required based on the primary sulfidisation equation (Equation 1.3).

### **7.3.3 Nucleation tank experiment**

Before any surveys were performed, an opportunity arose to use the Telfer SART nucleation tank as a batch reactor rather than a continuous reactor. This provided useful data for comparison to the laboratory scale experimental data from Chapter 6 which was performed in a batch reactor. The opportunity to use the Telfer SART nucleation tank as a batch reactor occurred due to a shutdown of the cyanidation circuit at the Telfer processing plant. Hence, the feed to the SART circuit was stopped, but the nucleation tank was not emptied during the shutdown period (36 hours).

The change in SART feed rate, sulfide addition, and acid addition for one hour leading up to the shutdown and the first hour after the shutdown are shown in Figure 7.2. During the shutdown, the feed was slowly reduced from between  $35 \text{ m}^3 \text{ h}^{-1}$  and  $40 \text{ m}^3 \text{ h}^{-1}$  to zero over one hour. Sulfide dosing was not reduced in a similar manner and, hence, it was expected that the tank would have more sulfide than required by stoichiometry of the primary sulfidisation equation (Equation 1.3). During this time, pH control remained on to keep the pH near the operational target value of 4.5. As the feed rate approached zero, sulfide addition and pH control were stopped.

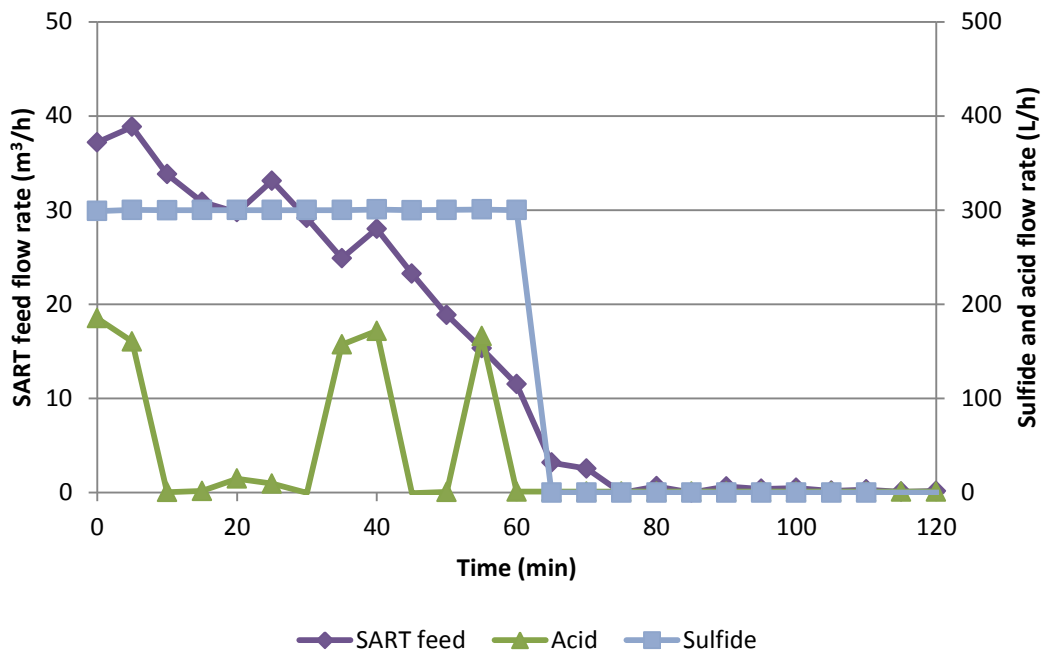
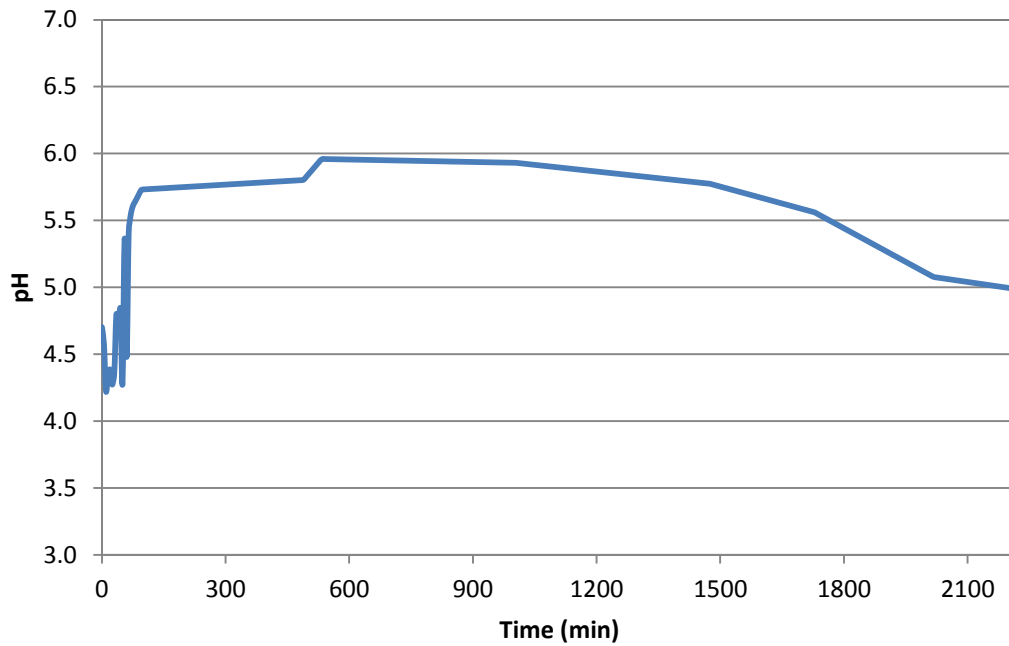


Figure 7.2 SART feed, sulfide, and acid addition flow rates at the beginning of the nucleation tank experiment.

Figure 7.3 shows the pH over time of the reactor during the shutdown period (36 hours), including the hour before the sulfide dosing and pH control was turned off. Once the feed to the nucleation tank ceased, there was a sharp increase in pH before the pH steadied and then started decreasing. The increase in pH was unexpected as the experiments with synthetic copper sulfide solutions (Section 6.3.3.1 and Section 6.3.5.1) had little change in pH when sulfide was overdosed. The change in other species in the reactor during this time is not known as no samples were able to be taken during the test.



**Figure 7.3 Change in pH over time during the nucleation tank experiment.**

While the result of this test shows no conclusive information related to the oxidation of the SART precipitate (Chapter 6), the pH change shows that there are reactions occurring with the Telfer SART solutions over time. The relevance of the results of this test become apparent when compared with the results from the plant surveys in the following sections and is discussed further in Section 7.3.4.4.

### **7.3.4 Surveys**

As the objective of the surveys was to determine if oxidation of the SART precipitate occurs over time on the industrial scale, the copper sulfide thickener in the Telfer SART plant is the focus of the survey results. This is due to the copper sulfide thickener having the largest residence time of the acidified section of the Telfer SART plant, along with the ability to sample the flows in (sample point C) and out (sample point D and F). Samples from the SART feed (sample point A) and sulfide addition (sample point B) were

used to determine the S:Cu ratio being feed to the SART plant once the two streams were mixed.

The results of sampling the cyanide recycle stream (sample point E) are not reported in the results because the thickener overflow (sample point D) is sufficient to determine if residence time is impacting SART at Telfer. Further, due to the gypsum thickener, there is a longer time period before any effect occurring becomes apparent in sample point E compared to sample point D. Similarly, the results from the copper product stream (sample point G) are not reported because the thickener underflow (sample point F) is sufficient to achieve the objective of the surveys.

#### *7.3.4.1 Survey one*

The sulfide dosing to the SART circuit for survey one gave an initial S:Cu ratio of 0.58 once the feed and sulfide were mixed. This S:Cu ratio is in the optimum range shown in Section 4.4.2 (0.55-0.60) and should theoretically yield high copper recoveries as there are few sulfide consuming impurities expected to be in the Telfer SART feed. Copper concentration in the SART feed (sample point A) was 17.4 mM, with the concentration measured at the thickener feed (sample point C) dropping to 3.2 mM. This yields a copper recovery of 81% during the nucleation stage of the Telfer SART plant.

Based on the sulfidisation model in Section 4.3.3 and the S:Cu of 0.58, the anticipated copper recovery at sample point C should be above 98%. There are several possible explanations for the reduced recovery at this sample point including precipitate oxidation during nucleation, side reactions consuming sulfide, or fluctuations in the consistency of the SART feed. As sample point C is the first sample point after the SART feed and sulfide are

mixed, it is not possible to determine the cause of the lower recovery at this sample point.

The average feed rate of the SART plant during the survey was  $40.5 \text{ m}^3 \text{ h}^{-1}$  resulting in a residence time for the copper sulfide thickener of 9.2 hours. Table 7-1 shows both the concentration and number of moles per hour of copper, sulfide, and thiocyanate in the solution phase moving through the copper sulfide thickener. The data shows a clear drop in copper recovery (22%) during the thickening stage of SART. No sulfide was detected in solution during the survey. Thiocyanate concentration increases in the thickener underflow (sample point F), but remains essentially the same in the thickener overflow (sample point D). Due to the small amount of solution which leaves the thickener underflow, however, there is little change in the total number of moles of thiocyanate during the thickening stage. No pH data is available for this survey due to equipment problems.

**Table 7-1 Survey one solution data for the copper sulfide thickening stage of the Telfer SART plant. The S:Cu ratio during the survey was 0.58 with a residence time of 9.2 hours.**

<b>Measurement</b>	<b>Thickener Feed</b>	<b>Thickener Overflow</b>	<b>Thickener Underflow</b>
Sample point	C	D	F
c(Cu) (mM)	3.2	7.0	7.4
c(S <sup>2-</sup> ) (mM)	0	0	0
c(SCN <sup>-</sup> ) (mM)	17.6	17.0	22.9
<b>Measurement</b>	<b>Thickener Feed</b>	<b>Combined Out</b>	
Cu recovery	81%	59%	
n(Cu) (mol h <sup>-1</sup> )	131	282	
n(S <sup>2-</sup> ) (mol h <sup>-1</sup> )	0	0	
n(SCN <sup>-</sup> ) (mol h <sup>-1</sup> )	713	692	

#### 7.3.4.2 Survey two

For the second survey, the measured S:Cu ratio from mixing the SART feed and sulfide was 0.66. The copper concentration at the SART plant feed (sample point A) was 45.2 mM which dropped to 4.7 mM after nucleation (sample point C). This gave a copper recovery of 89%. An 8% increase in copper recovery after nucleation can be observed in survey two compared to survey one due to the increased S:Cu ratio. The S:Cu ratio in the survey is above the optimum of 0.56 determined in Chapter 4, with S:Cu ratio's above 0.6 expected to yield copper recovery greater than 99%. As discussed in survey one, the lower than anticipated copper recovery could be caused by other species in the SART feed consuming sulfide or by oxidation of the precipitate over time (Chapter 6) when the slurry is in the nucleation tank.

The change in copper and sulfide concentration across the thickening stage of the Telfer SART plant is shown in Table 7-2. As with survey one, there is a clear increase in copper concentration in solution during thickening resulting in a 22% decrease in copper recovery to solids during thickening. Also, like observed in survey one, no sulfide was detected in solutions and a slight increase in thiocyanate concentration occurred in the thickener underflow. Nonetheless, there is little change in the total number of moles of thiocyanate during thickening, showing that thiocyanate generation is minimal. The thickener residence time for this survey was approximately 16.2 hours based on the plant feed rate of  $23.1 \text{ m}^3 \text{ h}^{-1}$ .

**Table 7-2 Survey two solution data for the copper sulfide thickening stage of the Telfer SART plant. The S:Cu ratio during the survey was 0.66 with a residence time of 16.2 hours.**

<b>Measurement</b>	<b>Thickener Feed</b>	<b>Thickener Overflow</b>	<b>Thickener Underflow</b>
Sample point	C	D	F
c(Cu) (mM)	4.7	14.6	14.6
c(S <sup>2-</sup> ) (mM)	0	0	0
c(SCN <sup>-</sup> ) (mM)	33.6	31.0	37.3
pH	4.42	4.49	4.25
<b>Measurement</b>	<b>Thickener Feed</b>	<b>Combined Out</b>	
Cu recovery	89%	67%	
n(Cu) (mol h <sup>-1</sup> )	109	337	
n(S <sup>2-</sup> ) (mol h <sup>-1</sup> )	0	0	
n(SCN <sup>-</sup> ) (mol h <sup>-1</sup> )	778	718	

During the second survey pH measurements indicated a small decrease between the thickener feed and underflow from 4.42 to 4.25. A slight increase in pH was observed between the thickener feed and overflow from 4.42 to 4.49. This change in pH is minor and does not contribute to the change in copper recovery seen with respect to the primary sulfidisation equation (Equation 1.3). The result, however, is different to that seen on the laboratory scale, where pH decreased over time when there was little to no excess sulfide present (Section 6.3.3.2, Section 6.3.3.3, and Section 6.3.5.2).

Results from analysis of the solids recovered in survey two are shown in Table 7-3. The results show no considerable change between the thickener feed (sample point C) and thickener underflow (sample point F). This is surprising given the change in the solution composition (Table 7-2), with a drop in copper concentration and increase in sulfide concentration expected in the solids. It is likely that the lack of change in the solids composition is due to the large recirculating load of solids in the Telfer SART plant masking the change in composition that is expected to be occurring.

The S:Cu ratio in the solids is 0.5. This ratio is expected to be higher (1.0) if oxidation of the precipitate during SART is occurring (Chapter 6) as the solution data suggests. Although the solids and solution data is in opposition, there are several factors which make the solution data more trustworthy. Firstly, the solids may have altered during drying and transport where the copper in solution should remain stable. Secondly, the solids did not completely dissolve during the aqua regia digestion. Finally, approximately 8% of the solids cannot be accounted for, even though the expected species were analysed for. Further experiments in Section 7.4 also add validation to the solution data; hence, the solid data has been disregarded.

**Table 7-3 Survey two solids analysis for the copper sulfide thickening stage of the Telfer SART plant. The S:Cu ratio during the survey was 0.66 with a residence time of 16.2 hours.**

Measurement	Thickener Feed	Thickener Underflow
Sample point	C	F
Cu (%)	72.0	71.6
S (%)	18.3	18.1
CN (%)	1.2	1.6
Fe (%)	0.7	0.8
Zn (%)	0.7	0.7
Au (ppm)	25	16
Ag (ppm)	384	334
Unaccounted (%)	7.8	7.9

#### 7.3.4.3 Survey three

For the third survey, the measured S:Cu ratio once the SART feed and sulfide were mixed was 1.52. This S:Cu ratio is approximately 2 times greater than reaction stoichiometry (0.5) with respect to the primary sulfidisation equation (Equation 1.3). Excess sulfide was measured at the thickener feed (sample point C), but was lower than what would be expected based on the S:Cu ratio after feed and sulfide mixing (Equation 1.3). This could be caused by either consumption of sulfide during the nucleation stage due to oxidation over time (Chapter 6) or a change in the way the SART plant was being fed during the survey period. Copper concentration in the SART feed (sample point A) was 27.2 mM and dropped to 1.0 mM at the SART thickener feed (sample point C). This is a recovery of 96% of the copper from the SART feed during nucleation.

Table 7-4 shows the survey data for the third survey. Unlike in the first two surveys, there was very little change in copper recovery during thickening (2%). Instead, consumption of excess sulfide in solution occurred (138 mol h<sup>-1</sup>). There was also a notable increase in pH across the thickener. Interestingly, when excess sulfide was present for laboratory scale experiments on residence time, there was no notable change in pH (Section 6.3.3.1 and Section 6.3.5.1). As with the previous surveys, there is an increase in thiocyanate concentration in the thickener underflow, but there is little change in the number of moles of thiocyanate during thickening. The residence time of the thickener during the third survey was 14.3 hours based on the plant feed rate of 26.2 m<sup>3</sup> h<sup>-1</sup>.

**Table 7-4 Survey three solution data for the copper sulfide thickening stage of the Telfer SART plant. The S:Cu ratio during the survey was 1.52 with a residence time of 14.3 hours.**

<b>Measurement</b>	<b>Thickener Feed</b>	<b>Thickener Overflow</b>	<b>Thickener Underflow</b>
Sample point	C	D	F
c(Cu) (mM)	0.98	1.69	1.24
c(S <sup>2-</sup> ) (mM)	5.55	0.32	0.19
c(SCN <sup>-</sup> ) (mM)	26.9	29.2	33.8
pH	4.73	5.66	5.22
<b>Measurement</b>	<b>Thickener Feed</b>	<b>Combined Out</b>	
Cu recovery	96%	94%	
n(Cu) (mol h <sup>-1</sup> )	26	44	
n(S <sup>2-</sup> ) (mol h <sup>-1</sup> )	146	8	
n(SCN <sup>-</sup> ) (mol h <sup>-1</sup> )	707	766	

Results from analysis of the solids recovered in survey three is shown in Table 7-5. As with survey two, the results show no large change between the thickener feed (sample point C) and thickener underflow (sample point F). This is likely due to the large recirculating load of solids the Telfer SART plant masking any change in solids composition during thickening.

Also similar to survey two is that the S:Cu ratio in the solids is 0.5 instead of 1.0, as the solution data and results from Chapter 6 suggest it should be. Due to several possible problems with the solids analysis, as discussed in Section 7.3.4.2, coupled with results from later experiments validating the solution data (Section 7.4), the solids data has been disregarded.

**Table 7-5 Survey three solids analysis for the copper sulfide thickening stage of the Telfer SART plant. The S:Cu ratio during the survey was 1.52 with a residence time of 14.3 hours.**

Measurement	Thickener Feed	Thickener Underflow
Sample point	C	F
Cu (%)	71.6	71.9
S (%)	18.1	18.3
CN (%)	0.7	1.1
Fe (%)	0.5	0.6
Zn (%)	0.7	0.7
Au (ppm)	15	20
Ag (ppm)	268	244
Unaccounted (%)	9.0	8.1

#### *7.3.4.4 Discussion of survey results*

It is apparent from the three surveys that there is a change in solution composition during the copper sulfide thickening stage of the Telfer SART process. In survey one and two, where little excess sulfide was present during thickening, there was a clear increase in copper in solution between the thickener feed (sample point C) and outlet (sample points D and F). This suggests redissolution of the copper from the precipitate during copper sulfide thickening. This result, for copper, is the same as the residence time experiments on synthetic copper cyanide solutions (Section 6.3.3.2, Section 6.3.3.3, and Section 6.3.5.2). From the observations made in Chapter 6, however, when copper redissolution occurs, a drop in pH and generation of thiocyanate is also expected. Interestingly, there was little change in pH or thiocyanate concentration for survey one and two. The lack of change in thiocyanate concentration, however, may be related to difficulties in measuring small concentration changes in high concentration solutions.

Survey three showed that, when excess sulfide is present, the excess sulfide in solution is consumed instead of copper redissolution occurring as was also observed in laboratory investigations of copper cyanide solutions (Section 6.3.3.1 and Section 6.3.5.1). Unexpectedly, the consumption of sulfide is also accompanied by an increase in pH over time, which did not occur in the Chapter 6 experiments. This increase in pH over time also occurred in the nucleation tank experiment (Section 7.3.3), which was expected to have a high S:Cu ratio.

It is clear from the surveys and the nucleation tank experiment (Section 7.3.3) that, while copper and sulfide concentration in solution respond the same way in the Telfer SART plant as they did in the synthetic copper cyanide experiments (Chapter 6), the pH did not. For this reason, it is still unclear as

to whether the concentration changes seen during thickening at the Telfer SART plant are related to precipitate oxidation as shown in Chapter 6. Hence, laboratory scale residence time experiments using Telfer SART solutions were conducted to determine if there is a link between the observations.

#### **7.4 Laboratory work using Telfer SART solutions**

To determine if the changes in species concentration and pH seen during copper sulfide thickening at the Telfer SART plant are related to oxidation, a series of laboratory experiments were carried out using Telfer plant solutions. These experiments were designed to verify that the sulfidisation precipitate generated using Telfer solutions is susceptible to oxidation as seen with synthetic solutions in Chapter 6. Further, the results of the laboratory scale investigation can be used to determine whether the observed species concentration and pH changes during the surveys were caused by oxidation of the SART precipitate and not some other factor such as fluctuations in how the SART plant was operating. Finally, such experiments also give the opportunity to determine if the Telfer solutions have a similar rate of precipitate oxidation over time compared to the synthetic solutions used in Chapter 6.

##### **7.4.1 Experimental methods**

A 10 L sample of Telfer SART feed solution was taken by filling a bucket to the top with Telfer SART feed (sample point A) and sealing the bucket with a lid. A sample of Telfer sulfide (sample point B) was taken by filling a 2 L poison bottle to the top and sealing the bottle with a lid. Both the SART feed and sulfide samples were then transported to CSIRO Process Science and Engineering's Waterford site for the experimental work.

Experiments using the Telfer SART solutions were performed using the residence time method explained in Section 3.4.3 with the large reactor (Section 3.2) set up as described in Section 3.3.1.2. During the experiments the solution was sampled (Section 3.5.1) and analysed for copper, sulfide, thiocyanate, and thiosulfate using high performance liquid chromatography (Section 3.6.4.1).

Free cyanide was determined using potentiometric titration (Section 3.6.3.2). Determination of the endpoint in the titrations, however, was difficult and generated a large error. This is due to the low CN:Cu ratio of the Telfer solutions and reduction of detection sensitivity due to the presence of thiosulfate in the solution (Breuer, Sutcliffe, and Meakin 2011). For this reason, free cyanide concentration is not reported for the residence time experiments with copper recovery used as the indicator for cyanide recovery.

For comparison, some experiments with synthetic copper cyanide solutions were conducted with the same copper and cyanide concentrations as the Telfer SART feed solution. These solutions were made up using the methods described in Section 3.1.2. Some comparison experiments were also conducted with laboratory sulfide solutions prepared as described in Section 3.1.3.

#### **7.4.2 Analysis of Telfer solutions**

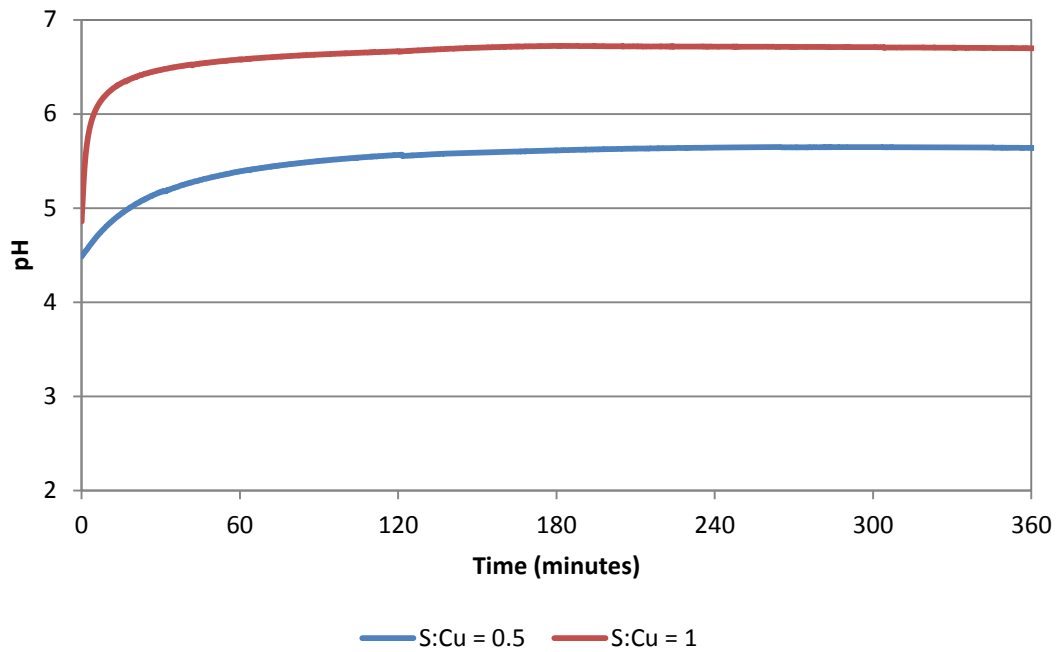
Before any experiments were performed, the Telfer SART feed and Telfer sulfide were both analysed to determine their respective species concentrations. The Telfer SART feed was found to contain 33.8 mM of copper with 78.1 mM of cyanide, giving a CN:Cu ratio of 2.3. To determine if any degradation occurred during storage, the Telfer SART feed was monitored over the course of the experiments. During this time cyanide

concentration decreased slightly, but this only caused a reduction in the CN:Cu ratio of 0.1. The Telfer SART feed also contained 35.7 mM thiocyanate, 3.5 mM thiosulfate, and 0.8 mM iron.

Sulfide concentration in the Telfer sulfide solution was quantified every time an experiment was performed. This was to prevent errors occurring due to the degradation of sulfide solution over time. The Telfer sulfide solution concentration ranged between 1.21 M and 1.19 M during the course of the test work.

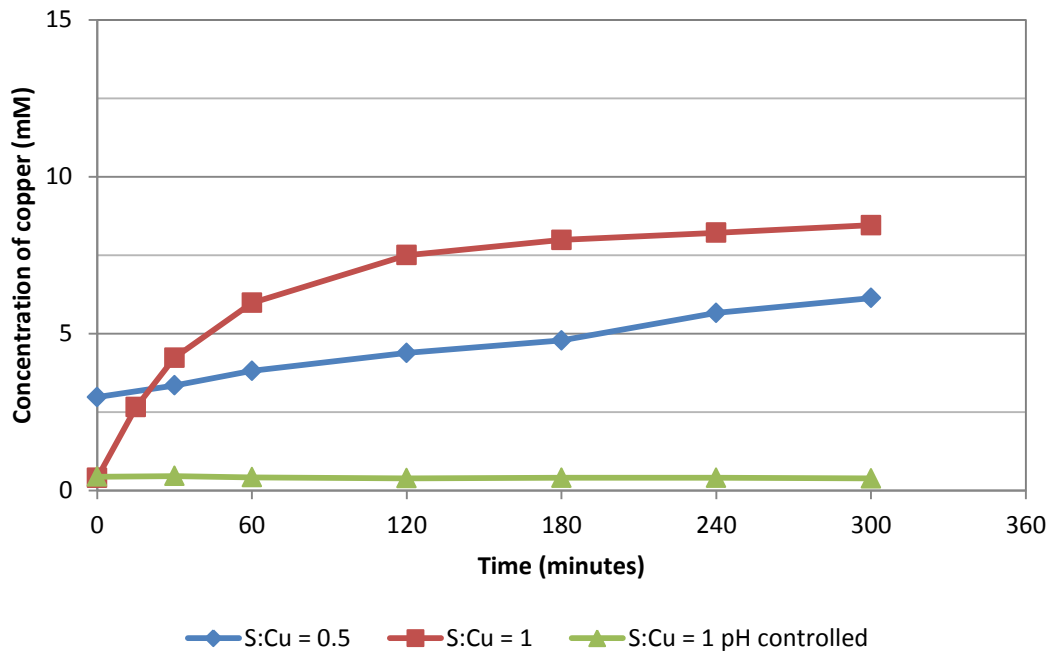
#### **7.4.3 Effect of sulfide dosing**

The effect of sulfide dosing on Telfer SART solutions was determined by running three experiments using both the Telfer SART feed and Telfer sulfide. The first two experiments were performed at S:Cu ratios of 0.5 and 1.0 respectively, with no control of pH once the initial acidification target pH (4.5) was achieved. Figure 7.4 shows the pH during the two non pH controlled experiments. The pH increased in both experiments over the first three hours before stabilising for the remainder of the experiment. As the pH of the experiment with a S:Cu ratio of 1.0 increased above 6, copper re-dissolution will occur due to a reverse in the primary sulfidisation reaction (Equation 1.3) as shown in Section 4.2.2. For this reason, a repeat of the experiment where the S:Cu ratio is 1.0 was performed with pH maintained at 4.5.



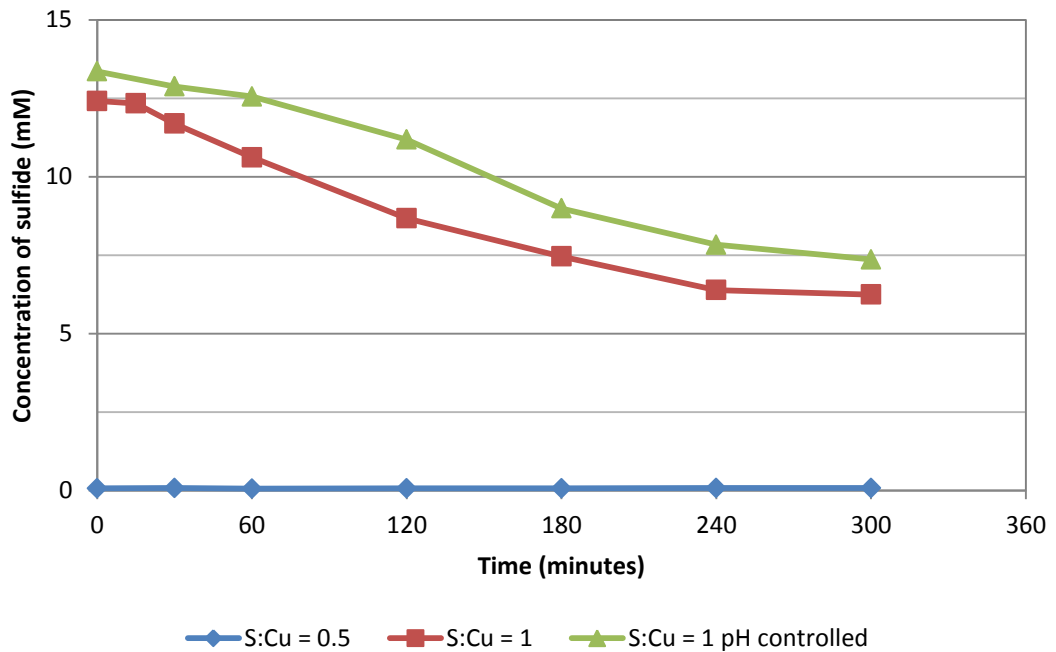
**Figure 7.4 Solution pH over time for Telfer SART feed and Telfer sulfide at different S:Cu ratios.**

Figure 7.5 shows the copper concentration in solution over time for the three experiments. The largest change in copper concentration happens for the S:Cu ratio of 1.0 when pH is not controlled. This can be attributed to the large pH change in that experiment as compared to the pH controlled experiment where the copper concentration in solution does not change. For the S:Cu ratio of 0.5, copper in solution also increases over time. The pH increase in the S:Cu ratio of 0.5 experiment (Figure 7.4) may explain a small amount of copper redissolution due to reversal of Equation 1.3. Nevertheless, the amount of copper redissolution (9.2%) cannot be explained solely by this mechanism as the pH only reaches 5.6, where high copper recoveries can still be expected (Section 4.2.2 and Section 4.3.3).



**Figure 7.5 Copper concentration over time for Telfer SART feed and Telfer sulfide at different S:Cu ratios.**

Figure 7.6 shows the soluble sulfide concentration for the three experiments. When there is excess sulfide in solution (S:Cu ratio of 1.0) the sulfide concentration decreases over time by a similar rate, whether the pH is controlled or not. There is, however, a slightly slower rate of sulfide consumption initially (30 min) when the pH is not controlled. This is due to sulfide released into solution as the pH increases in the non pH controlled experiment (reverse of Equation 1.3). As expected, little sulfide was detected in the S:Cu ratio of 0.5 experiment, verifying that copper redissolution in that experiment (Figure 7.5) is not caused by reversal of Equation 1.3.



**Figure 7.6 Sulfide concentration over time for Telfer SART feed and Telfer sulfide at different S:Cu ratios.**

The copper concentration, sulfide concentration, and pH change over time for the S:Cu ratio of 0.5 experiment and S:Cu ratio of 1.0 experiment when under pH control show the same trends to the results of the plant surveys. Nonetheless, the pH change seen in laboratory experiments was greater than that seen during the plant surveys. Except for these large pH increases, the trends in change of species concentration between the survey and laboratory data suggest that the plant survey results are indeed caused by residence time and not process fluctuations.

Changes in thiocyanate concentration were within experimental error. This is due to the large amount of thiocyanate in the Telfer solutions making detection of small concentration changes difficult to quantify. This problem also occurred in the surveys of the Telfer SART plant.

#### **7.4.4 Effect of oxygen**

While the plant surveys and laboratory work with Telfer solutions clearly show that residence time affects Telfer solutions, the results thus far do not show if the observations are caused by oxidation of the SART precipitate as seen in Chapter 6. Hence, the previous three experiments (Section 7.4.3) were repeated with an oxygenated headspace in the reactor to determine if oxidation is the cause of the concentration changes observed with the Telfer solutions.

##### **7.4.4.1 Sulfide to copper molar ratio of 0.5**

Figure 7.7 shows the pH for the air and oxygen headspace experiments using Telfer SART feed and Telfer sulfide when S:Cu ratio is 0.5. It is apparent that the change in pH is less for the oxygen headspace experiment compared to the air headspace. Little redissolution of the precipitate due to the reversal of Equation 1.3 is expected to occur in these experiments as the pH remained below 6, where high copper recovery is expected to occur (Section 4.2.2). Interestingly, the pH change seen in the oxygen rich experiment is also closer to that seen in the plant survey.

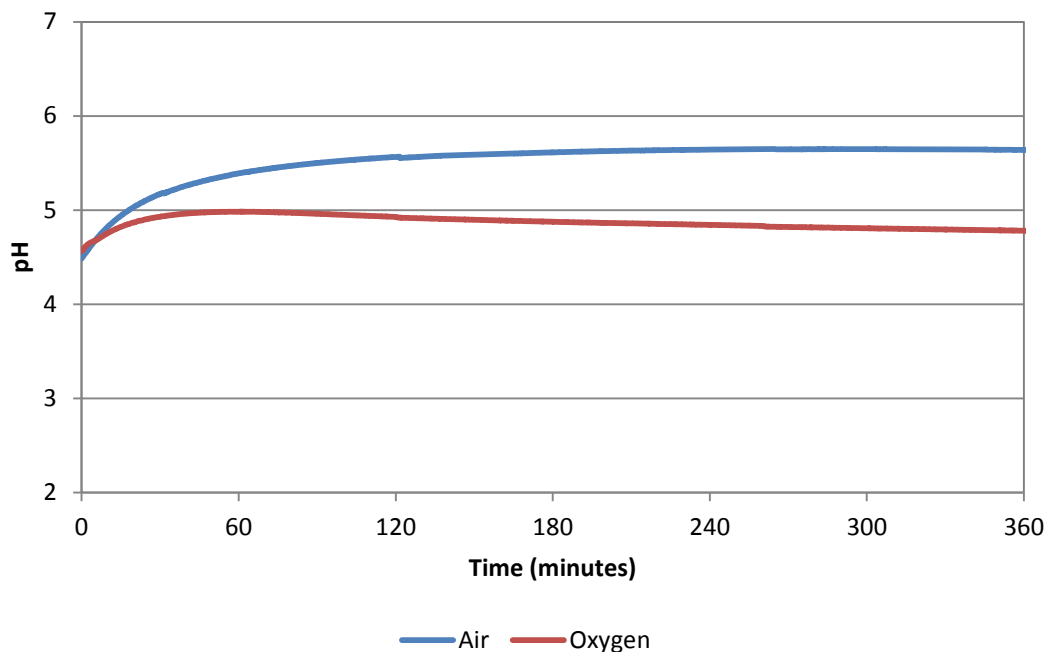


**Figure 7.7 Solution pH over time for Telfer SART feed and Telfer sulfide at an S:Cu ratio of 0.5 and with different headspace gas.**

Figure 7.8 shows the copper concentration in solution for both the air headspace and oxygen rich headspace when performing sulfidisation using the Telfer SART feed and Telfer sulfide at a S:Cu ratio of 0.5. The redissolution of copper occurs at a faster rate with an oxygen headspace than it does with an air headspace. This shows that redissolution of copper in the Telfer solutions is caused by oxidation of the precipitate over time, as was seen in sulfidisation of copper cyanide solutions in Chapter 6. For both experiments, there was little sulfide detected in solution at any time.

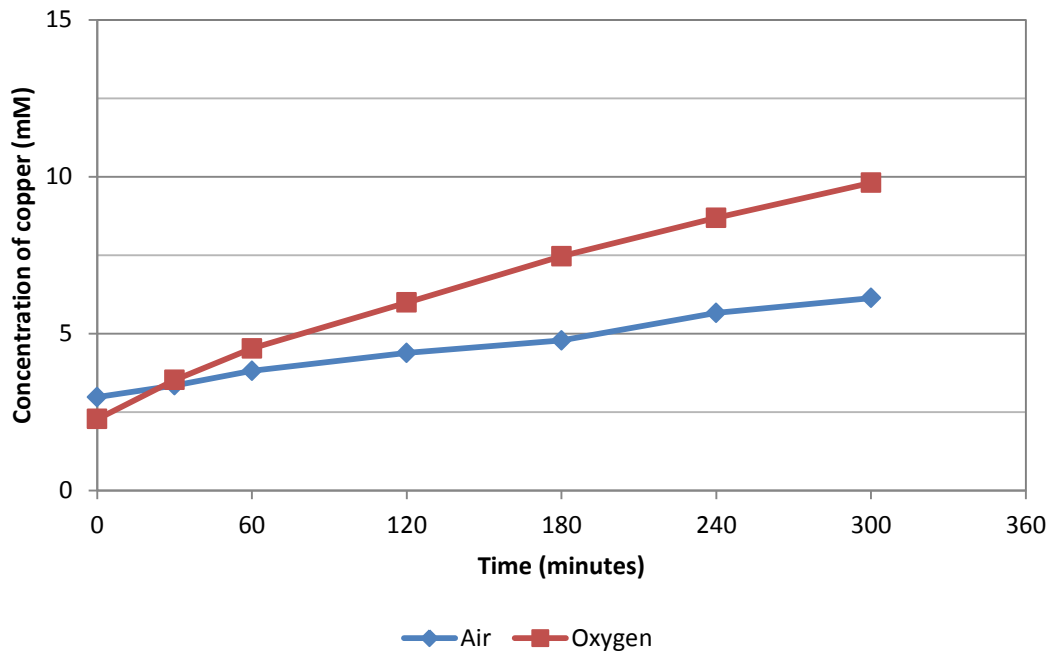
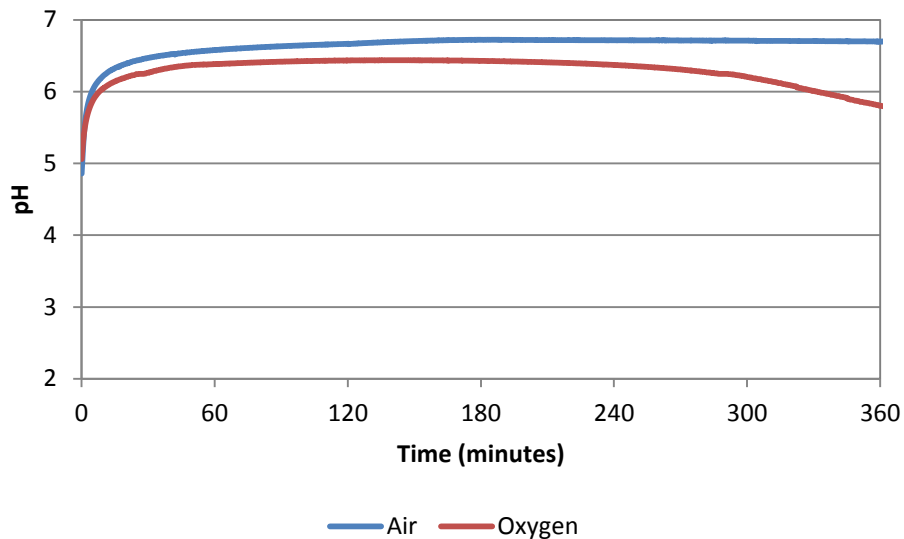


Figure 7.8 Copper concentration in solution over time for Telfer SART feed and sulfide at an S:Cu ratio of 0.5 and with different headspace gas.

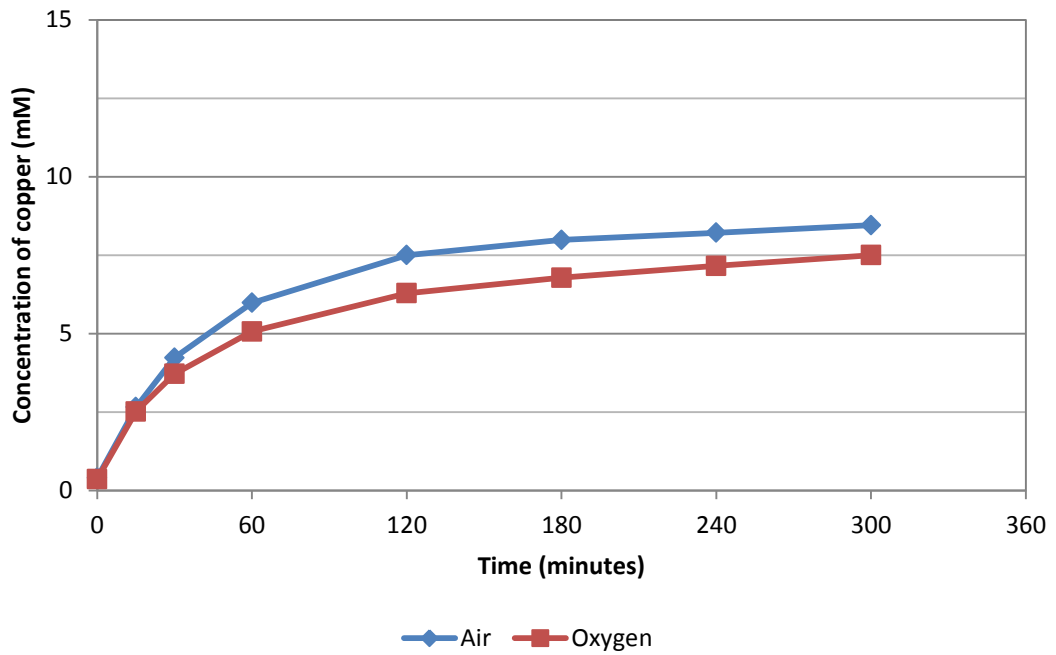
#### 7.4.4.2 Sulfide to copper molar ratio of 1.0 with no pH control

Figure 7.9 shows the pH of the solution for both the air headspace and oxygen rich headspace when S:Cu ratio is 1.0 using Telfer SART feed and sulfide. As with the S:Cu ratio of 0.5, the pH change in the oxygen rich headspace experiment increased less than seen in the air headspace. The pH change, however, rises above pH 6 for both experiments and therefore high copper recoveries cannot be expected due to the reversal of the primary sulfidation equation (Equation 1.3) as discussed previously in Section 7.4.3. Notably, the pH in the oxygen rich system begins to decrease towards the end of the experiment and may explain why at longer residence times, such as in the Telfer SART thickener, a large pH change was not observed.



**Figure 7.9 Solution pH over time for Telfer SART feed and Telfer sulfide at an S:Cu ratio of 1.0, an initial pH of 4.5, and with different headspace gas.**

The copper concentration over time for air and oxygen headspace experiments, when mixing the Telfer SART feed and Telfer sulfide at a S:Cu ratio of 1.0, is shown in Figure 7.10. Copper redissolution occurs at a similar rate in both experiments. This verified that the redissolution of copper is being caused largely by reversal of Equation 1.3 due to the pH rising rather than precipitate oxidation.



**Figure 7.10** Copper concentration in solution over time for Telfer SART feed and Telfer sulfide at an S:Cu ratio of 1.0, an initial pH of 4.5, and with different headspace gas.

Figure 7.11 shows the sulfide concentration in solution over time for the air and oxygen headspace experiments when mixing Telfer SART feed and Telfer sulfide at a S:Cu ratio is 1.0. It is apparent that, the rate at which sulfide was consumed in solution is faster in the oxygen headspace compared to the air headspace. The increased sulfide consumption in the oxygenated headspace experiment again verifies that oxidation of the precipitate is occurring, in this case causing sulfide consumption over time. This result is the same as observed when excess sulfide was present in sulfidisation investigations with copper cyanide solutions (Section 6.3.3.1 and Section 6.3.5.1).

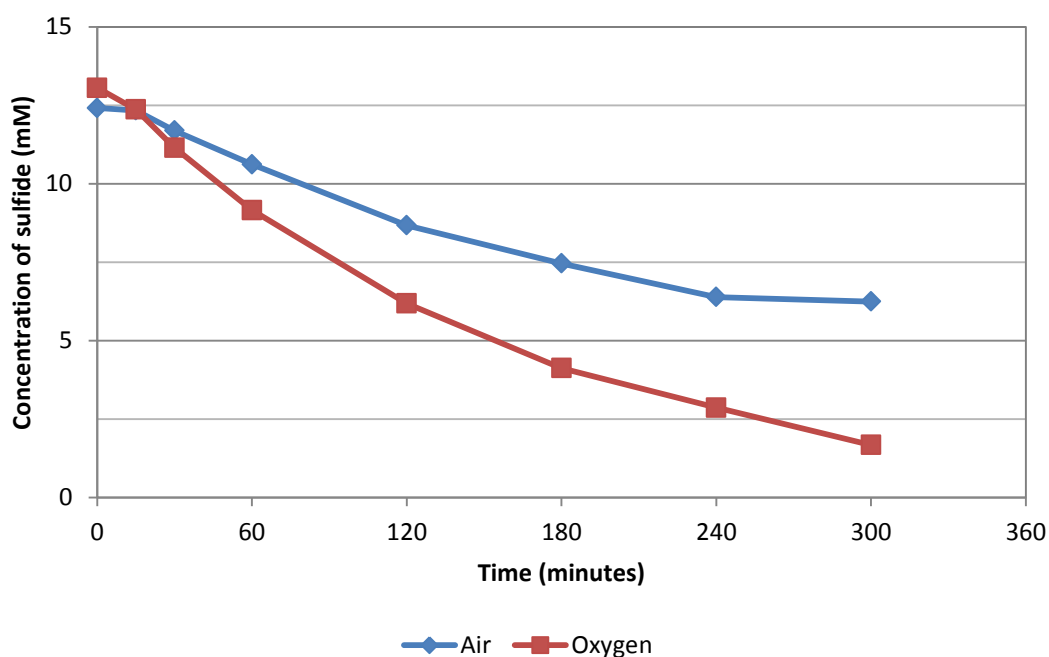


Figure 7.11 Sulfide concentration in solution over time for Telfer SART feed and Telfer sulfide at an S:Cu ratio of 1.0, an initial pH of 4.5, and with different headspace gas.

#### 7.4.4.3 Sulfide to copper molar ratio of 1.0 with pH control

Figure 7.12 shows the sulfide concentration in solution for the Telfer SART feed and Telfer sulfide experiment when S:Cu ratio is 1.0 and pH is held at 4.5. Once again, it is apparent that consumption of sulfide over time is faster in the oxygen headspace compared to the air headspace, reaffirming that oxidation is the cause of sulfide loss from the Telfer solutions.

The copper concentration in solution for the Telfer SART feed and Telfer sulfide is shown in Figure 7.13. No copper redissolution (Section 7.4.4.2) or oxidation (Section 7.4.4.1) was observed in the air headspace experiment as the pH was controlled and not all sulfide was consumed. For the oxygen headspace experiment, copper redissolution began towards the end of the experiment due to oxidation (Section 7.4.4.1).

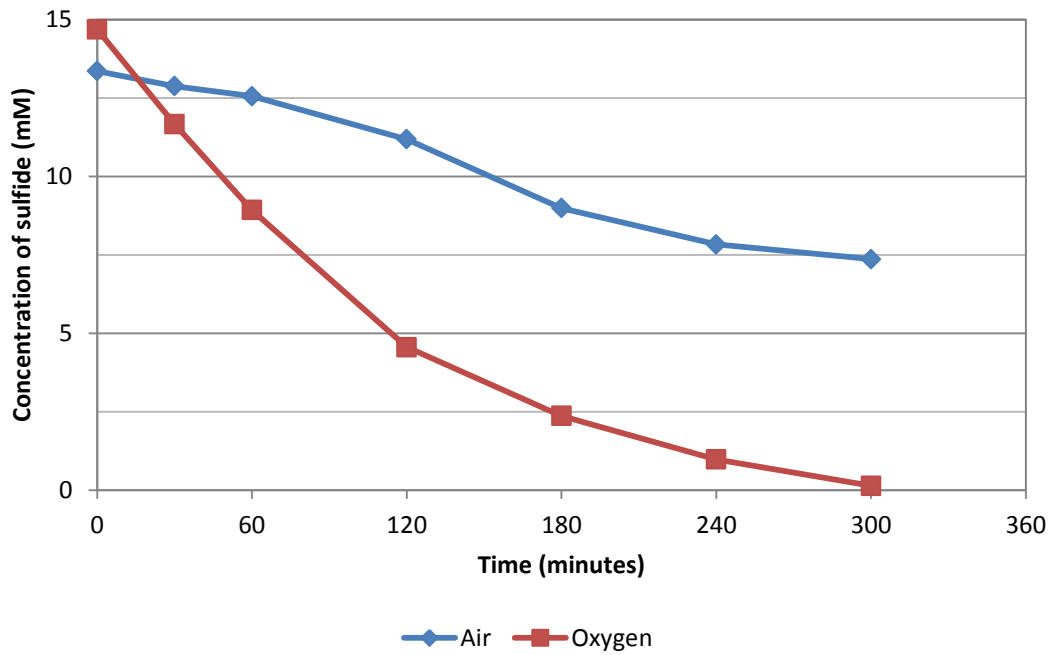


Figure 7.12 Sulfide concentration in solution over time for Telfer SART feed and sulfide at an S:Cu ratio of 1.0 with pH controlled at 4.5 and with different headspace gas.

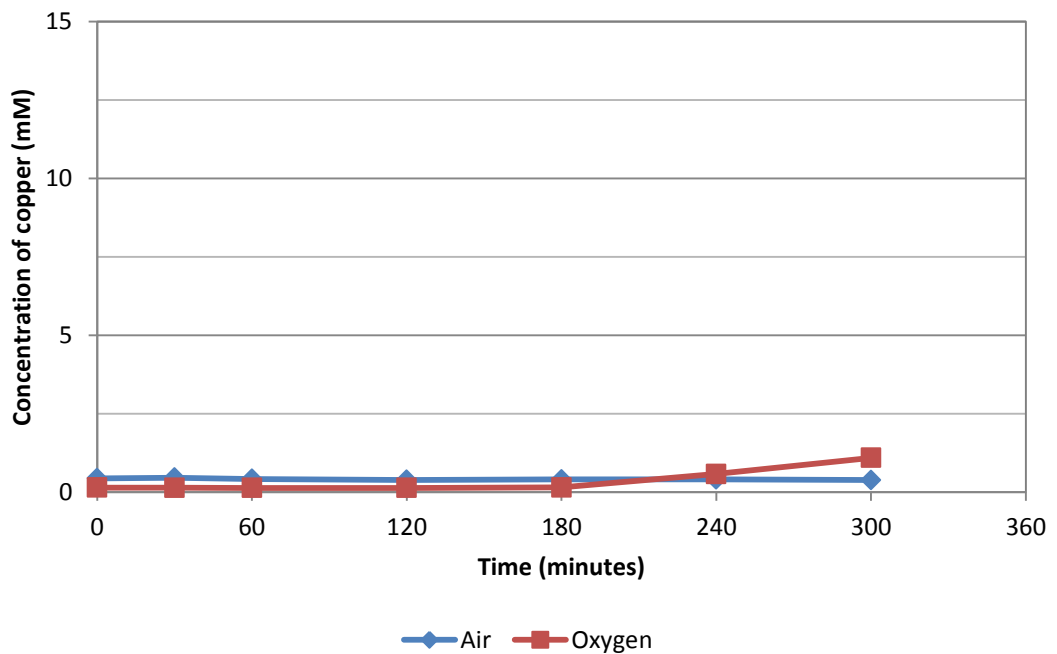


Figure 7.13 Copper concentration in solution over time for Telfer SART feed and sulfide at an S:Cu ratio of 1.0 with pH controlled at 4.5 and with different headspace gas.

#### **7.4.5 Discussion on oxidation in Telfer solutions**

The experiments with oxygenated headspace show that oxygen increases the rate of sulfide consumption or copper redissolution depending on the S:Cu ratio of the initial solution. Hence, it is apparent that the precipitate produced using Telfer SART feed and sulfide undergoes oxidation over time as seen in the synthetic copper cyanide sulfidisation experiments of Chapter 6.

The experiments using the Telfer solution all had increases in pH over time. This was not expected based on sulfidisation of synthetic copper cyanide solutions (Chapter 6), where the pH either remained constant (S:Cu > 0.5) or decreased over time (S:Cu ≤ 0.5). In any case, the pH response of the experiments with Telfer solutions are similar to the results of the plant surveys, which showed either no pH change at an S:Cu ratio near 0.5 (Section 7.3.4.2) or an increase in pH over time when S:Cu ratio was high (Section 7.3.4.3). Interestingly, the pH changes in the experiments with oxygenated headspaces were more closely related to the survey pH changes for similar S:Cu ratios.

It is important to note that, while oxygen does increase the rate of copper redissolution, this does not suggest that oxygen is the sole reason for the redissolution of copper at the Telfer SART plant. As the surface area to volume ratio of the large reactor (8.85 m<sup>-1</sup>) is far larger than that of the Telfer thickener (0.38 m<sup>-1</sup>), oxygen transfer will be significantly greater at the laboratory scale. Although this does not rule out oxygen as an oxidant source in the Telfer thickener, it was considered necessary to determine if the Telfer solution intrinsically has more potential for this oxidation reaction to occur compared to synthetic copper cyanide solutions. Further, such experiments could also determine if the different pH change over time, when using the

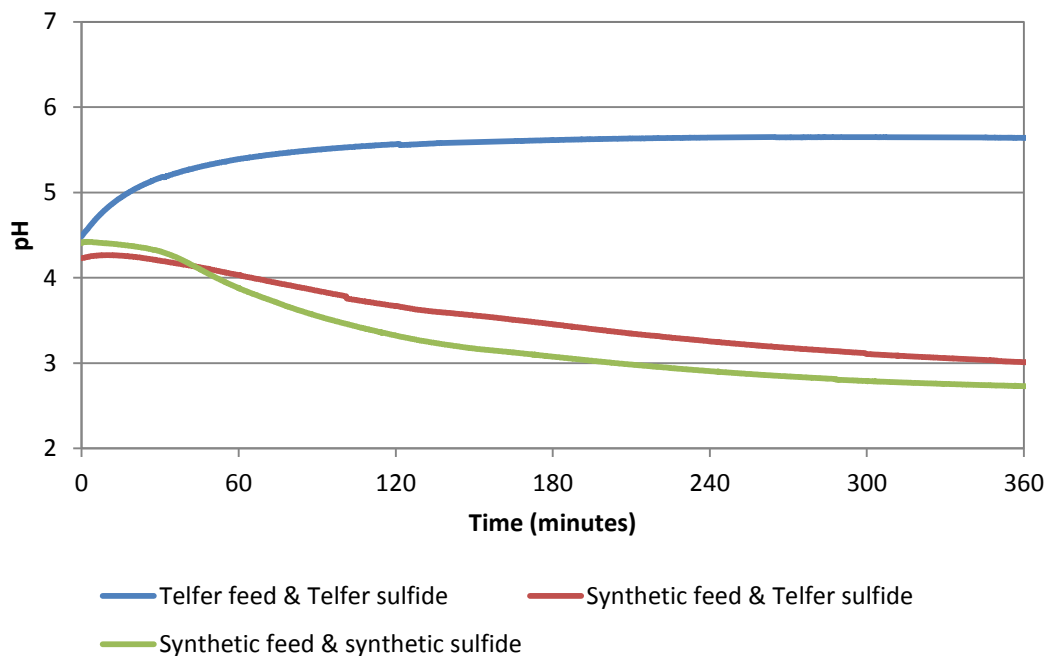
Telfer solutions compared to synthetic solutions (Chapter 6), is caused by the copper and cyanide concentrations of the Telfer SART feed or some other feature of the solution composition.

#### **7.4.6 Comparison to synthetic solution experiments**

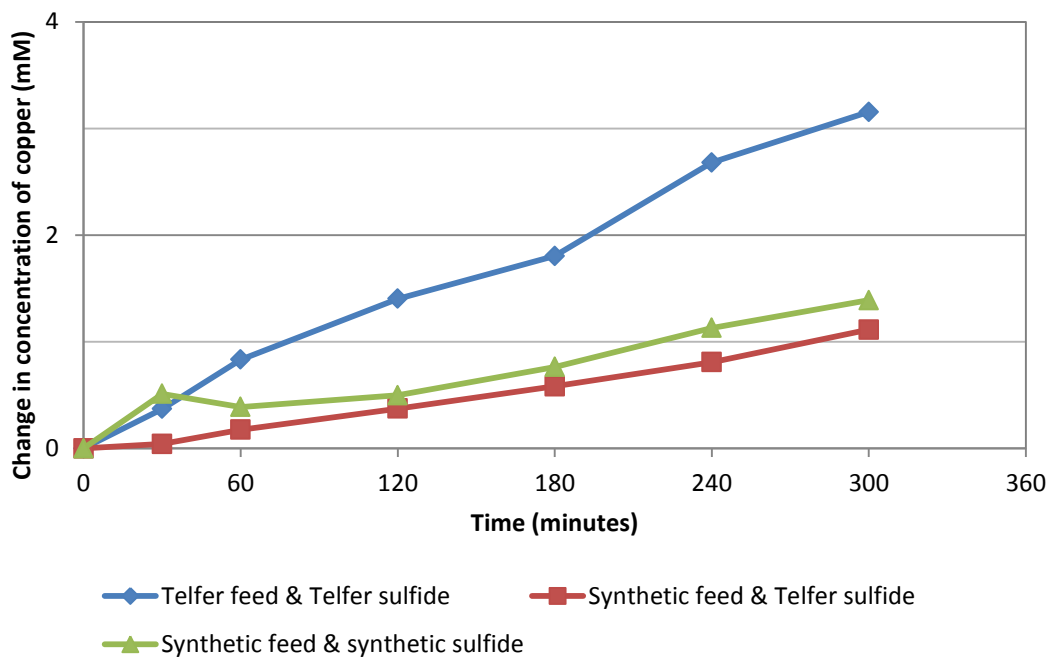
To determine if copper redissolution using Telfer SART feed occurs at the same rate as that of a synthetic copper cyanide solution of similar copper and cyanide concentration, a set of experiments were run with a comparable synthetic SART feed solution. These experiments will also show if the difference in pH change in the Telfer solution experiments compared to synthetic copper cyanide solution experiments of Chapter 6 is caused by the copper and cyanide concentration or some other feature of the Telfer solution. Copper (33.8 mM) and cyanide (78.1 mM) concentrations were the same in synthetic SART feed as that seen in the Telfer SART feed solution. Two experiments at a S:Cu ratio of 0.5 were then performed, one with the Telfer sulfide and one with sulfide prepared in the laboratory (Section 3.1.3). The results of these experiments were then compared to the experiment using Telfer SART feed and Telfer sulfide.

Figure 7.14 shows the pH over time for the Telfer SART feed with Telfer sulfide, the synthetic SART feed with Telfer sulfide, and the synthetic SART feed with synthetic sulfide, all at a S:Cu ratio of 0.5 and in an air headspace. It is clear from Figure 7.14 that the pH response over time for the Telfer SART feed solution experiment was very different from that of the synthetic SART feed solution experiments. Although there is a slight variation in the two synthetic SART feed experiments pH change, the trend is the same. These results suggest that there are other species present in the Telfer SART feed solution that are not present in the synthetic solutions which may be affecting the solution pH change over time.

The change in copper concentration over time for the Telfer SART feed with Telfer sulfide, the synthetic SART feed with Telfer sulfide, and the synthetic SART feed with synthetic sulfide all at a S:Cu ratio of 0.5 and in an air headspace are shown in Figure 7.15. The results show that, for both synthetic SART feed experiments, the rate of copper redissolution is less than that seen in the Telfer SART feed. As both the synthetic SART feed solutions had similar pH change and copper redissolution rates, it appears that the sodium sulfide used at Telfer has no impact on precipitate oxidation rate compared to the synthetic sulfide.



**Figure 7.14 Solution pH over time for various solution mixtures at a S:Cu ratio of 0.5 and initial pH of 4.5.**



**Figure 7.15** Change in copper concentration over time for various solution mixtures at a S:Cu ratio of 0.5 and initial pH of 4.5.

As the two synthetic SART feed experiments contained no thiocyanate initially, it was possible to determine the generation of thiocyanate over time in the experiments. A thiocyanate concentration increase of 0.33 mM was detected with the synthetic SART feed and Telfer sulfide over five hours. An increase of 0.26 mM was detected in the synthetic SART feed and sulfide experiment. This small generation of thiocyanate over time shows why thiocyanate changes were not detectable in the Telfer solutions due to the high initial thiocyanate concentrations (35.7 mM) masking the effect.

There are a number of possibilities which may explain the increased rate of dissolution seen when using the Telfer SART feed solution compared to the synthetic SART feed solution. First, the Telfer SART feed may contain other species which can act as an oxidant and hence increase the redissolution rate. Second, as other species in the feed solution can potentially become entrained in the precipitate (Chapter 5), there is a possibility that the crystal

lattice of the Telfer solution precipitate is different to that of the synthetic solution precipitate. This could result in an enhanced redissolution rate like that seen in the experiments. Finally, there may be a possibility that the increased redissolution rate in the Telfer SART feed is caused by a synergistic effect between the Telfer SART feed and sulfide solutions.

#### **7.4.7 Effect of impurities**

As the Telfer SART feed had a higher rate of copper redissolution compared to the synthetic SART feed, it is possible that some other species in the Telfer solution are contributing to the increased copper redissolution rate. The Telfer SART feed contained significant quantities of thiosulfate (3.5 mM) and thiocyanate (35.7 mM). Hence, the impact of these two species on the rate of copper redissolution was investigated to determine if they are the cause of the high redissolution rate seen in the Telfer solutions.

##### **7.4.7.1 Thiosulfate**

Figure 7.16 shows the change in copper concentration over time during sulfidisation of two synthetic SART feed solutions with an initial pH of 4.5, a S:Cu ratio of 0.5, and one solution containing 18 mM of thiosulfate. The thiosulfate concentration was selected so any impact thiosulfate has is clearly evident in the results. From Figure 7.16, it is apparent that thiosulfate has no impact on copper redissolution over time. Also, the thiosulfate concentration in solution did not change during the experiment. Thiocyanate generation (0.76 mM over 5 hours) was, however, higher than that seen in the same experiment without thiosulfate (0.26 mM over 5 hours). This is likely related to some thiosulfate reacting with cyanide to form thiocyanate. The solution pH for the experiment with thiosulfate did change by slightly less over time, but this appears to have no impact on copper redissolution.

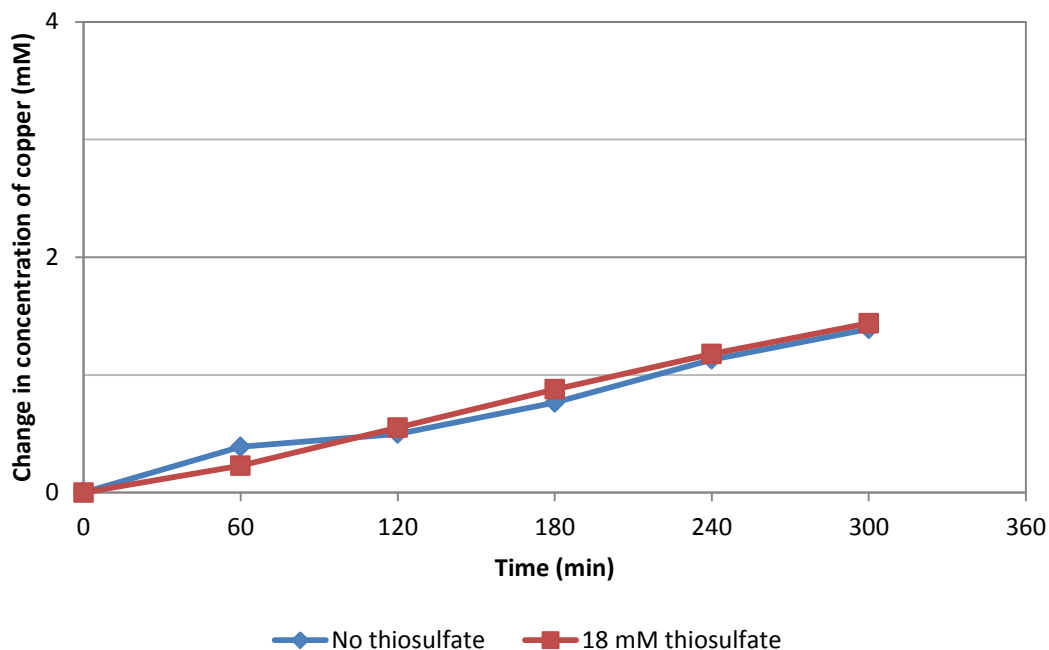


**Figure 7.16 Change in copper concentration over time for sulfidisation of a solution initially containing 33.8 mM copper solution with a CN:Cu ratio of 2.3, S:Cu ratio of 0.5, initial pH target of 4.5, and varied amounts of thiosulfate.**

#### 7.4.7.2 Thiocyanate

The impact of 15 mM thiocyanate on copper concentration in solution for the synthetic SART feed solution at an initial pH of 4.5 and with an S:Cu ratio of 0.5 is shown in Figure 7.17. As with thiosulfate, it is clear that thiocyanate has no impact on the rate of dissolution of copper from the precipitate. Thiocyanate generation was not detected due to the large thiocyanate concentration masking any effect as discussed at the end of Section 7.4.3. The change in pH over time was consistent between the solutions with and without thiocyanate.

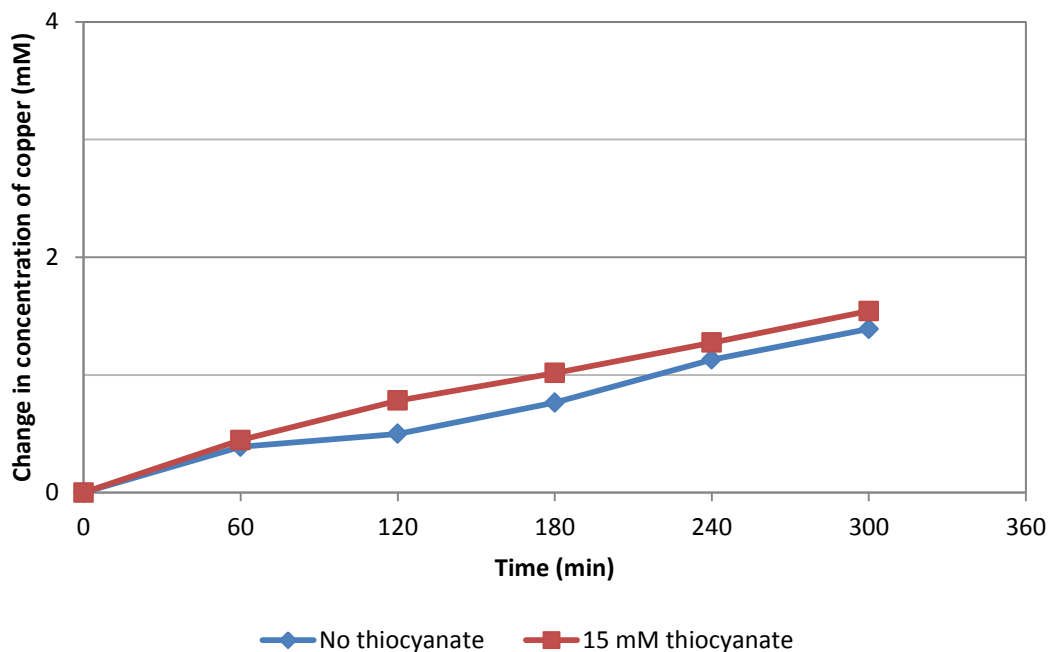


**Figure 7.17 Change in copper concentration over time for sulfidisation of a solution initially containing 33.8 mM copper solution with a CN:Cu ratio of 2.3, S:Cu ratio of 0.5, initial pH target of 4.5, and varied amounts of thiocyanate.**

## 7.5 Conclusions

The results of the plant survey and associated laboratory work show that, like with synthetic copper cyanide solutions (Chapter 6), under sulfidisation conditions oxidation of the sulfidisation precipitate occurs with Telfer solutions. This oxidation results in copper from the copper sulfide precipitate redissolving over time when no excess sulfide is present in solution. If excess sulfide is present, then copper does not redissolve, but the excess sulfide is consumed over time.

Interestingly, while copper and sulfide concentrations in solution have similar trends when comparing the Telfer SART solutions and synthetic copper cyanide solutions, the pH response is different. Specifically, the pH of the Telfer solution goes up over time whereas in the synthetic solution pH

either does not change ( $S:Cu > 0.5$ ) or decreases ( $S:Cu < 0.5$ ). What is also intriguing is that when excess sulfide is present, the increase in pH for the Telfer solutions are far more pronounced compared to when excess sulfide is not present in solution. As this change in pH is occurring at both the Telfer plant and in laboratory work with Telfer solutions, the cause must be a feature of the Telfer solution composition.

The results also show that sulfidisation precipitates generated with the Telfer SART feed solution have a faster rate of oxidation than synthetic copper cyanide solutions of the same concentrations as the Telfer SART feed. It was found that neither thiosulfate nor thiocyanate causes this increased copper redissolution rate for the Telfer solutions. There are several possibilities as to why this occurs for Telfer solutions including other oxidants in solution, differences in crystal structure due to impurity co-precipitation, or synergistic effects between Telfer SART feed and sulfide solutions.

## **8 CONCLUSIONS AND RECOMMENDATIONS**

### **8.1 Conclusions**

This study has developed knowledge in the area of sulfidisation for cyanide and copper recovery from gold cyanidation tailings. In particular, the process chemistry has been modelled so the optimum operating conditions could be determined, the impact of various impurities has been elucidated, and the research has resulted in the discovery and verification of the cause of poor performance for some industrial sulfidisation processes.

The impact of various process variables on sulfidisation in cyanide solutions was studied and the optimum operating conditions determined. Table 8-1 shows the S:Cu ratio, CN:Cu ratio, and pH which give the maximum copper recovery, maximum cyanide recovery, and minimum acid addition / initial copper concentration. Due to the responses having different optimums, an economic model was also created to show the optimum S:Cu ratio, CN:Cu ratio, and pH to maximise profit for a range of reagent cost and product value scenarios. This is also shown in Table 8-1. It was found that, within the reagent cost and product value ranges selected, the economic model optimum did not vary.

**Table 8-1 S:Cu ratio, CN:Cu ratio, and pH which give the optimum value for various responses during sulfidisation of copper cyanide solutions.**

<b>Response</b>	<b>Optimum type</b>	<b>S:Cu ratio</b>	<b>CN:Cu ratio</b>	<b>pH</b>
Copper recovery	Maximum	0.6	3	4
Cyanide recovery	Maximum	0.55-0.6	5	4
Acid addition / initial copper concentration	Minimum	0.4	3	5.5
<b>Economic model</b>	<b>Maximum</b>	<b>0.56</b>	<b>4</b>	<b>4</b>

Sensitivity analysis of the economic model showed that, when S:Cu ratio or CN:Cu ratio are not kept at their optimum values, profit can drop significantly. Hence, S:Cu ratio and CN:Cu ratio should be rigorously controlled during the industrial operation of a sulfidisation process. It should be noted that the CN:Cu ratio for optimum copper recovery is three. This value, however, would be detrimental to upstream processing for conventional gold cyanidation processes. Hence, a balance must be struck where CN:Cu ratio is minimised, to maximise sulfidisation profit, while not having a negative impact on upstream processes. For this reason, the ratio of four was selected as an optimum for a typical gold cyanidation process. The pH had a minor effect on profit compared to S:Cu ratio and CN:Cu ratio when operating at sub optimal conditions.

The presence of various impurities on sulfidisation of copper cyanide solutions showed a range of different impacts. Most interesting was that, whenever any metal precipitated, there was co-precipitation or adsorption occurring which resulted in recoveries of the other metals in solution. The amount of co-precipitation / adsorption increases with sulfide dosing; hence, sulfide overdosing should be limited if separation of metals is required. All of the impurities tested responded in different ways except for nickel, thiosulfate, and thiocyanate which exhibited no response.

Silver is selectively recoverable from all other metals tested as silver sulfide at a pH of 10 provided sulfide is not overdosed. It is also precipitated preferentially to all other metals tested over the entire pH range tested (pH 10 to 2).

Slight gold precipitation (< 30%) as gold sulfide occurs at low pH (< 3.5) and when excess sulfide is present. Hence, selective recovery of copper without recovering gold is viable provided pH is controlled above 3.5 and sulfide addition is stoichiometric to copper. This is beneficial when sulfidisation to recover copper is used before recovery of gold from solution. In the mixed metal experiments, gold precipitated between pH five and three depending on the amount of sulfide available, with gold recovery between 52.5% and 95.3% at pH 3 for different sulfide dosing. It is likely that this is due to a gold silver sulfide forming. The results suggest that gold recovery may be viable in some systems and its precipitation or rejection from the precipitate would need to be tested for each system. In some circumstances, tight control of pH and sulfide addition may be required to obtain the desired gold result.

Zinc is selectively recoverable from copper as a zinc sulfide at pH values around seven and above. If not recovered, zinc sulfide will redissolve as zinc

ions and aqueous dihydrogen sulfide as the pH is reduced below five. The presence of excess sulfide will aid in preventing zinc redissolution if desired. Zinc is also separable from silver as silver sulfide precipitates preferentially to zinc sulfide.

Iron (II) and iron (III) can both form copper iron cyanide precipitates below pH five. The precipitation of copper sulfide, however, occurs preferentially. The presence of iron causes increased acid consumption at low pH (< 4), likely due to the formation of protonated iron cyanide species. Hence, careful control of pH may be required when iron is present to limit unnecessary acid consumption. Iron also forms zinc iron cyanide precipitates at pH values less than eight when zinc is not precipitated as a sulfide and at low pH values (< 5) when zinc sulfide redissolves. Iron may also be forming other precipitates below pH four, although their nature was not determined.

The presence of chloride caused a reduction in the pH at which copper precipitation begins during sulfidisation. Nonetheless, the copper recovery was high for the usual sulfidisation operating conditions. Some co-precipitation / adsorption of chloride occurred which may impact the way sulfidisation is operated when integrated with a resin recovery process.

Ultimately, selective recovery of copper from other metals in cyanide solutions is achievable, but would require tight control of pH and sulfide addition during sulfidisation. It should also be noted that, while the pH values determined show when the various metals precipitate, slight variation may occur with concentration changes of the metals and cyanide in solution. Hence, the ranges shown in this research only serve as a guide to precipitation ranges and specific systems should be studied separately to determine exact precipitation ranges for metals in that system.

One of the most significant results from the research is the discovery that copper sulfide formed during sulfidisation of cyanide solutions undergoes oxidation. This oxidation reaction causes a transformation of the precipitate formed from roxbyite ( $\text{Cu}_7\text{S}_4$ , which is similar to  $\text{Cu}_2\text{S}$ ) to covellite ( $\text{CuS}$ ) over time. The reaction also results in copper redissolution and acid generation. Redissolution of copper ultimately causes a drop in copper and cyanide recovery during sulfidisation. A proposed equation for the reaction, which is similar to acid leaching equations for chalcocite ( $\text{Cu}_2\text{S}$ ) with a complexing ligand, is shown in Equation 8.1.



The release of copper into solution and a drop in pH occurs only when excess sulfide is not present, but a change in the precipitate structure from roxbyite ( $\text{Cu}_7\text{S}_4$ , which is similar to  $\text{Cu}_2\text{S}$ ) to covellite ( $\text{CuS}$ ) is still observed. The lack of copper and acid generation in solution is likely due to excess sulfide reacting with copper generated from Equation 8.1, as per the primary sulfidisation equation (Equation 1.3). The combination of Equation 8.1 and Equation 1.3 yields Equation 8.2, which is consistent with the experimental results. While Equation 8.2 prevents a drop in copper and cyanide recovery, it results an increase in reagent consumption during sulfidisation.



The rate of reaction for the conversion of the sulfidisation precipitate from a structure similar to chalcocite to that of covellite depends largely on oxygen transfer. Comparatively, copper and cyanide concentration have no major effect on the reaction rate.

A secondary reaction also occurs which causes the generation of thiocyanate in solution over time. The generation of thiocyanate over time is potentially caused by oxidation of covellite. The thiocyanate generation rate is increased in the presence of oxygen, although to a far lesser extent than the reaction causing conversion of the precipitate from a structure similar to chalcocite to covellite. Copper and cyanide concentration have no major effect on the reaction rate for thiocyanate generation.

It was also found that, at low pH and when no excess sulfide was present, copper redissolution ceases due to the formation of a copper thiocyanate precipitate. The pH at which this occurs depends on the amount of aqueous hydrogen cyanide in solution with less cyanide causing the pH to be higher. The highest pH where this occurred was approximately 3.5.

Industrial plant surveys, along with laboratory work with industrial solutions, also show that oxidation of sulfidation precipitates occur on an industrial scale. As with the synthetic solutions, this results in copper redissolution from the precipitate when excess sulfide is not present and sulfide consumption when it is. The response of pH during the plant surveys and associated laboratory work were not the same as that seen with synthetic solutions. This suggests that the difference in pH response is a result of the industrial solution composition.

The most intriguing result from experimentation with industrial solutions is that the rate of oxidation of the precipitate is faster in the industrial solution than it is in the synthetic one. Further testing showed that neither thiosulfate nor thiocyanate in the industrial solution were the cause of this increase in redissolution rate.

The oxidation of the sulfidisation precipitate over time shows that it is critical to minimise the residence time during sulfidisation as to keep copper and cyanide recoveries high without increasing reagent additions. This discovery should be considered when designing sulfidisation processes for industrial use.

## **8.2 Recommendations for future research**

While this study has determined the process optimums, impact of impurities, and cause of high sulfide consumption on the industrial scale during sulfidisation of copper cyanide solutions, there were several interesting observations which require further investigation. These fall into two main areas.

Firstly, more work can be done in the study of how other metals respond during sulfidisation of cyanide solutions. Particularly the interaction of gold, silver, and sulfide needs to be explored in greater detail to determine the nature of the precipitates formed. The chemistry of iron cyanide complexes at low pH also requires further work to elucidate what precipitates iron can form at low pH.

Secondly, while this study has shown the cause of high sulfide consumption during sulfidisation, a more detailed fundamental study could be performed on the oxidation of copper sulfide with cyanide as a complexing agent. Specifically, the mechanism which causes thiocyanate to be generated over time needs to be elucidated. The reason why copper thiocyanate precipitates at low pH over time, rather than copper cyanide, also needs to be determined. Finally, the impact of impurities over time needs to be studied in an effort to determine why test work on industrial solutions showed faster oxidation rates than synthetic solutions.

## 9 REFERENCES

- Adams, M, R Lawrence, and M Bratty. 2008. "Biogenic sulphide for cyanide recycle and copper recovery in gold-copper ore processing." *Minerals Engineering* 21 (6): 509-517.
- Adams, M, and V Lloyd. 2008. "Cyanide recovery by tailings washing and pond stripping." *Minerals Engineering* 21 (6): 501-508.
- Adams, M D, and J H Kyle. 2000. "Precipitation of cyanide as  $\text{Cu}_2\text{Fe}(\text{CN})_6$  compounds from cyanidation and detoxification circuits." In *Minprex 2000, Carlton, Victoria*, 201-206. Australasian Institute of Mining and Metallurgy.
- Alonso-González, O, F Nava-Alonso, and A Uribe-Salas. 2009. "Copper removal from cyanide solutions by acidification." *Minerals Engineering* 22 (4): 324-329.
- Anderson, M J, and P J Whitcomb. 2005. *RSM Simplified*. New York: Productivity Press.
- Australian Government Bureau of Resources and Energy Economics. 2012. Resources and Energy Statistics 2011. Accessed 19/1/2012, <http://www.bree.gov.au>.
- Australian Government Department of Foreign Affairs and Trade. 2011. Australia Fact Sheet. Accessed 19/1/2012, <http://www.dfat.gov.au/index.html>.
- Aydiner, C, M Kobya, and E Demirbas. 2005. "Cyanide ions transport from aqueous solutions by using quaternary ammonium salts through bulk liquid membranes." *Desalination* 180 (1-3): 139-150.
- Bachiller, D, M Torre, M Rendueles, and M Díaz. 2004. "Cyanide recovery by ion exchange from gold ore waste effluents containing copper." *Minerals Engineering* 17 (6): 767-774.

- Barter, J, G Lane, D Mitchell, R Kelson, R Dunne, C Trang, and D Dreisinger. 2001. "Cyanide management by SART." In *Cyanide: Social, Industrial and Economic Aspects*, eds C A Young, L G Twidwell and C G Anderson, 549-562. Warrendale: Minerals, Metals & Materials Soc.
- Bas, D, and I H Boyaci. 2007. "Modeling and optimization I: Usability of response surface methodology." *Journal of Food Engineering* 78 (3): 836-845.
- Bezerra, M A, R E Santelli, E P Oliveira, L S Villar, and L A Escaleira. 2008. "Response surface methodology (RSM) as a tool for optimization in analytical chemistry." *Talanta* 76 (5): 965-977.
- Botz, M, and S Acar. 2007. "Copper precipitation and cyanide recovery pilot testing for the Newmont Yanacocha project" *SME Annual Meeting, Denver, Colorado*: SME.
- Botz, M M, and T Mudder. 1998. "Cyanide recovery for silver leaching operations application of CCD-AVR circuits" *Randol gold and silver forum '98, Denver, Colorado*: Randol International.
- Breuer, P L, M I Jeffrey, and D M Hewitt. 2008. "Mechanisms of sulfide ion oxidation during cyanidation. Part I: The effect of lead(II) ions." *Minerals Engineering* 21 (8): 579-586.
- Breuer, P L, C A Sutcliffe, and R L Meakin. 2011. "Cyanide measurement by silver nitrate titration: Comparison of rhodanine and potentiometric end-points." *Hydrometallurgy* 106 (3-4): 135-140.
- Dai, X, and P L Breuer. 2009. "Cyanide and copper cyanide recovery by activated carbon." *Minerals Engineering* 22 (5): 469-476.
- Dai, X, P L Breuer, and M I Jeffrey. 2010. "Comparison of activated carbon and ion-exchange resins in recovering copper from cyanide leach solutions." *Hydrometallurgy* 101 (1-2): 48-57.

- Dai, X, A Simons, and P Breuer. 2012. "A review of copper cyanide recovery technologies for the cyanidation of copper containing gold ores." *Minerals Engineering* 25 (1): 1-13.
- Demopoulos, G P. 2009. "Aqueous precipitation and crystallization for the production of particulate solids with desired properties." *Hydrometallurgy* 96 (3): 199-214.
- Derringer, G C, and R Suich. 1980. "Simultaneous Optimisation of Several Variables." *Journal of Quality Technology* 12: 214-219.
- DIONEX Corporation. 2008. *IonPac AS7 Product Manual*.
- Donato, D B, O Nichols, H Possingham, M Moore, P F Ricci, and B N Noller. 2007. "A critical review of the effects of gold cyanide-bearing tailings solutions on wildlife." *Environment International* 33 (7): 974-984.
- Dreisinger, D, J Vaughan, J Lu, B Wassink, and P West-Sells. 2008. "Treatment of the Carmacks copper-gold ore by acid leaching and cyanide leaching with SART recovery of copper and cyanide from barren cyanide solution" *Hydrometallurgy 2008, Phoenix, AZ, United states: Society for Mining, Metallurgy and Exploration*.
- Dreisinger, D B. 2000. Cyanide recovery from aqueous ore processing solutions by solvent extraction. WO200043558-A; EP1165847-A; WO200043558-A1; AU200022722-A; US6200545-B1; ZA200002323-A; EP1165847-A1; EP1165847-B1; DE60003017-E; ES2200814-T3; AU772784-B2; CA2310111-C, filed 27 July 2000.
- Dymov, I, C J Ferron, and C A Fleming. 1997. "Development of a novel cyanide recovery process for an oxidised gold/silver ore" *Randol gold forum '97, Monterey, California: Randol International*.
- Environment Australia. 2003. *Cyanide Management*. Canberra: Department of Environment.

- Estay, H, J Becker, P Carvajal, and F Arriagada. 2012. "Predicting HCN gas generation in the SART process." *Hydrometallurgy* 113–114 (0): 131-142.
- Fisher, W W. 1994. "Comparison of chalcocite dissolution in the sulfate, perchlorate, nitrate, chloride, ammonia, and cyanide systems." *Minerals Engineering* 7 (1): 99-103.
- Fisher, W W, F A Flores, and J A Henderson. 1992. "Comparison of chalcocite dissolution in the oxygenated, aqueous sulfate and chloride systems." *Minerals Engineering* 5 (7): 817-834.
- Fleming, C A. 2005. "Cyanide Recovery." In *Advances in Gold Ore Processing*, ed. M D Adams, 703 - 727. Amsterdam: Elsevier.
- Fleming, C A, and M J Nicol. 1984. "The absorption of gold cyanide onto activated carbon III. Factors influencing the rate of loading and equilibrium capacity." *Journal of South African Institute of Mining and Metallurgy* 84 (4): 85-93.
- Fleming, C A, and J A Thorpe. 2003. Process for recovering cyanide from copper-containing feed material. US2003205533-A1; US6919030-B2, filed 6 November 2003.
- Fleming, C A, and C V Trang. 1998. "Review of options for cyanide recovery at gold and silver mines" *Randol gold and silver forum '98, Denver, Colorado*: Randol International.
- Ford, K, C Fleming, and R Henderson. 2008. "Application of the SART process to heap leaching of gold-copper ores at Maricunga, Chile." In *40th Annual Meeting of the Canadian Mineral Processors, Ottawa, Canada*. CIM.
- Gönen, N, O S Kabasakal, and G Özdil. 2004. "Recovery of cyanide in gold leach waste solution by volatilization and absorption." *Journal of Hazardous Materials* 113 (1-3): 231-236.

- Goulsbra, A, R Dunne, G Lane, D Dreisinger, and S Hart. 2003. "Telfer Project process plant design" *Eighth Mill Operators' Conference, Proceedings - Evolution and survival in the minerals industry, Parkville Victoria*: Australasian Institute of Mining and Metallurgy.
- Guzman, G, V Mamani, H Arevalo, S Vicuna, L Vargas, and B Burger. 2010. "SART / AVR circuit design and operation at Yanacocha gold mill."
- Han, B, Z Shen, and S R Wickramasinghe. 2005. "Cyanide removal from industrial wastewaters using gas membranes." *Journal of Membrane Science* 257 (1-2): 171-181.
- Hewitt, D M, P L Breuer, M I Jeffrey, and F Naim. 2009. "Mechanisms of sulfide ion oxidation during cyanidation. Part II: Surface catalysis by pyrite." *Minerals Engineering* 22 (13): 1166-1172.
- International Cyanide Management Institute. 2012a. The Cyanide Code. <http://www.cyanidecode.org/about-cyanide-code/cyanide-code>.
- International Cyanide Management Institute. 2012b. Directory of Signatory Companies. <http://www.cyanidecode.org/signatory-companies/directory-of-signatory-companies>.
- Kratochvil, D, N Chan, and A Hall. 2013. "Integrating SART into metallurgical flowsheets for cyanide recovery" *ALTA 2013 Gold Proceedings, Perth, Australia*: ALTA Metallurgical Services.
- Laitos, J G. 2012. The Current Status of Cyanide Regulations Engineering and Mining Journal. <http://www.e-mj.com/index.php/features/1656-the-current-status-of-cyanide-regulations>.
- Lewis, A, and R van Hille. 2006. "An exploration into the sulphide precipitation method and its effect on metal sulphide removal." *Hydrometallurgy* 81 (3-4): 197-204.
- Lewis, A E. 2010. "Review of metal sulphide precipitation." *Hydrometallurgy* 104 (2): 222-234.

- Littlejohn, P, D Kratochvil, and A Hall. 2013. "Sulfidisation-Acidification-Recycling-Thickening (SART) for Complex Gold Ores." *World Gold 2013, Brisbane*: Australasian Institute of Mining and Metallurgy.
- Lorösch, J. 2001. "Cyanide Recycling and Detoxification." In *Process and Environmental Chemistry of Cyanidation*, 402. Frankfurt: Degussa.
- Lower, G W. 1965. Leaching of copper from ores with cyanide and recovery of copper from cyanide solutions. US 3189435, filed 1 December 1964.
- Lower, G W. 1968. Leaching of copper from ores with cyanide and recovery of copper from cyanide solutions. US 3403020, filed 14 December 1964.
- Lu, J, D B Dreisinger, and W C Cooper. 2002. "Thermodynamics of the aqueous copper-cyanide system." *Hydrometallurgy* 66 (1-3): 23-36.
- MacPhail, P K, C A Fleming, and K W Sarbutt. 1998. "Cyanide recovery by the SART process for the Lobo-Marte Project, Chile" *Randol gold and silver forum '98, Denver, Colorado*: Randol International.
- Marani, D, J W Patterson, and P R Anderson. 1995. "Alkaline precipitation and aging of Cu(II) in the presence of sulfate." *Water Research* 29 (5): 1317-1326.
- Marchant, B. 2008. "Converting water into gold." *Water and Wastewater International* 23: 13-14.
- Marsden, J O, and C I House. 2006a. "Chemical Equilibria." In *The Chemistry of Gold Extraction*, 114. Littleton, Colorado: Society for Mining, Metallurgy, and Exploration.
- Marsden, J O, and C I House. 2006b. "Historical Developments." In *The Chemistry of Gold Extraction*, 1-17. Littleton, Colorado: Society for Mining, Metallurgy, and Exploration.
- Marsden, J O, and C I House. 2006c. "Reagent and Metals Recovery." In *The Chemistry of Gold Extraction*, 473 - 482. Littleton, Colorado: Society for Mining, Metallurgy, and Exploration.

- Milosavljevic, E B, L R Solujic, and M E Kravetz. 2004. "Use of organo-sulfur reagents for recovery and recycle of silver, copper, zinc and cyanide from precious metals cyanidation effluents" *2004 SME Annual Meeting Preprints, Denver, CO, United states*: Society for Mining, Metallurgy and Exploration.
- Moritz, K. 1954. "Reductions and oxidations of iron-cyanogen compounds of copper." *Analytica Chimica Acta* 10 (0): 401-404.
- Mudder, T, and M Botz. 2001. "An overview of cyanide treatment and recovery methods." In *The Cyanide Monograph*, eds T Mudder and M Botz, 481-500. London: Mining Journal Books Ltd.
- Mudder, T, M Botz, and A Smith. 2001a. "Treatment and Recovery of Cyanide." In *Chemistry and Treatment of Cyanidation Wastes*, 239-368. London: Mining Journal Books Ltd.
- Mudder, T, M Botz, and A Smith. 2001b. "Analysis of Cyanides." In *Chemistry and Treatment of Cyanidation Wastes*, 29-72. London: Mining Journal Books Ltd.
- Mudder, T, and A Goldstone. 2001. "The recovery of cyanide from slurries." In *The Cyanide Monograph*, eds T Mudder and M Botz, 202-241. London: Mining Journal Books Ltd.
- Muir, D M. 2011. "A review of the selective leaching of gold from oxidised copper–gold ores with ammonia–cyanide and new insights for plant control and operation." *Minerals Engineering* 24 (6): 576-582.
- Mullin, J W. 2004. "Co-precipitation." In *Crystallization*, 326-328. Oxford ;Boston: Butterworth-Heinemann.
- Osadchii, E G, and O A Rappo. 2004. "Determination of standard thermodynamic properties of sulfides in the Ag-Au-S system by means of a solid-state galvanic cell." *American Mineralogist* 89: 1405-1410.

- Paul, R L. 1984. "The role of electrochemistry in the extraction of gold." *Journal of Electroanalytical Chemistry and Interfacial Electrochemistry* 168 (1-2): 147-162
- Potter, G M, A Bergmann, and U Haidlen. 1986. Process of recovering copper and optionally recovering silver and gold by leaching of oxide and sulfide containing materials with water soluble cyanides. EP135950-A1; GB2145402-A; EP135950-A; AU8432399-A; DE3330795-A; NO8403220-A; JP60070133-A; BR8404242-A; ES8505212-A; US4587110-A; ZA8406623-A; GB2145402-B; CA1225241-A; RO91171-A; EP135950-B; DE3471953-G, filed 8 August 1984.
- Puigdomenech, I. 2010. *MEDUSA: Make equilibrium diagrams using sophisticated algorithms*. Stockholm: Royal Institute of Technology.
- Riveros, P A, R Molnar, and F Basa. 1996. "Treatment of a high-cyanide waste solution for cyanide and metal recovery." *Cim Bulletin* 89 (998): 153-156.
- Riveros, P A, R E Molnar, and V M McNamara. 1993. "Alternative technology to decrease the environmental impact of gold milling - A progress report on CANMET research activities in this field." *Cim Bulletin* 86 (968): 167-171.
- Ronie, A, P Lamberg, J Mansikka-aho, P Björklund, J Kentala, T Talonen, T Kotiranta, R Ahlberg, A Gröhn, O Saarinen, J Myyri, J Sipilä, A Vartiainen. 2012. *HSC Chemistry 7*. Pori: Outotec.
- Sceresini, B. 2005. "Gold-copper ores." In *Advances in Gold Ore Processing*, ed. M D Adams, 789 - 824. Amsterdam: Elsevier.
- Sceresini, B, and P Richardson. 1991. *Development and application of a process for the recovery of copper and complexed cyanide from cyanidation slurries, Randol Gold Forum : Cairns '91*. Golden: Randol Int Ltd.

- Sceresini, B J. 1992. Base metals recovery by adsorption of cyano complexes on activated carbon. WO9208812-A1; AU9189453-A; BR9106985-A; US5427606-A; AU663475-B, filed 29 May 1992.
- Shen, Z, B Han, and S R Wickramasinghe. 2006. "Cyanide removal from industrial praziquantel wastewater using integrated coagulation-gas-filled membrane absorption." *Desalination* 195 (1-3): 40-50.
- Solis, J S, P M May, and G Hefter. 1996. "Cyanide thermodynamics. Part 4.- Enthalpies and entropies of cyanide complexation of Cu, Ag, Zn and Cd." *Journal of the Chemical Society, Faraday Transactions* 92 (4): 641-644.
- Stat-Ease Inc. 2011. *Design Expert* 8.
- Vapur, H, O Bayat, H Mordogan, and C Poole. 2005. "Effects of stripping parameters on cyanide recovery in silver leaching operations." *Hydrometallurgy* 77 (3-4): 279-286.
- Venter, D, S L Chryssoulis, and T Mulpeter. 2004. "Using mineralogy to optimize gold recovery by direct cyanidation." *JOM* 56 (8): 53-56.
- Wang, X, and K S E Forssberg. 1990. "The Chemistry of Cyanide-Metal Complexes in Relation to Hydrometallurgical Processes of Precious Metals." *Mineral Processing and Extractive Metallurgy Review: An International Journal* 6 (1-4): 81-125.
- World Gold Council. 2012a. Demand and supply statistics. [https://www.gold.org/investment/statistics/demand\\_and\\_supply\\_statistics/](https://www.gold.org/investment/statistics/demand_and_supply_statistics/).
- World Gold Council. 2012b. Gold Facts. <http://www.goldfacts.org/en/faqs/>.
- World Gold Council. 2012c. Interactive gold price chart. [http://www.gold.org/investment/statistics/gold\\_price\\_chart/](http://www.gold.org/investment/statistics/gold_price_chart/).
- Young, C A. 2001. "Remediation technologies for the management of aqueous cyanide species" In *Cyanide: Social, Industrial and Economic*

*Aspects*, eds C A Young, L G Twidwell and C G Anderson, 549-562.  
Warrendale: Minerals, Metals & Materials Soc.

Young, C A, E J Dahlgren, and R G Robins. 2003. "The solubility of copper sulfides under reducing conditions." *Hydrometallurgy* 68 (1-3): 23-31.

Every reasonable effort has been made to acknowledge the owners of copyright material. I would be pleased to hear from any copyright owner who has been omitted or incorrectly acknowledged.

## 10 APPENDICES

### 10.1 Thermodynamic data

This section details the thermodynamic data used throughout the thesis. Gibbs free energy data was taken from the sources in Table 10-1 and is shown in Table 10-2 through to Table 10-8. Table 10-9 shows explanatory note for species labels in MEDUSA diagrams. All thermodynamic data is consistent between the different sources.

**Table 10-1 Source of thermodynamic data.**

Source letter	Reference
a	Roine et al. (2012)
b	Lu, Dreisinger, and Cooper (2002)
c	Young, Dahlgren, and Robins (2003)
d	Osadchii and Rappo (2004)

Table 10-2 Gibbs free energy data used  
for the Cu-CN-S-H<sub>2</sub>O system.

Species	$\Delta G_f^\circ$	
CN(-a)	41.18	b
CNS(-a)	22.1613	a
Cu	0	c
Cu(+2a)	15.7	c
Cu(+a)	12	c
Cu(CN)2(a)	97.6976	a
Cu(CN)2(-a)	61.66	b
Cu(CN)3(-2a)	95.6	b
Cu(CN)4(-3a)	134.8	b
Cu(CNS)4(-3a)	87.0188	a
Cu(HS)2(-a)	-5.68	c
Cu(HS)3(-a)	-11.94	c
Cu(OH)2	-74	c
Cu(OH)3(-a)	-118.6	c
Cu(OH)4(-2a)	-157.3	c
Cu(SCN)(+a)	34.7441	a
Cu1.75S	-18.7	c
Cu1.96S	-20.1	c
Cu2(OH)2(+2a)	-67.8251	a
Cu2O	-35.4	c
Cu2OH(+3a)	-16.4236	a
Cu2S	-20.4	c
Cu2S(HS)2(-2a)	-8.11	c
Cu2SO4	-156.43	a
Cu2SO4(a)	-154.288	a
Cu3(OH)4(+2a)	-151.42	a
CuCN	25.93	b
CuCNS	15.085	a
CuHS(a)	-2.85	c
CuO	-32	c
CuO(a)	-20.8313	a
CuO(T)	-30.5635	a
CuO*CuSO4	-189.354	a
CuO2(-2a)	-43.95	b
CuOH(+a)	-31	c
CuOH(a)	-25.6405	a

Species	$\Delta G_f^\circ$	
CuS	-12.8	c
CuS(HS)3(-3a)	-0.85	c
CuSO3(a)	-100.648	a
CuSO4	-165.43	c
CuSO4*2Cu(OH)2	-345.75	c
CuSO4*3Cu(OH)2	-434.44	c
CuSO4*3H2O	-333.882	a
CuSO4*5H2O	-449.3	c
CuSO4*H2O	-218.633	a
H2S(a)	-6.66	c
H2SO4	-164.894	a
H2SO4*2H2O	-286.7	a
H2SO4*3H2O	-345.098	a
H2SO4*4H2O	-402.906	a
H2SO4*6.5H2O	-546.278	a
H2SO4*H2O	-227.124	a
HCN(a)	28.61	b
HCNO(a)	-2.89	b
HCuO2(-a)	-61.88	b
HS(-a)	2.88	c
HS2O3(-a)	-127.183	a
HS2O4(-a)	-146.862	a
HS2O6(-a)	-256.546	a
HSO4(-a)	-180.68	c
OCN(-a)	-23.59	b
S	0	c
S(-2a)	20.548	a
S(M)	0.0198	a
S2(-2a)	19.0553	a
S2O3(-2a)	-123.96	a
S2O4(-2a)	-143.539	a
S2O5(-2a)	-189.024	a
S2O6(-2a)	-231.605	a
S3(-2a)	17.6572	a
S3O6(-2a)	-228.815	a
S4(-2a)	16.589	a
S4O6(-2a)	-248.627	a
S5(-2a)	15.8207	a
S5O6(-2a)	-228.331	a
S6(-2a)	15.8272	a

Species	$\Delta G_f^\circ$	
SO <sub>2</sub> (a)	-71.8343	a
SO <sub>3</sub>	-88.1433	a
SO <sub>3</sub> (-2a)	-116.287	a
SO <sub>4</sub> (-2a)	-177.94	c

Table 10-3 Gibbs free energy data used for Ag species in the Ag-Cu-CN-S-H<sub>2</sub>O system. All data is from reference "a".

Species	$\Delta G_f^\circ$
Ag	0
AgCN	37.5329
AgCNO	-13.7691
AgCNS	24.237
AgO	3.4641
AgO <sub>2</sub>	-2.6267
Ag <sub>2</sub> O	-2.671
Ag <sub>2</sub> O <sub>2</sub>	6.5529
Ag <sub>2</sub> O <sub>2</sub> (cub)	-8.7798
Ag <sub>2</sub> O <sub>3</sub>	28.9864
Ag <sub>1.64</sub> S	-9.7737
Ag <sub>2</sub> S	-9.6517
Ag <sub>2</sub> S(A)	-9.5628
Ag <sub>2</sub> S(B)	-9.346
AgSCN	24.2604
Ag <sub>2</sub> SO <sub>3</sub>	-98.3362
Ag <sub>2</sub> SO <sub>4</sub>	-147.733
Ag(+2a)	64.1902
Ag(+a)	18.4305
Ag(CN) <sub>2</sub> (-a)	73.0973
Ag(CN) <sub>3</sub> (-2a)	111.5382
AgHS(a)	0.2849
Ag(HS) <sub>2</sub> (-a)	0.0586
AgO(-a)	-5.4377
AgOH(a)	-21.9216
AgSO <sub>4</sub> (-a)	-160.96
AgS <sub>2</sub> O <sub>3</sub> (-a)	-117.125
Ag(SO <sub>3</sub> ) <sub>2</sub> (-3a)	-226.18

Species	$\Delta G_f^\circ$
Ag(SO <sub>3</sub> ) <sub>3</sub> (-5a)	-342.796
Ag(S <sub>2</sub> O <sub>3</sub> ) <sub>2</sub> (-3a)	-240.955

Table 10-4 Gibbs free energy data used for Au species in the Au-Cu-CN-S-H<sub>2</sub>O system. All data is from reference "a", except Au<sub>2</sub>S which is from reference "d".

Species	$\Delta G_f^\circ$
Au	0
AuCu	-5.6013
AuCu <sub>3</sub>	-7.0311
Au <sub>2</sub> O <sub>3</sub>	18.6088
Au(OH) <sub>3</sub>	-75.7294
Au(OH) <sub>3</sub> (P)	-75.7294
Au <sub>2</sub> O <sub>3</sub> *3H <sub>2</sub> O	-167.484
Au(+3a)	103.3159
Au(+a)	39.1742
Au(CN) <sub>2</sub> (-a)	68.1753
Au(HS) <sub>2</sub> (-a)	2.4878
Au <sub>2</sub> S	0.257

Table 10-5 Gibbs free energy data used for Au-Ag species in the Au-Ag-Cu-CN-S-H<sub>2</sub>O system. All data is from reference "d".

Species	$\Delta G_f^\circ$
Au	0
AuCu	-5.6013

Table 10-6 Gibbs free energy data used for Fe species in the Fe-Cu-CN-S-H<sub>2</sub>O system. All data is from reference "a".

Species	$\Delta G_f^\circ$
CuFeS <sub>2</sub>	-45.529
Cu <sub>5</sub> FeS <sub>4</sub>	-93.8234
CuO*Fe <sub>2</sub> O <sub>3</sub>	-205.969
Cu <sub>2</sub> O*Fe <sub>2</sub> O <sub>3</sub>	-220.015
Fe	0
Fe(A)	-0.0029
Fe <sub>0.945</sub> O	-57.9952
Fe <sub>0.947</sub> O	-58.6015
FeO	-59.8905
FeO <sub>1.056</sub>	-61.6194
FeO <sub>1.5</sub> (W)	-82.041
Fe <sub>2</sub> O <sub>3</sub>	-177.879
Fe <sub>2</sub> O <sub>3</sub> (G)	-174.788
Fe <sub>2</sub> O <sub>3</sub> (H)	-159.427
Fe <sub>3</sub> O <sub>4</sub>	-241.956
Fe <sub>3</sub> O <sub>4</sub> (H)	-203.856
Fe(OH) <sub>2</sub>	-116.389
Fe(OH) <sub>3</sub>	-168.088
Fe <sub>2</sub> O <sub>3</sub> *H <sub>2</sub> O	-233.23
Fe <sub>2</sub> O <sub>3</sub> *3H <sub>2</sub> O	-334.289
FeO*OH	-117.237
FeO*OH(L)	-115.351
Fe <sub>0.877</sub> S	-25.5329
FeS	-23.9692
FeS(ai)	1.5693
FeS <sub>2</sub>	-39.8572
FeS <sub>2</sub> (M)	-37.1686
Fe <sub>2</sub> S	-10.6842
Fe <sub>2</sub> S <sub>3</sub>	-67.0303
Fe <sub>7</sub> S <sub>8</sub>	-178.725
Fe <sub>9</sub> S <sub>8</sub>	-187.349
FeSO <sub>4</sub>	-197.153
Fe <sub>2</sub> (SO <sub>4</sub> ) <sub>3</sub>	-541.198
FeSO <sub>4</sub> *H <sub>2</sub> O	-257.952
FeSO <sub>4</sub> *4H <sub>2</sub> O	-428.672

Species	$\Delta G_f^\circ$
FeSO <sub>4</sub> *7H <sub>2</sub> O	-599.842
Fe(CN) <sub>2</sub> (a)	63.1767
Fe(CN) <sub>3</sub> (a)	121.9706
FeO(a)	-50.7151
Fe(OH) <sub>2</sub> (a)	-94.0319
Fe(OH) <sub>3</sub> (a)	-113.842
FeSO <sub>3</sub> (a)	-135.169
Fe <sub>2</sub> (SO <sub>3</sub> ) <sub>3</sub> (a)	-351.095
HFeO <sub>2</sub> (a)	-105.7
Fe(+3a)	-4.1069
Fe(+2a)	-21.875
Fe(CN) <sub>6</sub> (-3a)	174.3752
Fe(CN) <sub>6</sub> (-4a)	166.1138
Fe(CNS)(+2a)	17.0097
FeO(+a)	-53.0932
FeO <sub>2</sub> (-a)	-92.6416
FeOH(+2a)	-57.8297
FeOH(+a)	-65.8452
Fe(OH) <sub>2</sub> (+a)	-108.078
Fe(OH) <sub>3</sub> (-a)	-148.193
Fe(OH) <sub>4</sub> (-a)	-202.985
Fe <sub>2</sub> (OH) <sub>2</sub> (+4a)	-111.743
FeSCN(+2a)	17.0067
FeSO <sub>4</sub> (+a)	-184.656
HFe(CN) <sub>6</sub> (-3a)	160.3416
H <sub>2</sub> Fe(CN) <sub>6</sub> (-2a)	157.3482
HFeO <sub>2</sub> (-a)	-95.3529

Table 10-7 Gibbs free energy data used for Ni species in the Ni-Cu-CN-S-H<sub>2</sub>O system. All data is from reference "a".

Species	$\Delta G_f^\circ$
Ni	0
Ni(CN) <sub>2</sub>	36.9871
NiH <sub>0.5</sub>	1.4074
NiH <sub>0.59</sub>	1.6578
NiH <sub>0.68</sub>	1.918
Ni <sub>2</sub> H	2.7506

Species	$\Delta G_f^\circ$
NiO	-50.5701
Ni(OH)2	-107.037
Ni(OH)2(B)	-109.259
Ni(OH)3	-129.894
Ni2O3*3H2O	-258.149
NiO*OH	-75.7334
NiS0.84	-19.1455
NiS	-21.8356
NiS(A)	-21.0133
NiS(B)	-21.8356
NiS2	-29.8343
Ni3S2	-50.2728
Ni3S4	-69.7866
Ni6S5	-114.964
Ni7S6	-134.332
Ni9S8	-180.07
NiSO4	-181.543
NiSO4*H2O	-259.437
NiSO4*4H2O	-432.81
NiSO4*6H2O	-531.616
NiSO4*6H2O(B)	-531.773
NiSO4*7H2O	-588.316
NiO(a)	-54.2511
Ni(SCN)2(a)	29.6991
NiSO4(a)	-191.972
HNiO2(-a)	-81.9724
Ni(+2a)	-10.9194
Ni(CN)4(-2a)	107.4524
Ni(CN)5(-3a)	152.0764
NiCNS(+a)	9.0963
NiO2(-2a)	-64.1478
NiOH(+a)	-54.3177
Ni(OH)3(-a)	-140.321
Ni2OH(+3a)	-87.0982
Ni4(OH)4(+4a)	-225.421
NiSCN(+a)	8.7427
Ni(SCN)3(-a)	51.4059

Table 10-8 Gibbs free energy data used for Zn species in the Zn-Cu-CN-S-H<sub>2</sub>O system. All data is from reference "a".

Species	$\Delta G_f^\circ$
Zn	0
Zn(CN)2	32.1226
ZnO	-76.0396
Zn(OH)2	-132.868
Zn(OH)2(D)	-132.411
Zn(OH)2(E)	-132.658
Zn(OH)2(G)	-132.561
ZnO*2ZnSO4	-494.188
ZnS	-47.4464
ZnS(B)	-47.8967
ZnS(W)	-44.9811
ZnSO4	-207.634
ZnSO4*H2O	-270.558
ZnSO4*2H2O	-327.443
ZnSO4*6H2O	-555.491
ZnSO4*7H2O	-612.646
Zn(CN)2(a)	46.8547
Zn(CN)2(Ha)	31.7578
Zn(CNS)2(a)	7.8562
Zn(HS)2(a)	-47.468
ZnO(a)	-67.4178
ZnS(a)	-14.7526
ZnSO3(a)	-151.491
ZnSO4(a)	-216.273
ZnS2O3(a)	-158.64
HZnO2(-a)	-110.702
Zn(+2a)	-35.1941
Zn(CN)3(-a)	65.9778
Zn(CN)4(-2a)	86.7088
ZnCNS(+a)	-15.5612
ZnHS(+a)	-44.1896
Zn(HS)3(-a)	-48.4461
ZnO2(-2a)	-93.2765
ZnOH(+a)	-81.1863
Zn(OH)3(-a)	-168.621

<b>Species</b>	<b><math>\Delta G_f^\circ</math></b>
Zn(OH) <sub>4</sub> (-2a)	-209.457

**Table 10-9 Explanatory notes for symbols used in MEDUSA.**

Symbol	Description
(c)	Crystalline solid
(am)	Amorphous solid
(s)	Solid, nature not defined
(g)	Gas

## 10.2 Calculation of cyanide concentration

In a solution containing only free cyanide, the concentration of cyanide can be calculated from the following equation:

$$c(CN) = \frac{2 \times c(Ag) \times V(Ag_{total})}{V(Sample)}$$

Where  $c(CN)$  is the concentration of cyanide (mM),  $c(Ag)$  is the concentration of silver nitrate used (mM),  $V(Ag_{total})$  is the volume of silver nitrate added at the titration end point (mL), and  $V(Sample)$  is the volume of sample titrated (mL). To determine the amount of free cyanide in a solution containing cyanide, copper, and sulfide, the volume of silver which reacts with cyanide from copper cyanide and sulfide must be subtracted from the volume of

silver added in the titration. The volume of silver consumed by copper cyanides and sulfide is calculated in the following two equations:

$$V(Ag_{Cu}) = \frac{0.5 \times c(Cu) \times V(Sample)}{c(Ag)}$$

$$V(Ag_S) = \frac{2 \times c(S^{2-}) \times V(Sample)}{c(Ag)}$$

where  $V(Ag_{Cu})$  and  $V(Ag_S)$  is the volume of silver consumed by copper cyanide and sulfide respectively, and  $c(Cu)$  and  $c(S^{2-})$  are the concentrations of copper and sulfide in the sample respectively. This gives a final equation of:

$$c(CN) = \frac{2 \times c(Ag) \times \left( V(Ag_{total}) - \frac{0.5 \times c(Cu) \times V(Sample)}{c(Ag)} - \frac{2 \times c(S^{2-}) \times V(Sample)}{c(Ag)} \right)}{V(Sample)}$$

### 10.3 Coefficients of combined profit equation

Coefficients of Equations 4.22 through to 4.25.

$$b_1 = -0.712 \times V_{Cu} \times [Cu] + 0.780 \times V_A \times [Cu] + 0.780 \times V_B \times [Cu]$$

$$b_2 = -0.00776 \times V_{Cu} \times [Cu] - 2.55 \times V_{CN} \times [Cu] - 0.445 \times V_A \times [Cu] \\ - 0.445 \times V_B \times [Cu]$$

$$b_3 = 6.66 \times V_{Cu} \times [Cu] - 4.55 \times V_A \times [Cu] - 4.55 \times V_B \times [Cu] - V_S \\ \times [Cu]$$

$$b_4 = -0.0856 \times V_{Cu} \times [Cu] + 0.216 \times V_A \times [Cu] + 0.216 \times V_B \times [Cu]$$

$$b_5 = 8.05 \times V_{CN} \times [Cu]$$

$$b_6 = -0.092 \times V_{CN} \times [Cu]$$

$$b_7 = 0.129 \times V_{Cu} \times [Cu] - 0.337 \times V_A \times [Cu] - 0.337 \times V_B \times [Cu]$$

$$b_8 = 0.215 \times V_{CN} \times [Cu]$$

$$b_9 = -61.7 \times V_{Cu} \times [Cu] + 4.25 \times V_A \times [Cu] + 4.25 \times V_B \times [Cu]$$

$$b_{10} = -6.68 \times V_{CN} \times [Cu]$$

$$b_{11} = -0.23 \times V_{CN} \times [Cu]$$

$$b_{12} = 0.141 \times V_{CN} \times [Cu]$$

$$b_{13} = -0.00997 \times V_{CN} \times [Cu]$$